The University Of Sheffield.

Developing neuronal blockers for long-lasting pain relief

By:

Rebecca Bresnahan

A thesis submitted in partial fulfilment of the requirements for the degree of Doctor of Philosophy

The University of Sheffield

Faculty of Life Sciences

Department of Biomedical Science

June 2018

Acknowledgements

Firstly, I would like to thank my supervisor, Bazbek Davletov, for allowing me this opportunity, and for his support during this time. I would also like to thank all of the members of the Davletov lab. Thank you to Ciara Doran for teaching me countless cell culture techniques and for your advice and support. Thank you to Charlotte Leese for the endless preparations of proteins and for always having patience. A special thank you to Rose Hart for your friendship and for always being available for a good rant!

Additionally, I would like to thank Steve Hunt and his lab members for the in vivo techniques that I acquired during my visits to UCL. I would also like to acknowledge all of those who have shared any reagents or antibodies used in this project or have advised on any troubleshooting. There have been plenty of occasions! I would especially like to thank my advisor, Liz Seward, who has been, when times required, a source of much needed support and reassurance.

A massive thank you to my BMS besties, Catherine Buckley and Rachel Moore, for all of our date nights and unplanned pub evenings. I don't want to face a Pancake Tuesday without you two. Thank you to Shireen Gallagher for always being a text message away. You have been so understanding of my neglect of our friendship for the past 4 years. I promise to visit many gin gardens and eateries with you to make up for it. Thank you to my combat partner and personal mentor, Sue Hemsworth. Your advice has been invaluable. Thank you to my sister, Michelle, and my beautiful nieces, Eden and Esme (and Molly). You have been a constant reminder to me that there are more important things in life. I love you the world. Thank you to my mum. You are my rock and my best friend. I will never be able to repay you for your constant and unfaltering love and support (not to mention the taxi rides up and down the motorway). I love you so much. Thank you to my boyfriend, Neil Hansen. Thank you for the hugs and cuddles and reassurance (and, again, the taxi rides). A special thank you for always having a chippy and a cold craft beer ready for me on a Friday night. You know me so well, I love you.

Finally, thank you to anyone who I might have forgotten but who has offered a shoulder to cry on. This has been a difficult journey. Thank you all for everything.

Declaration

I, the candidate, confirm that all work and data shown in this thesis was conducted by myself, the author. Any work conducted by others has been appropriately referenced and acknowledged throughout the text.

Abstract

The inadequacy of available pharmacotherapy for managing chronic pain imposes a huge burden on both patients, healthcare services and the economy. The exploitation of biologics, specifically botulinum neurotoxin A (BoNT/A), is important for the development of novel long-acting analgesics. BoNT/A induces analgesia in numerous chronic pain models, via the disruption of SNARE-mediated cellular processes. To aid translation into humans, reengineering BoNT/A can eliminate its paralytic effects and improve its safety profile. BiTox/A, an elongated version of BoNT/A, was generated using SNARE-stapling technology and effectively reduced mechanical hypersensitivity in multiple pain models, presumably via actions at the A-nociceptors. Producing a chimera as efficacious against other clinical features of pain, including thermal hyperalgesia, requires the retargeting of BoNT/A's catalytic activity to different sensory neuron subpopulations. The light chain-translocation domain of BoNT/A (LcTd/A) was thus conjugated to the receptor binding domain (Rbd) of alternate BoNT serotypes, /C to /E. Staining of cultured sensory neurons revealed that conjugation of LcTd/A to BoNT/D-derived Rbd produced SNAP25 cleavage in a subpopulation of smaller myelinated neurons. Unexpectedly, intraplantar injection of the chimera into an inflammatory pain model potentially prolonged thermal hyperalgesia and failed to alter mechanical hypersensitivity. Conversely, LcTd/A conjugated to cholera toxin-derived binding domain attenuated the development of, and reversed, mechanical hypersensitivity in a post-operative pain model and a chemotherapy-induced peripheral neuropathy model, yet remained ineffective against thermal hyperalgesia.

BoNT/A's analgesic effect is hypothesised to be predominantly centrally-mediated. To determine whether this theory was also relevant to BiTox/A, the chimera's in vivo activity was examined. Cleaved SNAP25 was revealed in the ipsilateral ventral horn with sparse labelling in the dorsal horn, as well as in the peripheral afferent terminals, thus implying that a peripheral and central action contribute to the analgesic effect. After demonstrating penetration of the central nervous system, the application of toxin chimeras for drug delivery to the spinal cord was investigated using tetanus binding domain (Tbd). Tbd successfully chaperoned fluorescent tags and LcTd/A to the spinal cord. Attachment of a second Tbd to chimeras significantly increased the detectable fluorescence and amount of cleaved SNAP25 in the ventral horn. In conclusion, the smaller Aδ-nociceptors, targeted by BoNT/D-derived Rbd, likely contribute to the resolution of inflammation and the recovery of normal thermal sensation. Targeting of LcTd/A by cholera toxin resulted in a functional analgesic that displayed less penetration of the ventral horn, indicating a reduced motor effect. This chimera should thus be pursued as a potential long-lasting analgesic. Equally, tetanus proved an efficacious tool for spinal cord delivery. Attaching a second binding domain successfully increased its potency, emphasising the versatility and technical advancement of the SNARE-stapling approach.

Table of Contents

List of Figures

List of Tables

List of Abbreviations

AA	Amino Acid
AB5	A subunit interacting with a pentameric B subunit
ACh	Acetylcholine
ALS	Amyotrophic Lateral Sclerosis
AMPA	α-amino-3-hydroxy-5-methyl-4-isoxazolepropionic acid
ANOVA	Analysis of Variance
ATP	Adenosine triphosphate
BiTox/A	SNARE-stapled chimera constructed from LcTd/A conjugated to Rbd/A
BiTox/C	SNARE-stapled chimera constructed from LcTd/A conjugated to Rbd/C
BiTox/D	SNARE-stapled chimera constructed from LcTd/A conjugated to Rbd/D
BiTox/E	SNARE-stapled chimera constructed from LcTd/A conjugated to Rbd/E
BoNT/A	Botulinum Neurotoxin, Serotype A
BoNT/B	Botulinum Neurotoxin, Serotype B
BoNT/C	Botulinum Neurotoxin, Serotype C
BoNT/D	Botulinum Neurotoxin, Serotype D
BoNT/E	Botulinum Neurotoxin, Serotype E
BoNT/F	Botulinum Neurotoxin, Serotype F
BoNT/G	Botulinum Neurotoxin, Serotype G
BTIII	β-Tubulin III
CaMKII	Ca 2+ /calmodulin-dependent protein kinase II
CFA	Complete Freund's Adjuvent
CGRP	Calcitonin gene-related peptide
ChoBot	SNARE-stapled chimera constructed from LcTd/A conjugated to Cholera toxin AB5
cSNAP25	Cleaved SNAP25
CTB	Cholera Toxin Subunit B
CTB-488	Cholera Toxin Subunit B Alexa Fluor 488 Conjugate
Cy3	Cyanine Dye 3
DAPI	4′,6-diamidino-2-phenylindole
DMEM	Dulbecco’s modified Eagle medium
DRG	Dorsal Root Ganglion
ECL	Erythrina Cristagalli
GABA	γ-amino butyric acid

GAD	Glutamic Acid Decarboxylase
HC	Heavy Chain
HTM	High Threshold Mechanoreceptors
ICC	Immunocytochemistry
IHC	Immunohistochemistry
KCl	Potassium Chloride
Lc	Light chain
Lc/A	Light Chain of Botulinum Neurotoxin subtype A
LcTd/A	Light chain-Translocation domain of botulinum neurotoxin serotype A
LTM	Low Threshold Mechanoreceptors
MAG	Myelin Associated Glycoprotein
MAP	Mitogen-Activated Protein
MgCl2	Magnesium Chloride
MOR	μ-opioid receptors
NeuN	Neuronal Nuclei
NF200	Neurofilament 200 kDA
NGF	Nerve Growth Factor
NK1	Neurokinin-1
NMDA	N-methyl-D-aspartate
NMJ	Neuromuscular Junction
OG	Octyl β-D-glucopyranoside
P2X3	P2X purinoceptor 3
PAG	Periaqueductal Gray
PBS	Phosphate-Buffered Saline
PDPN	Painful Diabetic Peripheral Neuropathy
PFA	Paraformaldehyde
PGE2	Prostaglandin E2
PIPN	Paclitaxel-induced Peripheral Neuropathy
PKA	Protein Kinase A
PKC	Protein Kinase C
QST	Quantitative sensory testing
Rbd	Receptor binding domain
Rbd/A	Receptor binding domain of Botulinum Neurotoxin Serotype A
Rbd/C	Receptor binding domain of Botulinum Neurotoxin Serotype C
Rbd/D	Receptor binding domain of Botulinum Neurotoxin Serotype D
Rbd/E	Receptor binding domain of Botulinum Neurotoxin Serotype E

ROI	Region of Interest
rTMS	Repetitive Transcranial Magnetic Stimulation
RVM	Rostral Ventromedial Medulla
SDS	Sodium Dodecyl Sulphate
SMA	Spinal Muscular Atrophy
SNAP25	Synaptosomal Associated Protein of 25 kDa
SNARE	Soluble N-ethylmaleimide-sensitive factor Attachment Protein Receptor
SNI	Spared Nerve Injury
SV2	Synaptic Vesicle Protein 2
SV2/A	Synaptic Vesicle Protein 2 Isoform A
SV2/B	Synaptic Vesicle Protein 2 Isoform B
SV2/C	Synaptic Vesicle Protein 2 Isoform C
Syn	Syntaxin
Tbd	Tetanus binding domain
Td	Translocation domain
TetBot	SNARE-stapled chimera constructed from LcTd/A conjugated to Tbd
TG	Trigeminal Ganglion
TRPV1	Transient Receptor Potential Vanilloid receptor-1
v/v	Volume/Volume percentage
VAMP	Vesicle-Associated Membrane Protein
VAS	Visual Analogue Scale
w/v	Weight/Volume percentage
WB	Western Blot
WDR	Wide Dynamic Range
α-BTX	Alpha Bungarotoxin
α-BTX-488	α-Bungarotoxin-Alexa Fluor 488 Conjugate

Chapter 1. Introduction

Chronic pain is generally defined to be pain that outlasts the normal recovery period, following injury or damage. Clinically, it is recognised as pain that persists beyond 3 to 6 months (Treede et al., 2015). It is estimated that 19% of the European population suffer from chronic pain (Breivik et al., 2006). Analogous statistics have been reported within the Australian population with 17% of males and 20% of females identifying as chronic pain sufferers (Blyth et al., 2001). For approximately 40% of these chronic pain sufferers, pharmacological intervention provides inadequate pain relief (Breivik et al., 2006). This primarily results from a lack of medication, specifically intended for use in chronic pain conditions. Instead, pharmacological management of chronic pain relies upon a combination of anti-inflammatories, anti-epileptics, anti-depressants and opioids to acutely manage pain conditions (Dworkin et al., 2007). Often, these medications are associated with significant adverse effects which thus limits their use.

The huge economic burden imposed by chronic pain combined with its increased prevalence, associated with age, raises great concern about the future impact that chronic pain may have on healthcare services and society, given the aging population (Sleed et al., 2005; Phillips, 2009; Kaye et al., 2010). This concern has consequently led to an increased interest in developing novel pain therapeutics. Many avenues are being explored in order to produce therapeutics that selectively target pain signalling pathways. The use of Botulinum neurotoxin (BoNT) represents one such avenue being pursued. Specifically, when retargeted through protein modification, BoNT can be used to silence distinct populations of neuronal cell types for several months, following localised injection (Arsenault et al., 2013; Ferrari et al., 2013; Ma et al., 2014).

This introduction will now proceed to discuss chronic pain and the mechanisms by which it is hypothesised to arise before introducing BoNT subtype A (BoNT/A) and its clinical applications in pain at present. In addition, the protein engineering approaches being used to improve efficacy of BoNT/A as an analgesic, as well as its safety profile, and the success of these techniques will be described.

1.1 Chronic Pain

1.1.1 The epidemiology of chronic pain

1.1.1.1 Inflammatory Pain

Chronic pain forms an umbrella term for a multitude of pain conditions. Chronic inflammatory pain is the most prevalent with arthritis being the leading cause of pain, accounting for 40% of chronic pain sufferers in Europe (Breivik et al., 2006). Inflammatory pain is unique in comparison to other chronic pain conditions because it is largely nociceptive, meaning that there is an on-going stimulus which elicits the pain response. Inflammatory pain does, however, begin to comprise some neuropathic components as the disease progresses which result from the continuous activation of the pain signalling pathways (van Laar et al., 2012).

1.1.1.2 Neuropathic Pain

In contrast to inflammatory pain, neuropathic pain conditions feature pain signalling and pain sensation which persist in the absence of a noxious stimulus. Historically, neuropathic pain was referred to as “pain initiated or caused by a primary lesion or dysfunction in the nervous system” (Merskey and Bogduk, 2012). This definition has now been revised and neuropathic pain is instead specified as “pain caused by a lesion or disease of the somatosensory system” (Jensen et al., 2011). The latter definition prevents complications caused by whether pain is initiated by a primary or secondary lesion and also avoids conditions, such as complex regional pain syndrome with more complex aetiology, being misappropriated as neuropathic pain conditions (Backonja, 2003). Current estimates indicate that the prevalence of neuropathic pain is 7-10% in the UK population (van Hecke et al., 2014).

Within the neuropathic pain bracket there are several distinct conditions. For example, 2.4% of the population are estimated to suffer from peripheral neuropathies. The most prominent being painful diabetic peripheral neuropathy (PDPN) which presents in 26.4% of all type 2 diabetic patients (Martyn and Hughes, 1997; Davies et al., 2006). This statistic then increases to over 50% of type 2 diabetic patients over the age of 60 experiencing PDPN (Young et al., 1993). Peripheral neuropathies are also commonly developed following chemotherapy in cancer patients. They are estimated to occur in 90% of all cases due to the neurotoxic damage of nerves (Fallon, 2013). Both of these peripheral neuropathies typically present with a ‘gloves and stocking’ distribution due to the increased vulnerability of the longer peripheral nerves to neurotoxic damage (Said et al., 1983; Starobova and Vetter, 2017).

Alternatively, neuropathic pain can affect a specific body region, resulting from damage to a specific nerve. For example, trigeminal neuralgia, a rarer condition, which affects 0.03%- 0.3% of people, is believed to result from the focal demyelination of the trigeminal nerve due to compression of the nerve, most likely by blood vessels (Love and Coakham,

2001; De Toledo et al., 2016). Damage to nerves, typically the brachial plexus, commonly occurs following road traffic accidents. Brachial plexus injuries were identified in 1.2% of trauma patients and were particularly prevalent in patients involved in motor cyclist accidents (Midha, 1997). Notably, brachial plexus injuries account for 36% of all traumatic peripheral nerve injuries (Ciaramitaro et al., 2010).

Additionally, nerve damage can be inflicted by viral infection. For example, post-herpetic neuralgia is frequently experienced following herpes zoster infection. An Icelandic study stated that pain persisting past 3 months was reported in 1.8% of patients, aged below 60, infected with herpes zoster, whereas approximately 7% of patients aged over 60 had pain persisting beyond 3 months (Helgason et al., 2000). Conversely, an American study described post-herpetic neuralgia in 25%-50% of patients aged over 50 who had incurred herpes zoster (Schmader, 2002). Both studies, however, emphasised an increased severity and incidence associated with age. Postherpetic neuralgia presents in the infected nerve and the associated dermatome or dermatomes. This consequently produces a focal neuropathy rather than a global neuropathy, as is classically observed in PDPN and chemotherapy-induced peripheral neuropathy (Rowbotham et al., 1998).

1.1.1.3 Chronic Post-Surgical Pain

Post-operative pain occurs following 10–50% of surgical cases. It is most commonly associated with surgical procedures such as breast surgery, limb amputation, thoracotomy and major heart surgery (Kehlet et al., 2006). The highest incidence for post-surgical pain occurs after limb amputation (Kehlet et al., 2006; Macrae, 2008). Mastectomy is a frequently used surgical intervention for treating breast cancer. 22–72% of breast cancer patients experience postmastectomy pain syndrome, a post-surgical pain condition (Gottrup et al., 2000; Andersen and Kehlet, 2011). Within the UK, post-surgical pain is responsible for introducing an additional 140,000 patients with disabling chronic pain each year (Werner and Kongsgaard, 2014).

The pathophysiology of chronic post-surgical pain is not well understood. It is generally accepted that it must arise from a combination of local inflammation due to the cutting of tissue at the surgical site causing direct activation of nociceptors, as well as nerve damage due to the severing of nerves, or damage inflicted to nerves, during the surgical procedure. This subsequently introduces a neuropathic component (Macrae, 2008; Reddi and Curran, 2014). There is also a large role for psychological factors in post-surgical pain, such as catastrophising and attribution of blame, which are known to impact the development of chronic post-surgical pain and patient responsiveness to intervention (Macrae, 2008; Reddi and Curran, 2014).

1.1.2 Pathophysiology of chronic pain

Although chronic inflammatory pain conditions and neuropathic pain conditions can present differently clinically and arise from contrasting aetiologies, the same fundamental mechanisms are believed to underlie the development of all subclasses of chronic pain (Xu and Yaksh, 2011).

.

1.1.2.1 Pain signalling pathways

Acute nociception relies upon the activation of nociceptors, namely the high-threshold unmyelinated C-fibres and the lightly myelinated Aδ-fibres (Fig.1.1A). C-fibre nociceptors are polymodal and respond to thermal, mechanical and chemical stimuli, however, some

A.

Primary Afferent Fibre	Degree of Myelination	Axon Diameter (µm)	Conduction Velocity (m/s)	Sensory Modality
Aβ	Heavily myelinated	6 -12	16 - 100	Mechanical (innocuous), Proprioception
Aδ	Lightly myelinated	1 - 5	5 - 30	Mechanical (noxious), Thermal, Chemical
C	Unmyelinated	0.2 - 1.5	0.2 - 2	Mechanical (noxious), Thermal, Chemical, Itch

B.

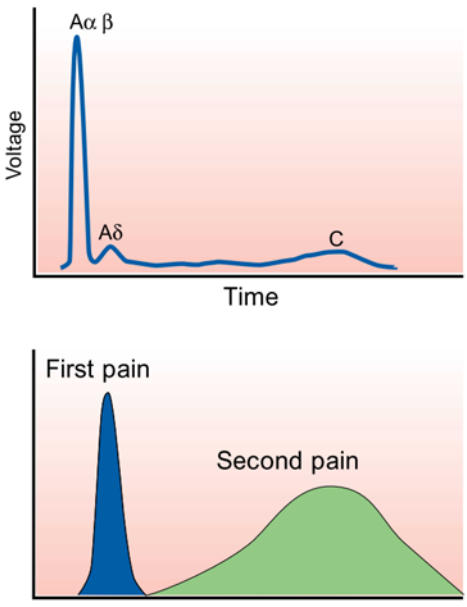

Figure 1.1 The properties of sensory neuron subtypes relate to the different pain qualities experienced. (A) *The table describes the three main classification groups for sensory neurons. Notably, the axon diameter (Pocock et al., 2018) and conduction velocity (Abraira and Ginty, 2013) are much greater in the Aβ-fibres than the other sensory subtypes. These properties correspond to the level of myelination.* ***(B)*** *Analysis of the compound action potential from a peripheral nerve reveals that the quality of pain experienced is dependent upon which sensory subpopulations are activated and their respective conduction velocities. Activation of Aδ-nociceptors correlates to a sharp pain (first pain), whereas activation of C-nociceptors produces the dull, aching, diffuse pain (second pain). Graph from Julius and Basbaum (2001).*

populations only respond to a subset of these stimuli (Caterina and Julius, 1999; Almeida et al., 2004). Additionally, C-fibres can be classified as either peptidergic or non-peptidergic, depending on their expression of neuropeptides (Caterina and Julius, 1999). Whilst Aδ-fibre nociceptors can also be polymodal, they are more commonly responsive to either mechanical or thermal stimuli, exclusively (Dubin and Patapoutian, 2010). In contrast the large diameter, myelinated Aβ-sensory afferents are low threshold mechanoreceptors and are responsive to innocuous stimuli, for instance, touch (Fig. 1.1A) (Abraira and Ginty, 2013).

All sensory neurons, including nociceptors, are pseudopolar neurons whose cell soma reside in the dorsal root ganglia, located outside of the spinal cord. The axons of sensory neurons project to the dorsal horn of the spinal cord where they form synapses with interneurons and wide dynamic range (WDR) neurons. Specifically, the C-fibre nociceptors terminate in lamina I-IIo (outer), known as the substantia gelantinosa, and the Aδ- nociceptors terminate in lamina I and V (Fig 1.2) (Todd, 2010). Conversely, the low threshold mechanoreceptors, the Aβ-fibre sensory afferents, project to lamina IIi (inner)-V (Todd, 2010). Whilst interneurons terminate locally within the spinal cord, the wide dynamic range neuron relay information from the peripheral nociceptive afferents to the higher regions of the central nervous system, including the somatosensory cortical areas, mainly via the lateral spinothalamic tract (Fig 1.3) (Todd, 2017).

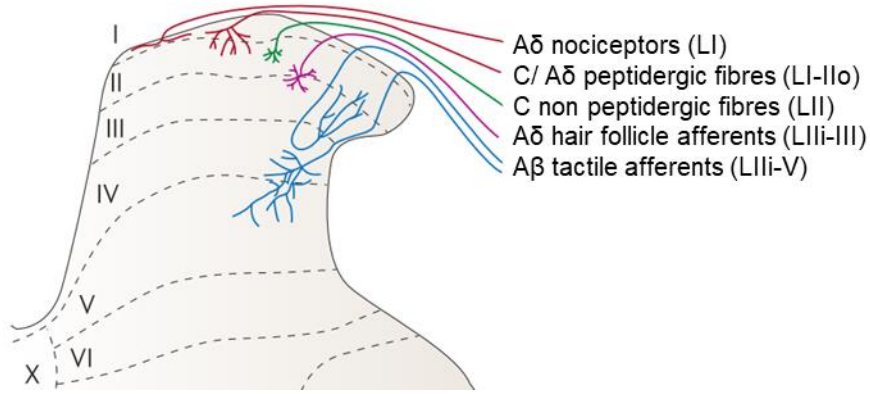

Figure 1.2 Primary afferents terminate within distinct laminae of the dorsal horn. *The central terminals of the sensory afferents project to the dorsal horn of the spinal cord. C-fibres terminate within the substantia gelatinosa. Specifically, the peptidergic C-nociceptors project to lamina I and lamina IIo (outer), whereas the terminals of non-peptidergic C-fibres remain confined to Lamina II. Aδ-nociceptors terminate in Lamina I, with some collaterals projecting to Lamina V. Additionally, Aδ-fibres which innervate the hair follicles, terminate in Lamina IIi (inner) and Lamina III, however, these are not relevant when studying the glabrous skin. The low-threshold Aβ mechanoreceptors conversely terminate between laminae IIi and V. Although not shown, projection neurons are predominantly found in lamina I, as well as being present in lamina III–VI. The interneurons are located largely within Laminae I-III. From Todd (2010).*

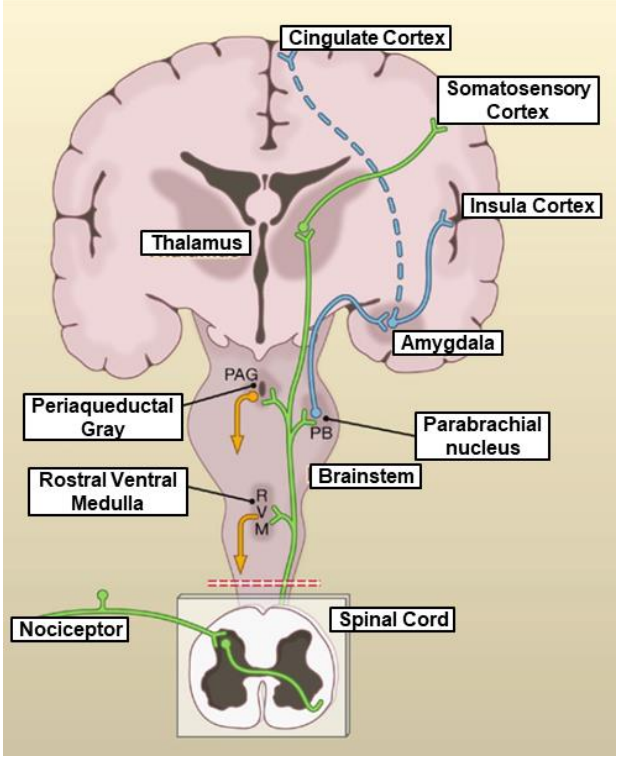

Figure 1.3 The lateral spinothalamic tract. *Nociceptors propagate noxious information from the periphery to the dorsal horn of the spinal cord (green pathway). Here, they synapse on to, and activate, second order projection neurons. Notably, the projection neurons decussate at the level of the spinal cord and access the contralateral lateral spinothalamic tract, before ascending to the ventral posterolateral nucleus of the thalamus. Information is then conveyed to the somatosensory cortices by third order neurons. Importantly, many of the projection neurons have collaterals which terminate within other central areas implicated in pain processing. Namely, the rostral ventral medulla and periaqueductal gray which are important for the descending inhibitory and facilitatory control of pain (orange arrows). Other collaterals project to the parabrachial nucleus and contribute to the emotional aspect of pain due to the subsequent activation of the amygdala and insula cortex (blue pathway). From Basbaum et al. (2009).*

Dissimilar to other the signalling tracts, the wide dynamic range neurons, the projection neurons, first decussate to the contralateral lateral spinothalamic tract, via the anterior white commissure of the spinal cord, before ascending to the thalamus. Specifically, upon reaching the thalamus, the projection neurons terminate within the ventral posterolateral nucleus of the thalamus where they synapse on to third order neurons. It is the third order neurons which are then responsible for transmitting sensory information to the higher cortical regions, such as the somatosensory cortices (Steeds, 2016). There is also evidence that within the spinothalamic tract, there are axon collaterals which project to other central structures involved in pain processing, such as the periaqueductal grey and the lateral brachial nucleus (Al-Khater and Todd, 2009).

1.1.2.2 Peripheral Sensitisation

1.1.2.2.1 Sensitisation of the peripheral terminal

It is changes that occur within the pain signalling pathway that lead to the chronification of pain. Peripheral sensitisation specifically refers to the increased excitability and reduced activation threshold of nociceptive neurons, within the peripheral nervous system (Julius and Basbaum, 2001). This is most commonly initiated by either nerve or

tissue damage which produces a local inflammatory response, resulting in the release of inflammatory mediators, including Adenosine triphosphate (ATP), histamine, bradykinin and nerve growth factor (NGF), as well as the recruitment of inflammatory cells (Okuse, 2007). The inflammatory mediators released bind to and directly activate the nociceptors (Amaya et al., 2013) whilst simultaneously stimulating the nociceptors to release their own subset of inflammatory mediators, including Substance P and Calcitonin gene-related peptide (CGRP) (Schaible et al., 2011). The additional release of inflammatory mediators from the nociceptors augments the local inflammation by promoting plasma extravasation and vasodilation. This process is referred to as neurogenic inflammation (Xanthos and Sandkühler, 2014).

Upon binding to nociceptive neurons, local inflammatory mediators promote the activation of intracellular signalling pathways that result in post-translational modifications being made to receptors and ion channels, such as phosphorylation, as well as increased gene expression and receptor trafficking (Bhave and Gereau IV, 2004). One of the best characterised targets of peripheral sensitisation is the capsaicin receptor, TRPV1 (transient receptor potential vanilloid receptor-1), which is specifically implicated in the development of thermal hyperalgesia (Huang et al., 2006). For example, it has been shown that NGF, a key component of the inflammatory soup, activates mitogen-activated protein (MAP) kinase signalling pathways in C-fibre nociceptors, resulting in increased trafficking of TRPV1 to the peripheral terminal (Ji et al., 2002). Meanwhile, other inflammatory mediators, for example, bradykinin, activate the Protein Kinase C (PKC) pathway which leads to the sensitisation of TRPV1 receptors already located at the plasma membrane, by increasing the probability of the channel opening, thus increasing the excitability of the neuron (Premkumar and Ahern, 2000; Huang et al., 2006).

Similar mechanisms have been demonstrated with respect to the ion channels. For example, prostaglandin E_2 (PGE_2) causes activation of the PKC and Protein Kinase A (PKA) kinases within the nociceptive afferents (Gold et al., 1998). The activation of these kinases results in an increased tetrodotoxin-resistant sodium current via the voltage gated sodium channels which precipitates in a decreased current threshold, required for neuronal firing (England et al., 1996; Gold et al., 1998). Additionally, the increased expression of sensory neuron specific tetrodotoxin-resistant PN3 sodium channel has been implicated in the development of mechanical allodynia and thermal hyperalgesia after injury in rat models of both neuropathic and inflammatory pain (Porreca et al., 1999)

Collectively, modifications made to receptors and ion channels, including their increased plasma membrane insertion, consequently impact the overall excitability of nociceptors. These changes in excitability correspond to the clinical features of chronic pain, such as

allodynia and hyperalgesia. The reduced activation threshold of nociceptors means that previously innocuous stimuli become sufficient to activate nociceptors, and thus, are now perceived to be noxious, analogous to allodynia. Conversely, the increased responsiveness of nociceptive neurons results in nociceptors eliciting a much larger neuronal response to a noxious stimuli, perceived as primary hyperalgesia, localised to the injury site (von Hehn et al., 2012). Additionally, if hyperexcitability develops in the neuron, then this can result in ectopic firing, associated with spontaneous pain attacks (von Hehn et al., 2012).

1.1.2.2.2 Recruitment of silent nociceptors

In addition to the increased excitability of neurons, peripheral sensitisation also features the recruitment of so called “silent nociceptors” (Gold and Gebhart, 2010). Silent nociceptors are insensitive to thermal and mechanical stimuli when in a non-pathological state and are estimated to account for nearly a quarter of all C-fibre nociceptors (Schmidt et al., 1995). After exposure to a chemical irritant, i.e. capsaicin or mustard oil, a proportion of these normally insensitive C-fibre nociceptors gain responsiveness to a sensory modality (Davis et al., 1993; Schmidt et al., 1995). Furthermore, within the population of C-fibre nociceptors already either exclusively mechano- or thermo-sensitive, a subset develop an additional sensory modality responsiveness to become mechano-heat-sensitive (Schmidt et al., 1995). Interestingly, Kress et al. (1992) reported a higher yield of recruited silent nociceptors after exposure to inflammatory mediators, compared with exposure to chemical irritation. This could be due to the physiological relevance of inflammatory mediators, compared to chemical irritants. Regardless, the activation of these previously unresponsive neurons act to increase the peripheral input and drive to the central synapse, providing spatial summation of the nociceptive signal (Kress et al., 1992; Schmidt et al., 1995).

1.1.2.3 Central Sensitisation

The enhanced activity of the peripheral nociceptive afferents, resulting from peripheral sensitisation, drives potentiation at the central synapse. This consequently augments the synaptic efficacy of the synapse which, in turn, causes increased excitability of the second order neurons in the central nervous system. The subsequent hyperexcitability of the pain signalling pathways, induced by the changes that occur within the central nervous system to amplify pain signalling, is thus referred to as central sensitisation.

This central mechanism for persistent pain was first realised by Woolf (1983). In the study, the flexor reflex withdrawal response, normally elicited to noxious stimuli, was measured in the α-motor neurons innervating the biceps femoris muscle in rats. Under normal physiological conditions, innocuous stimuli to the hindpaw did not produce a reflex response. Only with the application of noxious stimuli was the reflexive response observed. Conversely, after repeated application of a noxious heat source to the hindpaw that was of sufficient intensity to induce mild localised inflammation, innocuous stimuli were then able to elicit a reflex response from the motor neurons of the biceps femoris muscle. Additionally, an increased excitability and a reduced activation threshold was noted in the motor neurons, as well as an enlarged receptive field, and these changes persisted for several hours.

It was confirmed that the changes identified were due to a central mechanism after anaesthetic block, administered locally to the site of injury, failed to reverse the enlarged receptive fields of the motor neurons. This indicated that it could not be a peripherally-mediated mechanism otherwise the receptive fields would have immediately returned to their original size. Instead, it demonstrated that the enlarged fields were being centrally maintained. Furthermore, electrical stimulation of the low threshold Aβ- sensory neurons, normally irresponsive to noxious stimuli, caused the reflex to occur suggesting that Aβ-fibres were able to access the nociceptive pathway at the central level, again, implying a central mechanism. Additionally, the results could be replicated by low-frequency stimulation of the sural nerve, specifically at the frequency at which to activate C-fibre nociceptors. This stimulation again caused the reflexive response to be elicited by innocuous stimuli and provided evidence that it was the repeated activation of the C-fibre nociceptors that was driving plasticity within the central nervous system to enable nociceptive responses to Aβ-fibre stimulation. Woolf (1983) had inadvertently discovered the first evidence for long-term potentiation, a mechanism by which synaptic strength is increased and sustained over a period of time, in the dorsal horn.

1.1.2.3.1 Synaptic potentiation

The primary neurotransmitter used by sensory afferents is glutamate. Under normal physiological conditions, the amount of glutamate released is sufficient to cause post-synaptic depolarisation, however, it does not normally induce any long-term changes to the synapse. In contrast, in a pathological state were peripheral sensitisation has already been established, the nociceptors display an increased firing rate as well as an increased magnitude of action potentials. This consequently results in increased glutamate release at the central terminal, located in the dorsal horn, where the nociceptors synapse on to

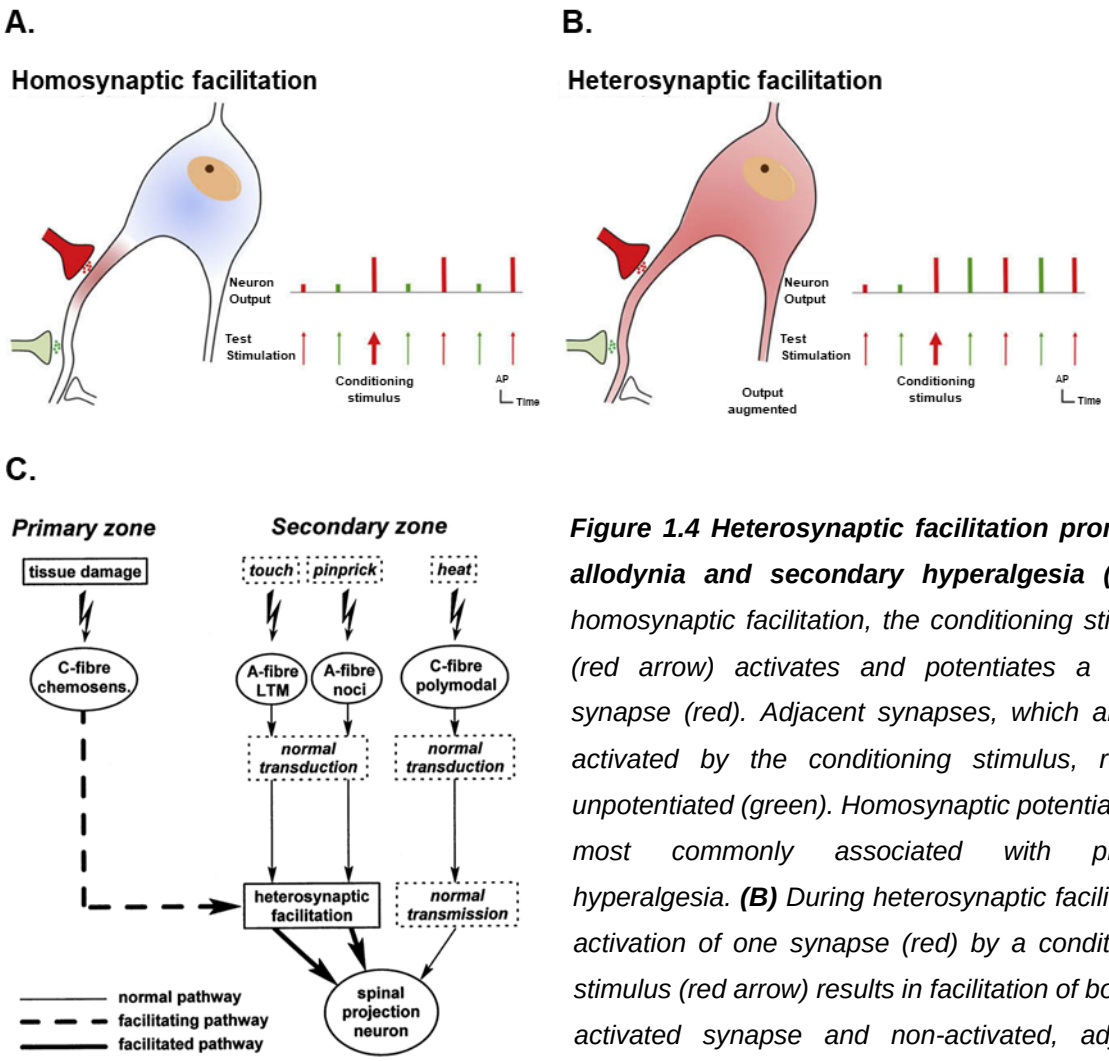

Figure 1.4 Heterosynaptic facilitation promotes allodynia and secondary hyperalgesia (A) *In homosynaptic facilitation, the conditioning stimulus (red arrow) activates and potentiates a single synapse (red). Adjacent synapses, which are not activated by the conditioning stimulus, remain unpotentiated (green). Homosynaptic potentiation is most commonly associated with primary hyperalgesia.* ***(B)*** *During heterosynaptic facilitation, activation of one synapse (red) by a conditioning stimulus (red arrow) results in facilitation of both the activated synapse and non-activated, adjacent synapse (green). Consequently, the synapse that did not receive the conditioning stimulus (green) displays augmented activity to subsequent stimulation (green bars in neuron output). From Latremoliere and Woolf (2009).* ***(C)*** *Heterosynaptic facilitation is initiated by the repeated or sustained activation of C-nociceptors at the site of injury and potentiates the synapses between the projection neurons and the Aβ low-threshold mechanoreceptors (LTM) and Aδ-nociceptors (A-fibre noci) that innervate the adjacent areas (secondary zone). Facilitation of the Aβ-fibre synapses produces noxious responses to innocuous touch (allodynia) whereas facilitation of Aδ-fibre synapses results in enhanced activation, following application of noxious stimuli (secondary mechanical hyperalgesia). C-fibres innervating the secondary zone do not display potentiation, hence explaining the absence of secondary thermal hyperalgesia. From Ziegler et al. (1999).*

both WDR projection neurons and interneurons. The increased glutamate release then produces a greater activation of amino-3-hydroxy-5-methyl-4-isoxazole propionate (AMPA) receptors to promote a much larger post-synaptic depolarisation. The simultaneous release of neuropeptides, such as Substance P and CGRP, can also contribute to this enhanced depolarisation. Consequently, the larger depolarisation leads to the removal of the voltage-dependent Mg^{2+} block from N-methyl-D-Aspartate (NMDA)

receptors which results in the influx of calcium into the neuron, as well as activating intracellular calcium stores to be released (Latremoliere and Woolf, 2009). The increase in cytosolic calcium initiates many intracellular signalling cascades, similar to peripheral sensitisation, mainly resulting in the activation of protein kinases (Basbaum et al., 2009).

One of the most well-characterised cellular targets of the activated signalling cascades is the AMPA receptors. Phosphorylation of AMPA receptors at the GluR1 subunit by PKC leads to their increased membrane insertion (Boehm et al., 2006) whilst phosphorylation of GluR1 by active CaMKII (Ca 2+ /calmodulin-dependent protein kinase II) converts AMPA receptors to a higher conductance state (Derkach et al., 1999). Likewise, activation of PKC has also been shown to induce the trafficking of NMDA receptors to the plasma membrane and to increase the frequency of channel opening (Lan et al., 2001). The increased availability of receptors, as well as their potentiated state, means that a larger post-synaptic current can generated by the same original level of stimulation, and consequently, a greater depolarisation of the neuron is observed. The synapse is thus regarded to be potentiated. The increased synaptic efficacy also means that the post-synaptic neuron can be activated by previously subthreshold stimuli and this attributes to the maintenance of the potentiation (Latremoliere and Woolf, 2009).

The mechanism described so far mainly refers to homosynaptic potentiation which is when synaptic efficacy is enhanced specifically in the conditioned synapse, meaning the synapse which receives and is being activated by the noxious conditioning stimulus (Fig 1.4A). Homosynaptic potentiation thus amplifies the signal being received directly from the activated peripheral afferent and therefore contributes to primary hyperalgesia, the exaggerated response to a noxious stimulus, applied to the site of injury (Ikeda et al., 2006). Heterosynaptic potentiation is more clinically relevant as it is responsible for the development of secondary hyperalgesia and allodynia, the additional pain phenotypes which cannot be fully accounted for by peripheral sensitisation (Fig 1.4C) (Woolf, 2011).

Heterosynaptic potentiation occurs when adjacent synapses, that are not activated by the conditioning stimulus, display altered synaptic efficacy such that subsequent activation of the unconditioned synapse results in an augmented postsynaptic response (Fig 1.4B). It has been suggested that diffusible nitric oxide, released from a synapse which has been facilitated by homosynaptic potentiation, could promote neurotransmitter release from locally situated synapses, that were not activated by the conditioning stimulus, to then induce potentiation (Jacoby et al., 2001). Allodynia specifically results from the heterosynaptic potentiation of the Aβ-fibre input to the dorsal horn projection neurons (Baba et al., 1999). Following heterosynaptic facilitation, information conveyed by the Aβ-fibres, regarding innocuous stimuli, now infiltrates and engages the nociceptive signalling pathways, due to the potentiation of the synapse. As a result, a

previously innocuous stimulus is therefore consequently perceived to be noxious. This phenomenon was observed by Woolf (1983) and has been replicated in subsequent studies (Thompson et al., 1993).

Conversely, it is the heterosynaptic potentiation of the central synapses of both Aβ- and Aδ-fibres, innervating the areas adjacent to the site of injury or inflammation, that is responsible for the development of secondary hyperalgesia (Ziegler et al., 1999; Magerl et al., 2001). Again, this potentiation relies upon the activation of C-fibre nociceptors to induce heterosynaptic facilitation at the central synapse of Aβ- and Aδ-fibres to dorsal horn second order neurons (Ziegler et al., 1999; Magerl et al., 2001). This has been demonstrated in human subjects whereby compression block of the A-fibres, confirmed by electrophysiological recordings, blocked the perception of secondary hyperalgesia, elicited by application of punctate mechanical stimuli, following intradermal injection of capsaicin (Ziegler et al., 1999; Magerl et al., 2001). Moreover, even when compression blockade of A-fibre conduction was performed, prior to the injection of capsaicin, and was then maintained for a period of time after capsaicin injection, mechanical secondary hyperalgesia was still perceived once the block was removed. This thus demonstrates that secondary hyperalgesia is still able to develop, despite the blockade of A-fibre volleys, and confirms that the development of secondary hyperalgesia relies upon the activation of C-fibre nociceptors at the immediate site of injury whose signalling remained intact throughout. It is the firing of these fibres that ensures that central changes are still induced and allows for these synaptic modifications to become effective once the A-fibre blockade is removed (Ziegler et al., 1999). This was further confirmed by the demonstration that anaesthetic block administered to the skin, prior to injection of capsaicin, and used to effectively block the firing of the C-fibres innervating the inflamed area, prevented the development of secondary hyperalgesia showing that it is C-fibre initiated (LaMotte et al., 1991).

Essentially, heterosynaptic facilitation results in the recruitment of subthreshold inputs by increasing the synaptic efficacy meaning that activity within these inputs is now sufficient to generate action potentials in second order neurons. This consequently manifests in the wide dynamic range neurons having enlarged receptive fields. They hence begin to respond to neurons that are either normally insufficiently activated by certain sensory modalities to elicit a response, or that innervate areas outside of the normal receptive field (Woolf and King, 1990; Latremoliere and Woolf, 2009).

1.1.2.3.2 Disinhibition within the dorsal horn

This understanding of central sensitisation has been expanded to not only acknowledge the contribution of synaptic potentiation as the sole cause of hyperexcitability in the pain signalling pathways, but now also incorporates the role of disinhibition within the dorsal horn. Disinhibition is specifically implicated in the presentation of allodynia and secondary hyperalgesia. The dorsal horn is densely populated by GABAergic and glycinergic inhibitory interneurons (Todd, 2017). When this inhibitory modulation is removed by application of GABA antagonists, an enhancement of A-fibre mediated excitation of the second order neurons in the superficial dorsal horn is observed (Baba et al., 2003). Reduced inhibitory neurotransmission is consistently demonstrated in models of nerve injury (Moore et al., 2002), alongside reports of apoptotic death of GABAergic inhibitory interneurons within the dorsal horn (Scholz et al., 2005). It was suggested that this apoptosis results from NMDA receptor-mediated excitotoxicity after MK-801, an NMDA antagonist, significantly reduced the number of apoptotic neurons (Scholz et al., 2005).

The death of inhibitory interneurons as the cause of reduced inhibitory modulation remains contentious as subsequent studies have failed to replicate this finding (Polgár et al., 2004). Instead, others have argued that although inhibition is decreased, specifically following nerve injury, the inhibitory circuitry remains intact, thus explaining why GABA analogues, such as pregabalin, are able to deliver analgesia in chronic pain conditions (Basbaum et al., 2009).

Similarly in inflammatory pain conditions, there is disinhibition of the dorsal horn neurons, however, it is instead associated with the loss of glycinergic inhibitory tone (Hösl et al., 2006). Following peripheral inflammation, PGE_2 is produced by cyclo-oxygenase enzymes within the spinal cord. Here, PGE_2 acts locally to cause the activation of the PGE_2 receptor subtype, EP2, which subsequently promotes activation of PKA (Reinold et al., 2005). Activated PKA then phosphorylates the glycine receptor subtype, GlyRα3, which consequently inhibits the activity of the receptor, thus disrupting glycinergic inhibition (Harvey et al., 2004). Mice lacking EP2 receptors displayed significantly reduced mechanical hyperalgesia compared to wild type mice following direct injection of, and induced production of, PGE_2 (Reinold et al., 2005). More impressively, mice lacking GlyRα3 receptor failed to develop any pain sensitivity after intrathecal injection of PGE_2 (Harvey et al., 2004). This mechanism of disinhibition is unique to chronic inflammatory pain and does not contribute to hyperalgesia developed following peripheral nerve injury (Hösl et al., 2006).

Regardless of the mechanism or cause of the disinhibition in the dorsal horn, the lack of inhibitory currents further augments the hyperexcitability observed in the pain signalling pathways, initiated by synaptic potentiation, by failing to inhibit the newly facilitated

inputs. The disinhibition of these circuits also contributes to the subsequent maintenance of the facilitated state as it fails to reverse the increased activity of the synapses and allows previously subthreshold inputs to continue to activate pain signalling pathways.

1.1.2.4 Alterations in the central processing of pain

In addition to the multiple changes to pain processing and signalling that have been described within the peripheral nervous system and the central spinal cord, altered pain processing has also been demonstrated in the central brain regions, most notably the "pain matrix". The "Pain Matrix" constitutes the areas of the brain involved in the processing and subjective experience of pain. These areas include, but are not limited to: the somatosensory cortices, the prefrontal cortices, the nucleus accumbens, the anterior cingulates cortex, the insula, the amygdala, the periaqueductal gray (PAG), the locus coerulus and the rostrovental medulla (Legrain et al., 2011).

Investigations of the pain matrix have highlighted altered activation patterns in chronic pain states. Functional neuroimaging techniques have specifically emphasised that there is increased activation of the anterior cingulate cortex, the insula and the prefrontal cortex observed in chronic pain patients (Tracey and Mantyh, 2007; Friebel et al., 2011). These brain regions all contribute to the emotional element of pain. Furthermore, structural MRI scans have consistently revealed reduced gray matter volume within the brains of chronic pain patients, compared to healthy controls. The most frequently affected areas are the anterior cingulate cortex, the insula and the dorsal pons, all of which are brain regions implicated in the pain matrix (May, 2008). Comparatively, cortical reorganisation has also been demonstrated specifically within the motor representation of body regions affected by chronic pain (Moxon et al., 2014; Nurmikko et al., 2016). Although, historically motor cortex reorganisation has been associated almost exclusively with phantom limb pain (Karl et al., 2001), more recent studies have shown that this reorganisation is apparent across multiple pain conditions, for example, in trigeminal neuropathy (Nurmikko et al., 2016).

Additional supraspinal mechanisms for the development and maintenance of chronic pain are attributed to the loss of inhibition and increased facilitation within the descending modulatory pathways, originating from the PAG and rostral ventromedial medulla (RVM) (Vanegas and Schaible, 2004). Reduced sensitivity to opioids has been identified in the PAG and the thalamus within a chronic constriction injury neuropathic pain model in mice (Hoot et al., 2011). Responsiveness to opioids is required for the activation of the PAG to stimulate descending inhibitory pathways within the RVM (Park et al., 2010). Notably, silencing the descending inhibition from the RVM by local application of lidocaine has

been shown to precipitate allodynia in wildtype rats (De Felice et al., 2011). The RVM also exhibits a descending facilitatory function, whereby it is able to augment and facilitate pain signalling in the spinal cord. In appreciation of this function, administrating lidocaine to the RVM in allodynic rats, following spinal nerve ligation, reversed allodynia (De Felice et al., 2011). This emphasises how an imbalance in the activity of the inhibitory and facilitatory pathways, originating from the RVM, can occur in chronic pain and thus can be implicated in its maintenance (Porreca et al., 2002; Vanegas and Schaible, 2004).

1.2 Botulinum Neurotoxin in chronic pain

The mechanisms of peripheral and central sensitisation, discussed above, both heavily rely upon SNARE (Soluble N-ethylmaleimide-sensitive factor Attachment Protein Receptor) dependent exocytosis. Primarily, SNARE-mediated exocytosis is required for the release of neurotransmitters and neuropeptides (Welch et al., 2000; Lisman et al., 2007; Dolly and O'Connell, 2012). Moreover, SNARE-mediated exocytosis is also necessary for the membrane insertion of receptors, implicated in the establishment of persistent pain, most notably TRPV1, AMPA and NMDA receptors (Lan et al., 2001; Lu et al., 2001; Morenilla-Palao et al., 2004).

Botulinum neurotoxin (BoNT) inhibits SNARE-mediated exocytosis by cleaving specific SNARE- proteins, dependent on the serotype, to thus prevent the formation of SNARE-complexes and the subsequent fusion of the vesicular and plasma membranes (Montecucco et al., 2005). Consequently, BoNT provides a tool by which to block the SNARE-dependent neurotransmitter release and membrane insertion of receptors that occurs during the induction and maintenance of chronic pain.

1.2.1 The structure of Botulinum Neurotoxin

Botulinum neurotoxin (BoNT) is produced by anaerobic *Clostridium botulinum* bacteria and exists in seven distinct serotypes, BoNT/A-G (Davletov et al., 2005). All botulinum neurotoxin serotypes are synthesised as a single polypeptide which is then cleaved by either bacterial or host cell proteases to form a heavy and a light chain. The two chains are linked by a disulphide bond, providing the characteristic multidomain protein structure (Fig 1.5A). Once cleaved, BoNT exists in its active form (Montecucco, 1994).

A.

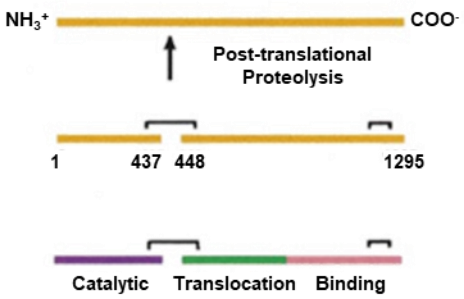

B.

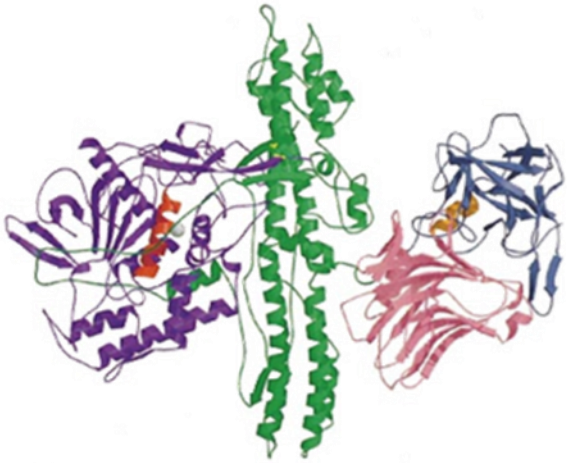

C.

```
   1 MPFVNKQFNY KDPVNGVDIA YIKIPNVGQM QPVKAFKIHN KIWVIPERDT FTNPEEGDLN
  61 PPPEAKQVPV SYYDSTYLST DNEKDNYLKG VTKLFERIYS TDLGRMLLTS IVRGIPFWGG
 121 STIDTELKVI DTNCINVIQP DGSYRSEELN LVIIGPSADI IQFECKSFGH EVLNLTRNGY
 181 GSTQYIRFSP DFTFGFEESL EVDTNPLLGA GKFATDPAVT LAHELIHAGH RLYGIAINPN
 241 RVFKVNTNAY YEMSGLEVSF EELRTFGGHD AKFIDSLQEN EFRLYYYNKF KDIASTLNKA
 301 KSIVGTTASL QYMKNVFKEK YLLSEDTSGK FSVDKLKFDK LYKMLTEIYT EDNFVKFFKV
 361 LNRKTYLNFD KAVFKINIVP KVNYTIYDGF NLRNTNLAAN FNGQNTEINN MNFTKLKNFT
 421 GLFEFYKLLC VRGIITSKTK SLDKGYNKAL NDLCIKVNNW DLFFSPSEDN FTNDLNKGEE
 481 ITSDTNIEAA EENISLDLIQ QYYLTFNFDN EPENISIENL SSDIIGQLEL MPNIERFPNG
 541 KKYELDKYTM FHYLRAQEFE HGKSRIALTN SVNEALLNPS RVYTFFSSDY VKKVNKATEA
 601 AMFLGWVEQL VYDFTDETSE VSTTDKIADI TIIIPYIGPA LNIGNMLYKD DFVGALIFSG
 661 AVILLEFIPE IAIPVLGTFA LVSYIANKVL TVQTIDNALS KRNEKWDEVY KYIVTNWLAK
 721 VNTQIDLIRK KMKEALENQA EATKAIINYQ YNQYTEEEKN NINFNIDDLS SKLNESINKA
 781 MININKFLNQ CSVSYLMNSM IPYGVKRLED FDASLKDALL KYIYDNRGTL IGQVDRLKDK
 841 VNNTLSTDIP FQLSKYVDNQ RLLSTFTEYI KNIINTSILN LRYESNHLID LSRYASKINI
 901 GSKVNFDPID KNQIQLFNLE SSKIEVILKN AIVYNSMYEN FSTSFWIRIP KYFNSISLNN
 961 EYTIINCMEN NSGWKVSLNY GEIIWTLQDT QEIKQRVVFK YSQMINISDY INRWIFVTIT
1021 NNRLNNSKIY INGRLIDQKP ISNLGNIHAS NNIMFKLDGC RDTHRYIWIK YFNLFDKELN
1081 EKEIKDLYDN QSNSGILKDF WGDYLQYDKP YYMLNLYDPN KYVDVNNVGI RGYMYLKGPR
1141 GSVMTTNIYL NSSLYRGTKF IIKKYASGNK DNIVRNNDRV YINVVVKNKE YRLATNASQA
1201 GVEKILSALE IPDVGNLSQV VVMKSKNDQG ITNKCKMNLQ DNNGNDIGFI GFHQFNNIAK
1261 LVASNWYNRQ IERSSRTLGC SWEFIPVDDG WGERPL
```

Figure 1.5 The 3D structure and amino acid sequence of Botulinum Neurotoxin A. (A) *BoNT/A is expressed as an inactive single polypeptide. Post-translational proteolysis leads to the formation of the disulphide bond between the light and heavy chain, producing the active dichain. The black brackets indicate where a disulphide bond exists. Noticeably, there is another disulphide bond present in the receptor binding domain.* ***(B)*** *A backbone trace of the 3D structure of BoNT/A illustrates the catalytic domain (purple), featuring a zinc ion (white sphere) and zinc-binding motif (red), required for the zinc-endopeptidase activity. The central pair of α-helices (green) indicate the translocation domain. The N-terminal of the receptor binding domain (pink) is assumed to aid the function of the c-terminal subdomain (blue) which contains the ganglioside binding site (orange) and mediates receptor binding. From Lacy and Stevens (1999).* ***(C)*** *The amino acid sequence of BoNT/A, determined by Thompson et al. (1990), delineates the catalytic domain (purple), translocation domain (green) and receptor binding domain (pink). The sequence contains 8 cysteines (C), 4 of which contribute to the disulphide bonds shown in* ***(A).***

All seven botulinum neurotoxin serotypes share a molecular mass of 150 kDa. This mass is split across the heavy chain (HC, Mr ~100 kDA), comprising both the receptor binding domain (Rbd, Mr ~50 kDa) and the translocation domain (Td, Mr ~50 kDa), and the light chain (Lc, Mr ~50 kDa), which contains the zinc-endopeptidase activity, necessary for the cleavage of SNARE-proteins (Schiavo et al., 2000) (Fig. 1.5B).

1.2.2 Mechanism of action

The Rbd, contained within the heavy chain, provides the neuron specific binding associated with the BoNTs. The majority of the serotypes, namely BoNT/A, -B, -E, -F and -G, utilise a dual receptor binding mechanism whereby the Rbd selectively binds to a protein receptor and a complex ganglioside, found on the membrane of neurons (Fig. 1.6A) (Rummel, 2012). In contrast, it has been demonstrated that BoNT/C and BoNT/D do not require a protein receptor and instead only bind to either gangliosides or phospholipids (Tsukamoto et al., 2005). The different serotypes bind to distinct complex gangliosides, enriched in neuronal membranes (Montal, 2010). The exact combination of protein receptors and gangliosides bound is dependent on the serotype and is discussed more in-depth in chapter 4.1.

The dual receptor binding of surface receptors and gangliosides, specifically, produces high affinity binding that allows BoNT to undergo receptor-mediated endocytosis and be internalised into cells (Fig 1.6B) (Montecucco, 1994). Once the holotoxin is captured inside the endosome, the acidic environment induces a pH-dependent conformational change to the Td, such that the Td inserts itself into the endosomal membrane, forming a channel that allows the Lc to translocate into the cytosol (Fig 1.6C). Concomitantly, the Lc unfolds from its globular structure which enables it to translocate through the narrow channel, produced by the insertion of Td (Koriazova and Montal, 2003). The Td thus acts a chaperone to allow the endosomal escape of the Lc, and additionally stabilises the Lc in its unfolded inactive state, during translocation (Fischer et al., 2008; Pirazzini et al., 2011).

Following endosomal escape, reduction of the disulphide bond, connecting the HC and the Lc, occurs (Fischer and Montal, 2007). It has been hypothesised that this reduction is performed by thioredoxin reductase-thioredoxin, located on the cytosolic surface of the endosomes (Pirazzini et al., 2014). The reduction of the disulphide bond results in the cytosolic release of the Lc. Subsequently, the return of the Lc to the neutral pH of the cytosol induces the refolding of the Lc to its active form (Montal, 2010).

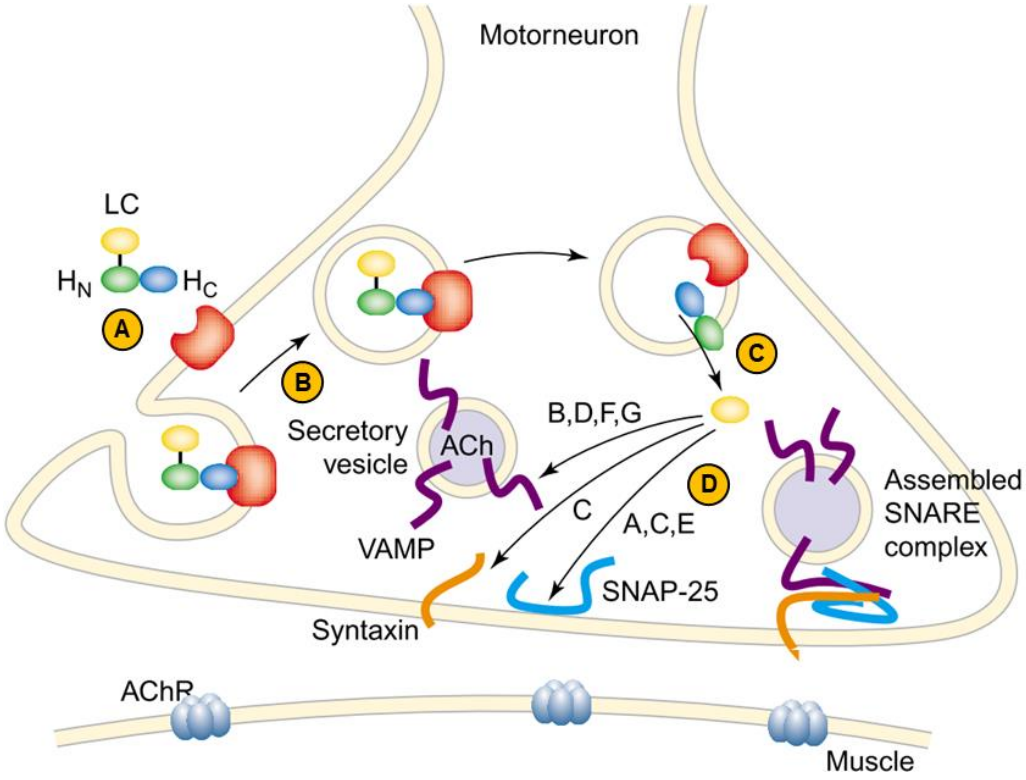

Figure 1.6 Schematic depicting the mechanism of action of Botulinum Neurotoxin (BoNT) at the neuromuscular junction. (A) *The BoNT receptor binding domain (Hc, blue) binds to the relevant gangliosides and protein receptors located on the presynaptic membrane.* ***(B)*** *This initiates receptor-mediated internalisation of BoNT into vesicles.* ***(C)*** *The ATPase pump, located on the vesicle membrane, generates an acidic environment. This induces a conformational change to promote the insertion of the translocation domain (HN, green) into the vesicular membrane, thus allowing the light chain (LC, yellow) to translocate across the membrane, into the cytosol, where reduction of the disulphide bond occurs.* ***(D)*** *The LC then diffuses through the cytosol to cleaves its SNARE-protein target, via its zinc-endopeptidase activity. The SNARE target varies dependent on the BoNT serotype. BoNT/A and -/E cleave SNAP-25 whilst BoNT/ B, -/D, -/F and -/G cleave VAMP (synaptobrevin). BoNT/C cleaves both syntaxin and SNAP-25. The cleavage of SNARE proteins prevents the formation of the SNARE-complex and prevents exocytosis of acetylcholine (ACh). Consequently, acetylcholine receptors (AChR) located on muscle fibres are no longer activated, producing flaccid paralysis. From Turton et al. (2002).*

Once returned to its active form, the Lc is able to mediate the proteolytic cleavage of SNARE-proteins via its intrinsic zinc-endopeptidase activity (Fig 1.6D). The specific SNARE-target is determined by the BoNT serotype. BoNT/A and -/E both cleave SNAP-25 (Synaptosomal associated protein 25) whereas BoNT/B, -/D, -/F and -/G cleave synaptobrevin, also referred to as vesicle-associated membrane protein (VAMP). In contrast, BoNT/C has two SNARE-targets as it cleaves both syntaxin and SNAP-25 (Davletov et al., 2005).

Intact SNARE proteins are necessary for vesicle fusion at the neuronal plasma membrane, which is essential for the release of neurotransmitter (Söllner et al., 1993). The action of BoNTS is historically associated with the blockade of neurotransmitter release from cholinergic presynaptic terminals, situated at the neuromuscular junction (Simpson, 1981). In this instance, cleavage of the SNARE proteins prevents vesicle fusion thus preventing the release of acetylcholine. This blockade of cholinergic neurotransmission consequently results in the failure to initiate muscle contraction and therefore produces the clinical manifestation of flaccid paralysis (Turton et al., 2002). BoNTs are, however, known to inhibit the release of other neurotransmitters and neuropeptides due to the fundamental role of SNARE-proteins in all release mechanisms (Purkiss et al., 2000; Welch et al., 2000; Cui et al., 2004; Durham et al., 2004).

1.2.3 Clinical evidence for the antinociceptive effect of BoNT/A

In addition to targeting different SNARE proteins, the seven BoNT serotypes also vary in their duration of action and their potency (Aoki and Guyer, 2001). Specifically, Botulinum Neurotoxin A (BoNT/A) has the longest duration of action of the seven serotypes and consequently, has been the serotype most frequently utilised for clinical applications (Foran et al., 2003). Notably, it is BoNT/A, specifically, that has been approved for the clinical management of chronic migraine (Dodick et al., 2010). Consequently, the use of BoNT/A in other pain chronic conditions is now being pursued (Drinovac et al., 2013). The most clinical and preclinical literature therefore exists with respect to BoNT/A, compared to the other serotypes (Pickett, 2010; Matak and Lacković, 2014). Accordingly, there has been a much more thorough investigation of its mechanism of action and a more comprehensive understanding reached. For the purposes of this project, the introduction will now mainly focus on discussing BoNT/A for the reasons detailed above.

The potential analgesic effect of BoNT was first recognised in conditions characterised by excessive muscle contractions and neuromuscular hyperexcitability. Treatment of conditions such as cervical and axial dystonia with BoNT/A effectively reduces the frequency and intensity of involuntary muscle contractions whilst concomitantly reducing the pain experienced in these disorders. In one study by Jankovic et al. (1990), 90% of patients with cervical dystonia reported significant global improvement in their condition, encompassing both spasms and pain. Furthermore, 93% of cervical dystonia patients who reported pain as a feature of their cervical dystonia described a marked reduction. On average, patients rated their pain as almost completely resolved, as indicated by an average pain response of 3.5 with 0 representing no improvement and 4 representing a complete resolution of pain. Likewise, Brin et al. (1987) demonstrated that 64% of

patients suffering cervical dystonia benefited from local injection of BoNT/A, reporting improved motor symptoms. A further 74% of these patients similarly described significantly reduced pain. Additionally, a study focused on the treatment of lower-limb spasticity in children with cerebral palsy, using BoNT/A, found that all 26 patients included in the study demonstrated significantly reduced pain according to pain scores collected at 3 months post-treatment (Lundy et al., 2009).

It was primarily assumed that the marked reduction in pain observed in spasticity disorders related to the paralytic properties of BoNT/A. Excessive muscle contractions can cause compression of the local blood vessels resulting in ischemia of the supplied tissue. Ischemia initiates an inflammatory response that includes the release of inflammatory mediators which, as detailed earlier, results in the activation and sensitisation of peripheral nociceptors (Mense, 2004; Pickett, 2010). Similarly, adenosine-5-triphosphate, released from cells suffering ischemic damage, will activate and sensitise neurons expressing the P2X purinoceptor 3 (P2X3) (Cook and McCleskey, 2002). Additionally, ischemia can also lead to a decrease in pH which can cause acid-sensing ion channels to activate and can eventually sensitise chemical-responsive nociceptors (Mense, 2004; Pickett, 2010).

Contrary to this explanation, however, there is evidence that the analgesic effect of BoNT/A exists beyond its muscle relaxant properties. For example, pain relief can persist after normal muscle contractility has returned. Freund and Schwartz (2003) showed that although the onset of muscle relaxation and analgesia occurred concurrently following intramuscular injection of BoNT/A to the masseter and temporalis muscles in temporomandibular disorder, the pain relief experienced continued after bite force, the measure of muscle contractility, returned to, and even surpassed, basal values. Conversely, in another study, Relja and Klepac (2002) observed significant pain relief in patients with cervical dystonia after injection of doses as low as 50 U BoNT/A, and as early as one week post-treatment. Improvement in spasticity, however, was only revealed two weeks post-treatment and, furthermore, required higher dosages, 100 and 150 U BoNT/A, to be observed. Notably, BoNT is more commonly measured in units when used in a clinical setting. A unit of BoNT refers to the median lethal dose (LD50) following intraperitoneal administration and is determined using a standardised mouse lethality assay (Dressler et al., 2012). One Unit is roughly equivalent to 28 pg of BoNT/A (Frevert, 2010).

Moreover, pain relief has been described in conditions with little or no association with muscular hyperactivity, for example, in chronic migraine, where BoNT/A is FDA-approved for clinical use (Dodick et al., 2010). This has led to further investigation of the possible applications of BoNT/A in other chronic pain conditions, namely in neuropathic

pain. Attal et al. (2016) conducted a randomised, placebo-controlled, multicentre clinical trial investigating the efficacy of BoNT/A in peripheral neuropathic pain, primarily resulting from either trauma or surgery. Patients were asked to rate their pain according to an 11-point numerical rating scale, 0 meaning no pain to 10 meaning maximum pain imaginable. Attal et al. (2016) reported an average pain reduction of almost 30% following two separate administrations of BoNT/A subcutaneous injections to the painful area, 12 weeks apart. Impressively, 50% of patients receiving BoNT/A treatment were deemed to be responders, meaning that they experienced an average pain reduction of greater than 50%. Interestingly, the severity of allodynia, as assessed using quantitative sensory testing, was the best predictor of whether a patient would be a responder. Brush evoked allodynia was significantly reduced by treatment with BoNT/A compared to placebo. Attal et al. (2016) reported that there was no effect of BoNT/A on normal sensation, similarly assessed using quantitative sensory testing (QST).

This observation of unaltered sensation, combined with the anti-allodynic effect of BoNT/A observed, has some important implications for the potential mechanism of action for BoNT/A in neuropathic pain. The lack of effect against normal sensation suggests that BoNT/A cannot be acting at the peripheral nerve terminals. If this was the case, one might expect to observe hypoesthesia, a reduction in normal sensation, resulting from reduced activation by stimuli. As described earlier, allodynia results from central sensitisation whereby normal activation of Aβ-fibres begins to initiate activity in pain signalling pathways, via changes that occur at the central synapse (Baba et al., 1999). This therefore implies that BoNT/A must be acting within the central spinal cord to somehow interrupt this signalling.

In contrast, a systematic review regarding the pharmacological management of neuropathic pain, conducted by the same research group a year earlier, highlighted that subcutaneous injection of BoNT/A should be only used as a third line option for the management of neuropathic pain (Finnerup et al., 2015). They advised that BoNT/A is particularly applicable for use in peripheral neuropathies that are predicted to result from a peripheral insult. Finnerup et al. (2015) did, however, specify that the conclusion of BoNT/A's efficacy was based on, and limited by, the low number of randomised controlled trials conducted, as well as their small sample size. These studies did, nevertheless, consistently report a therapeutic effect of BoNT/A. Additionally, Finnerup et al. (2015) included a larger, unpublished study in the meta-analysis that, in contrast to the small studies, reported no analgesic effect of BoNT/A in neuropathic pain. The size of this study relative to the others thus greatly impacted the overall perceived efficacy of BoNT/A. This led the research group to conduct their own clinical trial, detailed above, in

which they demonstrated a clear therapeutic effect, thus supporting the overall effectiveness of BoNT/A in neuropathic pain (Attal et al., 2016).

Such clinical observations verify that BoNT has analgesic properties, separate from its actions as a muscle relaxant. This has led to the hypothesis that BoNT/A may act directly at nociceptors. The preclinical evidence supporting this hypothesis will now be discussed.

1.2.4 Pre-clinical evidence for BoNT/A's analgesic effect

Preclinical investigations of the anti-nociceptive effect of BoNT/A in chronic migraine were able to elucidate a direct action at the nociceptors. Importantly, it is the meningeal afferents, a subpopulation of trigeminal neurons, that receive and propagate sensory information from the dura mater, where headaches and migraine are believed to originate, to the trigeminal nucleus caudalis (Melin et al., 2017). Incubation of cultured trigeminal ganglion neurons with BoNT/A did not affect the basal release of CGRP, however, significantly reduced CGRP release evoked by stimulation with potassium, as well as the chemical irritant, capsaicin (Durham et al., 2004). This effect was observed at clinically relevant doses of BoNT/A and after incubations as short as 3 hours.

Additional evidence for a direct effect of BoNT/A at the meningeal afferents is provided by the reduced trafficking of TRPV1 receptors noted in the trigeminal neurons after administration of BoNT/A (Shimizu et al., 2012). Notably, increased trafficking and membrane insertion of TRPV1 receptors is specifically implicated in the peripheral sensitisation of nociceptors (Ji et al., 2002). Following subcutaneous injection of BoNT/A to rats, reduced immunoreactivity for TRPV1 was observed at the soma and the nerve terminals of trigeminal ganglion neurons. It was shown that this was not due to decreased receptor expression, but instead resulted from decreased trafficking of TRPV1 receptors to the membrane. The reduced trafficking consequently rendered receptors to the cytosol where they were increasingly vulnerable to proteolytic degradation by the proteasome, thus explaining the perceived reduction in immunoreactivity (Shimizu et al., 2012).

Both studies highlight potential mechanisms by which BoNT/A could be mediating its analgesic effect in chronic migraine, predominantly showing that BoNT/A specifically acts by preventing modifications that occur during sensitisation. Accordingly, other preclinical studies have replicated these findings and recognised similar mechanisms in other pain conditions and in vitro models. It is believed that the pathophysiology of pain conditions arising from injury or insult to the trigeminal and dorsal root ganglion neurons is shared (Dolly and O'Connell, 2012). Consequently, any elucidated mechanisms for the analgesic action of BoNT/A in chronic migraine should be equally applicable to pain

conditions originating from distal peripheral sites that are instead innervated by DRG neurons.

This hypothesis appears to be valid. When added to DRG cultures, it was demonstrated that BoNT/A inhibited calcium-dependent release of substance P in response to both capsaicin and potassium stimulation, similar to the reduction of evoked-CGRP release observed in trigeminal ganglion cultures (Purkiss et al., 2000; Welch et al., 2000). Substance P and CGRP are both neuropeptides that are released from the central terminal of sensory afferents and contribute to central sensitisation (Basbaum et al., 2009). Notably, mice who lack the gene for either substance P or the substance P receptor, NK1, fail to display BoNT/A-mediated analgesia when subjected to inflammatory or neuropathic pain (Matak et al., 2017).

Moreover, comparable to Shimizu et al. (2012), Xiao et al. (2013) reported reduced immunoreactivity for TRPV1 receptors in the DRG, following intraplantar injection of BoNT/A in a rat neuropathic pain model. In the latter study, however, this was attributed to the reduced expression of TRPV1 receptors. Nevertheless, it has been repeatedly shown that BoNT/A does not alter the expression of TRPV1 but does impact its trafficking, mainly by interfering with PKC-induced translocation of TRPV1 receptors to the plasma membrane (Morenilla-Palao et al., 2004; Shimizu et al., 2012). It is thus likely that the reduced immunoreactivity, recognised by Xiao et al. (2013), was misinterpreted as reduced expression of TRPV1, but instead resulted from increased degradation of TRPV1 receptors, secondary to reduced receptor trafficking (Shimizu et al., 2012).

The effects so far described are largely confined to the primary nociceptive afferents, i.e. the trafficking of receptors to the peripheral terminal and the release of neuropeptides at the central terminal. Both changes are, however, integral to peripheral and central sensitisation which underlie the induction and maintenance of chronic pain conditions. It is therefore hypothesised that BoNT/A prevents the development of hyperexcitability in the pain signalling pathways, rather than simply blocking neurotransmission in nociceptive neurons, as might be expected given its silencing effects within the motor neurons. This hence explains why BoNT/A does not alter sensory thresholds or acute nociception in non-pathological states (Ji et al., 2002; Cui et al., 2004; Bach-Rojecky and Lacković, 2005, 2009; Attal et al., 2016).

The lack of effectiveness of BoNT/A against acute nociception is well demonstrated by the application of BoNT/A in the formalin model of inflammatory pain. Intraplantar injection of BoNT/A to rats, prior to formalin challenge, is ineffective against the first phase of inflammation, however, significantly reduces pain behaviour during the second phase (Cui et al., 2004). The first phase of inflammation represents the direct chemical

activation of nociceptors, immediately after injury, thus showing that BoNT/A does not block neurotransmission in the peripheral nociceptors. In contrast, the second phase reflects the hyperexcitability of the pain signalling pathways, resulting from peripheral and central sensitisation, indicating a more sustained pain state. Again, this illustrates that BoNT/A is acting to prevent the changes that induce sensitisation. The observed reduction in pain behaviour during the second phase corresponds to an inhibition of glutamate release from the peripheral afferents (Cui et al., 2004). Glutamatergic neurotransmission is essential for central sensitisation, thus emphasising that BoNT/A prevents the pain signalling necessary for the establishment of persistent pain, rather than affecting acute pain nociception (Woolf & Thompson, 1991).

This study again highlights the effectiveness of BoNT/A against mechanisms of sensitisation, specifically those initiated within the primary afferents. It does not, however, specify whether BoNT/A is most efficacious at preventing modifications which occur at the peripheral or central terminal of sensory afferents. There is now, however, a significant amount of literature gathered from in vivo studies, that places a greater emphasis on the effectiveness of BoNT/A against changes that occur at the central terminal, rather than at the peripheral terminal.

BoNT/A has been shown to produce analgesia in a number of animal models for a range of chronic pain conditions, including: inflammatory pain (Cui et al., 2004; Matak et al., 2017), orofacial pain (Matak et al., 2011), trigeminal neuropathy (Filipović et al., 2012), trigeminal neuralgia (Wu et al., 2016), muscle hyperalgesia “mirror pain” (Bach-Rojecky and Lacković, 2009; Drinovac et al., 2016), peripheral neuropathy (Bach-Rojecky et al., 2010; Marinelli et al., 2012; Drinovac et al., 2013; Matak et al., 2017), cancer tumour pain (Olbrich et al., 2017) and chemotherapy-induced peripheral neuropathy (Favre-Guilmard et al., 2009). In a number of these studies, intraneural injection of colchicine, an axonal transport blocker, consistently abolished the analgesia observed after peripheral injection of BoNT/A (Bach-Rojecky and Lacković, 2009; Matak et al., 2011; Filipović et al., 2012; Wu et al., 2016). This consequently indicates that axonal transport of BoNT/A to the central nervous system is essential for it to mediate its analgesic effect and suggests that the perceived analgesia does not result from the actions of BoNT/A at the peripheral terminal.

Further to this, it has been suggested that transcytosis of BoNT/A into second order neurons might contribute to its perceived analgesic effect. This hypothesis has mainly arisen after the observation of bilateral analgesia in global pain conditions, namely DPN and chemotherapy-induced peripheral neuropathy, following unilateral peripheral injection of BoNT/A (Favre-Guilmard et al., 2009; Bach-Rojecky et al., 2010). Accordingly, immunohistochemical studies have confirmed transcytosis of BoNT/A

(Antonucci et al., 2008; Restani et al., 2011). In one study, cleaved SNAP25 was produced in the tectum of rats following intravitreal injection of BoNT/A (Restani et al., 2011). Within the tectum, cleaved SNAP25 was not present in the terminals of the retinal ganglion cells but was instead detected in the adjacent structures, thus implying that cleaved SNAP25 was contained within the terminals of the second order tectal cells (Restani et al., 2011). The appearance of cleaved SNAP25 was prevented by injection of colchicine, highlighting that cleavage was due to the axonal transport of BoNT/A, and not via systemic diffusion, whilst an additional experiment confirmed that it was the active protease that undergoes axonal transport, and not the cleavage product (Restani et al., 2011).

In support of these claims, cleaved SNAP25, the cleavage product of BoNT/A, has been detected at the level of the lumbar spinal cord, following intraplantar injection of BoNT/A. Specifically, cleaved SNAP25 was visible in the ipsilateral ventral horn, surrounding the motor neurons, and in single nerve fibres, labelled in the ipsilateral dorsal horn (Matak et al., 2011, 2012; Drinovac et al., 2016). This demonstrates that the axonal transport of BoNT/A, and possibly the transcytosis, might also occur within the motor system and is likely to not be exclusively observed in the visual system.

Behavioural studies have also elucidated how BoNT/A might interact with inhibitory networks, thus contributing to the theory of its centrally-mediated analgesic effect. GABA-mediated inhibition was implicated in the anti-nociceptive effect of BoNT/A after intraperitoneal injection of GABA-A receptor antagonist, bicuculline, reversed the BoNT/A-associated analgesia in a formalin-induced inflammatory pain model and in a partial sciatic nerve transection neuropathic pain model (Drinovac et al., 2014). Importantly, in this study, as well as in a consequent study, intraplantar, intraperitoneal and intrathecal injection of bicuculline all successfully prevented the BoNT/A-induced anti-nociceptive effect, however, intracisternal injection of bicuculline, used to gain access to the brain regions where the descending inhibitory pathways originate from, did not (Drinovac et al., 2014, 2016). It was thus concluded that BoNT/A alters GABAergic transmission at the level of the spinal cord, and not supraspinally, in chronic pain conditions.

It has, however, been documented that intrathecal administration of antagonists to GABAergic and glycinergic receptors does precipitate a pain phenotype, akin to that observed following peripheral injury, most notably featuring tactile allodynia (Sivilotti and Woolf, 1994; Malan et al., 2002; Drew et al., 2004; Basbaum et al., 2009). Given that this assumed interaction between BoNT/A and the GABAergic network is solely based on the use of bicuculline, and provided that the pronociceptive effect of bicuculline is so pronounced even in naïve animals, it is possible that bicuculline could be acting

separately, away from interfering with the mechanism by which BoNT/A mediates allodynia, to still induce a pain phenotype.

There is, however, evidence to suggest that BoNT/A also influences the endogenous opioid system, present within the spinal cord (Drinovac et al., 2013, 2016). The activation of opioid receptors is an important mechanism by which inhibition is again initiated within the spinal cord (Dickenson, 1995). Injection of non-specific opioid receptor antagonist, naltrexone, prior to behavioural testing, prevented the observed anti-nociceptive effect of BoNT/A in both formalin-induced inflammatory pain and the partial sciatic nerve transection model of neuropathic pain (Drinovac et al., 2013). Moreover, injection of the selective μ-opioid receptor antagonist, naloxonazine, inhibited BoNT/A-induced analgesia in formalin-induced inflammatory pain and in carrageenan-induced mirror pain, hence emphasising the predominant involvement of μ-opioid receptors (Drinovac et al., 2016). This is not surprising given that μ-receptors represent 70% of the opioid receptors, present in the dorsal horn (Dickenson, 1995). Finally, similar to that demonstrated with bicuculline, a central action, specifically confined to the level of the spinal cord, was confirmed after intrathecal injection effectively abolished the analgesic effect in carrageenan-induced mirror pain whereas intercerebroventricular injection of naloxonazine failed to prevent the perceived analgesia (Drinovac et al., 2016). This again highlights a potential link between BoNT/A-mediated analgesia and the inhibitory networks of the spinal cord. It subsequently generates a more convincing argument of how BoNT/A might correct this disinhibition, characteristic of pain conditions.

In contrast to the neuron-specific actions so far described, some studies have suggested that BoNT/A might somehow interact with non-neuronal inflammatory cells to elicit an anti-inflammatory effect. Cleaved SNAP25 has been detected colocalised with markers of astrocytes and microglia following intraplantar injection of BoNT/A to mice (Marinelli et al., 2012). Another study demonstrated, using western blot, that intraplantar injection of BoNT/A to rats prevented the upregulation of pro-inflammatory interleukins, important to microglia activation, however, no immunohistochemical staining was either conducted or eluded to in order to confirm the colocalisation of cleaved SNAP25 with microglia (Zychowska et al., 2016). Similarly, it was highlighted that intraplantar injection of BoNT/A can reduce astrocyte expression and activation at the spinal cord of rats (Vacca et al., 2012). Again, although this study used immunohistochemistry to quantify the expression and activation of astrocytes, it did not investigate the colocalisation with cleaved SNAP25.

Interestingly, this inflammatory theory remains contentious as many studies have failed to detect any colocalisation between cleaved SNAP25, indicative of BoNT/A activity, and inflammatory cells, for example, astrocytes (Restani et al., 2011; Matak et al., 2012; Cai

et al., 2017). This is not unexpected given that astrocytes and other glial cells are known to express SNAP23, which is resistant to BoNT/A cleavage, rather than the neuronal SNAP25 (Hepp et al., 1999). It is thus logical to assume that any anti-inflammatory effect associated with BoNT/A, is most likely due to an indirect effect, resulting from the reduced neurotransmitter and neuropeptide release at the afferent terminals. This would then consequently prevent the recruitment and activation of inflammatory cells.

1.2.5 Protein engineering to optimise BoNT/A's anti-nociceptive activity

Despite the discrepancy on whether the actions of BoNT/A responsible for its anti-nociceptive effect are restricted to the primary afferents, or whether it does transcytosis into second order neurons of the spinal cord, the studies detailed above clearly and consistently demonstrate that BoNT/A does have an important action within the nociceptive pathway. All of these findings are, however, based on the use of BoNT/A in its native form whereby it is still able to access and block neurotransmission at the neuromuscular junction and, therefore, retains its paralytic activity. This thus limits the dosage of BoNT/A which can be safely used to induce analgesia without eliciting a paralytic effect. Reengineering techniques seek to remove the paralytic activity of BoNT/A and redirect its binding specifically to sensory neurons. In theory, this can be effectively achieved by replacing the Rbd of BoNT/A with an alternative targeting molecule, which displays greater affinity and specificity for subpopulations of sensory neurons, selective to pain pathways.

One method by which this is achievable is recombinant protein expression. This technique has been used to express a novel protein by fusing the gene that encodes BoNT/A, purposely excluding the gene section which encodes the C-terminal of the Rbd and that constitutes the ganglioside-binding pocket, with a gene encoding a single-chain variable fragment antibody against P2X purinoceptor 3 (P2X3), a receptor specific to nociceptive neurons (Ma et al., 2014). Accordingly, the protein produced specifically bound to cultured DRG neurons expressing P2X3. Cleaved SNAP-25 was successfully detected in DRG cultures after exposure to 0.1 nM of the chimera. Furthermore, the percentage of SNAP25 cleaved correlated with the degree of inhibition of CGRP release from treated DRG cultures, compared to untreated cultures. This indicates that the recombinant protein was successfully internalised via the intended target and retained BoNT/A's endopeptidase activity to provide a functional pain-specific outcome. Additionally, the reengineered protein displayed a 2×10^8 greater LD50 than native BoNT/A, indicating a much improved safety profile (Ma et al., 2014).

Recombinant expression is limited by the size of protein that can be produced, alongside additional issues with protein misfolding (Rosano and Ceccarelli, 2014). An alternative method for protein engineering is chemical conjugation. This method was previously used to conjugate LcTd/A to a lectin isolated from Erythrina cristagalli (ECL), after it was established that the lectin specifically bound gangliosides found on nociceptive neurons (Duggan et al., 2002). In this case, a protein cross-linking reagent was used to introduce reactive sulphydryl groups to both LcTd/A and ECL to enable the formation of a disulphide bond between the two components. The novel protein was able to internalise into neurons, and subsequently inhibited both substance P and glutamate release from embryonic DRG cultures. Additional in vivo lumbar recordings, following intrathecal injection, revealed that the LcTd/A-ECL conjugate reduced C-fibre responses by 75.8% and Aδ-fibre activity by 42.3% at the injection site, while Aβ-fibre responses were unaffected, highlighting selectivity for pain pathways (Duggan et al., 2002). Notably, however, neither of the two studies so far described attempted to assess the analgesic effect of the respective chimeras in behavioural pain models (Drew et al., 2004; Ma et al., 2014). It is therefore unknown whether their efficacy translates in vivo.

Another popular method of chemical conjugation is maleimide conjugation. This method was used by a separate group to conjugate the light chain of BoNT/A (Lc/A) to Substance P, thus deliberately excluding both the Rbd and the translocation domain of BoNT/A from the construct (Mustafa et al., 2013). The novel chimera was reportedly internalised by cultured diencephalon neurons and retained the ability to cleave SNAP25. This finding is surprising given that the translocation domain is required for the endosomal release of the Lc (Koriazova and Montal, 2003). It consequently suggests that the Lc can reach the cytosol unaided, and therefore, negates the importance of the translocation domain. Unconjugated Lc/A failed to internalise into cells, however, thus emphasising that a targeting domain is required for internalisation. Additionally, intracisternal injection of the Lc/A-Substance P construct significantly reversed thermal hypersensitivity in mice subjected to the paclitaxel-induced peripheral neuropathy model, compared to vehicle (Mustafa et al., 2013). Although not definitely shown, this implies that Lc/A-Substance P remained functional in vivo and indicates that the ability of Lc to access the cytosol, in the absence of the translocation domain, is not an artefact of culture.

Unfortunately, although maleimide conjugation produces uncleavable bonds, there are concerns about the long-term stability of the chimeras generated, specifically when subjected to blood plasma (Christie et al., 2015). Chemical reactions, such as thiol exchange, can promote instability in chimeras and are also capable of affecting the efficacy of the therapeutic unit of the chimera, even within a stable chimera. This issue

has even been recognised to affect certain FDA-approved maleimide conjugated drugs (Fontaine et al., 2015).

1.2.5.1 SNARE-stapling for protein engineering

The limitations associated with the current methods of recombinant protein expression and chemical conjugation have encouraged others to establish novel methods by which to achieve protein reengineering. Our own research group developed a 'stapling' technology which combines and exploits the two platforms of protein engineering, recombinant and protein conjugation, whilst acting within their limitations to overcome the issues so far described (Darios et al., 2010).

For this technique, individual functional protein domains are tagged with short SNARE-peptides, namely synaptobrevin and SNAP25, using recombinant protein expression (Darios et al., 2010; Ferrari et al., 2012). Since only single subunits are being expressed at one time, the protein size of the individual subunits remains within the constraints of recombinant protein expression. Once successfully expressed with the fused SNARE-tags, the individual subunits can then be assembled into a single multidomain protein by the addition of the SNARE-staple, syntaxin. The SNARE-peptides assemble into an irreversible, correctly orientated, tetrahelical complex, known as the SNARE-complex (Fig 1.7A). This assembly occurs within an hour at room temperature. Specifically, the assembly of the SNARE-complex does not require a chemical reaction and therefore is not susceptible to other reactive groups. The resultant complex is resistant to harsh detergents, including Sodium dodecyl sulphate (SDS), and therefore the assembled chimera can be detected by SDS-page gel (Fig 1.7B) (Darios et al., 2010). Additionally, this method enables a combinatorial approach to protein engineering. When all of the subunits of interest have been expressed with the relevant SNARE-tags, numerous combinations of distinct subunits can be produced which can then be tested to identify the optimum combination for a given function or outcome (Darios et al., 2010; Ferrari et al., 2012).

1.2.5.1.1 TetBot

This stapling method has so far been used to produce two novel chimeras that have both demonstrated analgesic properties in behavioural pain models. One of the chimeras, TetBot, was produced by conjugating the LcTd/A, expressed with the fused SNAP25 tag, to the Rbd of tetanus toxin, fused to the synaptobrevin tag, by addition of the syntaxin staple (Fig 1.7A) (Ferrari et al., 2013). Native Tetanus toxin undergoes retrograde

A.

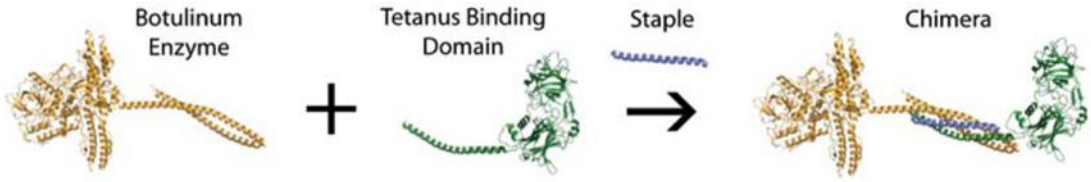

B.

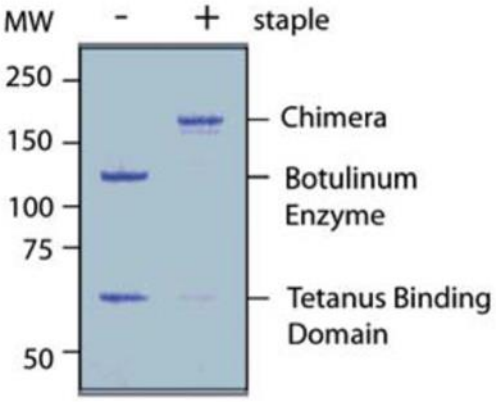

Figure 1.7 The modular assembly of botulinum neurotoxin A- tetanus toxin chimera by SNARE-tagging. ***(A)*** *The schematic illustrates the conjugation of LcTd/A, fused to SNAP25 (Botulinum Enzyme), to the tetanus binding domain (Tbd), fused to synaptobrevin, by addition of a staple, syntaxin. Central to the chimera (right), the tetrahelical SNARE-complex can be seen.* ***(B)*** *The coomassie-stained SDS-page gel shows that the conjugation reaction only occurs in presence of the staple and is successful at producing an irreversible, SDS-page resistant product. From Ferrari et al. (2013).*

transport to the spinal cord to elicit spastic paralysis (Surana et al., 2017). TetBot was therefore generated with the intention of targeting the active domain of BoNT/A to central neurons, whilst attempting to exclude its normal paralytic activity.

The introduction of the SNARE-complex into the centre of the chimera produced an elongated protein of approximately 23 nm which is almost double the length of native BoNT/A (Ferrari et al., 2013). When applied to isolated mouse hemidiaphragm muscles, TetBot was shown to be 11000 less effective at blocking muscle twitches than native BoNT/A. Impressively, intramuscular injection of 500 ng TetBot to mice did not produce any signs of motor paralysis and was not associated with any lethality. Consequently, it can be confirmed that TetBot displays a LD50 that is at least 10^5 fold greater than the LD50 of native BoNT/A. It has therefore been inferred that the chimera has restricted access to the neuromuscular junction (NMJ), resulting from the increased size of the protein combined with the tight synaptic cleft and ensheathing, characteristic of the NMJ (Ferrari et al., 2011).

TetBot was applied to hippocampal neuron cultures to examine its efficacy at central neurons. TetBot was imaged internalised into the synaptic terminals of hippocampal neurons and was shown, by western blot, to successfully cleave SNAP25 and thus retained the catalytic activity of BoNT/A (Ferrari et al., 2013). Furthermore, brain slices

containing the suprachiasmatic nucleus displayed significantly reduced circadian rhythms following incubation with TetBot, indicating a functional effect.

After confirming the lack of paralysis and retained functionality of the chimera, TetBot was trialled in the complete Freund's adjuvant (CFA)-induced inflammatory pain model. 100 ng TetBot was injected intrathecally to rats prior to induction of the pain model. TetBot did not influence basal mechanical sensitivity, however, significantly attenuated the mechanical hypersensitivity developed after intraplantar injection of CFA (Ferrari et al., 2013). Importantly, this analgesic effect was still apparent at 11 days post-CFA when the experiment was terminated, emphasising a long-lasting effect. Again, the analgesia occurred in the absence of any motor impairment.

In the experiments detailed, TetBot was administered directly to the target neurons. For example, intrathecal injection was used when targeting the central neurons of the spinal cord in the CFA-induced inflammatory pain model. This delivery method would have therefore provided direct access to the target neurons. Consequently, the experimental conditions did not attempt to exploit the axonal transport, associated with Tetanus toxin, although this was the original aim. Ideally, TetBot should have been injected to a peripheral site to investigate whether it would then undergo retrograde transport to penetrate the central neurons. Additionally, the vast majority of humans are immunised against tetanus toxin, and consequently, TetBot would most likely not be suitable for use in human medical care (Maple et al., 2000). Instead, TetBot would be most applicable for pain management in animals.

1.2.5.1.2 BiTox

The other chimera generated was BiTox which is an elongated version of native BoNT/A (Ferrari et al., 2011). BiTox was again constructed from the LcTd/A fused to the SNAP25 SNARE-peptide tag. The fused-subunit was then conjugated to the Rbd of BoNT/A, tagged with synaptobrevin, by addition of the SNARE-staple, syntaxin. This once more led to the formation of a truncated SNARE-complex within the chimera, which hence significantly increased the length of the protein. Accordingly, BiTox demonstrated reduced potency at blocking neurotransmission at the NMJ, similar to TetBot. Specifically, 75 minute incubation with 190 pM BiTox was required to reduce the amplitude of contractile responses in mouse hemidiaphragm preparations by 50% (Darios et al., 2010). By contrast, it has been separately shown that 2 pM of native BoNT/A was sufficient to reduce the amplitude of muscle twitches in hemidiaphragm preparations by 50%, within the same time allowance (Ferrari et al., 2013). This again

highlights that the paralytic activity of BoNT/A is greatly impaired by the SNARE-stapling approach.

Correspondingly, BiTox demonstrated greatly reduced lethality compared to native BoNT/A. Lethality with native BoNT/A was observed within 24 hours in mice after intraperitoneal injection of doses as low as 2 ng/kg (Ferrari et al., 2011). In contrast, mice receiving intraperitoneal injection of up to 200 ng/kg BiTox did not display any indication of muscular paralysis or compromised well-being. Again, this reveals an increased safety profile, associated with the reengineered proteins.

Subsequent in vitro investigations confirmed the functionality of BiTox. Specifically, incubation of isolated brain synaptosomes with BiTox inhibited both calcium-dependent and potassium-evoked glutamate release (Darios et al., 2010). The impairment of glutamate release was equivalent to that observed following incubation with BoNT/A, therefore emphasising that BiTox is as efficacious as native BoNT/A at blocking neurotransmission and neuronal function of central neurons. The compromised efficacy of BiTox is instead exclusive to the encapsulated NMJs.

The selectivity of BiTox for silencing other neuronal populations in preference to the motor neurons, in addition to its improved safety profile, encouraged the antinociceptive potential of BiTox to be assessed. Similar to native BoNT/A, intraplantar injection of BiTox did not affect basal mechanical or thermal sensory thresholds in naïve rats (Mangione et al., 2016). 200 ng BiTox administered via intraplantar injection, 1 day after pain model induction, produced only a partial and transient recovery of the basal mechanical withdrawal threshold in both CFA-induced inflammatory pain and the plantar incision post-operative pain model, compared to vehicle control.

By contrast, in a subsequent experiment, CFA was instead injected into the ankle joint, rather than intraplantar, while the mechanical withdrawal threshold continued to be measured at the plantar surface of the ipsilateral hindpaw. Under these conditions, intraplantar injection of BiTox 3 days after CFA-injection, significantly reduced mechanical hypersensitivity. Likewise, intraplantar injection of BiTox, prior to exposure to capsaicin, failed to alter primary thermal hyperalgesia, localised to the capsaicin injection site. Injection of BiTox did, however, effectively reduce secondary mechanical hyperalgesia in the adjacent area on the plantar surface of the hindpaw. The study did not, however, measure mechanical primary hyperalgesia following capsaicin injection. It is therefore not clear from this experiment whether BiTox is more effective against the sensory modality, i.e. thermal or mechanical pain, or the site of hyperalgesia, primary or secondary. Mechanical threshold was, however, assessed in both CFA-models and this, therefore, consequently implies that BiTox exhibits an effectiveness specifically against

secondary hyperalgesia, highlighting a potential action against central sensitisation (Mangione et al., 2016).

Separately, when intraplantar injection of 200 ng BiTox was administered 3 days post-spared nerve injury (SNI), a model of peripheral neuropathic pain, a significant reversal of the developed mechanical hypersensitivity was observed whereby the mechanical threshold returned to basal values. In contrast, vehicle-injected SNI rats continued to develop further mechanical hypersensitivity. Additionally, intraplantar injection of BiTox, 14 days prior to SNI, greatly attenuated the development of mechanical hypersensitivity. Notably, only a marginal decrease in mechanical threshold from basal values was detected in BiTox-injected rats, compared to vehicle injected rats (Mangione et al., 2016).

Mechanical hypersensitivity in neuropathic pain, likewise, results from central sensitisation (Nickel et al., 2012). Collectively, it suggests that, similar to native BoNT/A, BiTox might produce its analgesic effect predominantly via a centrally-mediated mechanism. In agreement with this, a delay in the analgesic effect following intraplantar injection of BiTox was consistently noted hence suggesting that this time might be necessary to allow for the axonal transport of the chimera. Opposingly, however, western blot analysis failed to reveal cleaved SNAP25 at the level of the dorsal horn in BiTox-injected animals (Mangione et al., 2016). Furthermore, evidence was provided for a peripheral mechanism after reduced capsaicin-induced plasma extravasation was observed in the BiTox-injected hindpaw compared to the uninjected contralateral paw (Mangione et al., 2016). A direct action at A-nociceptors was also suggested after mechanical, but not thermal hypersensitivity, was reduced, as thermal nociception is communicated by C-fibre nociceptors (Mangione et al., 2016). As a result of the conflicting evidence, it is currently unclear how BiTox mediates its analgesic effect and subsequently still remains to be clarified.

1.3 Hypotheses and Aims

Chronic pain represents a huge unmet clinical need. Whilst no chronic pain-specific pharmacotherapy exists, and while the aging population proceeds to grow, chronic pain will continue to place massive strain on both present and future healthcare services, as well as imposing ever-increasing pressure on the economy. In order to resolve this issue, it is important that therapeutics specifically intended for use in chronic pain conditions are developed. Between them, the studies described here illustrate how chemical and recombinant protein engineering methods can be utilised to design chimeras that incorporate the potent BoNT/A, in order to provide novel analgesics.

Within these studies, several important aims have already been achieved. Novel chimeras have repeatedly been demonstrated to effectively retain the catalytic activity of BoNT/A, via the detection of cleaved SNAP25 (Mustafa et al., 2013; Ma et al., 2014). Furthermore, the novel chimeras have displayed functionality by inhibiting pain mediator release from cultured neurons, and by producing analgesia in behavioural pain models (Duggan et al., 2002; Mustafa et al., 2013; Ma et al., 2014). Specifically, the chimeras generated using the pioneered SNARE-stapling technique exhibited reduced potency at the neuromuscular junction, thus circumventing the motor paralysis and lethality associated with BoNT/A, whilst simultaneously continuing to provide long-lasting pain relief (Ferrari et al., 2013; Mangione et al., 2016). It is essential that the mechanisms of action of these chimeras begin to be understood. From this perspective, Chapter 3 will focus on elucidating the in vivo activity of BiTox/A, the most successful chimera so far produced using the SNARE-stapling technology.

It is also important that novel chimeras continue to be developed. This is required in order to assess whether alternative combinatorial chimeric designs are more effective at producing analgesia in other pain conditions or are more efficacious at treating certain clinical presentations of chronic pain, e.g. thermal versus mechanical hypersensitivity. By maintaining the inclusion of LcTd/A, the future resultant chimeras will persist to cleave SNAP25 in neurons, and consequently block SNARE-mediated cellular processes. However, by combining LcTd/A with alternative targeting domains, using the combinatorial approach, possible with the SNARE-stapling technology, the catalytic activity of BoNT/A can be retargeted to separate subpopulations of sensory neurons.

Based on the distinct combinations of gangliosides and protein receptors bound by the alternative BoNT serotypes, it is hypothesised that the Rbd of the respective serotypes, conjugated to LcTd/A, will retarget the catalytic activity to distinct populations of sensory neurons, whilst continuing to avoid action at the NMJ (Chapter 4). The in vitro binding profile of BiTox, henceforth referred to as BiTox/A, due to the inclusion of Rbd/A, will thus be assessed and then compared to the binding profile of chimeras composed of the alternative BoNT Rbds, to investigate whether they do exhibit preferential binding to distinct sensory neuron subpopulations and whether this consequently conveys an alternate therapeutic effect in vivo. There is also the possibility of utilising the binding domains of unrelated toxins, such as cholera toxin. This will be investigated using the same technique in Chapter 6.

Additionally, a potential alternative clinical application for chimeras, separate from the management of chronic pain, will be explored (Chapter 5). Axonal transport to the central terminal of neurons has been either demonstrated or suggested for both native and re-engineered clostridial neurotoxins (Bach-Rojecky and Lacković, 2009; Mangione et al.,

2016; Matak et al., 2017), however, it is already known and accepted that tetanus toxin does undergo retrograde transport to reach the inhibitory interneurons, located in the spinal cord (Surana et al., 2017). It will therefore be investigated whether the binding domain of tetanus toxin can be exploited for the drug delivery of therapeutics to the central nervous system, as a proof of principle experiment, and whether optimisation and advancement of the SNARE-stapling method can augment this delivery. Furthermore, cholera toxin is similarly able to undergo axonal transport and therefore is well-established as a neuronal tracer (Angelucci et al., 1996). For this reason, the use of cholera toxin binding domain for drug delivery will also be examined.

The ultimate objective of this thesis does, however, remain the development of a novel pain therapeutic for use in chronic pain conditions. This will again be the investigated in Chapter 6, subsequent to findings made in Chapter 5, regarding a novel chimera constructed from the binding domain of cholera toxin conjugated to LcTd/A. In Chapter 6, the analgesic potential of the novel chimera, which utilises the binding domain of a non-clostridial toxin, will be determined.

Collectively, this thesis will demonstrate how the SNARE-stapling conjugation approach allows for the production of safe, long-lasting, non-paralytic analgesics, with the potential for use in human pain management.

Chapter 2. General Methods

2.1 Materials

2.1.1 Chimeras

All the chimeras and proteins that were used for either treating cell cultures or that were injected into animals are listed in the table below:

Table 2.1 *Details of chimeras used.*

Proteins and Chimeras	Enzymatic domain	Receptor binding domain	Source	Reference
BiTox/A	LcTd/A	Rbd/A	Recombinant (Expressed and purified by Dr Charlotte Leese)	(Ferrari et al., 2011; Mangione et al., 2016)
BiTox/C	LcTd/A	Rbd/C	Recombinant (Expressed and purified by Dr Charlotte Leese)	
BiTox/D	LcTd/A	Rbd/D	Recombinant (Expressed and purified by Dr Charlotte Leese)	
BiTox/E	LcTd/A	Rbd/E	Recombinant (Expressed and purified by Dr Charlotte Leese)	
ChoBot	LcTd/A	AB5	Recombinant (Expressed and purified by Dr Charlotte Leese)	
Cholera Toxin Subunit B Alexa Fluor 488	-	CTB	Recombinant (Purchased from ThermoFisher, Product No. C34775)	(Conte et al., 2009)
Tbd-Cy3	-	Tbd	Recombinant (Expressed and purified by Dr Charlotte Leese)	(Mavlyutov et al., 2016)
2xTbd-Cy3	-	2xTbd	Recombinant (Expressed and purified by Dr Charlotte Leese)	
TetBot	LcTd/A	Tbd	Recombinant (Expressed and purified by Dr Charlotte Leese)	(Ferrari et al., 2013)
2xTetBot	LcTd/A	2x Tbd	Recombinant (Expressed and purified by Dr Charlotte Leese)	

2.1.2 Antibodies

Below is a table documenting all the primary antibodies used for immunocytochemistry, immunohistochemistry and western blot.

Table 2.2 *Details of all primary antibodies used including the relevant dilutions used for Immunocytochemistry (ICC), Immunohistochemistry (IHC) and Western Blot (WB).*

Primary antibody	Abbreviation	Species raised in	Dilution	Catalogue number	Source
βIII-Tubulin	BTIII	Mouse	1:500 (ICC/IHC)	MAB1195	R&D systems
Calcitonin gene-related peptide	CGRP	Mouse	1:200 (IHC)	ab81887	Abcam
Cholera toxin B subunit	CTB	Rabbit	1:10000 (IHC)	C3062	Sigma
Cleaved SNAP25	cSNAP25	Rabbit	1:1500 (ICC) 1:2000 (IHC/WB)		In-house
Neurofilament 200	NF200	Mouse	1:400 (ICC) 1:200 (IHC)		In-house
Neuronal Nuclei (clone A60)	NeuN	Mouse	1:1000 (IHC)	MAB377	Merck Millipore
Peripherin	Peripherin	Mouse	1:200 (ICC)	MAB1527	Merck Millipore
SNAP25	SNAP25	Mouse	1:1000 (IHC)	SMI 81	Biolegend
SNAP25	SNAP25	Rabbit	1:3000 (WB)		In-house
Syntaxin 1	Syn1	Rabbit	1:2000 (WB)		In-house

The specificity of the in-house anti-cleaved SNAP25 antibody has been repeatedly verified within the laboratory (Fig. 2.1). Similarly, the inhouse anti-Neurofilament 200 antibody has been validated by Dr Ciara Doran who demonstrated that immunolabelling produced by the inhouse antibody colocalised to that produced by a commercial anti-Neurofilament 200 antibody (data not shown).

All secondary antibodies used for immunocytochemistry, immunohistochemistry and western blot are listed in the table below:

Table 2.3 *Details of all secondary antibodies used including the relevant dilutions used for Immunocytochemistry (ICC), Immunohistochemistry (IHC) and Western Blot (WB).*

Secondary antibody	Species raised in	Dilution	Catalogue number	Source
Anti-mouse IgG (H+L) Cross-adsorbed Alexa Fluor 488	Goat	1:2000 (ICC) 1:500 (IHC)	A11029	Life Technologies
Anti-rabbit IgG (H+L) Cross adsorbed Alexa Fluor 488	Goat	1:2000 (ICC) 1:500 (IHC)	A11034	Life Technologies
Anti-mouse IgG (H+L) Cross adsorbed Alexa Fluor 594	Goat	1:2000 (ICC) 1:500 (IHC)	A11005	Life Technologies
Anti-rabbit IgG (H+L) Cross adsorbed Alexa Fluor 594	Goat	1:2000 (ICC) 1:500 (IHC)	A11012	Life Technologies
Anti-rabbit IgG HRP linked	Donkey	1:24000 (WB)	NA934V	Amersham

A protein conjugate was also used for immunohistochemistry. Its details are documented in the table below.

Table 2.4 *Details of the protein conjugate used.*

Protein Conjugates	Abbreviation	Dilution	Catalogue Number	Source
α-Bungarotoxin Alexa Fluor 488 Conjugate	α-BTX-488	1:250 (IHC)	B13422	ThermoFisher

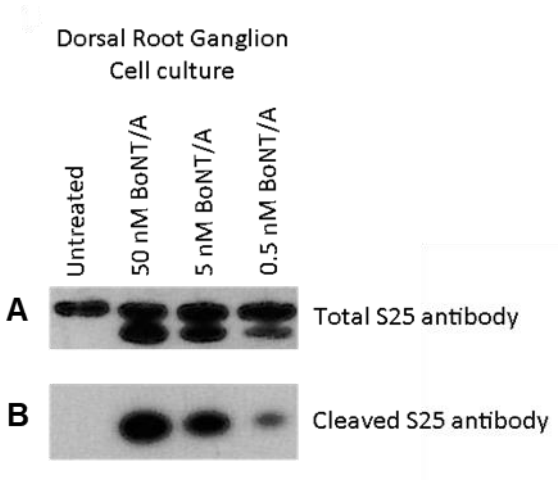

Figure 2.1 The anti-cleaved SNAP25 antibody is specific for the BoNT/A-cleavage product. (A) *Western blot analysis of dissociated dorsal root ganglion cultures, incubated with multiple concentrations of Botulinum neurotoxin A (BoNT/A), display dose-dependent cleavage of SNAP25. When the western blot is probed with the total SNAP25 antibody, immunoreactive to both whole, uncleaved SNAP25 and cleaved SNAP25, two bands are detected in each lane of the treated cultures. The top band represents full length, uncleaved SNAP25 whilst the bottom band represents the shorter, BoNT/A-cleavage product. Accordingly, only one band is detected in the untreated sample, representing whole SNAP25 and indicating that no cleavage of SNAP25 has occurred.* ***(B)*** *In contrast, probing using the specific anti-cleaved SNAP25 antibody reveals only one band. Thus, highlighting the specificity of the antibody for the BoNT/A-cleavage product and the lack of immunoreactivity for whole SNAP25. Resultantly, no band is detected in the untreated sample. Data provided courtesy of Dr C. Leese.*

2.1.3 Media and solutions used

All medias used are detailed in the table below, alongside their composition.

Table 2.5 *Details of the medias used.*

Media	Components
DRG wash media	DMEM/F12 with Glutamax (31331, Life Technologies), 10% heat-inactivated Horse serum (26050, Life Technologies) and 1% penicillin-streptomycin (P0781, Sigma)
DRG low-serum media	Neurobasal A medium (10888, Life Technologies), 1% heat-inactivated Horse serum (26050, Life Technologies), 1% penicillin-streptomycin (P0781, Sigma), 20 ng/ml NGFβ (SRP4304, Sigma), 1x B27 (17504-044, Life Technologies), 1% Glutamax (35050-061, Life Technologies) 20 µM uridine (U3003, Sigma), 20 µM 5'-Fluoro-2'-deoxyuridine (F0503, Sigma).
Cortical neuron media	Neurobasal medium (21103, Life Technologies), 1% penicillin-streptomycin (P0781, Sigma), 1x B27 (17504-044, Life Technologies), 1% Glutamax (35050-061, Life Technologies)

All solutions used are documented in the table below, alongside their composition.

Table 2.6 *Details of the solutions used.*

Solution	Composition
Blocking solution for Immunohistochemistry	5% (v/v) Goat serum (005-000-121, Jackson ImmunoResearch Laboratories, Inc), 0.3% (v/v) Triton X-100 (BP151-500, Fisher BioReagents) in 1x PBS.
Blocking solution for Western Blot	5% (w/v) Skim milk powder (70166, Sigma), 0.1% (v/v) Tween 20 (B337-500, Fisher BioReagents) in 1x PBS.
15% Bovine Serum Albumin	15% (w/v), DMEM/F12 with Glutamax (31331, Life Technologies), 10% heat-inactivated Horse serum (26050, Life Technologies) and 1% penicillin-streptomycin (P0781, Sigma).
DRG Lysis Buffer	50 mM HEPES, 150 mM NaCl, 1 mM EDTA, 1.5 mM $MgCl_2$, 10% glycerol, 1% Triton-X100 and 1:40 protease inhibitor in deionised water (Gift from Dr M. A. Nassar's Lab).
70% Ethanol	70% (v/v) Ethanol (20821.330, VWR Chemicals) in deionised water.
HEPES-buffered dissociation solution (pH 7.3)	1 mg/ml Dispase II (D4693, 0.85 U/mg, Sigma), 0.6 mg/ml Collagenase XI (C7657,1594 U/mg Sigma) in 155 mM NaCl (S/3160/60, Fisher Scientific), 4.8 mM HEPES sodium salt (H8651,Sigma), 5.6 mM HEPES (B299-500, Fisher BioReagents), 1.5 mM KH_2PO_4 (P/5240/53, Fisher Scientific) and 10 mM D-(+)-Glucose (G7528, Sigma) in deionised water.
Laminin	10 µg/ml laminin (L2020, Sigma), Sterile PBS
Membrane Transfer Buffer	20% (v/v) methanol and 10% (v/v) 10x transfer buffer (Fluka) in deionised water.
MES SDS running buffer	5% (v/v) 20x NuPAGE MES SDS running buffer (Life Technologies) in deionised water.
4% Paraformaldehyde (pH 7.4)	4% (w/v) Paraformealdehyde (A11313, Alfa Aesar and 158127, Sigma) in 1x PBS.

Solution	Composition
1x Phosphate-Buffered saline (PBS)	10% (v/v) 10x Phosphate-Buffered saline (1.37 M Sodium chloride, 0.027 M Potassium Chloride and 0.119 M Phosphate buffer) (BP399-20, Fisher Scientific) in deionised water (pH 7.4).
4x SDS Lysis Buffer	224 mM SDS, 250 mM Tris-HCl pH 6.8, 6.4 mM EDTA, 25% (v/v) glycerol, 1 mM $MgCl_2$ (223210010, ACROS organics) and 0.1 % (v/v) Benzonase nuclease (E1014-2KU, Sigma) and traces of bromophenol blue (BDH Chemical) in deionised water.
5% Sucrose	5% (w/v) sucrose (S/8600/53, Fisher Scientific) in 1x PBS.
30% Sucrose	30% (w/v) sucrose (S/8600/53, Fisher Scientific) in 1x PBS.
0.3% Triton in PBS	0.3% (v/v) Triton X-100 (BP151-500, Fisher Bioreagents) in 1x PBS.
0.1% Tween in PBS	0.1% (v/v) Tween 20 (B337-500, Fisher BioReagents) in 1x PBS.
Working solution for immunohistochemistry	2% (v/v) Goat serum (005-000-121, Jackson ImmunoResearch Laboratories, Inc), 0.3% (v/v) Triton X-100 (BP151-500, Fisher BioReagents) in PBS.

2.2 Dorsal Root Ganglion Culture

2.2.1 Coating plates

µClear 96-well plates (655090, Greiner Bio-One) were used for imaging experiments. 96-well plates were coated with 40 µl per well of 10 µg/ml laminin in PBS and left for 1 hour at 37 ^{o}C. Alternatively, for western blot experiments using dissociated dorsal root ganglion cultures, 24-well plates (3526, Costar) were used. 120 µl of 10 µg/ml laminin was added per well and again plates were then left for 1 hour at 37 ^{o}C. After 1 hour, the laminin solution was aspirated from the wells and the wells were then washed twice, firstly for 2 minutes and then for 5 minutes, with PBS before seeding cells.

2.2.2 Dissection of dorsal root ganglia

3-5 week old Sprague Dawley rats were culled by schedule 1 method (cervical dislocation followed by exanguination) in accordance with the UK Animals (Scientific Procedures) Act 1986. The skin overlying the spinal column was removed and the excess adipose tissue trimmed away using a blade (15C, Swann-Morton). The spinal column was excised from situ using iris scissors (WPI) and a dorsal laminectomy was performed using microscissors (WPI) to remove the dorsal roof and expose the spinal cord. The ventral body of the spinal column was then hemisected, again using iris scissors (WPI). The spinal cord was gradually pulled away from each hemisection to reveal the dorsal root ganglia. Each dorsal root ganglion was dissected out using fine tweezers (Dumont) and microscissors (WPI) and the central and peripheral spinal root were trimmed away. Trimmed DRG were collected into 1 ml PBS in a 1.5 ml eppendorf tube.

2.2.3 Preparation of culture

The PBS was removed from the DRGs in a culture hood (Class II biological safety cabinet, Airstream) and 1 ml of 1 mg/ml Dispase II (D4693, 0.85 U/mg, Sigma) and 0.6 mg/ml Collagenase XI (C7657,1594 U/mg Sigma) in HEPES-buffered dissociation solution was added (Baker and Bostock, 1997). The DRGs were incubated at 37 ^{o}C for 1.5 hour in a carbon dioxide incubator to allow for dissociation (Galaxy 170 S CO2 Incubator, New Brunswick). After 1.5 hr, DRGs were transferred to a 15 ml falcon tube and triturated rapidly in 1 ml of DRG wash media. The resuspended DRG mixture was then carefully pipetted and transferred to form a separate layer on top of 3 ml 15% BSA (in DRG Wash Media) and centrifuged for 10 minutes at 1500 rpm (21 ^{o}C, Asc 9, Desc 2) using a Rotina 46 R centrifuge (Hettich) centrifuge. The supernatant containing both DRG wash media and 15% BSA was next removed leaving a pellet of DRG neurons. 4 ml of DRG wash media was then added, the pellet resuspended, and the spin repeated (10 mins at 1500 rpm, 21 ^{o}C, Asc 9, Desc 2) using the same centrifuge. The supernatant was again removed, and the pellet was resuspended in the appropriate amount of DRG low-serum media to allow the cells to plated in 200 µl per well.

2.2.4 Incubation with chimeras

Dissociated dorsal root ganglia cultures were grown for 2 days prior to the addition of chimeras. Half (100 µl) of the low serum media was removed and replaced with fresh low serum media, containing the chimera, to give an end concentration of 10 nM of

chimera. The culture was then incubated with the chimera for 65 hours at 37 ^{o}C, 5% CO_2 in the cell culture incubator.

2.2.5 Immunocytochemistry

After 65 hours incubation with the respective chimeras, 170 µl of the media containing the chimera was removed from the wells and the cells were washed with 150 µl of ice cold PBS for 5 minutes before 10 minute fixation with 150 µl 4% PFA. Both steps were carried out on ice. The wells were then washed once with 150 µl PBS for 5 min before permeabilising the cells with 150 µl of 0.3% triton in PBS. The wells were then washed a further two times with 150 µl PBS (first wash 2 minutes, second wash 5 minutes). The cells were then incubated in 150 µl blocking solution for immunocytochemistry for 1 hour. Next, the blocking solution was removed from the wells and the cells were incubated for a further 1 hour with primary antibodies diluted in 150 µl immunocytochemistry specific blocking solution. This was again followed by two washes with 150 µl PBS, the first for 2 minutes and the second for 5 minutes, before incubation with the respective secondary antibodies and DAPI (Sigma), again diluted in 150 µl blocking solution, for 45 minutes. The cells were then washed at least 3 times with 150 µl PBS (the first wash for 2 minutes and then subsequent washes for 5 minutes), prior to imaging.

2.2.6 Epifluorescence microscopy of cell cultures

Images were acquired on a Leica DM IRB epifluorescence microscope at 20x magnification using MicroManager software. Three fields of view were imaged per well. To avoid investigator bias, the fields of view were selected by viewing the well at 5x magnification and positioning the field of view to be central to each of three set positions per well (Fig. 2.2), before then increasing the magnification to 20x. Each experiment was completed in triplicates.

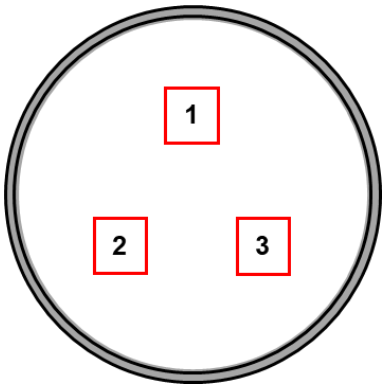

Figure 2.2 Selection of the fields of view when imaging dissociated dorsal root ganglion cultures. *The well of the 96 well plate was first viewed under 5x magnification to position the centre of the field of view at one of the three positions depicted. The magnification was then increased to 20x and the epifluorescent image was taken. This process was repeated until epifluorescent images had been taken at all three fields of view.*

2.2.7 Image analysis

Image analysis and quantification was performed using FIJI. Cells were judged to be neurons if they labelled positively with β-Tubulin-III (or Neurofilament 200 or Peripherin, dependent on the neuronal marker used) with an intact, healthy nucleus, assessed using the DAPI stain, and an intact cell membrane. The region of interest (ROI) of healthy neurons was then marked on the brightfield image, using the FIJI freehand selections tool (Fig 2.3). The multi-measure function was used to measure the area of the marked ROIs and the mean gray value intensity of the pixels contained within the individual ROIs, across the multiple image slices. This produced an Excel sheet which was then transferred to Microsoft Excel. Here, the cell diameter of neurons was calculated from the measured ROI area using the equation "=2*(SQRT(CELL/PI()))".

Colocalisation of cleaved SNAP25 with the neuronal markers was determined by a thresholding technique. The mean gray value threshold for each antibody stain is listed in Table 2.5. A higher threshold was set for the cleaved SNAP25 stain because this antibody produced a much brighter, more intense stain than the neuronal markers, possibly due to the use of the Anti-mouse IgG (H+L) Cross adsorbed Alexa Fluor 594 secondary antibody, opposed to Alexa Fluor 488, used to label the neuronal markers. The conditional formatting function within Microsoft Excel was used to highlight neurons whose immunofluorescence exceeded the set threshold.

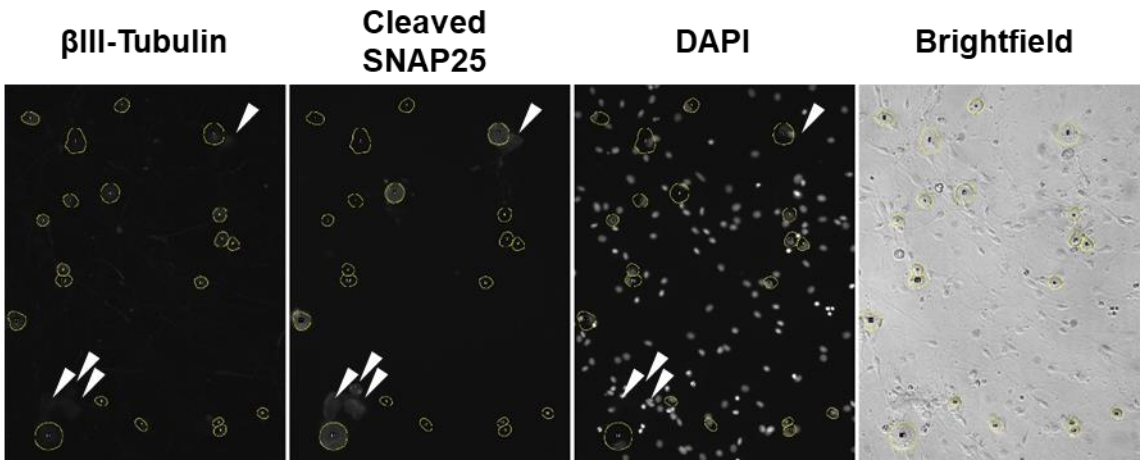

Figure 2.3 Marking of neurons and image quantification using FIJI. *Neurons were identified using the βIII-Tubulin stain (left panel). The health of neurons was then determined by identifying a DAPI-stained nucleus (3rd panel). Only the healthy neurons with intact nuclei were then outlined in the brightfield image (4th panel), using the freehand selection tool. The arrows indicate cells which appeared weakly positive for βIII-Tubulin but did not have a nucleus when viewing the DAPI image. The dead cells can be seen to produce non-specific immunofluorescence in the Cleaved SNAP25 image (2nd Panel).*

Antibody Stain	Mean gray value threshold applied
Cleaved SNAP25	>700
βIII-Tubulin	>300
Neurofilament 200	>300
Peripherin	>350

Table 2.7 *The mean gray value threshold applied to the antibody staining during immunocytochemistry.*

2.2.8 Statistical Analysis of DRG culture images

One-way analysis of variance (ANOVA) was used to assess the statistical relevance of immunocytochemistry data. Statistical significance was defined as $P<0.05$. In Chapter 4, Dunnett's multiple comparisons was used to specifically compare the binding of BiTox/A to each of the alternative botulinum chimeras. In chapter 6, however, the binding profile of three chimeras, BiTox/A, TetBot and ChoBot, was compared against each other. This meant that all pairwise comparisons were conducted, and therefore the Tukey's multiple comparisons test was used instead. All statistical analysis was conducted using GraphPad Prism 7. Results are presented as mean ± S.E.M.

2.3 Animals

All animal experiments were conducted under a UK Home Office Project License and complied with the UK Animals (Scientific Procedures) Act, 1986. Male and female rats were purchased from Charles River and breeding pairs were established. Male Sprague-Dawley rats (150-200 g) from the subsequent litters were then used in experiments. All animals were housed in a 12 hour light/dark cycle at 21 ^{o}C and in 55% relative humidity. Food and water was available ad libitum.

2.4 Injections

2.4.1 Preparation of clostridial chimeras for injection

Chimeras were prepared courtesy of Dr C. Leese. The appropriate amount of chimera was dissolved in the relevant volume of Buffer A to achieve the desired injection volume, most commonly 30 or 50 µl. For the vehicle control, the equivalent volume of 0.4% OG

(Octyl β-D-glucopyranoside) used to prepare the chimera, was diluted in Buffer A. Prior to injection, both solutions were maintained on ice to ensure their stability.

2.4.2 Intraplantar injection

Rats were individually anaesthetised in an induction chamber with 4% isoflurane (IsoFlo, Zoetis) in oxygen. Once immobile, the rat was then moved to an anaesthesia mask and placed in the prone position. The depth of anaesthesia was confirmed by loss of the pedal withdrawal reflex in the right hindpaw. The left hindpaw was next cleaned using 70% ethanol and a 0.3 ml U-100 Insulin syringe (Terumo), coupled to a 29-gauge needle, was inserted subcutaneously into the plantar aspect of the left hindpaw. The desired volume was then injected into the centre of the footpad, over approximately 5-10 seconds. The animal was then placed in a recovery cage and monitored for several minutes before being returned to its normal cage.

2.4.3 Intraperitoneal injection

Rats were anaesthetised with 4% isoflurane (in oxygen) in an induction chamber. Once anaesthetised, the rats were then removed and gently restrained whilst a 1ml syringe coupled to a 27-gauge needle (302200, BD Microlance) was inserted into the posterior quadrant of the abdomen, in order to access the peritoneum. The needle was angled so that it ran parallel to the line of the hind leg, as to avoid the abdominal organs. The necessary volume of substance was then delivered, and the needle withdrawn.

2.5 Experimental pain models

2.5.1 Chronic inflammatory pain model

Either 15 µl (Chapter 6) or 30 µl (Chapter 4) of Complete Freund's Adjuvant (F5881, Sigma) was delivered via intraplantar injection (as described in 2.4.1) to the central footpad to produce a stable inflammatory state (Stein et al., 1988).

2.5.2 Incisional post-operative pain model

For the post-operative pain model, rats were deeply anaesthetised in an anaesthesia induction chamber, using 4% isoflurane in oxygen, before being secured to an external anaesthesia mask in the prone position. The depth of anaesthesia was confirmed by loss of the pedal withdrawal reflex in the right hindpaw. The left hindpaw was then cleaned

thoroughly using 70% ethanol. An incision, approximately 1 cm in length, was then made to the left hindpaw, using a sterile blade (15A, Swann-Morton), extending from the centre of the foot pad towards the heel of hindpaw (Brennan et al., 1996). Pressure was then applied to the hindpaw for 1-2 minutes until any bleeding had stopped and the incision was sealed using VetBond tissue adhesive (3M). The rat was then returned to a recovery cage and monitored for 20 minutes to ensure the incision was effectively sealed before being returned to a clean cage.

2.5.3 Chemotherapy-induced peripheral neuropathy pain model

Rats were injected intraperitoneally (described in 2.4.2) with 2 mg/kg paclitaxel (10461, Cayman Chemicals), delivered in an injection volume of 1 ml/kg, as described previously (Polomano et al., 2001). The correct concentration of paclitaxel was prepared by diluting paclitaxel to 2 mg/ml in saline and then injecting the calculated volume, dependent on the weight of the individual rat. Rats received a total of 4 intraperitoneal injections of paclitaxel, administered on alternate days (day 0, 2, 4 and 6), providing a cumulative dose of 8 mg/kg paclitaxel per animal. A separate group of animals simultaneously received 4 IP doses of Cremophor EL (C5135, Sigma)/ Ethanol (1:1), used to dissolve paclitaxel, to provide a vehicle only group.

2.6 Behavioural studies

2.6.1 Hargreaves Test

Rats were placed in clear plastic boxes (20 cm x 20 cm x 14 cm) on top of a glass surface and allowed 30-45 minutes to acclimatise. Longer, however, specifically up to 1 hour, was allowed during initial baseline measurements. During the acclimatisation period, the rats were observed for exploratory behaviour. Only once this behaviour seized and rats appeared calm and less mobile, with only occasional bouts of grooming, was the test started. Thermal thresholds were determined by Hargreaves test using the Plantar Hargreaves' Test Apparatus (37370, Ugo Basile) (Hargreaves et al., 1988). Here, a laser heat source (60 IR), situated beneath the glass surface, was positioned under the central footpad of both the affected and unaffected hind paw. Once correctly positioned, a switch was used to activate the heat source and start an in-built electronic timer. The withdrawal latency for when the rat removed its paw from the heat source was electronically measured and confirmed by observation. To ensure that no tissue damage occurred during testing, a maximum withdrawal latency cut-off value of 20 seconds was imposed. A total of four readings were taken for each hindpaw and recorded with a minimum wait

of 5 minutes between each consecutive reading. The average withdrawal latency was then calculated from the four readings.

Urine and faeces were cleared for the duration of the test. Urine, especially, interferes with the heat absorption of the plantar surface of the paw, and with the reflection of the infrared beam, thus disrupting the reading (Ugo Basile, 2013).

2.6.2 Electronic von Freys

Rats were placed in individual plastic chambers (15cm x 36 cm x 18 cm) on top of an elevated wire mesh. Rats were allowed 30-45 minutes to acclimatise, however, a longer acclimatisation period was allowed during the initial baseline measurements. Once exploratory behaviour had stopped, and rats were still with only occasional short grooming periods, the test was started. Mechanical thresholds were assessed using electronic Von Frey equipment (EVF3, BioSeb) applied to the centre of the footpad of the affected and unaffected hind paw (Ängeby Möller et al., 1998). Pressure was evenly applied until the rat withdrew its hindpaw. The force at which the paw was removed was then electronically recorded. Four readings were taken per paw and a minimum interval of 5 minutes was imposed between consecutive readings. The average mechanical withdrawal threshold was then calculated from the four readings for each individual rat.

2.6.3 Evaluation of motor function

Two separate methods were used to assess motor function. Firstly, hindpaw digit spreading, following tail suspension, was used to examine motor innervation. Successful digit spreading of the hindpaw indicated sufficient intact motor innervation of the hindpaw (Wen et al., 2015). Secondly, a suspension test was used to assess muscle weakness and loss of muscle tone (Mangione et al., 2016). During this test, the rats were placed on a wire mesh. The mesh was then inverted and held approximately 30 cm over a cushioned cage. It was recorded whether rats were able to successfully grip the wire mesh or whether they fell immediately. Additionally, rats were observed for any signs of limping or dragging of the hindlimb, indicative of muscular paralysis, during normal exploratory behaviour.

2.6.4 Statistical Analysis

Two-way ANOVA was used to determine the statistical significance of the behavioural results. Sidak's multiple comparisons test was used, post-hoc, to determine whether any

statistical differences existed between treatment groups at each individual time point. Statistical significance was defined as $P<0.05$. All statistical analysis was conducted using GraphPad Prism 7. Results are presented as mean ± S.E.M.

2.7 Immunohistochemistry

2.7.1 Transcardial Perfusion

Rats were euthanized by an overdose of anaesthetic via intraperitoneal injection (described in 2.4.2) of pentobarbital (150 mg/kg) (JML), delivered under 4% isoflurane. Loss of the pedal withdrawal reflex and corneal reflex was used to confirm the depth of anaesthesia before proceeding with the perfusion. The rat was then placed in the supine position and a midline incision was made, extending up to the chest. The heart was accessed by cutting through the diaphragm and removing the ribcage using iris scissors (WPI). Once exposed, a 19-gauge needle (BD Microlance) was inserted into the left ventricle of the heart and secured using a needle holder (Arnold). Microscissors (WPI) were used to make an incision to the right atrium to allow the exit of fluids. The animal was perfused with 300 ml PBS followed by 300 ml 4% PFA. The animal was then released from the perfusion system and the relevant tissues were collected. These included the spinal cord, the dorsal root ganglia and glabrous skin, taken from the plantar surface of both hindpaws.

2.7.2 Preparation of tissue

Following the dissection, the tissues were post-fixed in 4% PFA for 4 hours at room temperature. The tissues were then transferred to 30% sucrose and stored at 4^{o}C until sectioned. Additionally, with regards to the spinal cord collected, an incision was made to the contralateral ventral horn using a blade (15C, Swann-Morton) to enable identification of the contralateral spinal cord during image analysis.

2.7.3 Sectioning of tissue

All tissue specimens to be processed were emerged in Cryo-M-Bed OCT embedding medium (53581-1, Bright) and frozen at -40 ^{o}C. 30 µm sections were prepared using a cryostat (OFT5000, Bright Instruments). Transverse spinal cord sections and glabrous skin sections were collected and consequently stored at 4 ^{o}C in 5 % sucrose in PBS as free-floating sections. Conversely, dorsal root ganglion sections were mounted directly

onto SuperFrost plus slides (ThermoFisher) and then stored at -20 ^{o}C until further immunohistochemical processing.

2.7.4 Immunohistochemical staining

Free-floating sections received three 10 minutes washes in PBS. Sections were then incubated with blocking solution (5% Goat serum, 0.03% Triton X-100 in 1x PBS) for one hour at room temperature before overnight incubation at 4 ^{o}C with the relevant primary antibodies, diluted in working solution (2% Goat serum, 0.03% Triton X-100 in 1x PBS). The next day, the sections were washed a further three times in 1x PBS. Again, each wash was 10 minutes long. Sections were then incubated with the corresponding secondary antibodies, diluted in the working solution for 2 hours. DAPI (Sigma) was also added at this stage. Sections underwent an additional three 10 minute washes in PBS before being mounted onto SuperFrost plus slides (ThermoFisher). The DRG slide-mounted sections were processed identically except for each set of three 10 minutes washes, the slides were instead washed 5 times for 5 minutes. PBS was again used for the washes. In both instances, the slides were allowed to air dry before adding Fluoromount aqueous mounting medium (Sigma) and applying a 22x64 mm coverslip (401/0188/52, BDH) to the slides, ready for immunofluorescent and confocal microscopy.

2.7.5 Imaging and microscopy of sections

Sections were imaged on a Leica DM IRB epifluorescence microscope at 5x, 10x, 20x and 40x magnifications, using MicroManager software. Where specified, images were acquired on a Nikon A1 TIRF confocal microscope at 40x magnification.

2.7.6 Image analysis

Image analysis and quantification was performed using FIJI. Similar to that described in 2.2.8, thresholding was again applied to quantify in vivo images. This technique is specifically used in Chapter 5. A predetermined threshold was first applied to the chosen image to select either the motor neurons of the ventral horn (5.3.2), or the whole of the tissue section (5.3.3). The FIJI analyse particles function was then used to generate an outline and calculate the area contained within the marked outline (tissue section, 5.3.3) or outlines (motor neurons, 5.3.2). Another threshold was then applied to highlight the area containing the other relevant immunofluorescent stain. Again, the analyse particles function was executed to create, outline and measure the area of the selected

immunofluorescence. This generated a summary excel sheet, detailing the total area measured within the outlines, which was then exported to Microsoft excel. The immunofluorescence was subsequently expressed as a percentage of the total area, either of the tissue section or of the motor neurons. A working example is shown in Figure. 2.4.

2.8 Western Blot

2.8.1 Protein extraction from whole Dorsal Root ganglia

Dorsal root ganglia from L3-L6 were collected as described in 2.2.2. In this instance, however, they were collected into ice cold PBS in individually labelled 1.5 ml Eppendorf tubes. Once the dissection was complete, the eppendorf tubes containing the individual DRGs were centrifuged at 13200 RPM for 1 minute and the excess PBS was removed. Each DRG was then individually transferred to a 0.1ml homogeniser and 40 µl of DRG lysis buffer was added. The DRG was homogenised for several minutes whilst being maintained on ice. Once sufficiently homogenised, the lysate was transferred back into an eppendorf tube which was then placed on a rotator for 1 hr and vortexed every 15 mins, whilst kept at 4 ^{o}C. The eppendorf tubes containing the lysate were then centrifuged at 13200 RPM for 1 minute. The supernatants were then collected into fresh eppendorfs before being placed in a heat block, set at 90 ^{o}C, for 3 minutes. The supernatant was then either loaded immediately onto a gel or stored in -20 ^{o}C until required.

2.8.2 Protein extraction from cultured neurons

1x SDS sample buffer was prepared by diluting 4x SDS buffer in deionised water and then adding 1 mM $MgCl_2$ and 0.1 % benzonase nuclease (Sigma). All media was aspirated from the wells of the 24-well plate. 60 µl of 1x sample buffer was added per well and the plate was then shaken for 10 minutes at 650 rpm, at room temperature, to lyse cells. The lysates were then collected into 1.5 ml eppendorf tubes and boiled for 3 minutes (>90 ^{o}C) before being centrifuged at 13200 RPM for 1 minute. Lysates were then either immediately loaded into a gel for western blot or stored at -20 ^{o}C for later use.

2.8.3 Western Blot

NuPAGE 12 % Bis-Tris pre-cast gels (Life Technologies) were loaded with a 5 µl Dual Colour protein ladder (Biorad) in the first lane and 13 µl of sample in the subsequent

A

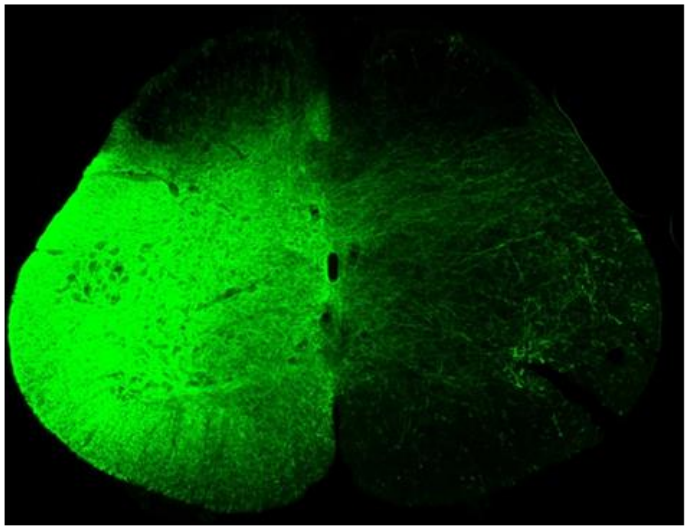

B

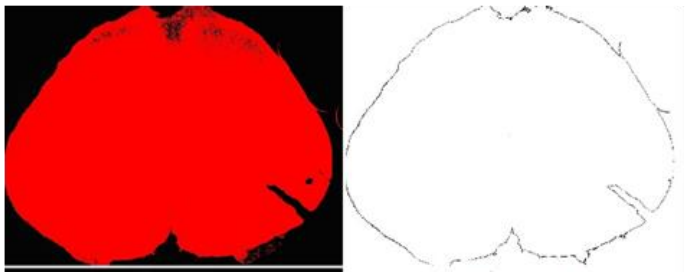

C

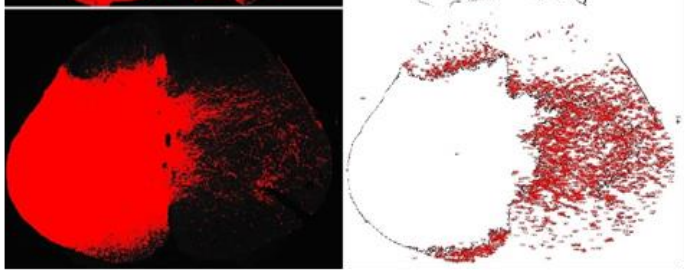

D

Whole section		Cleaved SNAP25		% Total slice area displaying cSNAP25
Minimum Threshold value	Area (mm^2)	Minimum Threshold value	Area (mm^2)	
15	3.576	24	1.887	52.8

Figure 2.4 Thresholding to quantify in vivo images. (A) *An epifluorescent image of cleaved SNAP25 (green) in the lumbar spinal cord, following intraplantar injection of 2xTetBot (Chapter 5).* ***(B)*** *A low threshold was applied to the epifluorescent image to select the whole of the tissue section (left). The FIJI analyse particles function was then used to generate an outline and calculate the area contained within (right).* ***(C)*** *A higher threshold was then applied to highlight only the area containing the cleaved SNAP25 stain (left). Again, the analyse particles function was performed to create, outline and measure the area of the cleaved SNAP25 stain (right).* ***(D)*** *The measurements were transferred to Microsoft excel to express the cleaved SNAP25 stain as a percentage of the total section area.*

lanes. Gels were run at 180 V constant and 300 W for 1 hour 50 min in an XCell SureLock system (Life Technologies) filled with NuPAGE MES SDS running buffer. Approximately 5 minutes before completion, an immunoblot PVDF membrane (BioRad) was activated by soaking it in methanol for 10-20 seconds. The membrane was then soaked in transfer buffer, along with two pieces of Whatmann paper. Once ran, the gel was then loaded into a transfer cassette and placed into a transfer tank (BioRad), filled with transfer buffer. The transfer cassette was ordered such that it contained: a foam sponge, whatmann paper, gel, a methanol-activated Immuno-Blot PVDF membrane, a second whatmann paper and a foam sponge. A freezer block was placed in the transfer tank and the transfer was run for 1 hour at constant 250 mA, 300 V and 300 W.

Once the transfer was complete, the membrane was gently washed with deionised water before incubation with 12 ml western blot blocking solution for 30 minutes at room temperature. The primary antibodies were then added directly to the blocking solution for overnight incubation at 4 ^{o}C. For all incubation and wash steps, the membrane was placed on a rocker. The following day, the membrane was rinsed and then received three 5 minutes washes in PBS with 0.1 % Tween-20. Next, the membrane was incubated with the respective secondary antibodies, again diluted in western blot blocking solution, for 30 minutes at room temperature. The membrane was then rinsed and underwent a further three 5 minutes washes in PBS with 0.1 % Tween-20. 0.4 ml of chemiluminescent solution (SuperSignal West Dura extended duration substrate, Thermo Scientific) was then added per membrane. The subsequent luminescence was visualised by exposing X-ray film (Amersham) to the membrane and then developing the X-ray film using an Optimax 2010 X-ray developer (Protec).

Chapter 3. In vivo characterisation of BiTox/A enzymatic activity following intraplantar injection

3.1 Introduction

BiTox/A has been shown to be analgesic in neuropathic pain conditions, however, it is not yet clear how BiTox/A is producing these therapeutic effects. It has been suggested that BiTox/A binds to, and is enzymatically active in, A-nociceptors (Mangione et al., 2016). This theory is largely based on the observation that native BoNT/A, when added to dorsal root ganglion (DRG) cultures, inhibits calcium-dependent release of substance P in response to both capsaicin and potassium stimulation (Purkiss et al., 2000; Welch et al., 2000). It is namely the C-fibre and the Type I Aδ-fibre mechano-heat sensitive nociceptors that are responsive to capsaicin stimulation (Magerl et al., 2001). For this reason, it was assumed that one of these fibres types must be targeted by BiTox/A.

Data generated by Mangione et al. (2016) then demonstrated that administration of BiTox/A specifically attenuated secondary hyperalgesia in pain models whilst primary hyperalgesia remained unaffected. This again indicates the involvement of Aδ-nociceptors, as well as possibly, Aβ- sensory neurons. Secondary hyperalgesia arises from increased input from the low threshold mechanoreceptors, the Aβ-fibre neurons, and the Aδ-nociceptors, to the pain signalling pathways, such that they begin to drive, and augment, the activity of these pain pathways (Ziegler et al., 1999). This occurs at the level of the central spinal cord and is believed to result from heterosynaptic facilitation, as a consequence of central sensitisation (Treede et al., 1992; Ziegler et al., 1999; Woolf, 2011). From the collective evidence, it was thus suggested that the A-nociceptors must be implicated in the analgesic effects of BiTox/A (Mangione et al., 2016).

Regardless of which sensory neuron subtypes are involved, it still remains unclear whether these analgesic effects are peripherally or centrally mediated. A central effect was suggested due to the perceived delay noted in the therapeutic effect of BiTox/A (Mangione et al., 2016). Western blot analysis of tissue taken from BiTox/A-injected animals, nevertheless, failed to detect cleaved SNAP25 at the central level of dorsal horn in the spinal cord, or in the dorsal root ganglia, implying a peripherally-mediated effect (Mangione et al., 2016). Skin tissue from the plantar surface of the injected hindpaw was not, however, included in the western blot analysis. It is therefore unknown whether cleaved SNAP25 would have been detected in the periphery either. As a result, this data does not completely discredit a central effect.

Consequently, here, the binding profile of BiTox/A will be investigated in vivo, using the in-house anti-cleaved SNAP25 antibody as a marker of BiTox/A's enzymatic activity, and as an indirect reporter to determine the location of BiTox/A. This method will be used to confirm whether BiTox/A is active in the A-nociceptors in vivo, and potentially, will help to elucidate the mechanism by which BiTox/A-induced analgesia is produced. Specifically, whether this is by blocking neurotransmission in the peripheral afferents, or by preventing the development of central sensitisation at the level of the spinal cord.

3.2 Results

3.2.1 Cleaved SNAP25 is visualised in the sensory neurons of the glabrous skin following intraplantar injection of BiTox/A

Immunohistochemical processing of glabrous skin sections, isolated from the plantar surface of the BiTox/A-injected hindpaw, revealed SNAP25 cleavage within the sensory neurons (Fig. 3.1A). Briefly, the sensory neurons were identified using pan-neuronal marker, βIII-Tubulin, which labels all nerve fibres, including both sensory and motor fibres. The location of the nerve terminals can, however, be used to distinguish the sensory nerve fibres from the motor nerve fibres. Sensory nerve fibres terminate more superficially within the dermis. Specifically, sensory nerve terminals are concentrated proximal to the epidermis. Motor neurons instead project to muscle fibres which are located much deeper in the skin, beneath the dermis.

Cleaved SNAP25 was not visualised in the sensory neurons of the contralateral hindpaw or in ipsilateral paw of vehicle-injected animals. Neither was cleaved SNAP25 observed in the paw skin tissue of naïve animals.

Further immunostaining indicated that cleaved SNAP25 colocalises with neurofilament 200 (NF200) -positive nerve fibres, a marker of myelinated neurons (Fig. 3.1B, Top panel), as well as IB4 (Fig. 3.1B, Middle panel) which labels non-peptidergic neurons (Stucky and Lewin, 1999). Cleaved SNAP25 was visualised within a subset of CGRP positive neurons (Fig. 3.1B, Bottom panel). Subjective observations, however, suggest that cleaved SNAP25 colocalised most readily with NF200. Importantly, the labelling for cleaved SNAP25 was shown to colocalise with the staining produced by the anti-SNAP25 antibody, which is immunoreactive to both whole and cleaved SNAP25, in BiTox/A-injected animals (Fig. 3.1C).

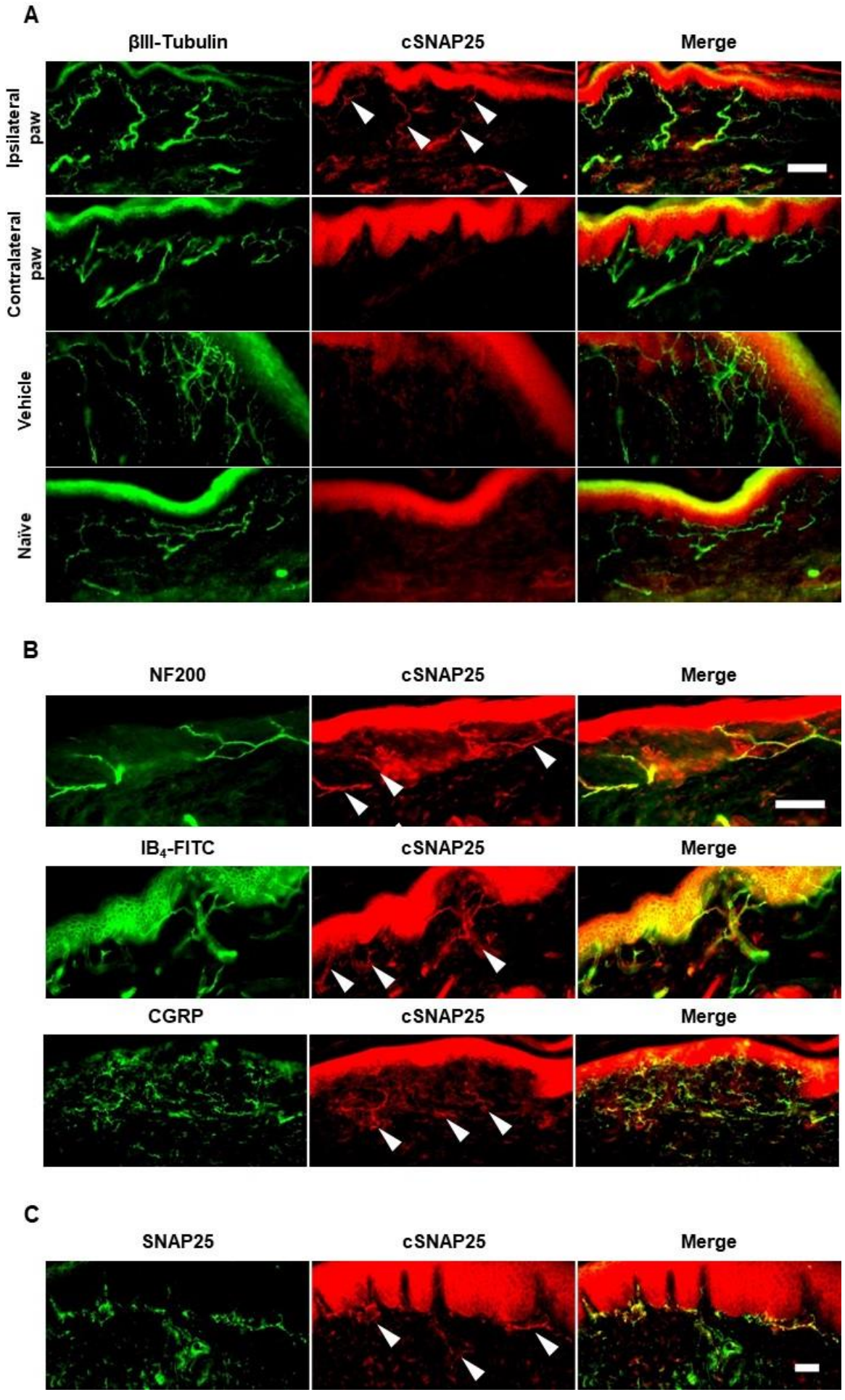
A
βIII-Tubulin
cSNAP25
Merge
Ipsilateral paw
Contralateral paw
Vehicle
Naïve
B
NF200
cSNAP25
Merge
IB4-FITC
cSNAP25
Merge
CGRP
cSNAP25
Merge
C
SNAP25
cSNAP25
Merge

Figure 3.1 Cleaved SNAP25 is detected in the sensory nerve terminals of the glabrous skin after intraplantar injection of BiTox/A. *4-5 week old male Sprague-Dawley rats received intraplantar injection of either 200 ng/ 30 µl BiTox/A (N=3) or 30 µl vehicle (N=2). 7 days post-injection rats were perfused and glabrous skin tissue was taken from both hindpaws.* ***(A)*** *Epifluorescent images of 30 µm glabrous skin sections, isolated from the ipsilateral hindpaw, revealed cleaved SNAP25 (red) in the sensory neurons, marked using βIII-Tubulin (green), within the dermis (N=3). Cleaved SNAP25 was not detected in the contralateral hindpaw of BiTox/A-injected rats (N=3), in the ipsilateral hindpaw of vehicle-injected rats (N=2) or in naïve rats (N=2). Scale bar = 100 µm* ***(B)*** *Cleaved SNAP25 (red) colocalised with both NF200 (top panel, green, N=2) and IB4 labelled neurons (middle panel, green, N=2) and was also observed in a subset of CGRP-positive neurons (bottom panel, green, N=2) in the BiTox/A-injected hindpaw. Scale bar = 100 µm* ***(C)*** *Cleaved SNAP25 staining (red) also colocalised with staining produced by a SNAP25 antibody, reactive to both full length and cleaved SNAP25 (green). Scale bar = 50 µm. Positive cleaved SNAP25 staining is indicated by the white arrowheads. The large, intense area of green and red fluorescence visible at the superior edge of the images is due to autofluoroscence generated by the dermis and epidermis of the skin sections and can thus be ignored.*

3.2.2 Cleaved SNAP25 is visualised at the neuromuscular junctions of the glabrous skin following intraplantar injection of BiTox/A

In agreement with previous studies, no motor paralysis was observed following intraplantar injection of 200 ng BiTox/A (Ferrari et al., 2011; Mangione et al., 2016). Rats continued to span the digits of their hindpaws normally when elevated and continued to be able to successfully grasp and remain suspended from an inverted wire mesh. Despite the perceived lack of motor paralysis, cleaved SNAP25 staining was detected at the neuromuscular junction (NMJ), labelled using α-Bungarotoxin-AlexaFluor488 (αBTX-488), and moreover, could also be seen in the nerve fibres innervating the NMJ (Fig. 3.2A, Top panel). Unexpectedly, SNAP25 cleavage was similarly visualised at the NMJ in skin isolated from the contralateral hindpaw (Fig. 3.2A, Second panel). Cleaved SNAP25 was not, however, present at the neuromuscular junction of vehicle-injected rats or naïve rats (Fig. 3.2A, Third and Bottom panel).

Again, cleaved SNAP25 was shown to colocalise with whole SNAP25 labelling following BiTox/A injection, confirming that the cleaved SNAP25 antibody is labelling neurons which normally express SNAP25 (Fig. 3.2B).

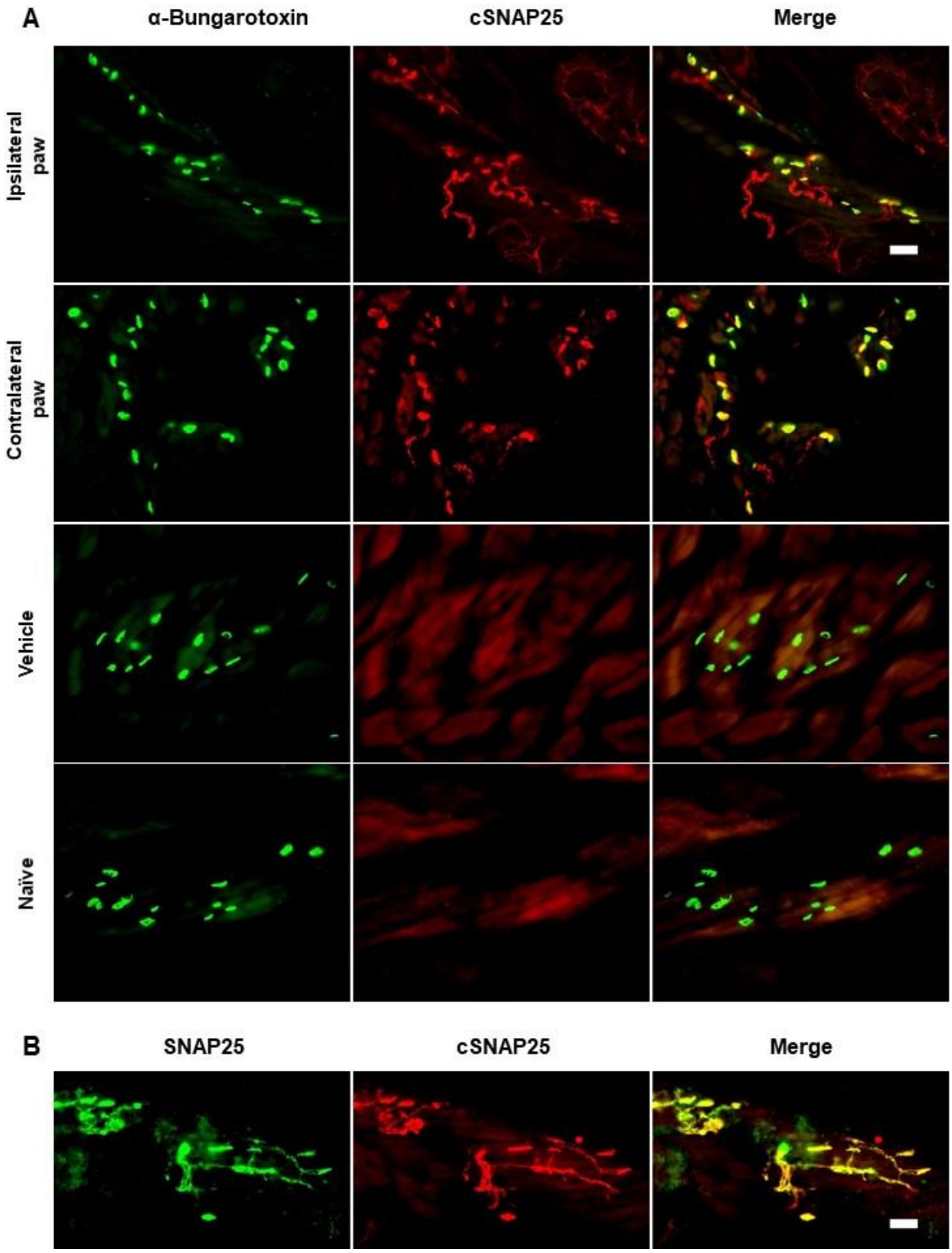

Figure 3.2 Cleaved SNAP25 is detected at the neuromuscular junction of the hindpaw after intraplantar injection of BiTox/A. (A) *Cleaved SNAP25 immunolabelling (red) was detected at the neuromuscular junction, marked using α-bungarotoxin-488 (green), in the ipsilateral (N=3) and contralateral hindpaw (N=3) in 200 ng/ 30 µl BiTox/A-injected animals. Cleaved SNAP25 was not detected in the ipsilateral paw of vehicle-injected rats (N=2) or naïve animals (N=2). Scale bar = 50 µm* ***(B)*** *Immunolabelled cleaved SNAP25 (red) colocalised with SNAP25 staining (green), immunoreactive to both full length and cleaved SNAP25, at the neuromuscular junction. Scale bar = 50 µm.*

3.2.3 Cleaved SNAP25 is detected in other innervated structures contained within the skin

Cleaved SNAP25 was also found localised to other structures within the skin. Namely, cleaved SNAP25 was detected at the sweat glands (Fig. 3.3, Top panel) and blood vessels (Fig. 3.3, Bottom panel). Both of which receive neuronal innervation from the sympathetic nervous system.

3.2.4 SNAP25 cleavage is not detected in the lumbar dorsal root ganglia following intraplantar injection of BiTox/A

Although SNAP25 cleavage was detected in the peripheral sensory nerve terminals, cleaved SNAP25 could not be detected at the level of the dorsal root ganglia (DRGs). Multiple methods were used to confirm this. Firstly, DRG cultures were produced from ipsilateral and contralateral DRG, taken from the lumbar levels L3-L5, of rats which, 5 days previously, had received intraplantar injection of 300 ng BiTox/A. Staining of these cultures did not reveal positive labelling for cleaved SNAP25 in any of the DRG from the investigated lumbar levels, ipsilateral or contralateral to the injected paw (Fig. 3.4A). To confirm that this was not a result of cells potentially being lost during the culturing

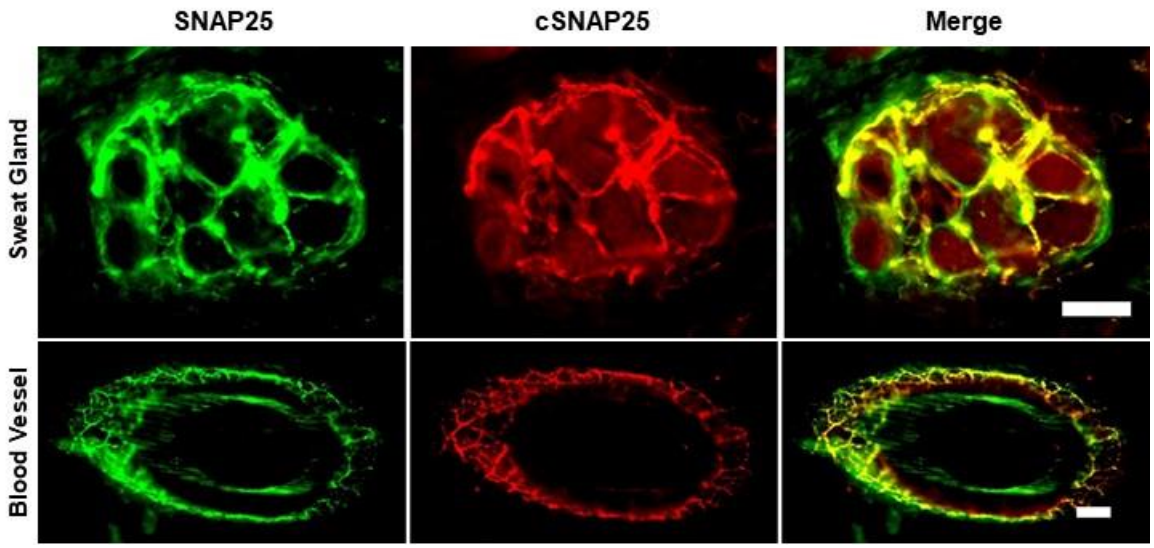

Figure 3.3 Cleaved SNAP25 is detected at the sweat glands and blood vessels of the glabrous skin after intraplantar injection of BiTox/A*. Cleaved SNAP25 immunolabelling (red) is found colocalised with SNAP25 staining (green), labelling both whole and cleaved SNAP25, at the sweat glands and the blood vessels located in the glabrous skin of the 200 ng/ 30 µl BiTox/A-injected hindpaw (N=3). Scale bars = 50 µm.*

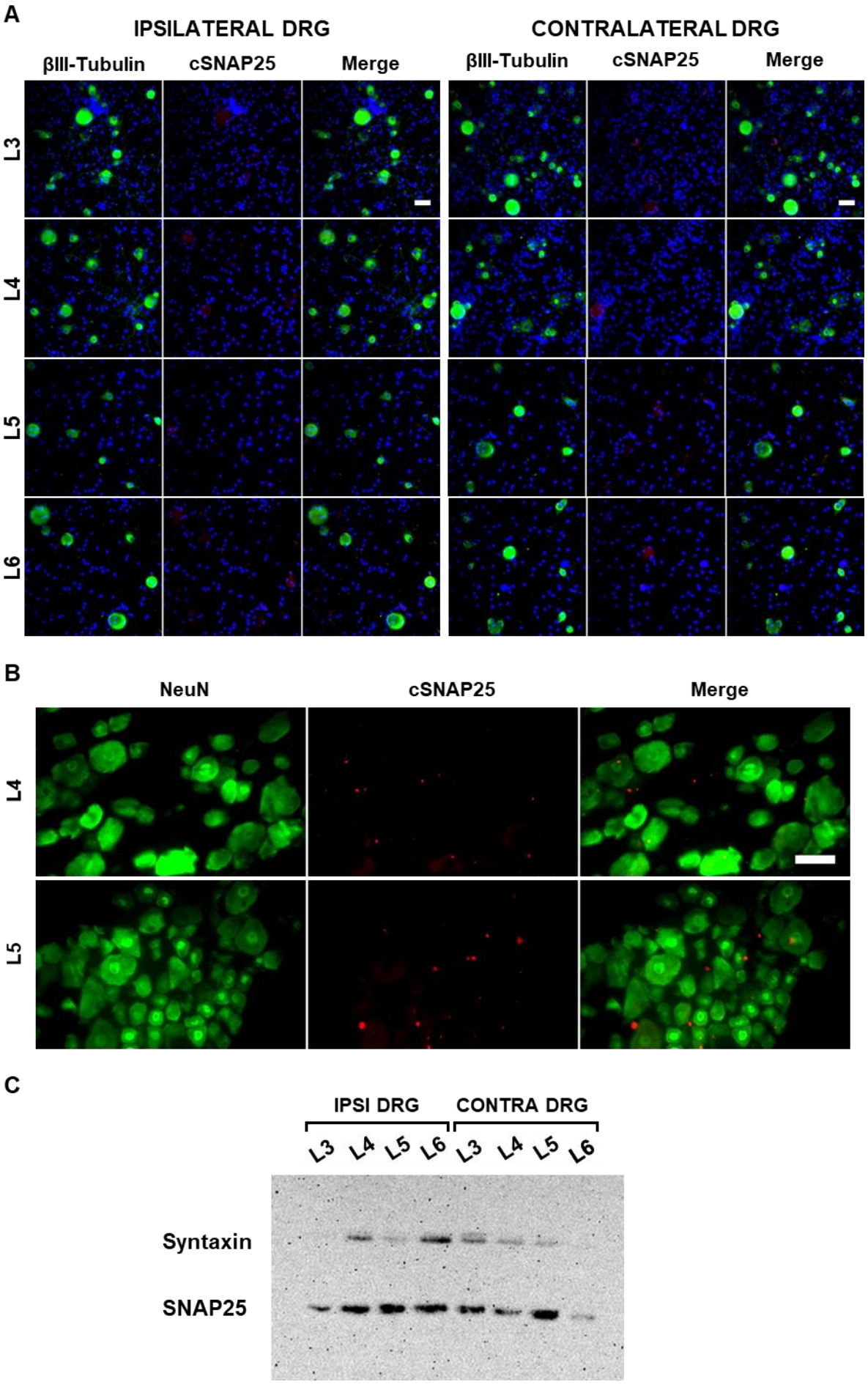
A
IPSILATERAL DRG
CONTRALATERAL DRG
βIII-Tubulin
cSNAP25
Merge
βIII-Tubulin
cSNAP25
Merge
L3
L4
L5
L6
B
NeuN
cSNAP25
Merge
L4
L5
C
IPSI DRG
CONTRA DRG
L3
L4
L5
L6
L3
L4
L5
L6
Syntaxin
SNAP25

Figure 3.4 Cleaved SNAP25 is absent in the dorsal root ganglia following intraplantar injection of BiTox/A. (A) *A 6 week old female Sprague-Dawley rat (N=1) received intraplantar injection of 300 ng/ 30 µl BiTox/A and was culled 5 days later. Dissociated dorsal root ganglia cultures were prepared from the ipsilateral and contralateral L3-L6 DRGs. Cleaved SNAP25 immunofluorescence (red) was not detected in any sensory neurons, marked by βIII-Tubulin (green), in DRG cultures from any level, either ipsilateral or contralateral to the injected paw. Scale bar = 50 µm.* ***(B)*** *Cleaved SNAP25 (red) was not detected in 30 µm DRG sections, prepared from the ipsilateral L4 and L5 DRG, taken from a 4 week old male rat (N=1) which had received intraplantar injection of 100 ng/ 20 µl BiTox/A 8 days previously. NeuN marks the sensory neuron soma (green). Scale bar = 50 µm.* ***(C)*** *Western blot analysis was performed on lysates prepared from ipsilateral and contralateral DRGs (L3-L6) dissected from a 6 week old female Sprague-Dawley rat (N=1) which had received intraplantar injection of 300 ng/ 30 µl BiTox/A 5 days earlier. Western blot, probed with an antibody immunoreactive to whole and cleaved SNAP25, displayed bands for whole SNAP25 for each DRG. No bands for cleaved SNAP25 were detected. Syntaxin was included as a loading control.*

protocol, the DRG of 100 ng BiTox/A-injected rats were removed and cryosectioned. Immunolabelled DRG sections were also negative for cleaved SNAP25 (Fig. 3.4B). Finally, lysates were prepared from individual DRGs, again taken from the lumbar levels L3-L5, both ipsilateral and contralateral to the 300 ng BiTox/A-injected hindpaw. Western blot, likewise, failed to recognise any cleaved SNAP25 in DRG isolated from the lumbar region (Fig. 3.4C).

3.2.5 Cleaved SNAP25 is observed in the ventral horn of the lumbar spinal cord following intraplantar injection of BiTox/A.

Again, despite the lack of motor paralysis observed, cleaved SNAP25 was detected within the ventral horn of the lumbar spinal cord of rats receiving intraplantar injection of BiTox/A. Specifically, cleaved SNAP25 was identified between levels L3-L5 of the spinal cord, as well as at the sacral region, S1 (Fig. 3.5A) with the strongest labelling visualised at L5. This staining was absent at L5 in vehicle-injected and naïve rats (Fig. 3.5B).

Labelling of the spinal cord sections with SNAP25 showed that although SNAP25 is expressed globally across the spinal cord, both in the dorsal and ventral horn, cleaved SNAP25 is only detected in a proportion of these nerve fibres and these fibres centre around the ipsilateral motor neurons of Lamina IX (Fig. 3.6A). Specifically, cleaved SNAP25 is not detected within the motor neuron soma themselves and is not present at the outer membrane. Instead, it appears to be contained within the neurons, presumably

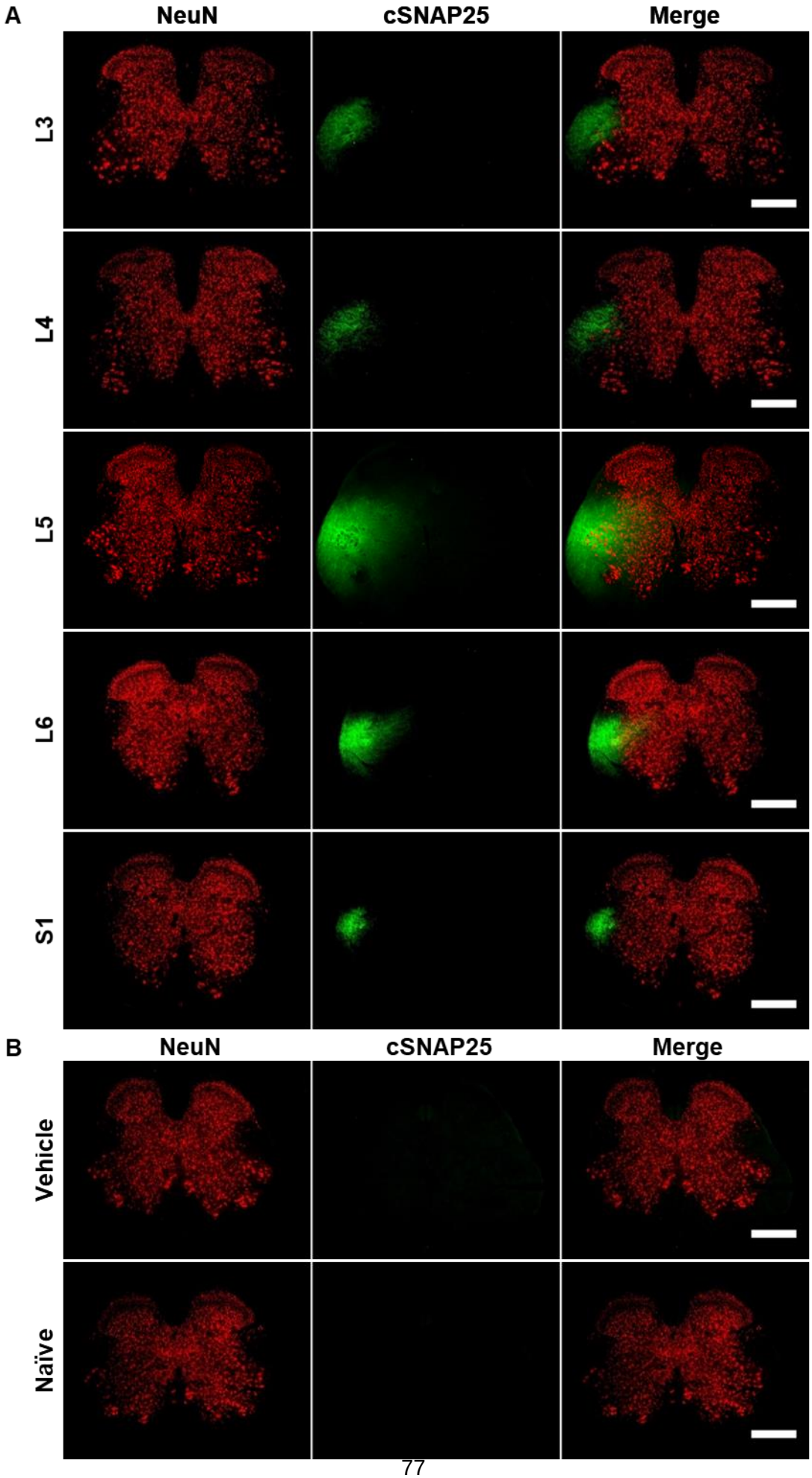
A
NeuN
cSNAP25
Merge
L3
L4
L5
L6
S1
B
NeuN
cSNAP25
Merge
Vehicle
Naïve

Figure 3.5 Cleaved SNAP25 is detected in the lumbar spinal cord after intraplantar injection of BiTox/A *4-5 weeks old male Sprague-Dawley rats (N=3) received intraplantar injection of 200 ng/ 30 µl BiTox/A.* ***(A)*** *Representative images were taken of cleaved SNAP25 staining (green) at L3-6 and S1 of the spinal cord. NeuN was used to label the neuronal soma (red). Cleaved SNAP25 staining was most intense at L5.* ***(B)*** *Cleaved SNAP25 staining is not observed in the lumbar spinal cord of vehicle-injected or naïve rats. Scale bar = 0.5 mm.*

interneurons, which synapse on to the motor neurons (Fig. 3.6B). This is clearly demonstrated by the absence of any overlap between the cleaved SNAP25 and NeuN stains when images are taken at different slices throughout a single spinal cord section (Fig. 3.6C).

3.2.6 Small amounts of cleaved SNAP25 are observed in the dorsal horn following intraplantar injection of BiTox/A

With regards to the dorsal horn, cleaved SNAP25 was sparsely detected in the dorsal horn in comparison to large area of SNAP25 cleavage visualised in the ventral horn (Fig. 3.6B). Specifically, single neurites containing cleaved SNAP25 were detected in the ipsilateral dorsal horn (Fig. 3.7, Top panel) which were largely absent in the contralateral dorsal horn (Fig. 3.7, Bottom panel).

3.3. Discussion

Here, the experimental conditions of Mangione et al. (2016) were replicated by injecting 200ng BiTox/A intraplantar into the hindpaw of Sprague-Dawley rats, with the intent to elucidate the mechanisms by which BiTox/A elicits its analgesic effect. Immunohistochemical staining revealed SNAP25 cleavage, considered to be indicative of BiTox/A's enzymatic activity, concentrated in the sensory and motor neurons of the glabrous skin of the injected hindpaw and in the ipsilateral ventral horn of the lumbar spinal cord.

3.3.1 BiTox/A cleaves SNAP25 in myelinated sensory neurons in vivo

Specifically, cleaved SNAP25 was visualised in both the NF200-positive neurons and the IB4-positive neurons, contained within the glabrous skin. This labelling suggests that BiTox/A internalises into myelinated, non-peptidergic neurons. Cleaved SNAP25 was also detected within a subset of CGRP-positive neurons. The expression of the

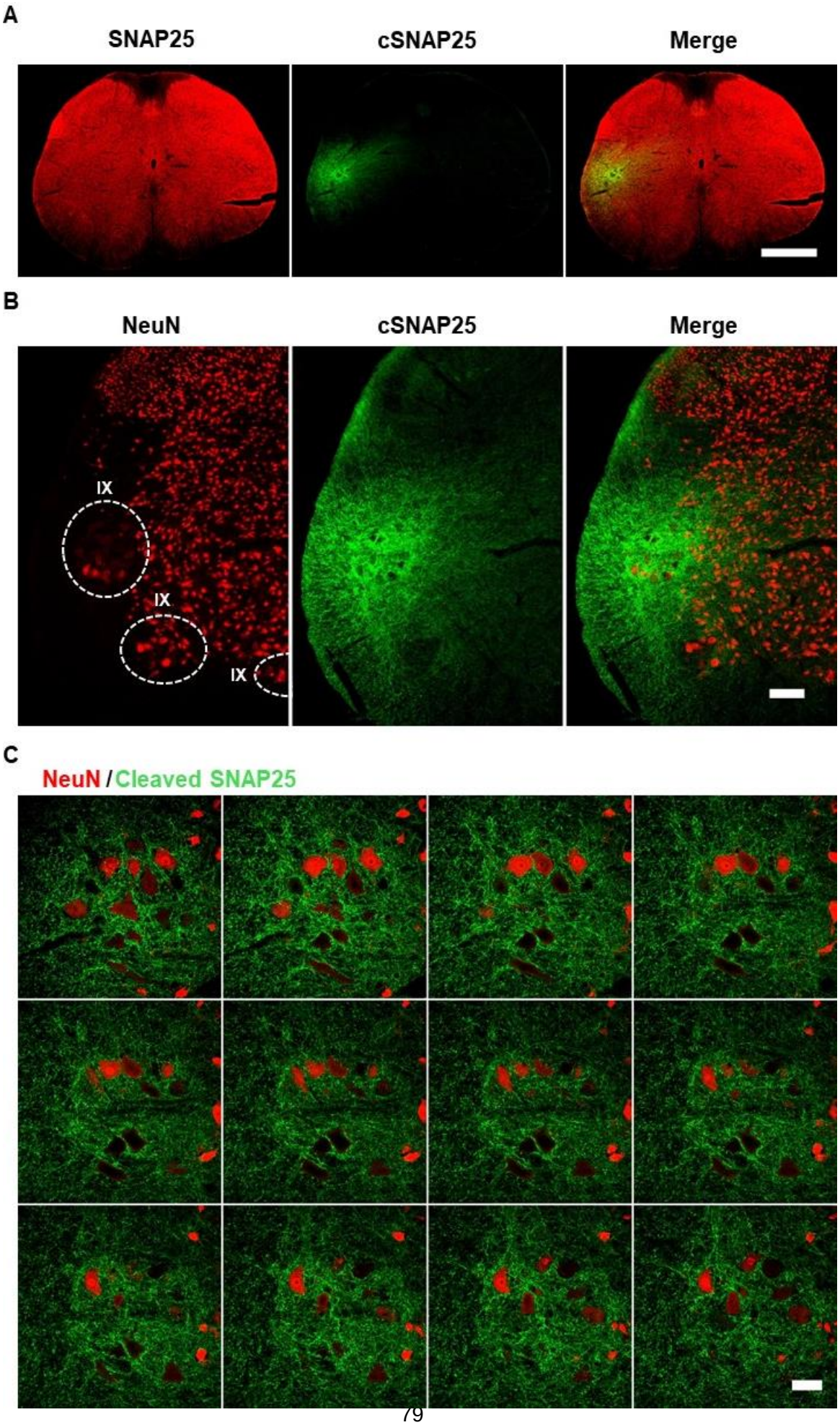
A
SNAP25
cSNAP25
Merge
B
NeuN
cSNAP25
Merge
IX
IX
IX
C
NeuN / Cleaved SNAP25

Figure 3.6 Cleaved SNAP25 is found concentrated around the motor neuron soma in lamina IX of the lumbar spinal cord. (A) *Spinal cord sections produced from a 4.5 weeks old male Sprague-Dawley rat (N=1) injected intraplantar with 200 ng/ 30 µl BiTox/A 7 days previously, displayed cleaved SNAP25 (green) colocalised with SNAP25 staining (red), immunoreactive to full length and cleaved SNAP25. Scale bar = 0.5 mm.* ***(B)*** *Higher magnification image of the ipsilateral L5 spinal cord, isolated from 200 ng/ 30 µl BiTox/A injected rats (N=3), acquired using a Nikon A1 TIRF confocal microscope. Cleaved SNAP25 (green) is observed surrounding the lateral lamina IX (dashed line) motor neuron pool (NeuN, red). Scale bar = 50 µm.* ***(C)*** *Stacked images were acquired using the Nikon A1 TIRF confocal microscope throughout the depth of a L5 lumbar spinal cord section and illustrate that cleaved SNAP25 (red) is excluded from the motor neuron soma (red). Scale bar = 20 µm.*

neuropeptide, CGRP, indicates that these neurons are peptidergic. This is in keeping with other in vitro studies that have reported reduced CGRP release from neuronal cultures which have been incubated with BiTox/A (Durham et al., 2004) . Similarly, in vivo studies have demonstrated decreased CGRP release from the sensory afferents of the bladder following intravesical delivery of BoNT/A (Chuang et al., 2004).

Subjective observation of the skin sections suggested that there was a higher colocalisation of cleaved SNAP25 staining with NF200 labelling than CGRP labelling in sensory nerve terminals. These observations are subjective and purely speculative. The immunofluorescence in sensory neurons was unable to be quantified as it was not clear following immunostaining, whereabout in the plantar surface the skin section had been isolated from. Additionally, cleaved SNAP25 was not consistently detected within every skin section, therefore, a method could not be standardised to allow for a fair comparison to be made. Despite this, within a single slice, cleaved SNAP25 would be routinely visualised within every NF200 positively labelled neuron present. In contrast, cleaved SNAP25 would only be detected within a subset of CGRP-positive nerve fibres, even when investigating one individual skin section.

Regardless, the detection of cleaved SNAP25 at the peripheral injection site suggests that the analgesic effect of BiTox/A should at least partially be due to a peripheral mechanism. The Aδ- and Aβ- neurons, labelled by NF200, are more strongly implicated in central sensitisation (Latremoliere and Woolf, 2009). It is thus possible that the cleavage of SNAP25 in these neurons could be having an indirect effect on central sensitisation by removing the peripheral drive which leads to increased excitability at the central synapse, thus explaining the effectiveness of BiTox/A against secondary hyperalgesia (Mangione et al., 2016).

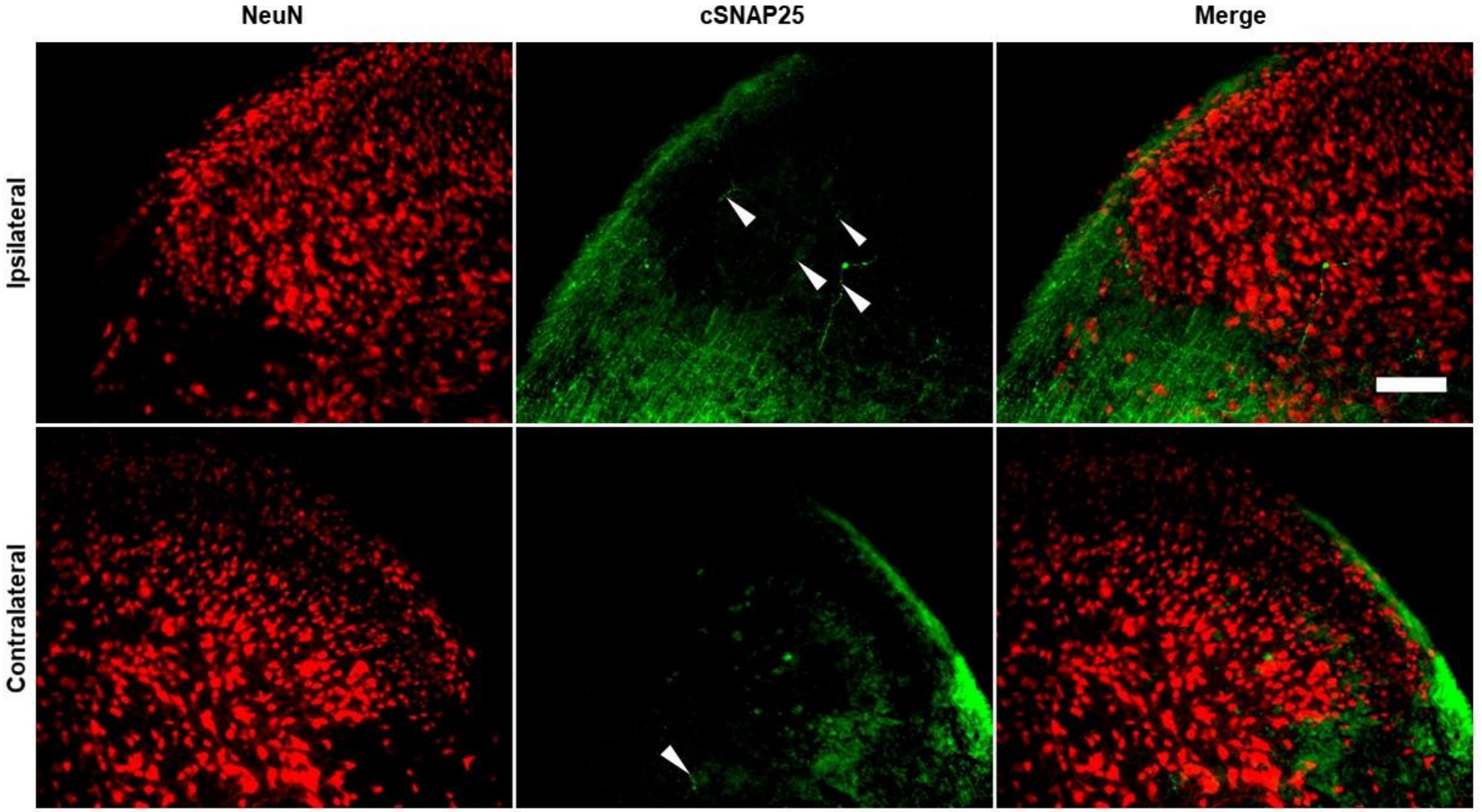
NeuN
cSNAP25
Merge
Ipsilateral
Contralateral

Figure 3.7 Cleaved SNAP25 is detected in single, sparse nerve fibres in the dorsal horn of the lumbar spinal cord. *Higher magnification images of the dorsal horn of spinal cord sections prepared from 4-5 week old Sprague-Dawley rats (N=3), 7 day after intraplantar injection of 200 ng/ 30 µl BiTox/A, show single nerve fibres displaying immunolabelling for cleaved SNAP25 (green) in the ipsilateral dorsal horn (top panel). Neuronal soma are labelled by NeuN (red). Cleaved SNAP25 is not readily detected in the contralateral dorsal horn (bottom panel). A single, small cleaved SNAP25- positive nerve fibre can be seen around lamina VI, at the base of the dorsal horn. Scale bar = 100 µm.*

Cleaved SNAP25 detected in a subset of CGRP-expressing neurons could likely explain the reduced plasma extravasation and inflammatory oedema, measures of local inflammation, observed in inflammatory models after intraplantar injection of BiTox/A (Mangione et al., 2016). CGRP is released from the peripheral nerve terminals of sensory afferents and contributes to neurogenic inflammation. It is hence logical that blocking this release would reduce local inflammation (Kilo et al., 1997). Surprisingly, however, C-fibre mediated thermal hyperalgesia at the site of inflammation remains unaffected by intraplantar injection of BiTox/A (Weng et al., 2012; Mangione et al., 2016). This would suggest that the reduction in CGRP release is primarily mediated via actions at the Aδ-nociceptors, which also display expression of CGRP, although less so than the C-nociceptors, as C-fibre signalling does not appear to be affected (McCarthy and Lawson, 1990). This could provide explanation for why, despite the reduction in local inflammation by BiTox/A observed, that C-fibre mediated thermal hyperalgesia is still developed.

3.3.2 The possible significance of SNAP25 cleavage detected at autonomic structures

Notably, SNAP25 cleavage was also detected at the blood vessels and sweat glands, located in the glabrous skin, following intraplantar injection of BiTox/A. Cleaved SNAP25 is normally reported at these structures following administration of native BoNT/A (Rhéaume et al., 2015) and represents the internalisation of BoNT/A into cholinergic autonomic neurons (McCorry, 2007). Accordingly, BoNT/A is used to treat conditions such as axillary hyperhidrosis, characterised by excessive sweating (Heckmann et al., 2001; Mirkovic et al., 2018).

The SNAP25 cleavage noted in the autonomic nervous system could potentially represent another, yet unexplored, possible therapeutic mechanism for the analgesic effect of BiTox/A. Sympathetic blockade and sympathectomy have been used to treat chronic pain conditions, such as complex regional pain syndrome (Straube et al., 2013;

O'Connell et al., 2016) and post-herpetic neuralgia (Kumar et al., 2004). Xie et al. (2016) demonstrated that performing a microsympathectomy reduced local inflammation and subsequent pain behaviour in a model of lower back pain in Sprague-Dawley rats. During this procedure, the ipsilateral gray rami, containing the postganglionic sympathetic fibres that project to the L4 and L5 sensory nerve branches, were severed. BiTox/A could be eliciting a similar effect by blocking neurotransmission in the sympathetic neurons, specifically those which innervate the hindpaw, thus limiting the inflammation which occurs in, and augments, pain conditions.

Native botulinum neurotoxin has already been used to successfully prolong the analgesic effect of a sympathetic nerve block (Choi et al., 2015). Importantly, however, this finding was based on a case study including only two patients. Furthermore, although sympathetic blockade has been routinely used to treat chronic pain conditions, its efficacy remains questionable (Straube et al., 2013; O'Connell et al., 2016). Lack of adequate controls and the poor quality of data consequently generated by these trials, means that conclusions about the efficacy of sympathetic blocks cannot be made. Moreover, Xie et al. (2016) noted the beneficial effect of microsympathectomy specifically with reference to a condition with a large inflammatory component. The analgesic effect of BiTox/A was most prominent in neuropathic conditions which do not have a strong inflammatory component (Mangione et al., 2016). Overall, it is therefore unlikely that an action at autonomic neurons is the mechanism by which BiTox/A is eliciting its analgesic effect.

3.3.3. The absence of cleaved SNAP25 in the dorsal root ganglia

Despite the SNAP25 cleavage detected at the peripheral nerve terminals, cleaved SNAP25 was not detected in dorsal root ganglia where the somas of the pseudopolar sensory neurons are located. Although all three methods used to detect SNAP25 cleavage employed only an N of one, each method repeatedly confirmed the absence of cleaved SNAP25 within the dorsal root ganglia, thus increasing the overall validity of this observation. This finding is not entirely surprising given that SNAP25 is a synaptic protein, involved in the release of neurotransmitter, and is thus more localised to the axons and axonal terminals, rather than the neuronal soma (Oyler et al., 1989; Tao-Cheng et al., 2000). Consequently, high levels of SNAP25 would not be expected in the dorsal root ganglia which could explain the absence of SNAP25 cleavage. It would thus be recommended to investigate the distribution of the SNAP25 in the dorsal root ganglia, by immunolabelling with the SNAP25 antibody, to determine whether this is the case.

Interestingly, Matak et al. (2011) investigated the analgesic effect of BoNT/A, following intraganglionic injection, after observing that peripheral injection of BoNT/A to the whisker pad of rats reduced formalin-induced orofacial pain and produced cleaved SNAP25 in the dorsal horn of the ipsilateral trigeminal nucleus caudalis. While they similarly observed a reduction in formalin-induced orofacial pain behaviours following intraganglionic injection, this effect was only observed when BoNT/A was injected two days prior to formalin challenge. BoNT/A injected 24 hours before the formalin test, or co-administered with colchicine, which blocks axonal transport, failed to elicit an antinociceptive effect. This consequently implies that the dorsal root ganglia are not the site of action for BoNT/A. Instead, the delay necessary to observe the analgesic effect indicates that BoNT/A still requires axonal transport to another area to produce analgesia, thus supporting the absence of cleaved SNAP25 in the DRG reported here.

3.3.4 BiTox/A does produce SNAP25 cleavage at the central spinal cord

In contrast, whilst investigating whether BiTox/A might have a centrally-mediated analgesic effect, cleaved SNAP25 was found readily detected at the level of the spinal cord, specifically concentrated around lamina IX of the ipsilateral ventral horn, as reported previously following intraplantar injection of native BoNT/A (Matak et al., 2012, 2017; Drinovac et al., 2016). Comparable to other studies that investigated native BoNT/A, sparse individual nerve fibres, displaying cleaved SNAP25 immunolabelling, were identified within the ipsilateral dorsal horn after intraplantar injection of BiTox/A (Matak et al., 2011, 2012, 2017; Drinovac et al., 2016). This strongly suggests that axonal transport of BiTox/A to the central nervous system does occur. Notably, cleaved SNAP25 was not detected within the motor neuron cell bodies, as delineated by NeuN, but instead appeared to be present in a network of nerve fibres, surrounding the motor neurons, hypothesised to be interneurons.

Cai et al. (2017) dispute this observation, claiming that cleaved SNAP25 is instead confined within the dendritic arborisations of the motor neuron pool. They were able to demonstrate this by injecting Cholera toxin B subunit Alexa Fluor 488 conjugate (CTB-488), a neuronal tracer, used to label the motor neurons of the ventral horn, and showed that this colocalised with the cleaved SNAP25 immunostain. There were, however, many fibres displaying cleaved SNAP25 that did not colocalise with CTB-488. Similar to the findings reported here, cleaved SNAP25 was visualised adjacent to the plasma membrane, outside of the external edge of the NeuN stain here, and the CTB-488 stain in their study. This cleaved SNAP25 staining appeared to look like end-feet, projecting to the motor neurons, which they did not acknowledge or account for. As stated earlier,

SNAP25 is a synaptic protein and therefore it would be expected that SNAP25 would be concentrated at the axonal terminals, and not at the plasma membrane of the cell soma (Tao-Cheng et al., 2000) as Cai et al. (2017) suggest.

Cleaved SNAP25 being contained solely within the motor neuron dendritic arborisations seems unlikely given the expanse and density of the cleaved SNAP25 stain. Specifically, at L5, the cleaved SNAP25 staining can be seen extending into the white matter of the spinal cord, as well as in single fibres projecting up to the dorsal horn. This data instead suggests that BiTox/A might transcytose into second order neurons. Evidence for the transcytosis of BoNT/A has been already provided by two separate studies (Antonucci et al., 2008; Restani et al., 2011). For example, Restani et al. (2011) demonstrated this by intravitreal injection of BoNT/A to the eye of rats which resulted in detectable cleaved SNAP25 in the tectum. 3 days post-BoNT/A intraocular injection, the optic nerve was severed, thus preventing any further axonal transport of BoNT/A protease before BoNT/E was then injected directly into the tectum. BoNT/E also cleaves SNAP25, however, BoNT/E removes 26 amino acids from the c-terminal, whereas BoNT/A only cleaves a 9 amino acid fragment. This enables the two cleavage products to be easily distinguished. After injection of BiTox/E, BiTox/A-cleaved SNAP25 was no longer detected in the tectum. BoNT/A-cleaved SNAP25 was, however, able to be detected again after the duration of action for BoNT/E had passed. The re-emergence of BoNT/A- cleaved SNAP25 indicated that the active protease had transcytosed into these second order neurons, rather than simply the BoNT/A cleavage product. Moreover, in both studies they were able to show that the cleavage of SNAP25 resulted from the axonal transport of BoNT/A, and not systemic spread, as SNAP25 cleavage was no longer detected following pre-injection of colchicine (Antonucci et al., 2008; Restani et al., 2011). Restani et al. (2011) also pre-emptively administered colchicine to the ipsilateral eye to show that detection of cleaved SNAP25 in the contralateral dorsal horn, likewise, relied upon axonal transport and discredited a systemic effect, thus contradicting Cai et al. (2017) who attributed the distal cleavage of SNAP25 to the systemic diffusion of BoNT/A.

Provided the limited amount of SNAP25 cleavage detected in the dorsal horn compared to the much larger amount of cleavage visualised in the ventral horn, the SNAP25 cleavage localised around the motor neurons could hold significance for the analgesic effect of BiTox/A. Although sensori-motor connectivity is described within the spinal cord, it is mainly concerned with the sensory input modulating reflexive responses elicited by the motor neurons (Cook and Woolf, 1985; Sivilotti and Woolf, 1994). Interestingly, however, repetitive transcranial magnetic stimulation (rTMS), targeted to the motor cortex, successfully produces analgesia in approximately 40% of refractory neuropathic pain patients (Lefaucheur et al., 2004, 2006, 2011, 2014; Lima and Fregni, 2008;

Nurmikko et al., 2016) whereas rTMS is ineffective against pain when targeted to the sensory cortex (Hirayama et al., 2006). It could thus be a possibility that modulation of the motor pathways, in the case of rTMS, the descending inhibitory motor pathways, could be beneficial in pain conditions.

In contrast, a range of behavioural studies have demonstrated the involvement of a number of neurotransmitters, specifically associated with pain signalling, in BoNT/A-induced analgesia including Substance P and its receptor, NK1 (Matak et al., 2017), GABA (Drinovac et al., 2014, 2016), and μ-opioids (Drinovac et al., 2013, 2016). Others have identified an anti-inflammatory component to the analgesic effect of BoNT/A, suggesting the involvement of Schwann cells (Marinelli et al., 2012), astrocytes (Marinelli et al., 2012; Vacca et al., 2012) and interleukins (Zychowska et al., 2016). Multiple studies have, however, contradicted this theory, reporting that there was no colocalisation of cleaved SNAP25 with GFAP, a marker of astrocytes, during immunostaining (Restani et al., 2011; Matak et al., 2012; Cai et al., 2017). Additionally, western blot analysis has further shown that BoNT/A has no effect on the expression of GFAP in the spinal cord or DRG (Zychowska et al., 2016).

The involvement of Substance P was recognised after using two strains of knockout mice. In one strain the gene encoding Substance P had been removed, whilst the other strain lacked the NK1 receptor gene (Matak et al., 2017). The anti-nociceptive effect of intraplantar BoNT/A in both an inflammatory pain model and a neuropathic pain model could not be replicated in either strain, hence implying that Substance P must have a role in the BoNT/A-induced analgesia. This is consistent with in vitro findings that incubation of neuronal cultures with BoNT/A inhibits the stimulated release of Substance P (Purkiss et al., 2000; Welch et al., 2000).

Conversely, GABA and μ-opioids were both implicated in the centrally-mediated therapeutic action of BoNT/A after intrathecal injection of GABA-A receptor antagonist, bicuculline, and μ-opioid receptor antagonist, naloxonazine, in rats, prevented the analgesic effect of BoNT/A against mechanical hypersensitivity in a mirror pain model (Drinovac et al., 2016). Furthermore, intraperitoneal injection of naloxonazine was also able to prevent the anti-nociceptive effect of BoNT/A in both a formalin inflammatory pain model and a sciatic nerve partial transection neuropathic pain model (Drinovac et al., 2013). Both experiments also demonstrated decreased formalin-evoked c-Fos activation in the dorsal horn of the spinal cord following intraplantar injection of BoNT/A. This effect was eliminated by knockout of substance P related genes (Matak et al., 2017) and separately, by injection of opioid antagonist, naltrexone (Drinovac et al., 2013) and GABA antagonist, bicuculline (Drinovac et al., 2014). None of these studies, however, investigated or demonstrated the colocalisation of cleaved SNAP25 with any markers of

the proteins mentioned. From this perspective, it would be recommended to conduct further immunolabelling of the spinal cord, isolated from BiTox/A-injected rats, to investigate whether any of the aforementioned proteins are co-expressed in the nerve fibres displaying cleaved SNAP25.

One study, however, argues that regardless, the amount of SNAP25 cleavage that occurs at the level of spinal cord is not sufficient to block neurotransmission at the central synapse (Lawrence et al., 2012). This was suggested after compartmentalised exposure of the neurites of cultured superior cervical ganglion neurons to native BoNT/A did not influence synaptic transmission between the cell bodies contained within the central compartment, despite that, at this time point, SNAP25 cleavage was readily detected in the cell soma. In contrast, global administration of BoNT/A to all culture chambers, consequently meaning that BoNT/A would gain direct access to the cell bodies, did significantly reduce the frequency of spontaneous excitatory postsynaptic currents, with currents completely abolished in four of the seven cells recorded (Lawrence et al., 2012). This suggests that although BoNT/A protease does reach the soma, it does not do so in sufficient amounts as to block neurotransmission.

This theory does, however, help to explain the lack of motor paralysis observed following intraplantar injection of BiTox/A (Ferrari et al., 2011; Mangione et al., 2016) and native BoNT/A (Cui et al., 2004; Matak et al., 2012; Wu et al., 2016), despite the SNAP25 cleavage noted in the ventral horn in both instances. Nevertheless, the study was conducted in vitro and, therefore, might not truly represent the actions of BoNT/A in vivo. For example, it has repeatedly been demonstrated that the anti-nociceptive effect of BoNT/A requires axonal transport after observing that injection of colchicine abolished BoNT/A-induced analgesia (Antonucci et al., 2008; Bach-Rojecky and Lacković, 2009; Matak et al., 2011, 2012; Restani et al., 2011; Wu et al., 2016). This provides strong evidence that BoNT/A does have a centrally mediated analgesic effect and further suggests that, in vivo, SNAP25 cleavage at the central level is adequate to block neurotransmission.

3.3.5 Cleaved SNAP25 is detected at the neuromuscular junction after peripheral injection of BiTox/A

With regards to the absence of any motor impairments following intraplantar injection of BiTox/A, it is important to acknowledge that cleaved SNAP25 was, however, detected at the neuromuscular junction, notably, of both the ipsilateral and contralateral hindpaw. This observation proved contrary to the theory proposed by Ferrari et al. (2011), that the increased molecular size of BiTox/A, compared to native BoNT/A, would negate its

access to the tight cleft of the NMJ. Instead, it appears that BiTox/A must still retain the ability to access the NMJ but may do so on a more restricted basis, provided the lack of paralysis observed. Specifically, the nerve terminals of the C- and Aδ nociceptors lack encapsulation and therefore could be more susceptible to penetration by BiTox/A, consequently creating a preference for binding of the sensory neurons above the motor neurons (Hall and Treinin, 2011). In future, however, more sensitive methods for the assessment of motor function should be used. For example, using the Digit Abduction Scale to systematically score digit spreading rather than a more subjective all or nothing approach (Broide et al., 2013), or by using CatWalk gait analysis to reveal any less obvious alterations in gait (Kappos et al., 2017).

The detection of cleaved SNAP25 at the NMJ of contralateral paw also raises concerns over systemic diffusion. It seems highly unlikely, however, that the protease would have arrived at the NMJ, following systemic diffusion, as cleaved SNAP25 was not detected in the sensory neurons of the contralateral paw. As described earlier, cleaved SNAP25 has previously been demonstrated in structures contralateral to the injection site. The appearance of cleaved SNAP25, contralateral to the injection site, was successfully prevented by pre-injection of colchicine, thus highlighting the role of axonal transport and transcytosis (Restani et al., 2011). Provided the importance of interconnectivity between the lumbar motor neuron pools for locomotion (Cazalets et al., 1995), it is feasible that BiTox/A could have transcytosed across these pathways to enter the contralateral motor neurons. This does, however, remain to be confirmed by injection of colchicine.

3.3.6 Conclusion

In conclusion, here, the first evidence for the cleavage of SNAP25 by BiTox/A in vivo has been successfully demonstrated. Although not definitively shown, after considering both the data presented here, and the evidence discussed with respect to native BoNT/A, it is most likely that BiTox/A is eliciting its therapeutic effect, via both a peripheral and a centrally-mediated mechanism. It is likely that by blocking neurotransmission in the peripheral sensory afferents, BiTox/A also indirectly prevents central sensitisation (Aoki, 2005). Future experiments are, however, necessary to effectively demonstrate this hypothesis. Further immunolabelling of the spinal cord sections will be required to determine which subtypes of central neurons BiTox/A is catalytically active in. This labelling should primarily be based on the observations made during the behavioural studies by Matak et al. (2017) and Drinovac et al. (2013, 2014, 2016) and should include co-staining of cleaved SNAP25 with anti-GAD65 (a marker for GABAergic neurons), anti-NK1 (a marker for Substance P receptors) and anti-MOR (a marker for μ-opioid

receptors) antibodies. It would also be beneficial to repeat the behavioural studies, detailed in Mangione et al. (2016), whilst including a pre-emptive injection of colchicine to confirm that the analgesic effect of BiTox/A is at least partly dependent upon a central mechanism. This will also verify that any central or contralateral cleaved SNAP25 staining observed does result from axonal transport of the active protease, and not from systemic diffusion. During these behavioural studies, additional motor assessments should also be carried out to ensure that any subtler motor impairments have not gone undetected. After conducting the further experiments detailed, the true significance of the enzymatic activity observed can then be appropriately deduced.

Chapter 4. The substitution of the receptor binding domain of Botulinum Neurotoxin A with that of alternative botulinum serotypes targets the enzymatic activity of Botulinum Neurotoxin A to additional subpopulations of sensory neurons

4.1 Introduction

It was recently demonstrated that intraplantar injection of BiTox/A, investigated in the previous chapter, prevents the development of, and reverses, the mechanical hyperalgesia observed in a rat model of peripheral neuropathic pain (Mangione et al., 2016). Unfortunately, however, the therapeutic application of BiTox/A in inflammatory pain conditions appears to be more limited. BiTox/A promoted a prolonged reduction in secondary hyperalgesia in an inflammatory pain model but was largely ineffective at reversing thermal hypersensitivity at the site of injury. Secondary hyperalgesia is hypothesised to result from the Aβ-fibres of low-threshold mechanoreceptors gaining access to the nociceptive signalling pathway, as a result of central sensitisation (Cervero et al., 2003; Latremoliere and Woolf, 2009). This suggests that the analgesic benefits of BiTox/A are largely due to its actions at the large Aβ-fibres rather than C-fibre nociceptors which would be activated direct at the site of injury. To effectively treat inflammatory pain conditions, it is thus necessary to retarget BiTox/A to a different subpopulation of sensory neurons, namely the nociceptors.

One way by which to achieve this is by utilising the other serotypes of Botulinum Neurotoxin (BoNT), of which seven exist, BoNT/A-G. The different serotypes are known to bind to different combinations of polysiagangliosides and membrane proteins, due to variations in the amino acid sequence of the Hc domain (Tsukamoto *et al.*, 2005; Montal, 2010; Strotmeier *et al.*, 2010). For example, BoNT/A binds to the ganglioside GT1b, and preferentially, the protein receptor, synaptic vesicle 2C (SV2C), although it does retain affinity for all three isoforms (SV2A, SV2B and SV2C) (Rummel et al., 2004; Dong et al., 2006; Rossetto, 2017). BoNT/E meanwhile, also displays affinity for GT1b but only binds two of the synaptic vesicle isoforms, SV2A and SV2B (Dong et al., 2008; Montal, 2010; Rossetto, 2017). Conversely, BoNT/C binds to GD1b, in addition to GT1b, but does not require a protein receptor for internalisation (Tsukamoto et al., 2005; Rummel et al., 2009). Similarly, there is no known protein receptor for BoNT/D (Rummel et al., 2009) and it further lacks the ganglioside-binding pocket present in the other serotypes. Instead, BoNT/D is believed to utilise the phospholipid, phosphatidylethanolamine (Tsukamoto et al., 2005).

The differential ganglioside binding profiles of the BoNT serotypes suggests that they would display different patterns of neuronal binding, dependent on the expression of

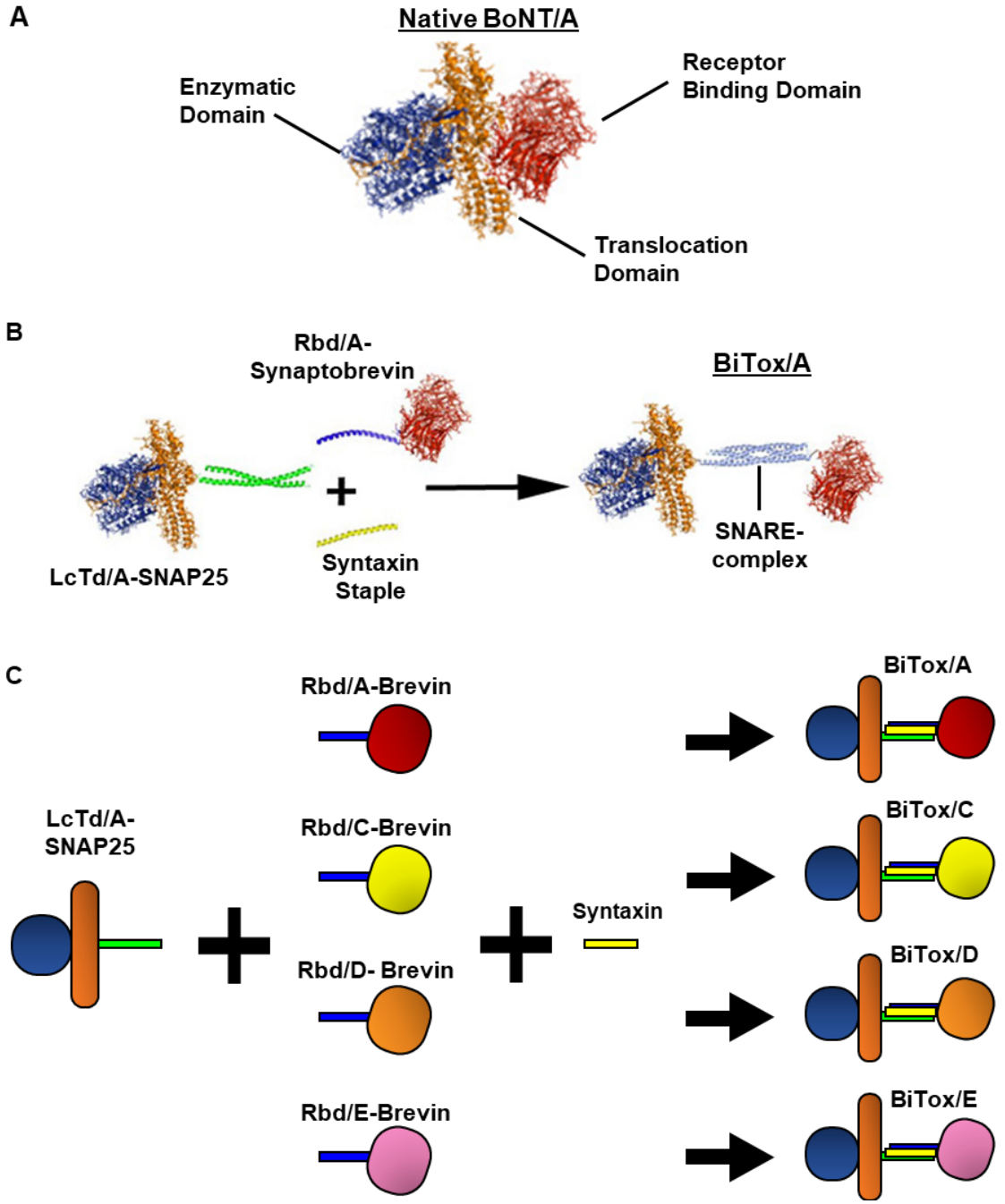

Figure 4.1 SNARE-tagging and stapling enables the production of alternative BiTox chimeras. ***(A)*** *Native BoNT/A consists of an enzymatic domain (light chain, Lc, blue), a translocation domain (Td, orange) and a receptor binding domain (Rbd, red).* ***(B)*** *For SNARE-stapling, BoNT/A was separated into the LcTd/A (blue, orange) and the Rbd/A (red). LcTd/A was expressed fused with a SNAP25 tag (green), whilst Rbd/A was expressed fused to synaptobrevin (blue). The chimera, BiTox/A (right), was produced after addition of the syntaxin staple (yellow). The assembled SNARE-complex is visible central to the chimera.* ***(C)*** *To generate the alternate BiTox chimeras, the Rbd of other serotypes were separately expressed fused to synaptobrevin (-brevin), as depicted in the schematic. Importantly, LcTd/A-SNAP25 and syntaxin were used consistently in the formation of each chimera. The substitution of Rbd/A-Brevin for Rbd/C-Brevin, Rbd/D-Brevin and Rbd/E-Brevin produces BiTox/C, BiTox/D and BiTox/E, respectively (Right). The clostridial chimera molecular model was created using the following structures, accessible in the Protein Data Bank archive (http://www.rcsb.org): 3BTA (BoNT/A), 1N7S (SNARE complex).*

certain gangliosides and protein receptors by different subpopulations of sensory neurons (Ashton et al., 1990; Bajjalieh et al., 1994). The receptor binding domains of the botulinum serotypes could thus be utilised to selectively retarget the enzymatic activity of BoNT/A to specific subpopulations of sensory neurons, including those involved in inflammatory pain.

Here, it will be investigated whether retargeting BoNT/A by recombining the cleavage promoting, enzymatic domain of BoNT/A, with the receptor binding domain (Rbd) of alternative botulinum serotypes, will alter the population of sensory neurons to which BoNT/A natively targets, and furthermore, whether this will augment its analgesic properties.

4.2. Results

4.2.1 Stapling the Light Chain Translocation Domain of Botulinum Neurotoxin A to the Receptor Binding domain of alternative botulinums results in functional toxins which retain the ability to cleave SNAP25 in vitro

The Light Chain-Translocation domain of Botulinum Neurotoxin A (LcTd/A), containing the enzymatic domain, was recombined with the receptor binding domain (Rbd) of BoNT/A, using our established stapling technology, to create the previously published BiTox/A (Fig. 4.1B) (Ferrari et al., 2011). LcTd/A was further conjugated to the Rbd of alternative botulinum neurotoxin serotypes C, D and E, to produce the chimeras: BiTox/C, BiTox/D and BiTox/E, respectively (Fig. 4.1C). LcTd/A contains the zinc-endopeptidase activity of BoNT/A which mediates the cleavage of SNAP25. The functionality of the novel chimeras was first assessed to evaluate whether they retained the catalytic activity of LcTd/A after reengineering.

Western blot revealed that after 65 hour incubation with 10 nM of each chimera, all four novel chimeras successfully produced SNAP25 cleavage in dissociated dorsal root ganglion cultures (Fig. 4.2A) confirming that they retained their efficacy. Incubation with 10 nM LcTd/A-αSNAP25, containing only the enzymatic activity of BoNT/A, without any targeting domain, also resulted in detectable SNAP25 cleavage, however, the percentage of total SNAP25 cleaved was significantly lower than that observed after incubation with the engineered chimeras, with the exclusion of BiTox/E (One-way ANOVA, $F_{(5,\ 18)}$=22.61; BiTox/A vs. LcTd/A-αSNAP25, P<0.05; BiTox/C vs. LcTd/A-αSNAP25, P<0.01; BiTox/D vs. LcTd/A-αSNAP25, P<0.05; BiTox/E vs. LcTd/A-αSNAP25, P=0.18, Fig. 4.2B). No cleavage was detected following the addition of 0.4% OG, the vehicle control that peptide staples are dissolved in to enable the formation of chimeras, or in untreated cultures.

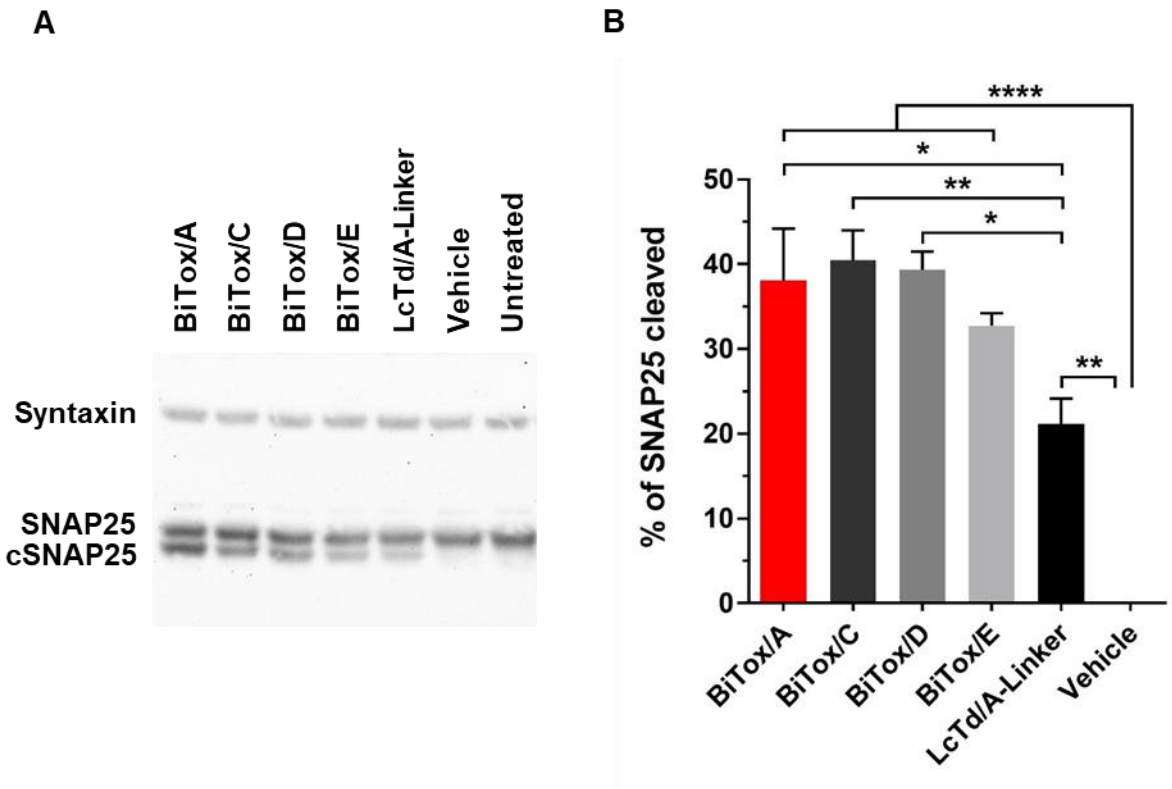

Figure 4.2 Clostridial chimeras containing LcTd/A retain the catalytic activity of BoNT/A in vitro. (A) *Western blots of dorsal root ganglion cultures were probed with a whole SNAP25 antibody following 65 hour incubation with 10 nM of each Chimera (N=4). Cleaved SNAP25 was detectable in all cultures incubated with active chimeras but was absent in untreated cultures and cultures incubated with 0.4% OG vehicle control. Syntaxin was included as a loading control.* ***(B)*** *The graph shows cleaved SNAP25 expressed as a percentage of total SNAP25, after quantification of the immunoblots. In the chimeras BiTox/A-/D, the conjugation of a Rbd to LcTd/A increased the percentage of SNAP25 cleaved compared to unconjugated LcTd/A-αSNAP25. All data is presented as mean ± S.E.M, * p<0.05, ** p<0.01, **** p<0.0001.*

Notably, Syntaxin 1 was chosen as a loading control. Syntaxin is an essential component of the SNARE complex and therefore is indicative of the number of SNARE complexes in the culture (Wilhelm et al., 2014). Syntaxin levels remained consistent between culture conditions, thus indicating that the separate cultures had a similar level of SNARE proteins available for cleavage.

4.2.2 The biodistribution of cleaved SNAP25 in cultured dorsal root ganglion neurons following incubation with alternative BiTox constructs suggests that substitution of Rbd/A can target the enzymatic activity of BoNT/A to additional sensory neuron subpopulations.

After confirming that the novel chimeras remained potent, it was next assessed whether the attachment of an alternative receptor binding domain was able to retarget the catalytic activity of LcTd/A to different subpopulations of sensory neurons. After 65 hour incubation with 10 nM of each chimera, an inhouse anti-cleaved SNAP25 antibody, specific for cleaved SNAP25 and lacking immunoreactivity for whole SNAP25, was used to report the proteolytic activity of LcTd/A in healthy, viable sensory neurons, as identified using anti-βTubulin III antibody, a pan-neuronal marker, in combination with DAPI, a nuclear marker.

Immunolabelling of dorsal root ganglion cultures indicated that the novel chimeras, BiTox/C, /D and /E, did not produce SNAP25 cleavage in a significantly distinct population of sensory neurons, based on soma size, compared to BiTox/A (One-way ANOVA, $F_{(4,154)}$ =2.265, P=0.065, Fig. 4.3A). BiTox/C did cleave SNAP25 in neurons with a slightly larger mean cell diameter (29.7 ± 1.5 µm) than BiTox/A (27.6 ± 1.3 µm), although the difference was not significant. Cleaved SNAP25 was, however, detected in a smaller percentage of neurons following incubation with BiTox/C, opposed to BiTox/A (Fig. 4.3B). Again, this difference was not significant (One-way ANOVA, $F_{(6,24)}$ = 3.589, P=0.772).

In contrast, SNAP25 cleavage was detected in a slightly larger percentage of neurons following incubation with BiTox/D than after incubation with BiTox/A (Fig. 4.3B). The mean cell diameter of neurons displaying SNAP25 cleavage after incubation with BiTox/A and BiTox/D was very similar (27.6 ± 1.3 µm and 27.3 ± 1.2 µm respectively, Fig. 4.3A), however, the distribution of neurons displaying cleaved SNAP25 differed between the two. Neurons displaying positive SNAP25 cleavage post-incubation with BiTox/A, as well as with BiTox/C, were mainly congregated at the upper values of the histogram whereas the distribution of neurons displaying SNAP25 cleavage after incubation with BiTox/D appeared almost bimodal with one peak visible around 18 µm and a second around 26-28 µm (Fig. 4.4B). Conversely, the neurons positive for cleaved SNAP25 after incubation with BiTox/E were evenly distributed between 20 and 30 µm.

In accordance with this observation, the average cell diameter of neurons showing SNAP25 cleavage after incubation with BiTox/E was 25.0 ± 2.0 µm suggesting that BiTox/E binds to a population of smaller sensory neurons than BiTox/A. Incubation with BiTox/E, however, resulted in an approximately 60% reduction in the number of neurons displaying SNAP25 cleavage compared to after incubation with BiTox/A. Even so, this difference was not shown to be significant (One-way ANOVA, $F_{(6,24)}$ = 3.589, P=0.217).

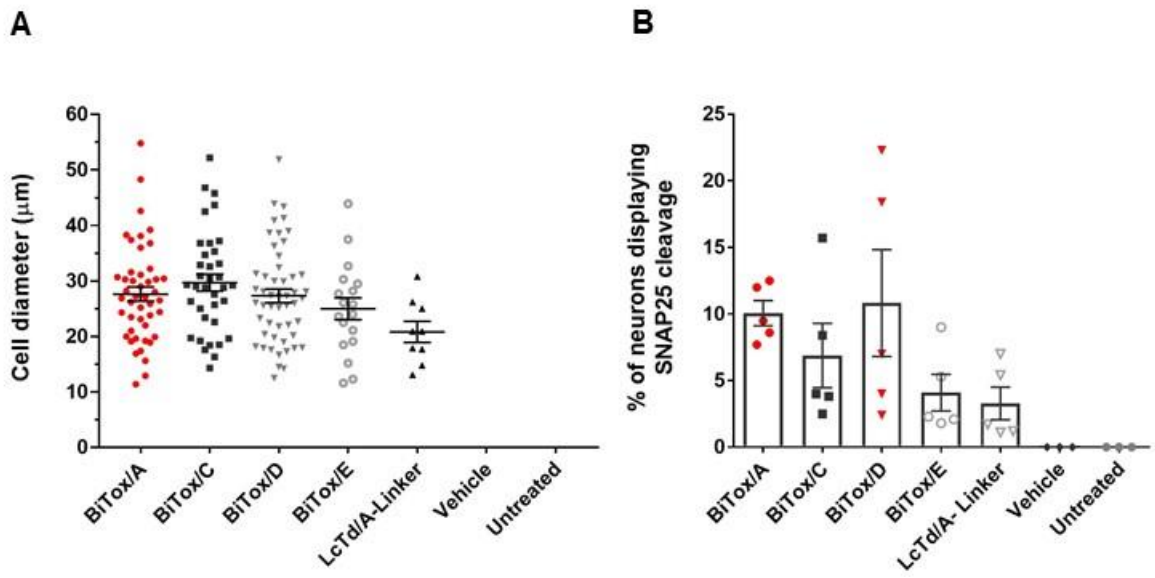

Figure 4.3 Substitution of BoNT/A Rbd with the Rbd from alternative BoNT serotypes does not significantly alter the targeting of the enzymatic activity BoNT/A to other subpopulations of sensory neurons. (A) *10 nM of each chimera was added to 2 day old dorsal root ganglion cultures and incubated for a further 65 hours (BiTox/A - BiTox/E, LcTd/A-αSNAP25: N=5, n=3; Untreated, 0.4% OG: N=3, n=3). Neurons were identified using pan-neuronal marker, βTubulin III. Incubation with BiTox/A resulted in SNAP25 cleavage, as detected using anti-cleaved SNAP25 antibody, in neurons with a soma diameter of 27.6 ± 1.3 μm. BiTox/C (29.7 ± 1.5 μm) and BiTox/D (27.3 ± 1.2 μm) failed to result in SNAP25 cleavage in a significantly different population of neurons. There was a trend for BiTox/E (25.0 ± 2.0 μm) and LcTd/A-αSNAP25 (20.8 ± 1.9 μm) to produce SNAP25 cleavage in neurons with a smaller mean cell diameter.* ***(B)*** *The number of neurons displaying detectable SNAP25 cleavage was expressed as a percentage of the total number of neurons identified in each culture. The percentage of neurons displaying SNAP25 was not significantly affected by the substitution of Rbd/A for the Rbd of another botulinum serotype. All data is presented as mean ± S.E.M.*

Similarly, 10 nM LcTd/A-αSNAP25 produced SNAP25 cleavage in neurons with a smaller average cell diameter (20.8 ± 1.9 μm), and in a yet smaller percentage of neurons (3.3 ± 1.2 %) than BiTox/A. Although, again, neither difference was significant (One-way ANOVA for cell diameter, $F_{(4,155)}$ =2.265, P=0.1054, Fig. 4.3A; One-way ANOVA for % of neurons displaying SNAP25 cleavage, $F_{(6,24)}$ = 3.589, P=0.1297, Fig. 4.3B). No trend in the cell diameter of neurons displaying cleaved SNAP25 was observed after incubation with LcTd/A-αSNAP25. Instead, cells displaying positive cleaved-SNAP25 staining appeared randomly throughout the frequency distribution histogram, thus supporting the hypothesis that a receptor binding domain is required for specific binding and internalisation into discreet neuronal subpopulations (Fig. 4.4B).

In agreement, a previous study showed that the LcTd portion of BoNT alone, is sufficient for entering neurons (Fischer et al., 2008). The LcTd is believed to exploit the constitutive endocytic pathway, to gain access to cells, rather than undergoing receptor-mediated endocytosis, normally associated with BoNTs. This mechanism is augmented by the presence of the attached -αSNAP25 peptide. This would most likely interact with the other components of the SNARE complex that might become exposed at the cell membrane, post-exocytosis, thus aiding nonspecific uptake into cells. The Rbd is instead only necessary to act as a chaperone, mediating neuronal specificity, and increasing the efficiency of neuronal uptake, hence explaining the lower percentage of neurons displaying SNAP25 cleavage. Being satisfied by this explanation, together with only being interested in determining a way to direct the LcTd/A of BiTox/A to specific, alternate populations of neurons, the binding profile of LcTd/A-αSNAP25 was not further investigated. Importantly, cleaved SNAP25 staining was not observed in cultures incubated with vehicle or in untreated cultures, thereby confirming that SNAP25 cleavage resulted from the addition of active protease to the cultures.

In summary, although certain trends were noted, none of the observed differences were shown to be significant. This lack of significance could be due to the negatively skewed distribution of the cell soma size observed in DRG cultures. This skew can be clearly seen in the frequency distribution histograms (Fig. 4.4B). The data sets display a natural bias towards smaller diameter neurons. This is because the protocol used to prepare DRG cultures favours the yield of smaller neurons, opposed to larger diameter neurons, as the larger neurons are more prone to being ruptured and lost during the trituration steps. Therefore, even if SNAP25 cleavage is detected in a very small proportion of small diameter neurons, it could severely distort the mean cell diameter of neurons displaying cleaved SNAP25, mitigating any perceived difference between the alternative BiTox constructs. For this reason, it was important to investigate the two populations of neurons, the larger myelinated neurons and the small unmyelinated neurons, separately. The neuronal markers, Neurofilament 200 and Peripherin, were used to identify and distinguish the two populations of neurons, respectively (Goldstein et al., 1991; Fornaro et al., 2008).

4.2.3 Cleaved SNAP25 is detected in a subpopulation of smaller myelinated sensory neurons after substitution of Rbd/A for the Rbd of alternative serotypes.

Anti-Neurofilament 200 antibody recognises heavy weight (200 kDa) neurofilament and is used to identify myelinated fibres. It labels large Aβ sensory neurons as well as more thinly myelinated Aδ sensory neurons. Both are described as large-light coloured

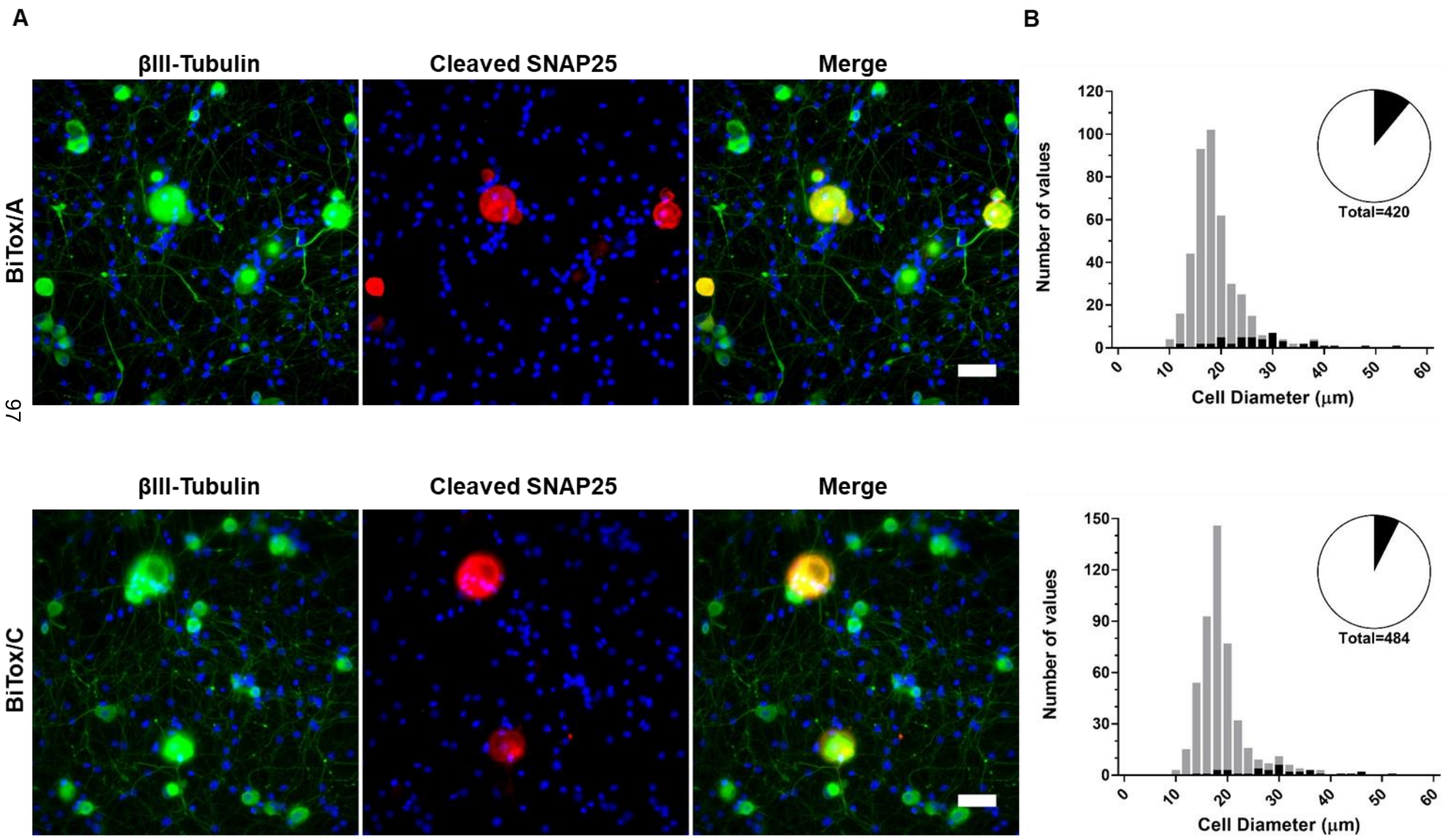
A
B
βIII-Tubulin
Cleaved SNAP25
Merge
BiTox/A
BiTox/C
Number of values
Cell Diameter (μm)
Total=420
Total=484

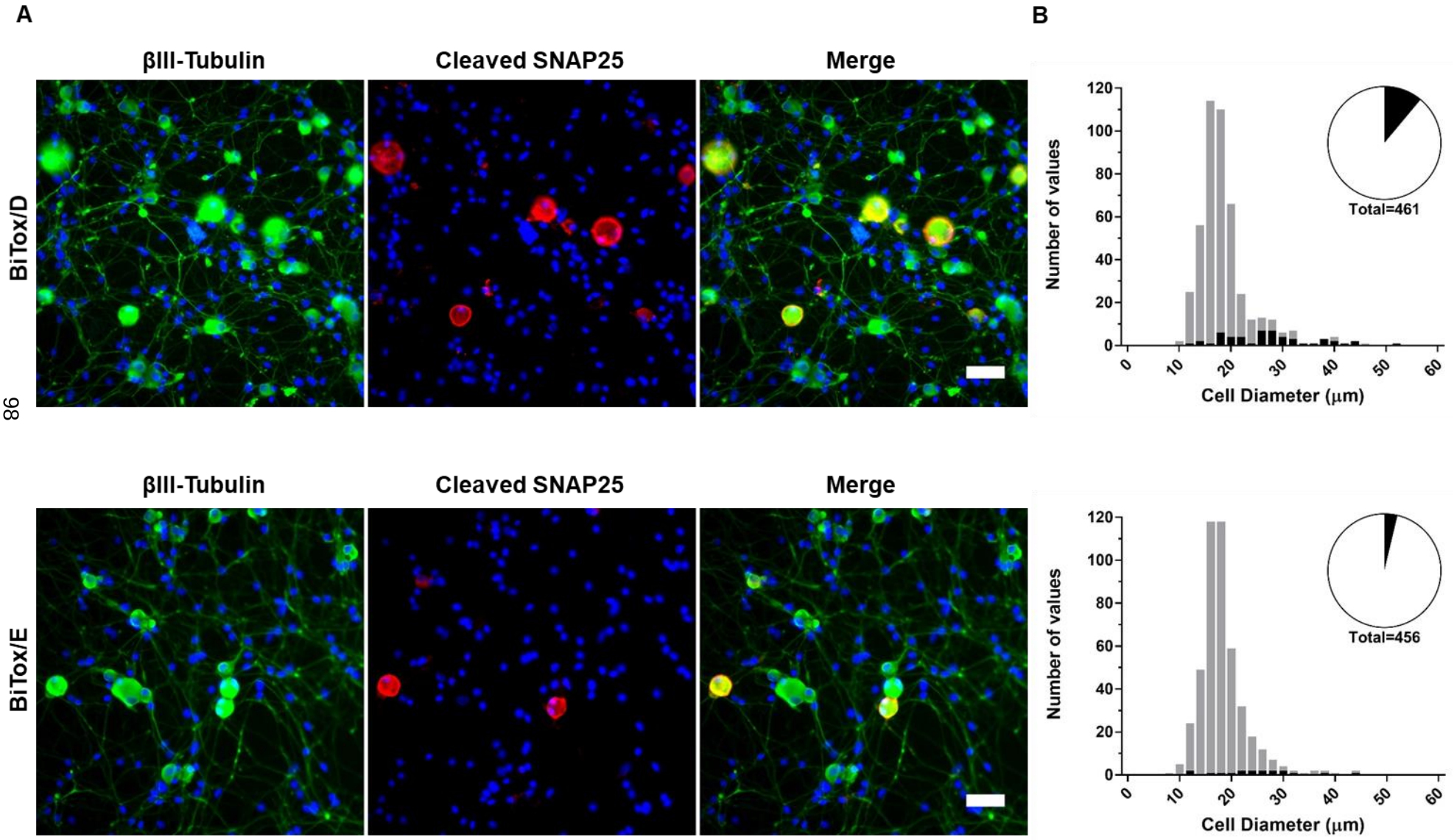
A
B
βIII-Tubulin
Cleaved SNAP25
Merge
BiTox/D
BiTox/E
Number of values
Cell Diameter (μm)
Total=461
Total=456
0
10
20
30
40
50
60
0
20
40
60
80
100
120

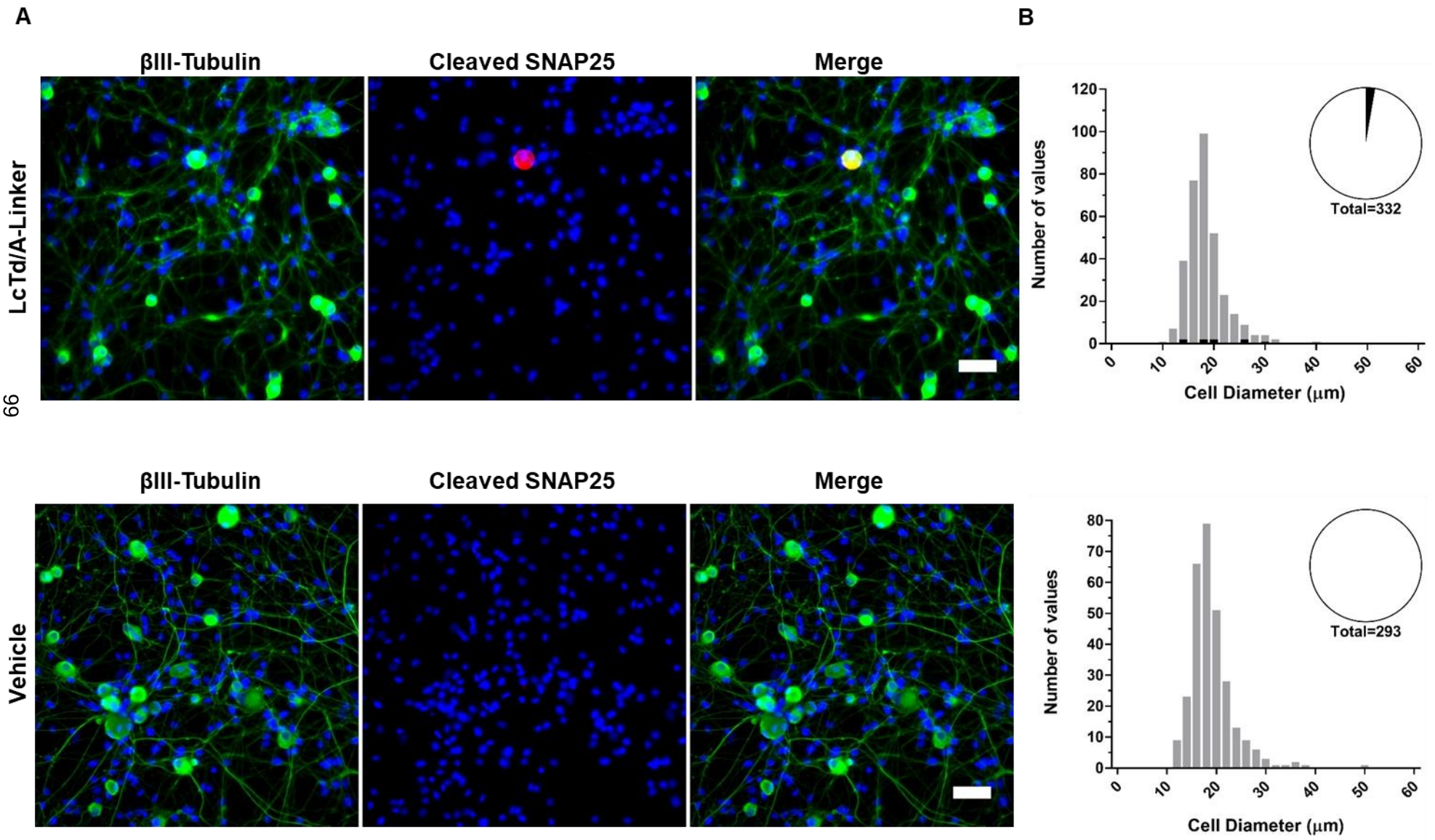
A
βIII-Tubulin
Cleaved SNAP25
Merge
LcTd/A-Linker
βIII-Tubulin
Cleaved SNAP25
Merge
Vehicle
B
Number of values
Cell Diameter (μm)
Total=332
Number of values
Cell Diameter (μm)
Total=293

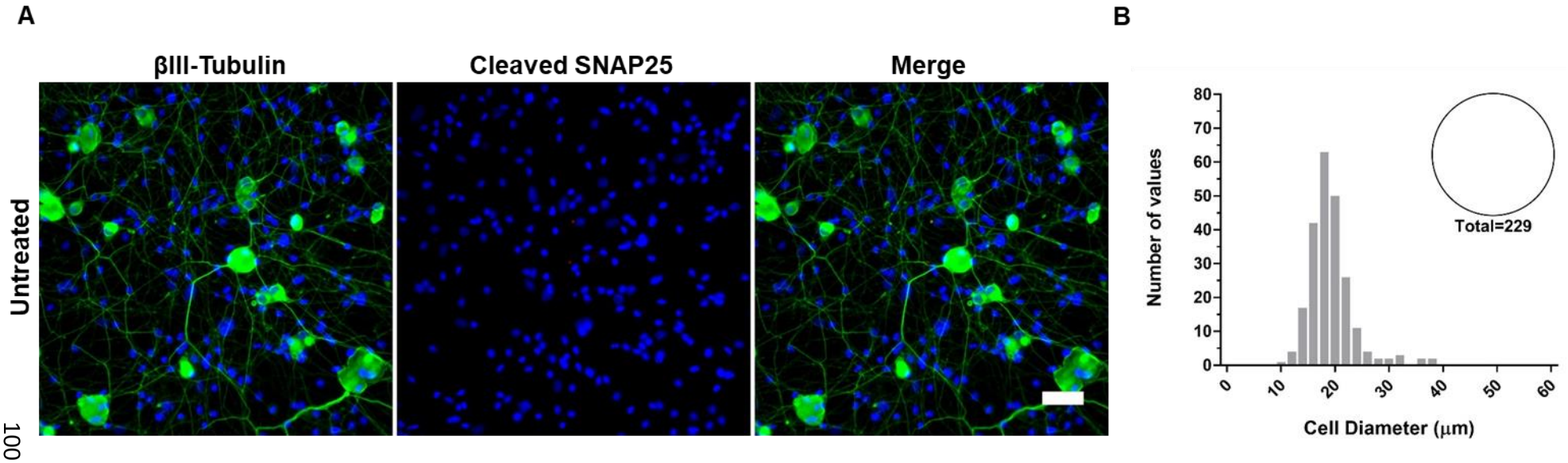

Figure 4.4 Representative images of cleaved SNAP25 staining in chimera-treated dorsal root ganglion cultures (A) *Representative images taken using an epifluorescent microscope of the immunocytochemical staining of cleaved SNAP25 (red) in neurons (green), identified using pan-neuronal marker, βTubulin III, following 65 hour incubation with each chimera (BiTox/A - BiTox/E, LcTd/A-αSNAP25: N=5, n=3; Untreated, 0.4% OG: N=3, n=3). The viability of neurons was confirmed by the presence of a healthy, intact nucleus using DAPI stain (blue).* ***(B)*** *The frequency distribution histograms generated show the distribution of the soma diameter of neurons displaying SNAP25 cleavage (black) following incubation with the different chimeras, compared to the total population of identified neurons, which were negative for cleaved SNAP25 (grey). The pie charts in the top right corner of the histograms illustrate the percentage of the neurons, labelled positively for cleaved SNAP25 (black), from the total number of neurons identified. Scale bar=50 μm.*

neurons. It does not, however, show immunoreactivity for unmyelinated C-fibres (Lawson et al., 1984; Lawson and Waddell, 1991).

After using anti-NF200 antibody to isolate only the myelinated neurons, it was shown that substituting the Rbd/A of BiTox/A for that of other serotypes had a significant effect on the mean cell diameter of NF200-positive neurons, displaying cleaved SNAP25 (One-way ANOVA, $F_{(3,120)} = 6.291$, P=0.0005, Fig. 4.4A). SNAP25 cleavage was detected in a subpopulation of significantly smaller NF200-positive neurons after 65-hour incubation with BiTox/D (23.7 ± 1.2 µm) and BiTox/E (20.6 ± 1.3 µm), compared to BiTox/A (28.2 ± 1.2 µm) (One-way ANOVA, *Dunnett's multiple comparisons test*, $F_{(3,120)} = 6.291$; BiTox/A vs BiTox/D P=0.0204; BiTox/A vs BiTox/E P=0.0002, Fig. 4.4A). More notably, the two peaks first observed in the frequency distribution histogram of neurons, identified using BTIII, and displaying SNAP25 cleavage after incubation with BiTox/D (Fig. 4.4B), were

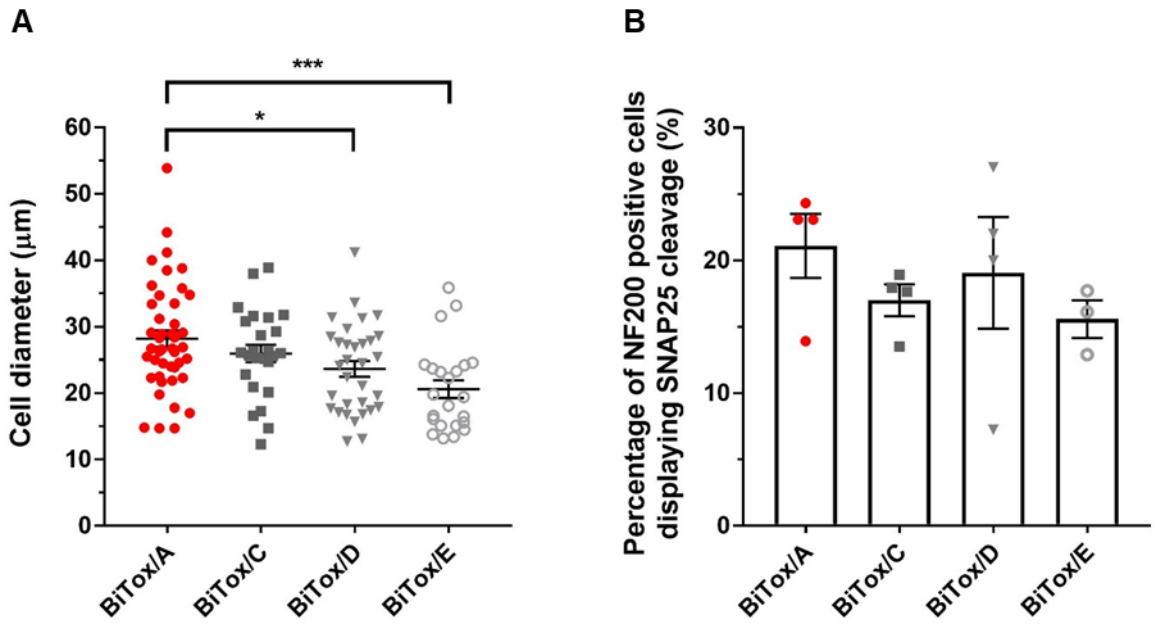

Figure 4.5 Cleaved SNAP25 is detected in a subset of smaller myelinated (Aβ and Aδ) fibre sensory neurons after substitution of Rbd/A for the Rbd of alternative serotypes. *10 nM of each chimera was added to 2 day old dorsal root ganglion cultures and incubated for a further 65 hours (BiTox/A, -/C, -/D: N=4, n=3; BiTox/E: N=3, n=3).* ***(A)*** *Quantification of cleaved SNAP25 in myelinated neurons, identified using anti-neurofilament 200 antibody (NF200), revealed that BiTox/A (28.2 ± 1.2 µm) produced SNAP25 cleavage in a subset of significantly larger myelinated neurons compared to BiTox/D (23.7 ± 1.2 µm) and BiTox/ E (20.6 ± 1.3 µm).* ***(B)*** *Expressing the number of NF200-positive neurons co-labelled for cleaved SNAP25 as a percentage of the total number of NF200-positive neurons per culture revealed no significant differences between chimeras. All data is presented as mean ± S.E.M, * p<0.05, *** p<0.001.*

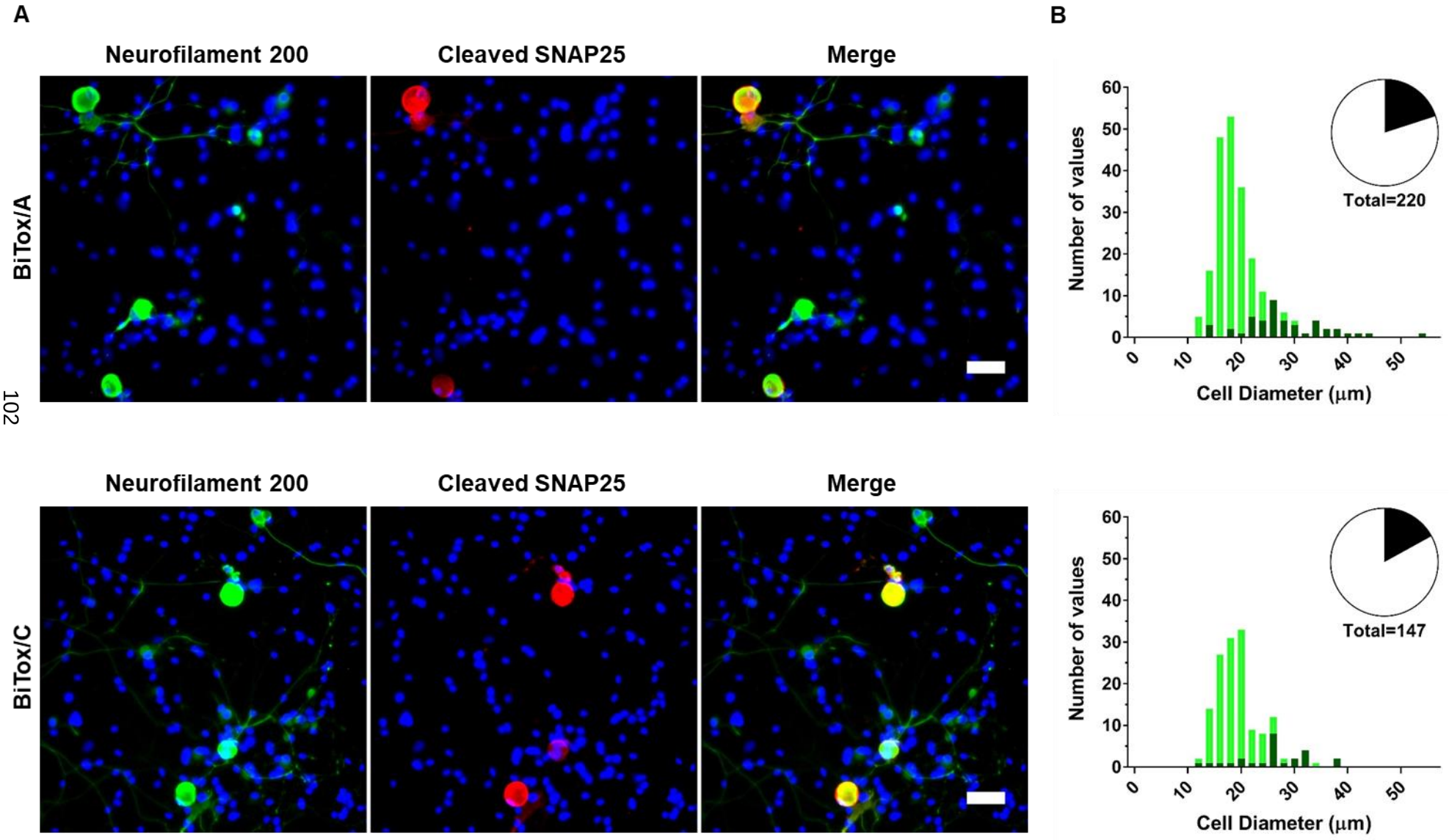
A
B
Neurofilament 200
Cleaved SNAP25
Merge
BiTox/A
BiTox/C
Number of values
Cell Diameter (μm)
Total=220
Total=147
0
10
20
30
40
50
60

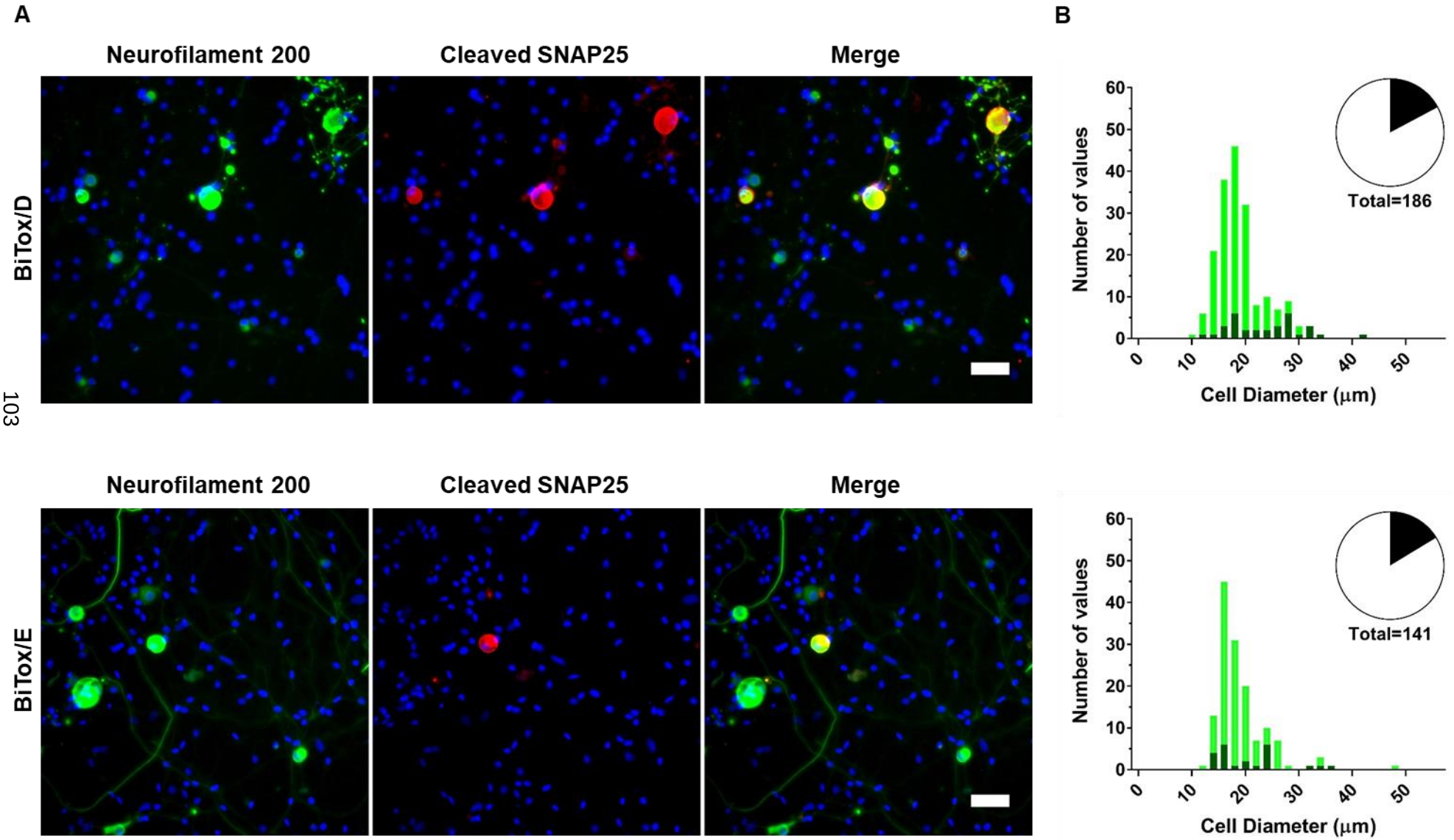
A
B
Neurofilament 200
Cleaved SNAP25
Merge
BiTox/D
BiTox/E
Number of values
Cell Diameter (μm)
Total=186
Total=141

Figure 4.6 Representative images of cleaved SNAP25 staining in myelinated dissociated sensory neurons. (A) *An epifluorescent microscope was used to take representative images of dorsal root ganglion cultures (BiTox/A, -/C, -/D: N=4, n=3; BiTox/E: N=3, n=3) showing the colocalisation of cleaved SNAP25 (red) and Neurofilament 200 (green) after 65 hr incubation of 2 day old cultures with BiTox/A-E. DAPI (blue) indicates the nucleus of cells.* ***(B)*** *Frequency distribution histograms illustrate the distribution of the cell diameter of NF200 positive neurons displaying cleaved SNAP25 (dark green) after incubation with the alternative chimeras, compared to NF200 positive neurons which were negative for cleaved SNAP25 (light green). The pie charts in the top right corner of the histograms illustrate the percentage of the neurons, labelled positively for cleaved SNAP25 (black), from the total number of NF200 positive neurons identified. Scale bar=50 µm.*

replicated in the BiTox/D histogram of NF200-positive neurons (Fig. 4.6B). There was no significant difference between the average cell diameter of neurons positively co-labelled for both NF200 and cleaved SNAP25, following incubation with BiTox/A and BiTox/C (One-way ANOVA, *Dunnett's multiple comparisons test*, P=0.4625). Furthermore, there was no significant difference in the percentage of NF200-positive neurons displaying cleaved SNAP25 between BiTox/A and any of the alternative BiTox constructs (One-way ANOVA, $F_{(3,11)} = 0.7355$, P= 0.5524, Fig. 4.5B).

4.2.4 SNAP25 cleavage is not detected in a significantly different subpopulation of small diameter neurons after substituting Rbd/A of BiTox/A for the Rbd of alternative serotypes.

Peripherin is a 57 kDa neuron-specific intermediate filament, predominantly expressed in the peripheral nervous system (Portier et al., 1983; Parysek and Goldman, 1988). With regards to the dorsal root ganglia, peripherin is preferentially expressed in the small, unmyelinated neurons and is thus used to characterise this subpopulation of sensory neurons (Parysek and Goldman, 1988; Ferri et al., 1990; Goldstein et al., 1991). Anti-peripherin antibody was therefore used to identify the small, unmyelinated neurons, namely the C-fibres nociceptors, after incubation with the alternative BiTox constructs, to investigate whether there were any similar, notable trends in the binding of unmyelinated neurons, and consequent cleavage of SNAP25, as was previously demonstrated in myelinated neurons.

Substitution of the Rbd/A in BiTox/A did not have a significant effect on the mean cell diameter of peripherin-positive neurons in which cleaved SNAP25 was detected (One-way ANOVA, $F_{(3,59)} = 1.806$, P= 0.1560, Fig. 4.7A). Incubation with BiTox/C did result in SNAP25 cleavage being visualised in neurons with a larger mean cell diameter (22.9 ±

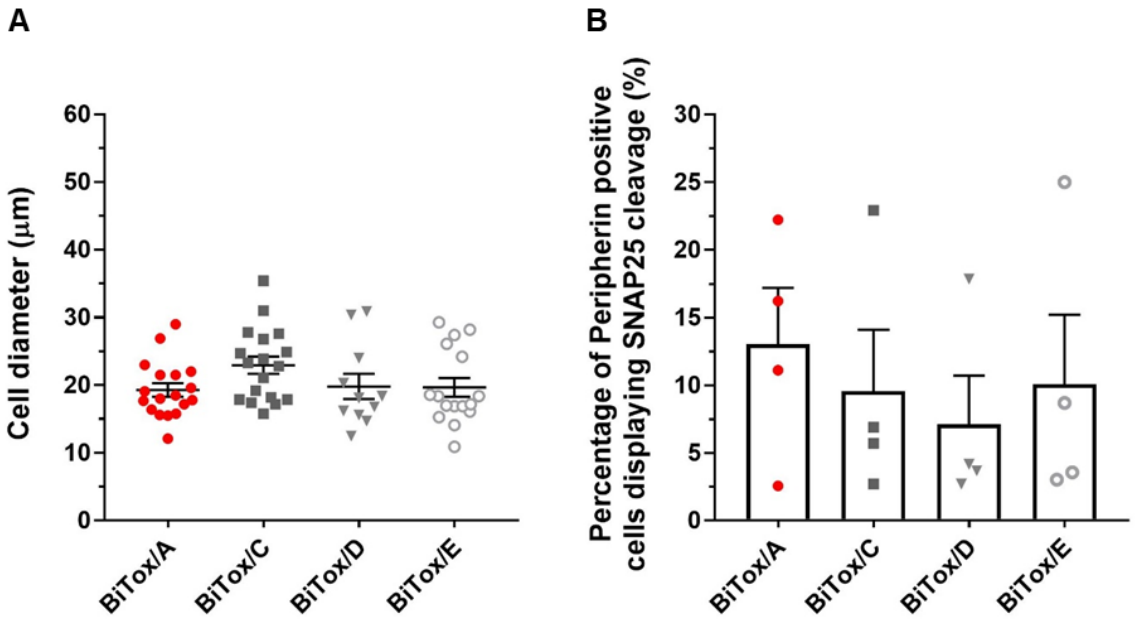

Figure 4.7 Substitution of Rbd/A does not influence the detection of cleaved SNAP25 in small diameter neurons. *10 nM of each chimera (BiTox/A-E) was added to 2 day old Dorsal root ganglion cultures (N=4, n=3) for a 65 hour incubation.* ***(A)*** *Immunolabelling of treated cultures using peripherin to identify the unmyelinated sensory neurons did not reveal any significant differences in the mean cell diameter of neurons colabelled for peripherin and cleaved SNAP25, dependent on treatment with an alternative chimera.* ***(B)*** *The number of neurons colabelled for peripherin and cleaved SNAP25 was calculated as a percentage of the total number of peripherin positive neurons per culture (N=4). Incubation with alternative chimeras did not significantly affect the percentage of colabelled neurons. All data is presented as mean ± S.E.M.*

1.3 µm) than BiTox/A (19.3 ± 1.3 µm) but this difference was not shown to be significant (One-way ANOVA, $F_{(3,59)} = 1.806$, P= 0.1040, Fig. 4.7A). Incubation with BiTox/D (19.8 ± 1.9 µm) and BiTox/E (19.7 ± 1.4 µm) produced SNAP25 in a subpopulation of peripherin-positive neurons with a very similar mean cell diameter to BiTox/A. Incubation with the alternative BiTox chimeras had no significant effect on the percentage of peripherin-positive neurons displaying cleaved SNAP25 (One-way ANOVA, $F_{(3,12)} = 0.3058$, P= 0.8208, Fig. 4.7B).

4.2.5 Intraplantar injection of BiTox/D is suspected to prolong thermal hyperalgesia in Complete Freund's Adjuvant rat model of inflammatory pain

Following the observations made in the previous experiments, BiTox/C was not pursued any further as it did not produce SNAP25 cleavage in a statistically different population of sensory neurons compared to BiTox/A. In contrast, both BiTox/D and -/E produced SNAP25 cleavage in a subpopulation of significantly smaller myelinated neurons.

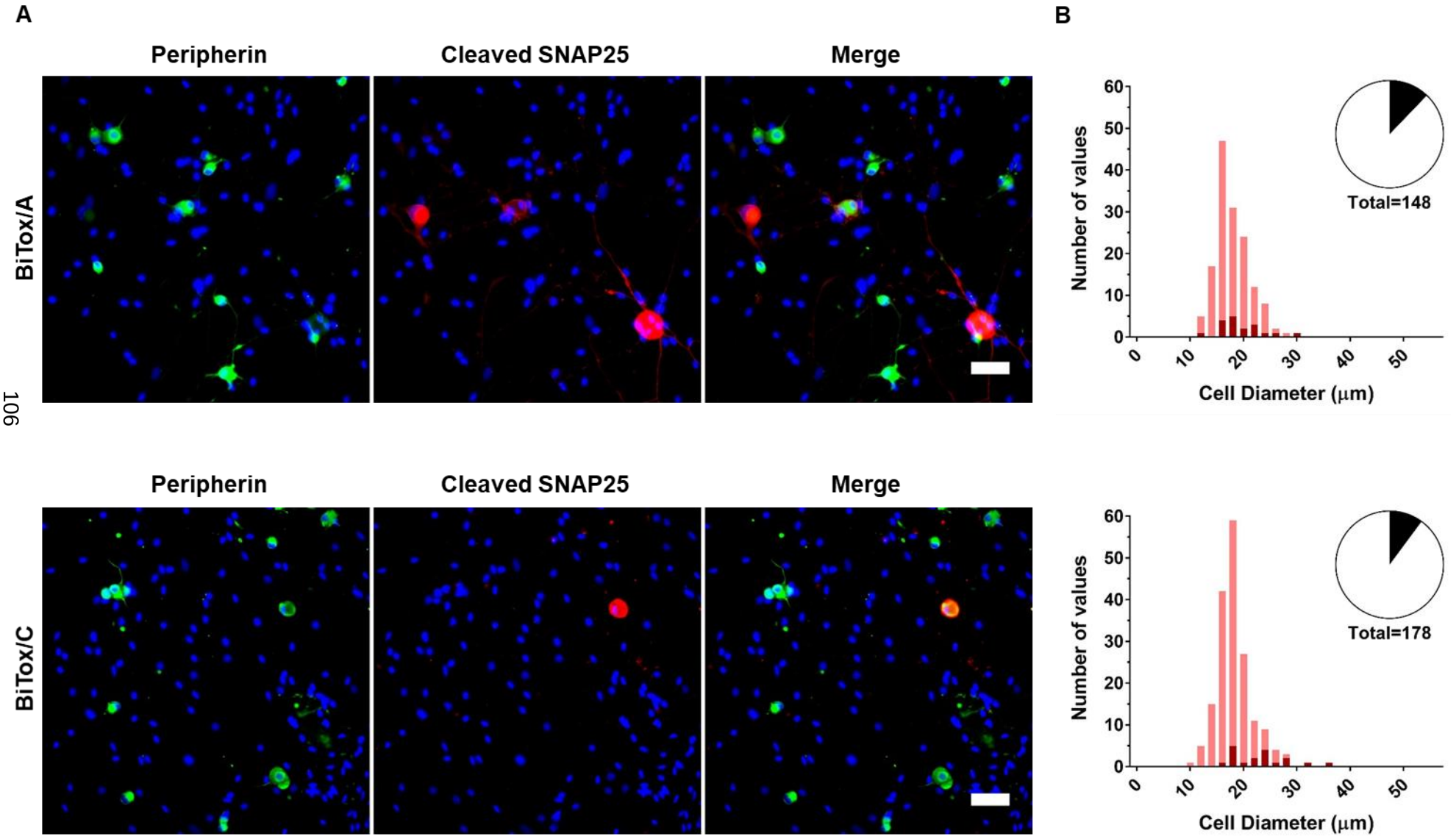
A
B
Peripherin
Cleaved SNAP25
Merge
BiTox/A
BiTox/C
Number of values
Cell Diameter (μm)
Total=148
Total=178
0
10
20
30
40
50
60

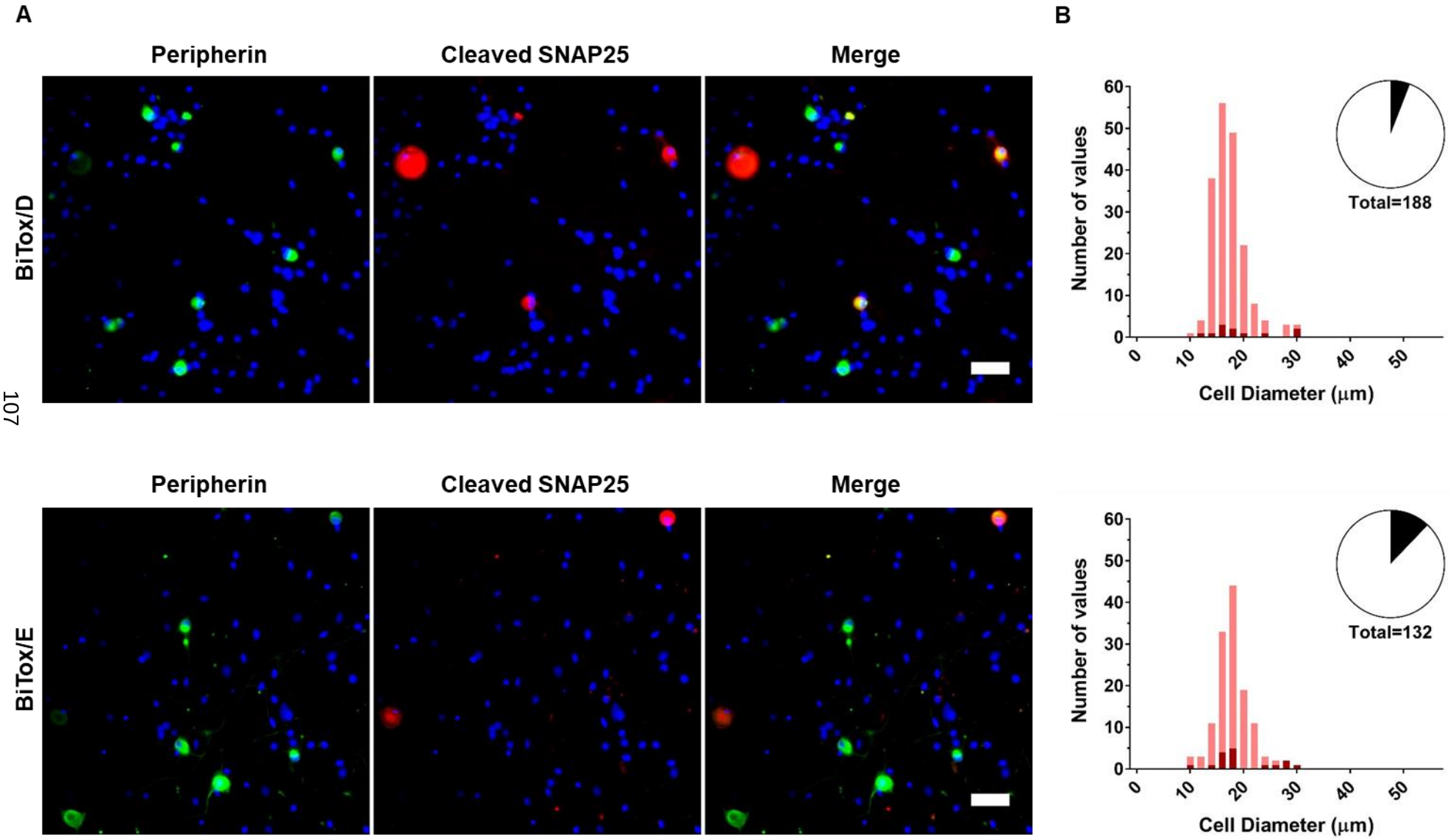
A
Peripherin
Cleaved SNAP25
Merge
BiTox/D
BiTox/E
B
Number of values
Cell Diameter (μm)
Total=188
Total=132

Figure 4.8 Representative images of cleaved SNAP25 staining in unmyelinated dissociated sensory neurons. (A) *Representative images of dorsal root ganglion cultures were taken using an epifluorescent microscope after 65 incubation with chimeras, BiTox/A-/E (N=4, n=3). Cleaved SNAP25 (red) is visualised in both peripherin-positive neurons (green) and peripherin-negative neurons. DAPI (blue) marks the cell nuclei.* ***(B)*** *Frequency distribution histograms illustrate the distribution of the cell diameter of peripherin positive neurons, displaying cleaved SNAP25 (red), after incubation with the alternative chimeras, combined with the distribution of peripherin-positive neurons which were negative for cleaved SNAP25 (pink). In the inserted pie charts, peripherin-positive neurons displaying cleaved SNAP25 (black) are expressed as a percentage of the total number of peripherin-positive neurons counted. Scale bar=50 µm.*

After reviewing the data for both chimeras, BiTox/D and BiTox/E, it was decided that BiTox/D would be investigated further. Incubation with BiTox/E consistently produced SNAP25 cleavage in a smaller proportion of neurons than the other chimeras, thus implying that BiTox/E might not be as efficacious. In contrast, the percentage of neurons displaying cleaved SNAP25 after incubation with BiTox/D was very similar to that after incubation with BiTox/A. BiTox/D also had the added benefit of cleaving SNAP25 in what appeared to be two separate subpopulations of sensory neurons, one subpopulation of smaller diameter, myelinated neurons and another subpopulation of larger diameter, myelinated neurons. This suggests that BiTox/D may be binding to the large Aβ- neurons and the medium sized Aδ-fibre nociceptors.

It was specifically chosen to trial BiTox/D in an inflammatory pain model given the implications of Aδ- and C-fibre nociceptor activation in chronic inflammatory pain. During inflammation, inflammatory mediators are released which activate and sensitise the C-fibre and Aδ-fibre nociceptors, whilst also stimulating them to release their own inflammatory mediators (Averbeck et al., 2000; von Hehn et al., 2012). This increased excitability and activity of peripheral nociceptors, consequently drives increased firing and glutamate release at the central synapse in the dorsal horn, resulting in central sensitisation (Latremoliere and Woolf, 2009). Cleavage of SNAP25 in the primary afferents should prevent the initial neurotransmission of pain from nociceptors to second order neurons, during the acute stage of CFA-induced inflammation, but also, the chronification of pain due to changes which occur at the central synapse, secondary to the increased firing of primary afferents.

Consequently, based on this hypothesis, the analgesic effects of BiTox/D were investigated in the Complete Freund's Adjuvant model of inflammatory pain. At baseline, prior to injection of either vehicle or BiTox/D, the thermal (Sidak's multiple comparisons test, *Baseline,* P= 0.9976, Fig. 4.9A) and mechanical (Sidak's multiple comparisons test,

Baseline, P= 0.8899, Fig. 4.9B) thresholds were not significantly different between the two groups of animals. The thermal and mechanical thresholds remained comparable between the two groups following intraplantar injection of vehicle and BiTox/D to the left hindpaw on day -4 (Sidak's multiple comparisons test, *Thermal Day -3,* P= 0.9923, *Day 0*, P= 0.5161, *Mechanical Day -3 and 0,* P> 0.9999). Both vehicle and BiTox/D-injected rats developed thermal hyperalgesia (Fig. 4.9A) and mechanical hypersensitivity (Fig. 4.9B) following intraplantar injection of Complete Freund's Adjuvant (CFA) to the ipsilateral hindpaw on day 0. By day 14-post CFA injection, rats receiving intraplantar injection of vehicle showed an almost complete recovery to basal thermal threshold values. Rats which received BiTox/D, however, displayed significantly lower thermal thresholds compared to vehicle-injected rats (Sidak's multiple comparisons test, *Day 14*, P= 0.0317, Fig. 4.9A). Further to this, the average thermal threshold for BiTox/D injected rats appeared to plateau by day 3 post-CFA with the average withdrawal latency remaining stable around 6 s, even at day 14 post-CFA, thus suggesting a prolonged period of thermal hyperalgesia.

Although there was no main effect of treatment on the average thermal threshold (Two-way ANOVA, *Treatment*, $F_{(1,10)} = 1.362$, P= 0.2703, Fig. 4.9A), there was a significant interactive effect of treatment over time (Two-way ANOVA, *Interaction,* $F_{(8, 80)} = 2.885$, P= 0.0071). When taken and analysed separately, treatment with BiTox/D, opposed to vehicle, did not influence thermal threshold measurements taken prior to injection of CFA (Two-way ANOVA, *Treatment: BL - Day 0,* $F_{(1,10)} = 0.4429$, P= 0.5208) but did significantly affect thermal threshold after the establishment of the pain model (Two-way ANOVA, *Treatment: Day 1-14 t* $F_{(1,10)} = 5.821$, P= 0.0365). This demonstrates that whilst BiTox/D does not affect basal thermal thresholds, it does affect thermal hypersensitivity once a pain phenotype has been induced.

With regards to the mechanical threshold, there was no main effect of treatment with BiTox/D opposed to vehicle (Two-way ANOVA, *Treatment,* $F_{(1,10)} = 0.19$, P= 0.6722, Fig. 4.9B), or overall interactive effect of treatment over time (Two-way ANOVA, *Interaction* $F_{(8, 80)} = 0.668$, P= 0.7180). The reversal of mechanical hypersensitivity was unaffected by injection of BiTox/D with both groups of animals following the same recovery trajectory.

The recovery of the mechanical threshold does, however, appear to be much slower than that observed of the thermal threshold. It was attempted to extend the experiment to investigate when either sensory threshold would fully recover, however, the experiment had to be terminated on day 18 after lacerations were noticed on left hindpaw of two of the BiTox/D-injected rats (Fig. 4.9E). This again supports the notion that BiTox/D-injected rats remained hypersensitive, even to the point of what appears to be self-injury.

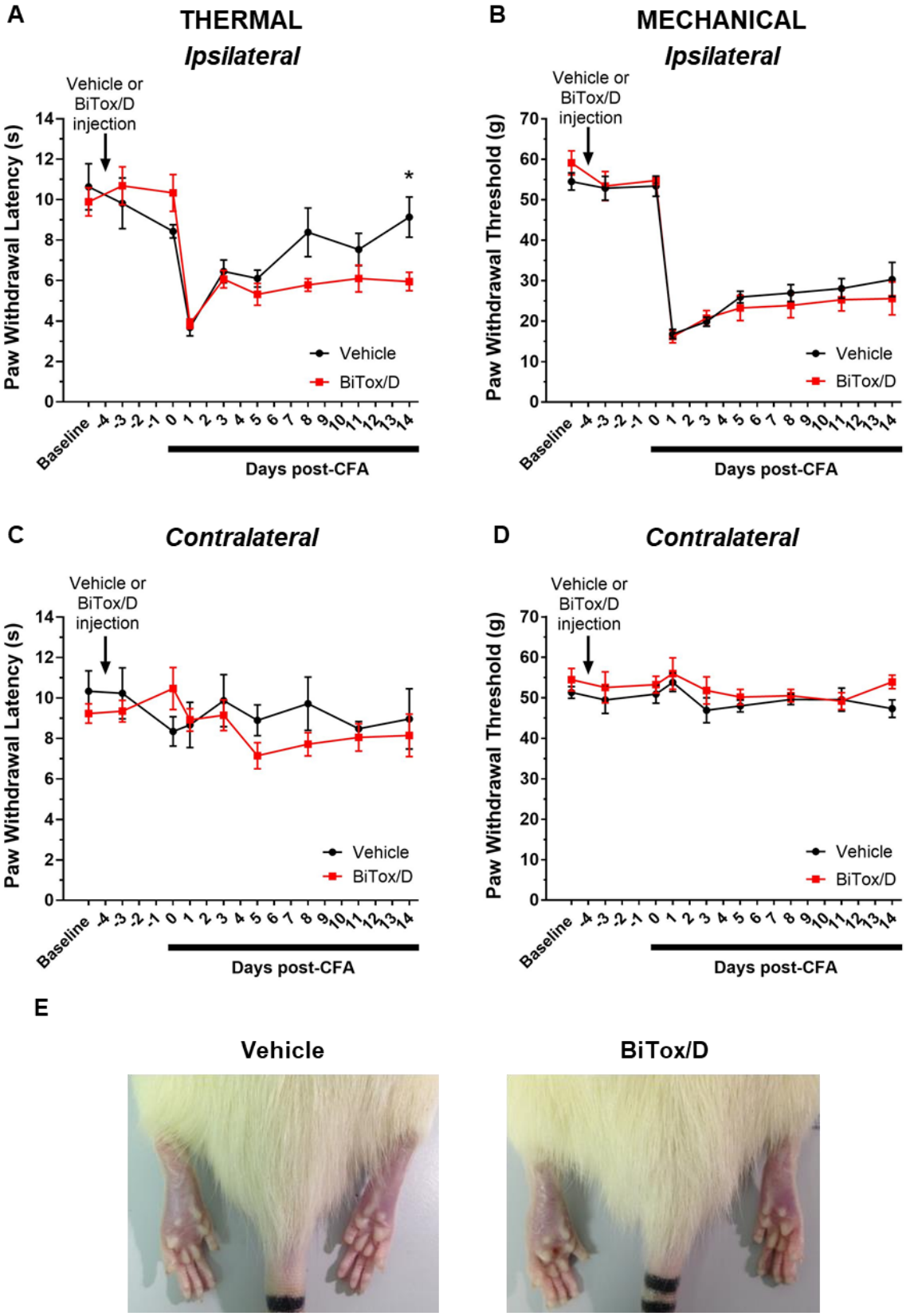

Figure 4.9 BiTox/D potentially prolonged thermal hyperalgesia in a Complete Freund's Adjuvant (CFA) inflammatory pain model. *7 week old Sprague Dawley rats received a 30 µl intraplantar injection of either 300 ng of BiTox/D (N=6) or vehicle (N=6), followed by an intraplantar injection of 30 µl CFA 4 days later (Day 0). The thermal and mechanical basal thresholds were assessed during two separate sessions. Consequently, the Baseline value represents the average of the two baseline readings.* ***(A)*** *The average basal withdrawal latency, measured using*

Hargreaves Plantar test, was not significantly different between BiTox/D- and vehicle-injected rats, and was not affected by injection of BiTox/D. A reduced paw withdrawal latency was observed 24 hours after CFA injection in both groups, with no significant difference in thermal thresholds detected between groups (Day 1). BiTox/D- injected rats consistently displayed lower thermal thresholds than vehicle-injected rats following CFA injection. On day 14, this difference was shown to be significant. ***(B)*** *There was no significant difference in mechanical threshold, assessed using Electronic von Frey, between groups at baseline. Both groups developed mechanical hyperalgesia 24 hours after CFA injection with no significant differences detected in mechanical threshold between the two groups at any later time point.* ***(C)*** *Thermals thresholds and* ***(D)*** *mechanical thresholds were also measured in the contralateral, uninjected paw. Both modalities remained stable in the contralateral paw of both groups and were unaffected by injection of CFA or BiTox/D to the ipsilateral paw.* ***(E)*** *On day 18, it was observed that two of BiTox/D injected rats had wounds on the foot pad of the CFA-injected hindpaw. Consequently, the experiment was terminated meaning that no later time points could be recorded. All data points are shown as mean ± S.E.M, * p<0.05.*

Importantly, the thermal (Two-way ANOVA, *Treatment*, $F_{(1,10)} = 3159$, P= 0.5865, Fig. 4.9C) and mechanical thresholds (Two-way ANOVA, *Treatment*, $F_{(1,10)} = 1.468$, P= 0.2535, Fig. 4.9D) of the contralateral paw were unaffected by intraplantar injection of BiTox/D to the ipsilateral paw.

4.2.6 Cleaved SNAP25 is detected in the ventral horn following intraplantar injection of BiTox/D in a rat inflammatory pain model

Immunohistochemical processing of spinal cord sections revealed SNAP25 cleavage in the lateral portion of the ventral horn within the lumbar regions L5 (Fig. 4.10, second panel) and L6 (Fig. 4.10, fourth panel), ipsilateral to the intraplantar injection site in BiTox/D- injected rats. No SNAP25 cleavage was detected in vehicle-injected animals (Fig. 4.10, first and third panel). Higher magnification images of the ventral horn of rats that received BiTox/D demonstrate that cleaved SNAP25 is not present within the motor neuron soma or at the membrane of motor neurons, but instead, appears to be localised within the interneuron terminals, synapsing on to the motor neurons (Fig. 4.11, top panel).

Higher magnification images of the ipsilateral dorsal horn also revealed single neurites displaying SNAP25 cleavage extending up to the substantia gelatinosa, the superficial laminae of the dorsal horn where the nociceptors terminate (Fig. 4.11, bottom panel). These neurites appear to project from the network of interneurons, contained within the ventral horn, showing SNAP25 cleavage.

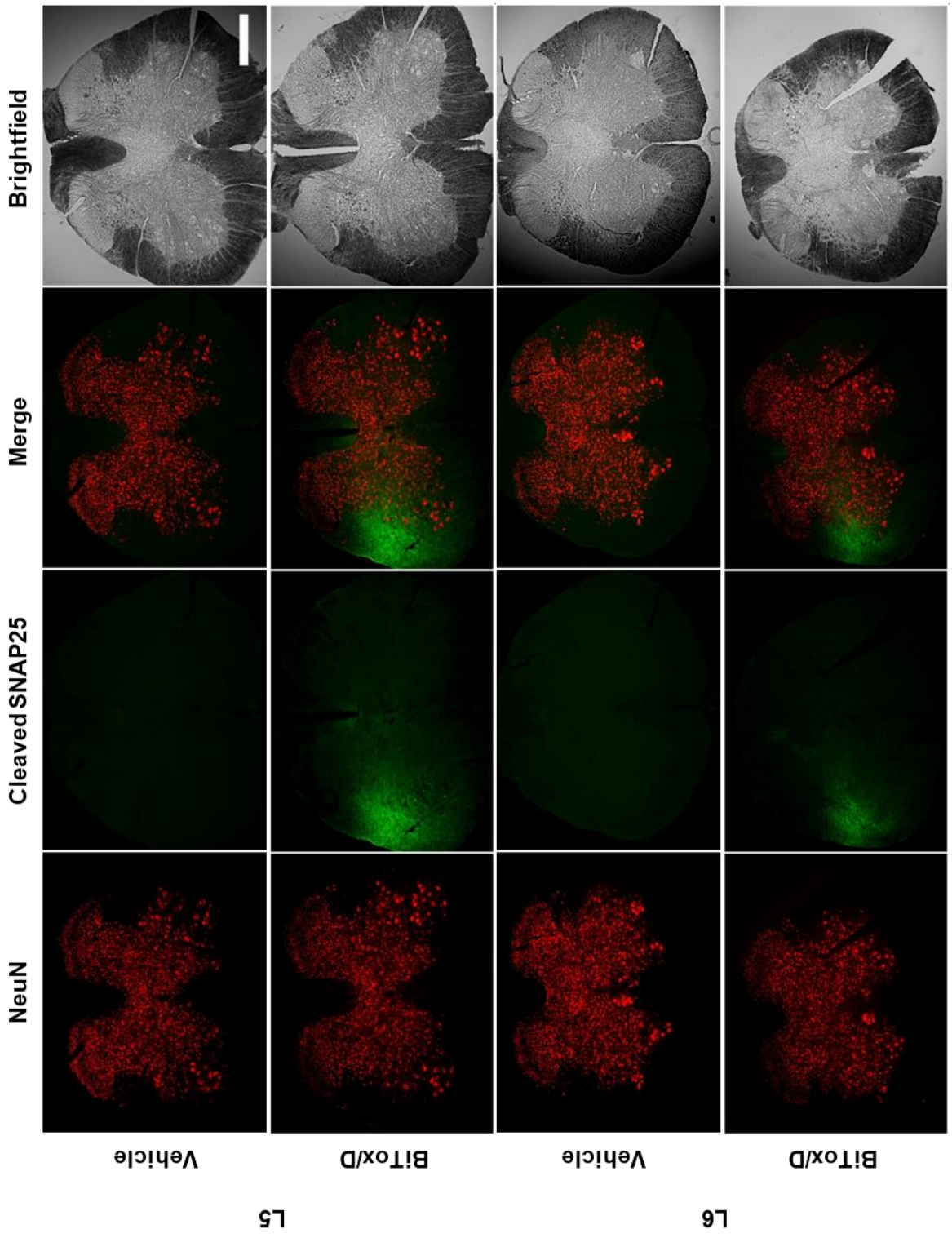

Figure 4.10 Cleaved SNAP25 is detected in the ventral horn following intraplantar injection of BiTox/D in an inflammatory pain rat model. *Vehicle-injected rats (N=3) and BiTox/D-injected rats (N=3) were perfused with 4% paraformaldehyde on day 15 post-CFA injection and 30 µm spinal cord sections were prepared and stained. The spinal cord was marked with an incision to the ventral horn, contralateral to the injection site. SNAP25 cleavage (green) was detected ipsilateral to the intraplantar injection site at the spinal cord levels, L5 (2nd panel) and L6 (4th panel) in BiTox/D-injected rats, but not in vehicle injected rats (1st and 3rd panels). Scale bar= 0.5 mm*

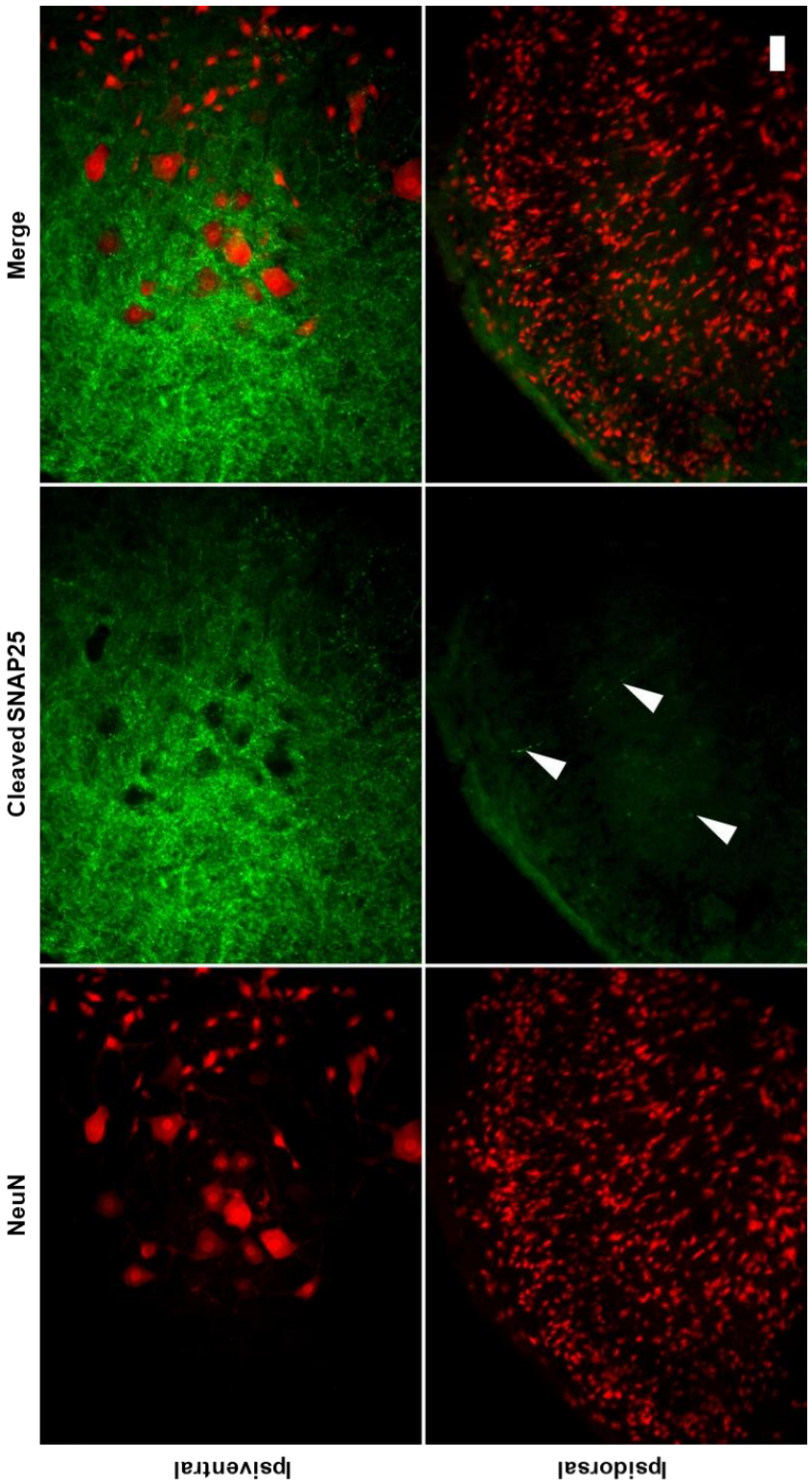

Figure 4.11 Higher magnification images of the ipsilateral spinal cord reveal cleaved SNAP25 within single neurites. *Higher magnification epifluorescent microscopy images of spinal cord sections isolated from BiTox/D-injected rats revealed that cleaved SNAP25 (green) does not colocalise with the motor neurons, marked using NeuN (red), of the ipsilateral ventral horn following BiTox/D injection (top). Instead, cleaved SNAP25 is visualised within a network of neurites surrounding the motor neurons. Further investigation of the ipsilateral dorsal horn (bottom) showed single neurites (white arrowheads), containing cleaved SNAP25, projecting to the outer layers of the dorsal horn, termed the substantia gelatinosa. Scale bar=50 µm.*

4.3 Discussion

The ability to silence distinct subpopulations of sensory neurons is important for the future design of long-lasting analgesics. It presents the opportunity to be able to treat the various clinical features of chronic pain conditions. For example, primary thermal hyperalgesia occurs due to the peripheral sensitisation of nociceptors at the site of injury, the Aδ- and C- fibres. By contrast, secondary hyperalgesia is due to changes in the phenotype of Aβ-fibres, such that they begin to produce a noxious response to innocuous stimuli (Latremoliere and Woolf, 2009). By discovering therapeutics that can target both small and large diameter neurons, it may be possible to prevent both peripheral and central sensitisation, and consequently, the establishment and maintenance of certain pain conditions.

Based on the knowledge that the different serotypes of botulinum neurotoxin utilise distinct combinations of gangliosides and protein receptors to gain entry into neurons (Montal, 2010), and that the composition of these respective gangliosides and proteins varies between subtypes of sensory neurons (Ashton et al., 1990), it was hypothesised that the different serotypes would preferentially bind to selective subpopulations of sensory neurons. To test this hypothesis, the LcTd/A of BoNT/A, containing the zinc-endopeptidase activity, and thus responsible for cleaving SNAP25, was conjugated to the receptor binding domain of BoNT/A, /C, /D and /E, to produce the chimeras, BiTox/A, /C, /D and /E, respectively. LcTd/A was specifically chosen as the active domain so that the inhouse anti-cleaved SNAP25 antibody could then be used as a reporter to provide an indirect measure of the novel chimeras' activity.

4.3.1 The in vitro binding profile of BiTox/A generates further support for the binding profile recognised in vivo

The in vitro investigation of the binding profile of BiTox/A, conducted in this chapter, highlighted that BiTox/A most likely preferentially binds to the larger Aβ-sensory neurons. Following incubation with BiTox/A, SNAP25 cleavage was detected in sensory neurons with the largest cell diameter as well as in neurons showing the highest level of immunoreactivity for NF200, indicative of heavy myelination, associated with the larger Aβ-sensory fibres. These observations are consistent with that reported during the in vivo investigation of BiTox/A's sensory binding profile (See 3.2.1). Following intraplantar injection of BiTox/A, cleaved SNAP25 was readily detected in both NF200- and IB4-positive sensory neurons, located in the glabrous skin of the injected hindpaw, thus representing the larger, myelinated, non-peptidergic neurons. Namely, the Aβ- fibres.

Additionally, cleaved SNAP25 was visualised in a subset of CGRP-positive neurons following intraplantar injection of BiTox/A. Expression of CGRP has been recognised in all subclasses of sensory neurons, Aβ-, Aδ- and C- fibres, however, CGRP is predominantly expressed in the small, unmyelinated C-fibres (McCarthy and Lawson, 1990; Lawson et al., 2002; Bae et al., 2015). It is thus possible that this population of CGRP-positive nerve fibres, displaying cleaved SNAP25, noted in vivo, could be equivalent to the small subpopulation of the peripherin-positive neurons, recognised to be unmyelinated, C-nociceptors, that showed SNAP25 cleavage during the present in vitro investigation. This, however, remains to be confirmed by further in vitro immunolabelling using the anti-CGRP antibody. It is, nevertheless, possible that any discrepancies in the predicted binding of BiTox/A could derive from the method of investigation, i.e. in vitro investigation performed here, opposed to observations made in vivo in the previous chapter.

4.3.2 In vitro investigation of the binding profiles of alternative BiTox chimeras confirms that the enzymatic domain of BoNT/A can be retargeted to alternate neuronal subpopulations

Here, it was demonstrated that all four chimeras successfully retained their functionality in vitro following conjugation and persisted to cleave SNAP25 in sensory neurons. Subsequent staining of dorsal root ganglion cultures with pan-neuronal marker, βIII-tubulin, proved to be minimally informative due to the skewed size distribution of neurons in culture. Although soma size has historically been used to determine cell type, this method is flawed as it does not consider the overlap in soma size between large and small sensory neurons (Harper and Lawson, 1985). The emergence of neuronal markers specific to subtypes of sensory neurons, in combination with soma size, has greatly improved the ability to distinguish the classic subtypes: Aβ-, Aδ- and C-fibre sensory neurons (Usoskin et al., 2010).

Consequently, Neurofilament 200 and peripherin were chosen to identify the large, myelinated neurons and small, unmyelinated neurons, respectively. This was done with the intention that separating the two populations would eliminate the skewness of the data and help to elucidate any significant differences in the binding profiles of the alternative chimeras (Goldstein et al., 1991). After isolating only the myelinated neurons, significant differences were successfully demonstrated between the mean cell diameter of neurons in which cleaved SNAP25 was detected following incubation with the four chimeras. Both BiTox/A and -/C produced SNAP25 cleavage in myelinated neurons, as identified using NF200, with a larger cell diameter, indicative of large diameter Aβ-fibre

neurons. The neurons responsible for normal touch sensation and implicated in the development of secondary hyperalgesia. Conversely, following incubation with BiTox/D and BiTox/E, SNAP25 cleavage was observed in a subpopulation of significantly smaller myelinated neurons, suggestive of the smaller diameter, lightly myelinated Aδ-fibre nociceptors.

There was still no significant difference noted between the mean cell diameter of peripherin-positive neurons, identified to be unmyelinated nociceptive neurons, which displayed cleaved SNAP25 after incubation with the alternative BiTox chimeras, compared to BiTox/A. This finding is not surprising given that the gangliosides found in the cell membrane of neuronal axons, which BoNTs utilise during the internalisation process, specifically GT1b, GD1a and GM1, are also known to act as ligands for myelin-associated glycoprotein (MAG) (Ogawa-Goto et al., 1992; Yang et al., 1996; Vinson et al., 2001; Vyas et al., 2002). MAG serves as an adhesion molecule, recruiting myelinating glial cells, i.e. the Schwann cells, to the axonal membrane, and is thus integral for the maintenance of myelination (Posse de Chaves and Sipione, 2010). The neuronal membranes expressing the correct ganglioside combinations for the binding of BoNTs are, therefore, most likely to be myelinated neurons. It is thus expected that any difference in binding profiles between botulinum serotypes would be detected within the population of myelinated neurons. Furthermore, this concept is supported by the observation that cleaved SNAP25 was consistently detected in a larger percentage of neurofilament-positive neurons than peripherin-positive neurons, inferring that BoNTs show a higher affinity for myelinated neurons.

Even with the use of the two antibodies, anti-NF200 and anti-peripherin, to separate the two populations of sensory neurons, there was still considerable similarity visible between the histograms of peripherin- and NF200- positive neurons. The histograms did, however, resemble those depicted by Ferri et al. (1990) who showed all peripherin-positive neurons to be between 10-40 µm in cell diameter, and all NF200-positive neurons be between 20-60 µm in cell diameter, thus highlighting that there is substantial overlap between the size distribution of the two populations. Not dissimilarly, here, peripherin positive neurons were described to be 10-30 µm and NF200 positive neurons 10-50 µm in cell diameter. Despite this overlap, the two antibodies have previously been shown to be largely mutually exclusive in their expression in dorsal root ganglion neurons (Ferri et al., 1990; Goldstein et al., 1991; Fornaro et al., 2008). Accordingly, any similarity in the size distributions does not mitigate the validity of the antibodies.

Contrary to this, in another in vivo study, it was reported that almost a quarter of all NF200 positive neurons were actually unmyelinated neurons, and vice versa, that a significant proportion peripherin positive fibres were actually large-Aβ myelinated fibres

(Bae et al., 2015). These observations were made whilst utilising an in vivo method, staining whole sections, and in the absence of any injury. It does, therefore, question the suitability of the two antibodies. Instead, they suggest that Substance P, Calcitonin Gene-Related Peptide, and isolectin-IB4 are more appropriate markers when assessing subpopulations of neurons.

The observed differences in the staining of neurons could, however, be due to the nature of the tissue used. Bae et al. (2015) specifically examined the localisation of neurofilaments in the trigeminal ganglia whereas, all the aforementioned studies, which verified the exclusive nature of NF200 and peripherin, were all conducted on dorsal root ganglia. Although not with specific reference to the expression of neurofilaments, RNA sequencing has demonstrated significant differences in the protein expression profiles between dorsal root and trigeminal ganglion neurons (Kogelman et al., 2017). This therefore suggests that although the two antibodies are mutually exclusive in DRG, these findings cannot be applied or extrapolated to the trigeminal ganglion neurons.

The exclusiveness of the two antibodies has, however, been demonstrated whilst conducting in vivo staining of whole DRG sections, opposed to in dissociated cultures, as was the method used here. With regards to the protocol for producing dissociated DRG cultures, it is important to realise that the removal of DRGs requires mutliple axotomies, making it, essentially, an in vitro model of neuropathic pain. Interestingly, Fornaro *et al.* (2008) compared the perceived expression of NF200 and peripherin in vivo and in vitro, using DRG sections and DRG explant cultures, respectively. The two neurofilaments were again shown to be expressed in almost entirely separate populations of neurons in vivo. In contrast, whilst neurofilament 200 and peripherin were still exclusively detected in two distinct populations of neurons immediately after explant, staining 2 days post-explant instead revealed that all neuronal somas were postive for peripherin but yet none were immunoreactive for NF200. Furthermore, by day 10 only a small proportion of DRG neurons in the explant were reported to be NF200-positive and these were located mostly at the peripheral edge of the explant. Additionally, RNA analysis conducted at the same time points indicated that whilst peripherin expression was reduced 2 days after explant, its expression levels greatly increased between days 2 and 10 post-explant, thus suggesting that peripherin has a role in axonal regrowth and regeneration in sensory fibres, consistent with other studies (Larivière et al., 2002). Conversely, the expression levels of NF200 remained low and, although they did recover slightly, the expression levels were not significantly regained.

This data illustrates that the process of axotomy, even more so a feature in the protocol for dissociated dorsal root ganglion cultures, than explants, could greatly disturb the normal expression levels of both NF200 and peripherin, and therefore, impact any

conclusions made. Similarly, in another study, Ferri et al. (1990) showed that capsaicin treatment of rodent neonates increased the percentage of neurons costained for both NF200 and peripherin, reiterating, again, that injury impacts the expression of these filaments. They specifically suggest that there is a shift in NF200-positive neurons towards expressing peripherin after treatment with capsaicin. This could explain why the negative skew is still apparent in the NF200 frequency distribution histograms shown here.

In consideration of this, it would be recommended to use cultures which have been maintained for longer periods of time before studying the effects of BoNTs. By this time point, it would be expected that the axons should have seized growing and that protein expression levels should stabilise back to normal physiological levels. For this study, chimeras were added 2 days post-culture and cultures were not then collected until 5 days post-culturing. According to Fornaro et al. (2008), the expression levels should begin recovering from 2 days post-culture so, although expression would be low, the proteins should be expressed in their correct populations and, therefore, minimally impact the data presented here. Furthermore, in contrast to their findings, the data presented here clearly shows a substantial proportion of NF200-positive neurons 5 days after culturing. This suggests that perhaps there is a quicker recovery of expression levels in dissociated cultures than in DRG explants.

It is also worth noting that there is a slight disparity in cell diameter shown here, compared to that described elsewhere. The maximum diameter of peripherin-positive and NF200-positive neurons, reported by Ferri et al. (1990), was around 10 µm larger than that reported here. This could again be explained by the method used. As discussed earlier, the process of trituration during the culturing of dorsal root ganglion cells subjects the larger neurons to a great deal of sheer force, potentially rupturing them, and consequently mitigating them from the culture. It could, therefore, also be beneficial to utilise DRG explant cultures, rather than dissociated cultures, in order to avoid the loss of the larger diameter neurons. Dissociated cultures do, however, have the added advantage of allowing equal, as well as increased penetration of all neurons. Hence why they were selected for the screening of BoNTs in this study (Passmore, 2005).

Another consideration to make is the age of the animals used. The majority of studies collected DRGs from rats weighing 300-350 g which suggests that they were approximately 8-11 weeks old, and would thus be considered young adults (McCutcheon and Marinelli, 2009; Brower et al., 2015). In this current work, the rats used were 3-4 week old, weighing less than 100 g, and equivalent to pubescents (McCutcheon and Marinelli, 2009). This could account for the overall smaller cell diameter noted. It has previously been documented that neurons continue to increase in soma size with age,

as well as there being a shift noted in the proportion of large versus small diameter neurons (Hatai, 1902). The use of pubescent rats was jusitified as it achieved a compromise between the ease of imaging and the increased viability of neurons taken from animals of a younger age (Manfridi and Forloni, 1992; McCutcheon and Marinelli, 2009) versus the maturity of neurons and expression profiles associated with adult cultures, compared to embryonic neurons (Melli and Höke, 2009).

In summary, NF200 and peripherin are reliable markers for separating the respective populations of myelinated and unmyelinated sensory neurons, when isolated from dorsal root ganglia, and have therefore been used appropriately in this study. Furthermore, the size distribution of both peripherin- and NF200-positive neurons shown here are analogous to that reported previously in vivo (Ferri et al., 1990). It was therefore acceptable to reach the conclusion that BiTox/D and BiTox/E do bind to a subpopulation of significantly smaller NF200- positive neurons and to proceed on this basis.

4.3.3 Pursuing BiTox/D as a potential analgesic

Upon reflection of the data, BiTox/D was chosen to be investigated as a potential analgesic. Although both BiTox/D and BiTox/E produced SNAP25 cleavage in a subpopulation of significantly smaller myelinated neurons than BiTox/A, incubation with BiTox/D led to cleaved SNAP25 being detected in a greater proportion of neurons compared to Bitox/E. This was shown on both Western Blot and following quantification of all neurons, marked using βTubulin III. Furthermore, the observation was made that BiTox/D consistently cleaved SNAP25 in two distinct subpopulations of sensory neurons, one subpopulation of smaller diameter, myelinated neurons, around 18 µm in cell diameter, and another of larger diameter, myelinated neurons, around 28 µm in cell diameter. This suggests that BiTox/D may be binding to both the myelinated large Aβ-neurons and the smaller, more thinly myelinated Aδ-fibre nociceptors.

It is not surprising, however, that BiTox/D displays the most distinct binding profile compared to the other chimeras investigated. BoNT/D displays the least homology in its amino acid sequence compared to other serotypes (Rummel et al., 2009; Strotmeier et al., 2010) and its method of internalisation remains the most contested. One theory states that, unlike other serotypes, Rbd/D does not utilise gangliosides but instead binds to the phospholipid, phosphatidylethanolamine (Tsukamoto et al., 2005). Conflicting evidence, however, claims that whilst Rbd/D is missing key residues in the ganglioside binding pocket, conserved between the other serotypes, it instead contains two carbohydrate binding pockets, one believed to have affinity for sialic acid, similar to tetanus, and another for which the ligand has yet to be identified (Strotmeier et al., 2010).

Accordingly, it has also been reported that Rbd/D binds to the b-series of gangliosides, GT1b and GD1b, comparable to the other serotypes, as well as GD2 (Strotmeier et al., 2010; Kroken et al., 2011). Additionally, there is no known protein receptor for BoNT/D. It is however, agreed that BoNT/D must utilise some component of the synaptic vesicles as its uptake is greatly increased upon stimulation of the neurons (Rummel et al., 2009; Kroken et al., 2011).

Overall, the internalisation method of Rbd/D remains relatively unclear. The unique neuronal binding profile determined here for BiTox/D does, however, support the notion that BoNT/D displays affinity for, and interacts with, alternate lipids, and possibly proteins, compared to the other serotypes.

4.3.4 Neuronal blockade of Aδ nociceptors potentially causes prolonged thermal hyperalgesia in inflammatory pain

BiTox/A is hypothesised to bind to the larger Aβ fibres based on its ability to successfully reduce secondary hyperalgesia in inflammatory pain conditions and its lack of effectiveness at treating primary hyperalgesia, localised to the site of injury (Mangione et al., 2016). Correspondingly, here it was shown that following incubation of cultures with BiTox/A, cleaved SNAP25 was detected in the larger myelinated neurons. Most noticeably, all NF200-positive neurons with a cell diameter greater than 30 µm displayed positive SNAP25 cleavage.

It was therefore speculated that incubation with BiTox/D, similar to BiTox/A, would continue to block the activity of the larger Aβ low-threshold mechanoreceptors that innervate the area adjacent to site of injury and are responsible for the phenomenon of secondary hyperalgesia, as well as the Aδ nociceptors, located at the site of inflammation. The additional action at Aδ-nociceptors would thus block neurotransmission from these neurons and consequently prevent primary hyperalgesia and the development of neurogenic inflammation (Latremoliere and Woolf, 2009). It was therefore believed that BiTox/D would effectively treat both clinical features, primary and secondary hyperalgesia, of inflammatory pain conditions.

Unfortunately, it was instead suspected that pre-treatment with BiTox/D might prolong thermal hyperalgesia at the site of inflammation. Only partial recovery of the thermal threshold was seen. Interestingly, immunotherapy treatment of neuroblastoma using anti-GD2 antibodies, whilst being very successful at treating neuroblastoma, is associated with severe visceral pain, requiring management with morphine (Cheung et al., 1987; Handgretinger et al., 1992, 1995). This perceived pain has been attributed to the activation of the complement cascade system which acts to heighten an inflammatory

response (Sorkin et al., 2010). GD2 has previously been demonstrated to be one of the possible interactive partners of BoNT/D (Kroken et al., 2011). If correct, it is therefore possible that the binding of BiTox/D to GD2 could augment the inflammatory response to CFA, by activating the complement system, thus maintaining the inflammatory state in BiTox/D-injected animals, whilst vehicle-injected animals recover.

Administration of anti-GD2 antibodies in rats is, however, more associated with producing mechanical hyperalgesia, consistent with a neuropathic pain phenotype, opposed to thermal hyperalgesia, which is affected here, and is more characteristic of inflammatory pain conditions (Sorkin et al., 2002). Nevertheless, induction of pain by bolus injection of anti-GD2 antibodies results in a lower mechanical threshold being required for the activation of Aδ- fibres specifically, compared to saline-treated animals. Contrarily, no significant difference in mechanical activation threshold for C-fibres is noted (Xiao et al., 1997). This suggests a preference of anti-GD2 antibodies to target Aδ- nociceptors, presumably due to GD2 expression. Together with the data presented here, indicating that BiTox/D is targeting Aδ-nociceptors, this proposes that BiTox/D and anti-GD2 antibodies could display similar binding patterns and thereby supports the theory that they could potentially share similar pathophysiologic mechanisms.

Furthermore, Weng et al. (2012) showed that only C-fibre firing and excitability is altered in CFA-induced inflammatory pain. This therefore negates the involvement of Aδ-nociceptors in primary hyperalgesia. The ineffectiveness of BiTox/D at treating thermal hyperalgesia consequently supports the notion that BiTox/D specifically binds the Aδ-nociceptors because, if these findings are correct, then only blockade of neurotransmission in the C-fibres would be expected to produce analgesia.

Regardless, the retargeting of LcTd/A to the smaller myelinated neurons, hypothesised to be Aδ -fibre nociceptors, using Rbd/D, did not affect the development of mechanical or thermal hyperalgesia following injection of CFA, thus implying that these neurons are not implicated in the establishment of chronic inflammatory pain conditions. The observation that thermal hyperalgesia persisted past the normal recovery experienced by vehicle-injected rats suggests that Aδ-nociceptors may, however, be important for the resolution of inflammation, and the subsequent reversal of thermal hyperalgesia.

4.3.5 SNAP25 cleavage within the spinal cord suggests that BiTox/D could have a centrally mediated effect

Comparable to that demonstrated following intraplantar injection of BiTox/A, cleaved SNAP25 was detected at the level of the spinal cord in animals that received intraplantar injection of BiTox/D, thus confirming that BiTox/D successfully retains the enzymatic

activity of LcTd/A in vivo. It also indicates that BiTox/D must be retrogradely transported from the peripheral injection site to the spinal cord. Retrograde transport of both BoNT/A and BoNT/B has previously been demonstrated in vivo (Antonucci et al., 2008; Restani et al., 2011; Matak et al., 2012). This retrograde transport was shown to be essential for the analgesic effect of BoNT/A in formalin-induced pain (Bach-Rojecky and Lacković, 2009) and acidic saline-induced hyperalgesia (Matak et al., 2011), after the observed analgesia was eliminated by intraneural injection of colchicine, an axonal transport blocker, to the sciatic nerve. With regards to BiTox/D, this could mean that the prolonged thermal hyperalgesia, suspected to occur, might not be due to the actions of BiTox/D at the sensory afferents in the periphery, as so far discussed, but could instead, at least in part, be due to changes in spinal cord processing.

A central mechanism for the analgesia produced by BoNT/A was first demonstrated in the formalin inflammatory pain model. Treatment with intraplantar BoNT/A injection, prior to formalin challenge, was ineffective against the first phase of inflammation, however, significantly reduced pain behaviour during the second phase (Cui et al., 2004). The first phase of inflammation represents the direct chemical activation of nociceptors by formalin at the periphery, whereas the second phase reflects changes in excitability, resulting from peripheral and central sensitisation. Similarly, BoNT/B was shown to reduce substance P release in the ipsilateral dorsal horn, subsequent to intrathecal injection of capsaicin (Marino et al., 2014), as well as preventing phosphorylation of pGluA1 and Akt, known markers of central sensitisation, following intrathecal injection of the glutamate receptor agonist, N-methyl-D-aspartate (NMDA) (Sikandar et al., 2016). BoNT/B did not, however, reduce local edema in the carrageenan-injected paw (Sikandar et al., 2016). Again, this suggests that the main analgesic effect of BoNTs is mediated at the level of the spinal cord by preventing the increase in neuronal excitability associated with central sensitisation. The evidence presented, however, explains a pro-analgesic effect, whereas, here, BiTox/D has been described to be pro-hyperalgesic. Nevertheless, this effect could likewise be due to a centrally mediated mechanism.

Specifically, cleaved SNAP25 is visualised in close proximity to the motor neurons in the ipsilateral ventral horn of the lumbar spinal cord, isolated from BiTox/D-injected rats. However, it is absent in the soma and at the membrane of motor neurons. Again, this is reminiscent of the SNAP25 cleavage noted after peripheral injection of BiTox/A. It is important to note that there were no signs of motor paralysis or motor deficits visible in either vehicle- or BiTox/D injected rats. Both groups were able to suspend from an inverted wire mesh for prolonged periods of time, indicative of normal motor function and tone (Marino et al., 2014; Mangione et al., 2016). This consequently questions the significance of the SNAP25 cleavage observed in the ventral horn.

Cleaved SNAP25 was also found present in a few single neurites which extended up to the substantia gelatinosa, the superficial laminae of the dorsal horn, where the Aδ- and C- fibre nociceptors terminate (Todd, 2010). It is unclear whether the SNAP25 cleavage present in the dorsal horn is being detected in fibres projecting up from the main network of cleaved SNAP25-positive fibres, originating in the ventral horn, possibly from interneurons or fibres involved in proprioception (Betley et al., 2009) or nocifensive spinal motor reflexes to noxious stimuli (Sivilotti and Woolf, 1994), or whether it is being detected in a remote population of dorsal horn neurons, secondary to anterograde transport in the peripheral afferents. Matak et al. (2012) likewise detected small amounts of cleaved SNAP25 in the dorsal horn after intramuscular injection of BoNT/A, but attributed this to the axonal transport of BoNT/A in spinal sensory neurons. The cleavage was consequently used to explain BoNT/A's observed analgesic effects.

Further investigation is still required to confirm whether this staining is indeed contained within interneurons, and if so, to determine the nature of these neurons, specifically, whether they are excitatory or inhibitory. It is thus possible that if cleaved SNAP25, produced by BiTox/D, is localised within GABAergic interneurons, specifically in the dorsal horn, that it could then suggest that BiTox/D is leading to the disinhibition of the pain signalling pathway, thereby augmenting the pain response, and subsequently maintaining central sensitisation. All claims remain purely speculative at present and require further investigation.

4.3.6 Conclusion

Based on the behavioural evidence provided, BiTox/D was not further pursued for testing in other pain models. BiTox/A thus currently remains the most promising analgesic. Provided the lack of success in generating a chimera specifically for treating inflammatory conditions, alternate uses of clostridial chimeras were consequently explored.

Chapter 5. Utilising clostridial toxins for spinal cord delivery for use in neurological diseases

5.1 Introduction

There is currently a large amount of interest in utilising tetanus toxin, as well as other clostridial neurotoxins, as a drug delivery tool to treat diseases of the central nervous system (Toivonen et al., 2010). Native tetanus toxin binds to the presynaptic motor neuron terminals at the neuromuscular junction. Tetanus then undergoes retrograde transport to the motor neuron soma, located in the ventral horn of the spinal cord (Surana et al., 2017). By selectively expressing only the binding domain of tetanus toxin (Tbd), and conjugating or fusing this to a potential therapeutic, for example, a small molecule drug, a protein of interest or a gene for expression, the binding domain can be used to navigate the conjugated therapeutic to the motor neuron presynaptic terminals. The Tbd can consequently chaperone the conjugated therapeutic to the motor neuron soma in the spinal cord, via axonal transport. This mechanism of drug delivery circumvents the blood-spinal cord barrier to penetrate the central nervous system. Its specificity of binding also prevents off-target effects thus making it an attractive tool for application in central nervous system diseases. Specifically, those involving the motor system, such as Amyotrophic lateral sclerosis (ALS) and spinal muscular atrophy (SMA) (Figueiredo et al., 1997; Francis et al., 2004; Ciriza et al., 2008; Chian et al., 2009).

These investigations so far, have focused on the attachment of a single Tbd to a single therapeutic molecule, using a simple one to one ratio. The attachment of a second binding domain should augment the efficacy of Tbd during drug delivery. The binding of a ligand to a receptor is determined by specific binding kinetics, most notably including on- and off-rate constants (Peuker et al., 2013). During binding, the ligand and receptor associate (the on-rate) and dissociate (the off-rate) several times (Corzo, 2006; Peuker et al., 2013). The presence of two binding domains would imply that as one receptor binding domain dissociates away from the receptor, the other binding domain which, as part of the same chimera, would be in close proximity to the receptor, would then be available to associate with the now vacant receptor. This hence increases the overall association time of the chimera with the receptor, and prevents the chimera from drifting away from the receptor during dissociation. In principle, this should increase the binding of the chimera to its receptor, thus improving its availability for, and overall rate of, internalisation, subsequently increasing the chimera's efficacy.

There are, however, concerns for the immunogenicity associated with tetanus toxin when pursuing it as a potential drug delivery tool. It is estimated that over 80% of the English

population under 40 years of age, and 53% of those over 60 years of age, are immunised against tetanus toxin (Maple et al., 2000). This means that a chimera containing Tbd could potentially be attacked and removed by immune cells before being able to produce any therapeutic effect. Only if the Tbd- containing chimera is internalised rapidly by neurons before eliciting an immune response, will the chimera be able to provide any therapeutic benefit (Toivonen et al., 2010). For this reason, here, the alternate toxin, Cholera toxin, was also investigated for use in drug delivery.

Similar to Tbd, the b subunit of cholera toxin is capable of undergoing both anterograde and retrograde transport after peripheral application, and is subsequently used as a well-established, effective neuronal tracer (Stoeckel et al., 1977; Angelucci et al., 1996; Conte et al., 2009). The majority of humans are not immunised against cholera toxin due to its low prevalence in developed countries, as a result of increased sanitation (Azurin and Alvero, 1974), thus making it an ideal candidate for development.

Consequently, in this chapter, it will be investigated whether the attachment of a second receptor binding domain can improve the efficacy of protein delivery to the central nervous system. Additionally, it will be determined whether cholera toxin does offer an efficacious alternative to Tbd for drug delivery.

5.2 Results

5.2.1 Tbd-Cy3 is retrogradely transported to the motor neurons in the ventral horn of the lumbar spinal cord following intraplantar injection

Tbd-Cy3 was prepared by Dr C. Leese, using the established stapling technique. Briefly, Tbd was fused to synaptobrevin whilst Cy3 was conjugated, via maleimide chemical conjugation, to the SNARE peptide SNAP25. Following the addition of syntaxin, the staple, a stable fluorescent chimera was produced (Mavlyutov et al., 2016). The attachment of the fluorescent label, -Cy3, enabled the location of Tbd to be inferred. Following intraplantar injection of 7.5 µg Tbd-Cy3 to the left hindpaw, Cy3 immunofluorescence was detected in the soma of motor neurons, located in the ventral horn of the lumbar spinal cord, ipsilateral to the injection site. Specifically, at the L5 region of the spinal cord (Fig. 5.1). No Cy3 immunofluorescence was observed in the contralateral ventral horn.

5.2.2 The penetration of the lumbar spinal cord motor neurons by Tbd-Cy3 is increased by the attachment of a second tetanus binding domain

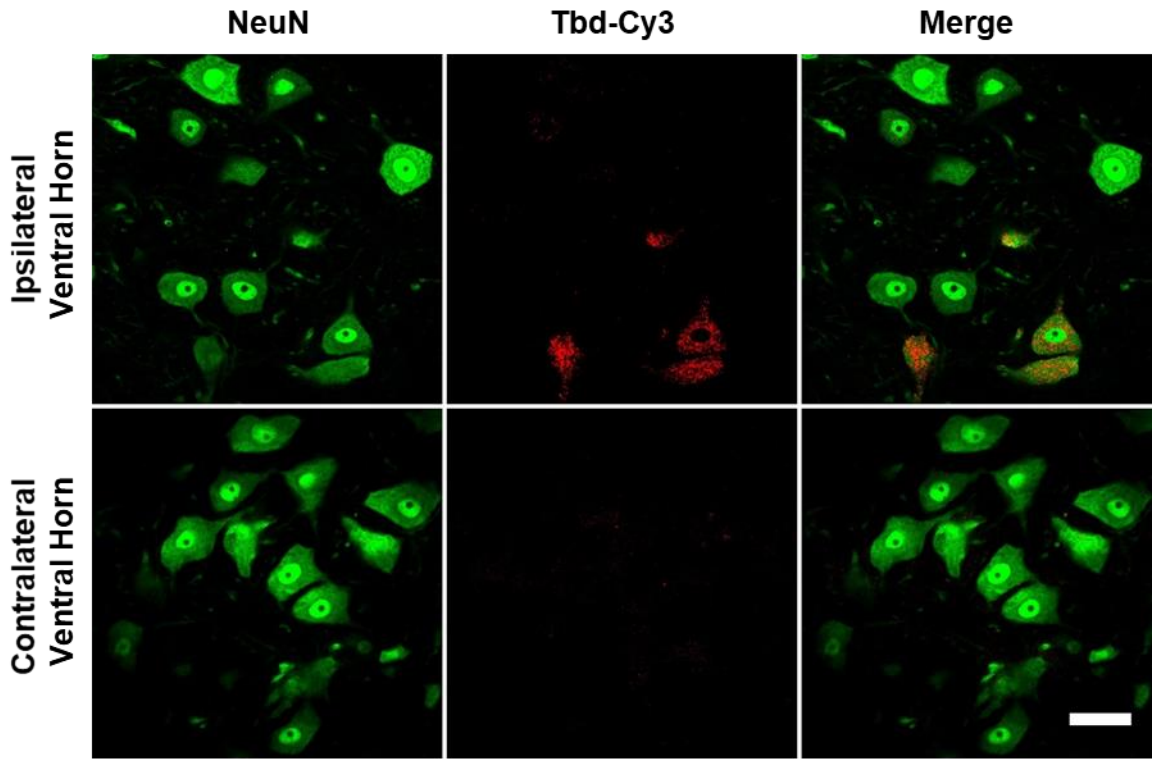

Figure 5.1 Tbd-Cy3 is visualised in the motor neurons of the ventral horn of the lumbar spinal cord following intraplantar injection. *Male 5 week old Sprague-Dawley rats received intraplantar injection of 7.5 µg/ 50 µl Tbd-Cy3 (N=2). Rats were perfused 7 days post-injection and the spinal cord was collected and cryosectioned. Representative images taken on a Nikon A1 TIRF confocal microscope show -Cy3 immunofluorescence (red) detected in the ipsilateral ventral horn of the lumbar spinal cord, specifically within the motor neurons marked by NeuN (green). Cy3 immunofluorescence was absent in the contralateral ventral horn. Scale bar= 20 µm*

The previous experiment confirms that Tbd remains functional after attachment of a fluorescent label. It was demonstrated that Tbd can still effectively internalise into neurons and undergo retrograde transport to the spinal cord, resulting in detectable immunofluorescence in the ventral horn. Consequently, the amount of immunofluorescence in the motor neurons of the spinal cord was utilised to provide an indirect measure of internalisation and retrograde transport.

To investigate whether the attachment of a second receptor binding domain could significantly enhance the binding of a protein, a second Tbd was attached to the fluorescent Tbd-Cy3 chimera. In short, the first Tbd and the -Cy3 label both remained fused to the same SNARE peptides. The second Tbd was expressed fused to the syntaxin peptide which was originally utilised as the “staple” peptide. Accordingly, no additional staple was required as all components of the SNARE complex were now contained within the individual subunits. Additionally, at this stage, the efficacy of cholera

toxin subunit B was also studied using a commercially available recombinant Cholera Toxin Subunit B Alexa Fluor 488 Conjugate (CTB-488) to determine whether cholera might provide a possible alternative delivery tool to tetanus toxin.

All three chimeras were administered via intraplantar injection. Rats received a single injection of either 7.5 µg of Tbd-Cy3, 7.5 µg of 2xTbd-Cy3 or 20 µg of CTB-488 to left hindpaw. Quantification of immunofluorescence in the motor neuron soma in the spinal cord revealed that injection of the different compounds did significantly affect the amount of immunofluorescence detected in the motor neuron soma located in the ipsilateral ventral horn to the injected hindpaw (One-way ANOVA, $F_{(2,15)} = 11.43$, $P=0.001$, Fig. 5.2C). Specifically, attachment of the second Tbd resulted in an almost ten-fold increase in the amount of immunofluorescence detected in motor neurons compared to Tbd-Cy3, consisting of only a single binding domain (Tukey's multiple comparisons test, $P < 0.001$, Fig. 5.2A and 5.2C). Additionally, significantly more immunofluorescence was observed after injection of 2xTbd-Cy3 compared to CTB-488 (Tukey's multiple comparisons test, $P<0.05$, Fig. 5.2A, 5.2B and 5.2C). CTB-488 did produce more immunofluorescence than Tbd-Cy3 in the motor neurons, however, this difference was not shown to be significant.

5.2.3 Attachment of a second tetanus binding domain to TetBot increases the efficacy of the BoNT/A enzymatic domain to cleave SNAP25 in the spinal cord.

Next, it was important to determine whether Tbd can deliver a large protein or enzyme to the spinal cord, and whether this ability to deliver a large protein is once more improved by the attachment of a second binding domain. Fluorescent probes such as Cy3 are usually very small in comparison to fully functional proteins. Cyanine fluorescent dyes specifically have a molecular weight below 1 kDa (Southwick et al., 1990; Mujumdar et al., 1993). Consequently, fluorescent probes do not largely impact the motility or binding of the proteins to which they are fused. In contrast, the enzymatically-active LcTd/A has a molecular weight of 100 kDa and can therefore greatly perturb the native binding and transportation of a targeting protein.

To test this hypothesis, two separate chimeras were prepared. In the first chimera, LcTd/A was conjugated to a single Tbd, and in the second, LcTd/A was conjugated to two Tbds, using a similar method to that previously described in this chapter. The two chimeras were thus referred to as TetBot and 2xTetBot, respectively. The inclusion of LcTd/A meant that the cleaved SNAP25 antibody could again be used to provide a reliable reporter for LcTd/A enzymatic activity. It could therefore be easily recognised where LcTd/A had been active, and from this, then surmise where the LcTd/A had been transported to, and how effectively.

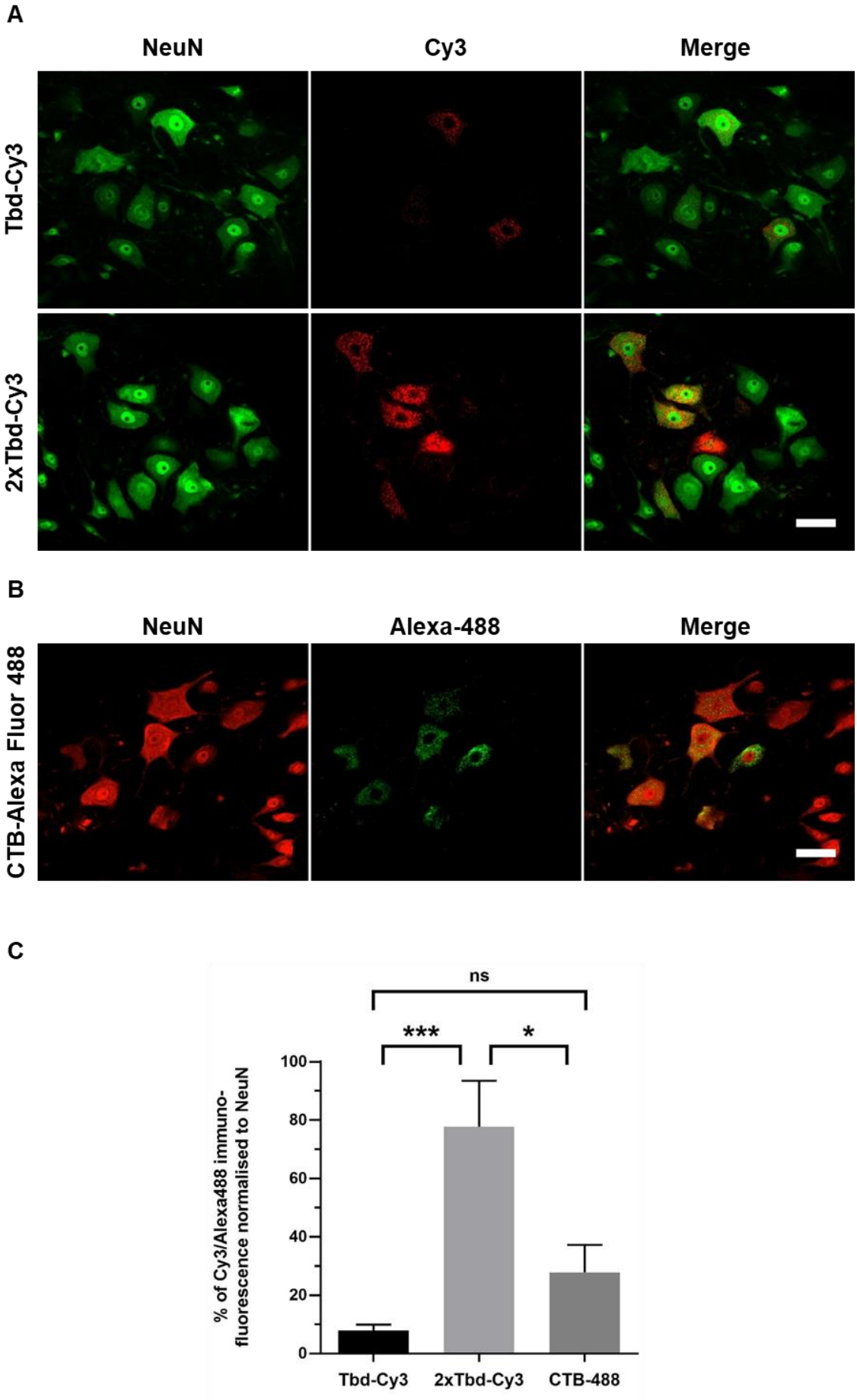
A
NeuN
Cy3
Merge
Tbd-Cy3
2xTbd-Cy3
B
NeuN
Alexa-488
Merge
CTB-Alexa Fluor 488
C
ns
***
*
% of Cy3/Alexa488 immuno-fluorescence normalised to NeuN
100
80
60
40
20
0
Tbd-Cy3
2xTbd-Cy3
CTB-488

Figure 5.2 The penetration of the lumbar spinal cord motor neuron soma by Tbd-Cy3 is increased by the attachment of a second tetanus binding domain. *Male 5 week old Sprague-Dawley rats received an intraplantar injection to the left hindpaw of either 7.5 µg/ 50 µl Tbd-Cy3 (N=2), 7.5 µg/ 50 µl 2xTbd-Cy3 (N=2) or 20 µg/ 30 µl CTB-AlexaFluor488 (N=2). Animals were then perfused 7 days later. The fixated spinal cord was taken and cryosectioned for immunohistochemistry. Images were acquired using a Nikon A1 TIRF confocal microscope.* ***(A)*** *Immunolabelling of ipsilateral lumbar spinal cord sections revealed -Cy3 (red) immunofluorescence colocalised with the NeuN stain, used to visualise the motor neurons (green), after injection of both Tbd-Cy3 and 2xTbd-Cy3. Scale bar= 20 µm* ***(B)*** *Spinal cord sections isolated from CTB-AlexaFluor488-injected animals similarly displayed Alexa-488 immunofluorescence (green) contained within the ipsilateral motor neurons (red). Scale bar= 20 µm* ***(C)*** *Quantification of the resultant immunofluorescence, using a thresholding technique, showed that injection of 2xTbd-Cy3 produced significantly more detectable immunofluorescence than injection of either Tbd-Cy3 and CTB-AlexaFluor488. All data presented as mean ± S.E.M., * p<0.05, *** p<0.001.*

Western blot analysis of dorsal root ganglion cultures incubated with increasing concentrations of both TetBot and 2xTetBot demonstrated that cleaved SNAP25 can be readily detected following 65 hour incubation with 2xTetBot at concentrations as low as 3.2 pM. In contrast, SNAP25 cleavage was only visualised following incubation with concentrations of 80 pM TetBot and above (Fig. 5.3C). This therefore implies that 2xTetBot has a higher efficacy than TetBot.

Similarly, quantification of the cleaved SNAP25 staining following intraplantar injection of 300 ng TetBot and 300 ng 2xTetBot into separate groups of animals, revealed that a significantly larger area of the spinal cord displayed positive SNAP25 cleavage following administration of 2xTetBot compared to TetBot (Unpaired t-test, $t_{(4)}$ =4.775, P=0.009, Fig. 5.3B). SNAP25 cleavage was visible in the ipsilateral ventral horn of the lumbar spinal cord following injection of both 2xTetBot and TetBot (Fig. 5.3A). Lumbar spinal cord sections prepared from 2xTetBot injected rats, however, showed a much greater medial spread of SNAP25 cleavage. Dense cleaved SNAP25 staining was seen reaching to the central canal of the spinal cord with additional projections decussating to the contralateral spinal cord (Fig. 5.3A). Furthermore, following intraplantar injection of 2xTetBot, the dense SNAP25 cleavage staining was observed as far dorsal as laminae V and VI of the dorsal horn. Additionally, single cleaved SNAP25-positive neurites were also seen extending more sparsely through to the superficial dorsal horn (Fig. 5.3A). In contrast, spinal cord sections prepared from TetBot injected rats displayed SNAP25 cleavage in a smaller area which was concentrated around laminae IX of the ventral horn, and was restricted to the ipsilateral spinal cord (Fig. 5.3A).

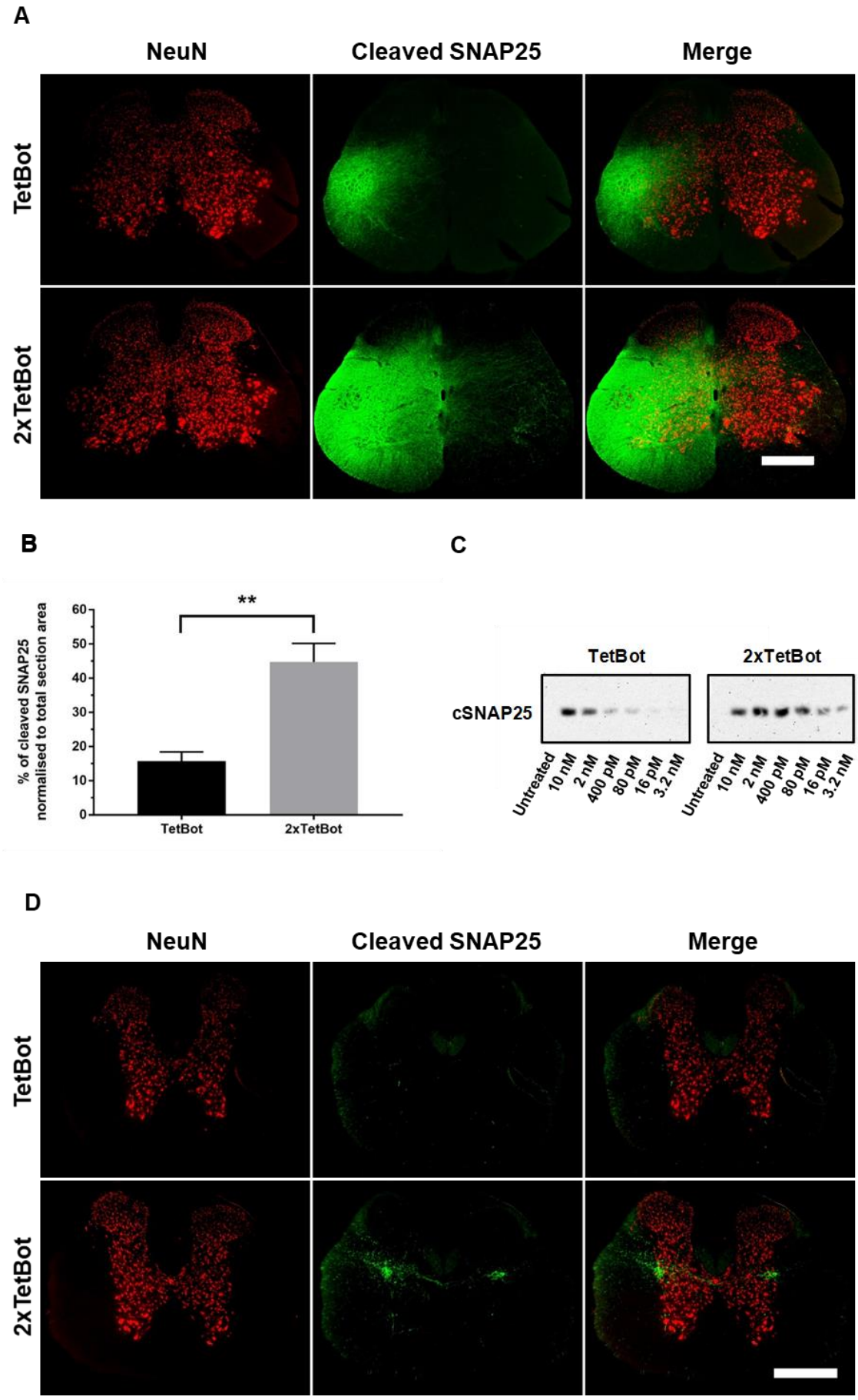
A
NeuN
Cleaved SNAP25
Merge
TetBot
2xTetBot
B
**
% of cleaved SNAP25 normalised to total section area
60
50
40
30
20
10
0
TetBot
2xTetBot
C
TetBot
2xTetBot
cSNAP25
Untreated
10 nM
2 nM
400 pM
80 pM
16 pM
3.2 nM
Untreated
10 nM
2 nM
400 pM
80 pM
16 pM
3.2 nM
D
NeuN
Cleaved SNAP25
Merge
TetBot
2xTetBot

Figure 5.3 Greater penetration of the lumbar rat spinal cord is observed after intraplantar injection of 2xTetBot. *Male 6 week old Sprague-Dawley rats received an intraplantar injection to the left hindpaw of either 300 ng/ 50 µl TetBot (N=3) or 300 ng/ 50 µl 2xTetBot (N=3). After 6 days, the animals were culled and the spinal cord was isolated. The spinal cord was marked by an incision to the contralateral ventral horn before sectioning.* ***(A)*** *Images were acquired using the Leica epifluorescence microscope. Cleaved SNAP25 (green) was visualised in the ipsilateral ventral horn of both TetBot- and 2xTetBot-injected rats but was absent in the neuronal soma, labelled using NeuN (red). Scale bar= 0.5 mm* ***(B)*** *Quantification of the staining at L5 of the spinal cord revealed that 2xTetBot (N=3, n=2) resulted in a significantly larger area of cleaved SNAP25 staining relevant to the total section area (44.7 ± 5.4%) than single TetBot (N=3, n=2) (15.6 ± 2.8%)* ***(C)*** *Western blot (N=1) of dorsal root ganglion cultures following 65 hr incubation with TetBot and 2xTetBot were probed with a cleaved SNAP25 antibody. SNAP25 cleavage was clearly detectable at concentrations as low as 3.2 nM after incubation with 2xTetBot, in comparison to 80 pM TetBot.* ***(D)*** *Staining of the thoracic lumbar region revealed bilateral SNAP25 cleavage in 2xTetBot-injected rats. This staining was absent in TetBot-injected rats. Scale bar= 0.5 mm. All data presented as mean ± S.E.M. ** p<0.01.*

Moreover, cleaved SNAP25 was detected at the thoracic level of the spinal cord after intraplantar injection of 2xTetBot (Fig. 5.3D) but not after intraplantar injection of TetBot. This suggests that the attachment of a second Tbd encourages transcytosis into second order projections neurons meaning that 2xTetBot may have transcytosised twice.

As was observed after injection of BiTox/A and BiTox/D, neither TetBot- or 2xTetBot-injected animals exhibited any visible signs of muscular paralysis, such as lameness or inability to grasp, despite the widespread SNAP25 cleavage observed at the level of the spinal cord. This is particularly surprising given the great expanse of SNAP25 cleavage detected in 2xTetBot injected animals, specifically.

5.2.4 Cleaved SNAP25 is not readily detected in the lumbar spinal region following intraplantar injection of ChoBot

The utility of Cholera Toxin Subunit B to deliver proteins of interest to the spinal cord was still investigated despite that CTB-488 was not shown to be more efficacious than single Tbd-Cy3 at internalising to neurons and undergoing retrograde transport, and remained less efficacious than 2xTbd-Cy3, due to the concerns over the immunogenicity predicted to occur when using tetanus toxin.

LcTd/A was again used as the protein of interest to study the ability of cholera binding domain to deliver proteins to the spinal cord. In this instance, LcTd/A was conjugated to the AB_5 domain of cholera toxin (for a more in-depth description, see 6.2.1). Briefly, AB_5

contains the receptor binding domain of cholera, the previously investigated B subunit, which interacts in a pentameric arrangement (B_5) with the rod-like structure, the A2 domain (A). The A1 domain which mediates the enzymatic active of cholera toxin was purposely excluded from the chimera. Resultantly, the chimera includes five binding domains.

In contrast to TetBot and 2xTetBot, immunohistochemical staining of the lumbar spinal cord showed few single fibres containing cleaved SNAP25 in the ipsilateral ventral horn after intraplantar injection of ChoBot (Fig. 5.4A). Staining of spinal cord sections using anti-CTB antibody, however, revealed positive CTB staining in the motor neurons of the ipsilateral ventral horn (Fig. 5.4B). This consequently suggests that CTB is unable to effectively chaperone LcTd/A to the central spinal cord.

5.3 Discussion

The blood-brain barrier remains a major obstacle for the delivery of therapeutic proteins to the central nervous system. Clostridial neurotoxins gain entry to the central nervous system via retrograde transport within nerve fibres, thereby circumventing the blood-brain barrier (Caleo and Schiavo, 2009). Consequently, clostridial neurotoxins represent one avenue being explored to achieve neuronal drug delivery. Here, it has been demonstrated that tetanus toxin can be used to effectively deliver both small fluorescent compounds, and much larger functional enzymes, to neuronal soma, situated within the central nervous system. Furthermore, it has been shown that the established stapling technique can be successfully used to enhance the efficacy of chimeras by constructing a chimera comprising of two receptor binding domains.

5.3.1 Attachment of a second targeting domain successfully augments the efficacy of chimeras

Here, the attachment of a second Tbd to the Tbd-Cy3 construct resulted in an almost ten-fold increase in the amount of fluorescence detected in the motor neuron soma in the ventral horn. Similarly, the conjugation of a second binding domain to the active chimera, TetBot, produced nearly three times as much SNAP25 cleavage in the lumbar spinal cord. The evidence from both experiments clearly supports the hypothesis that the presence of two targeting domains significantly increases the binding of chimeras. As a result, more material is being internalised into neurons and is consequently then reaching the central nervous system, following retrograde transport. Hence, enhancing the perceived efficacy of the chimeras.

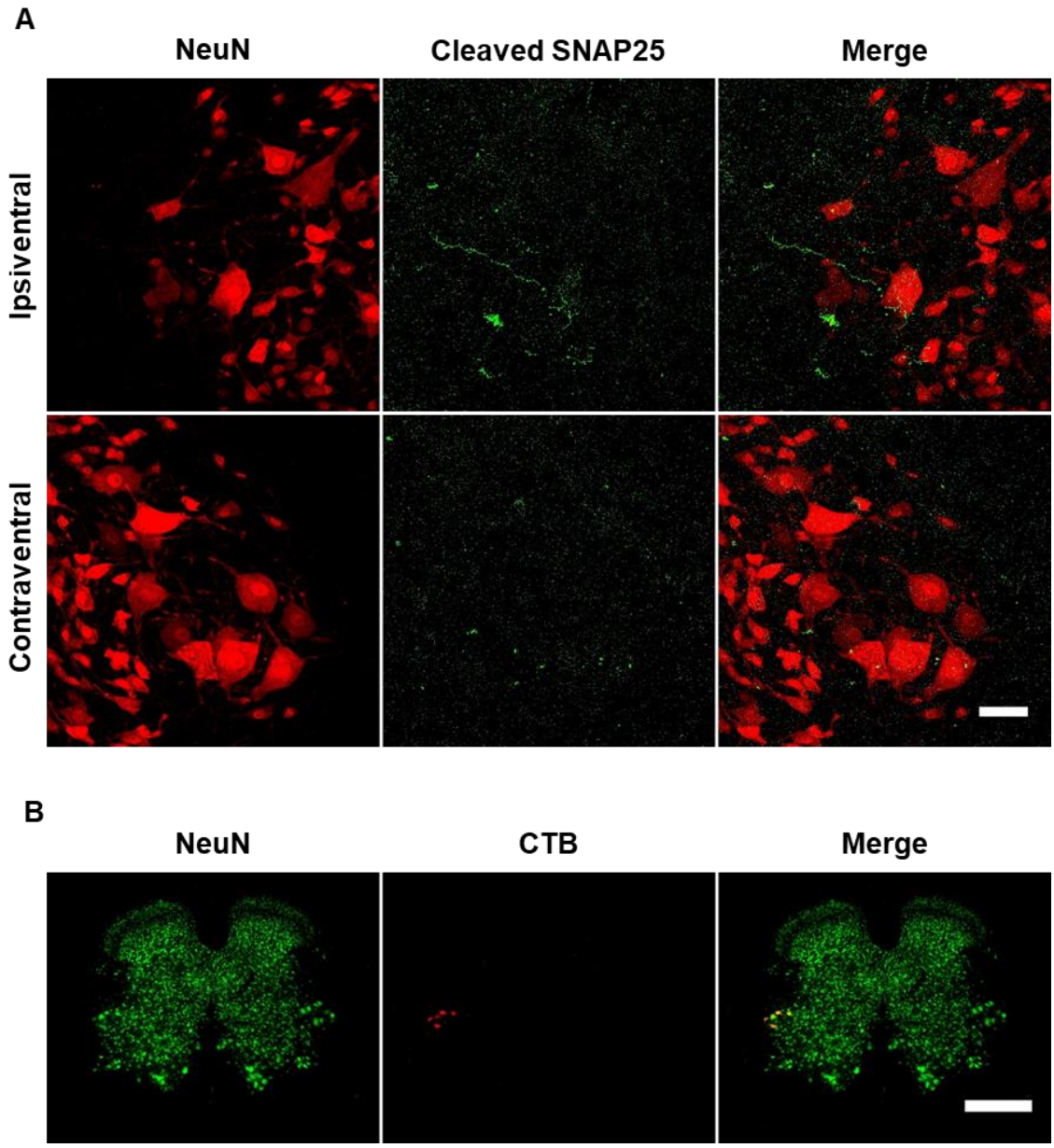

Figure 5.4 Limited SNAP25 cleavage is visualised in the lumbar spinal cord after intraplantar injection of ChoBot. *4 weeks old male Sprague-Dawley rats (N=2) received intraplantar injection of 200 ng/ 30 µl ChoBot.* ***(A)*** *Imaging of the lumbar spinal cord was conducted using a Nikon A1 TIRF confocal microscope. Lumbar spinal cord sections isolated from ChoBot-injected rats (N=2) show only single fibres positive for cleaved SNAP25 (green) within the ipsilateral ventral horn. No SNAP25 cleavage was detected in the contralateral ventral horn. Motor neurons are labelled using NeuN (red). Scale bar= 20 µm* ***(B)*** *Low magnification images of the spinal cord were acquired using the Leica epifluorescence microscope. Anti-CTB antibody (red) was used to detect the Cholera B subunit (CTB) at the level of the spinal cord whilst NeuN (green) was used to label all neuronal soma. Positive staining in the lumbar spinal cord for CTB (red) colocalised with the motor neurons of the ventral horn, following intraplantar injection, demonstrating that the B-subunit of ChoBot is retrogradely transported to the spinal cord. Scale bar= 0.5 mm*

This is most likely due to an increased interaction time between the chimera and the receptor of interest. As described earlier, the theory of binding kinetics depicts an on- (association) and off- (dissociation) rate constant for ligand-receptor interactions (Corzo, 2006; Peuker et al., 2013). The presence of a second binding domain would greatly increase the probability of the chimera continuing to interact with the receptor. As one binding domain dissociates away from the receptor, the other binding domain would be immediately available to bind to the now vacant receptor. This would thus prevent drift and would increase the overall chimera-to-receptor interaction time, henceforth, improving the internalisation rate. A similar finding has been demonstrated in native proteins that naturally contain two binding domains. For example, fibronectin-binding proteins, F1 and F2, of the bacterium, streptococcus, require both binding domains for optimal binding of the proteins to their targets (Jaffe et al., 1996).

The attachment of a second binding domain to a functional enzyme was important to demonstrate that Tetanus toxin could be used to deliver large cargo, opposed to small fluorescent markers. The SNAP25 cleavage detected confirmed that the attachment of two separate binding domains did not interfere with the enzymatic activity of LcTd/A. In contrast, the presence of a second binding domain greatly augmented the perceived catalytic activity of the chimera, as demonstrated by the large expanse of SNAP25 cleavage, both dorsally and medially, visualised in the spinal cord of rats injected intraplantar with 2xTetBot. Conversely, SNAP25 cleavage was mostly contained within the ipsilateral ventral horn following injection of TetBot. Noticeably, cleaved SNAP25 was detected in fibres extending to the contralateral spinal cord and into the ipsilateral dorsal horn of the lumbar spinal cord. Additionally, cleaved SNAP25 was detected at the higher thoracic level of the spinal cord in rats receiving intraplantar injection of 2xTetBot. Together, the evidence suggests that the presence of the double binding domain, aids the transcytosis of the LcTd/A into second order neurons. In its native form, tetanus is retrogradely transported, via motor neurons, to the ventral horn, where it transcytoses into interneurons (Surana et al., 2017). The SNAP25 cleavage observed in the thoracic region implies that the chimera may be capable of transcytosing across multiple synapses, after the addition of a second Tbd, whereas the transcytosis of the single binding domain TetBot appears to be more restricted.

5.3.2. The potential evidence for transcytosis introduces the possibility of delivering therapeutics to higher central nervous system regions

Moreover, the fact that SNAP25 cleavage was detected in the thoracic region generates interest as to whether peripheral injection of 2xTetBot could be used to deliver

therapeutic proteins to higher regions of the central nervous system, for example, the brainstem. Cleaved SNAP25 appears to be visualised in the lateral reticulospinal tract, a descending motor pathway, important for locomotion (Watson and Harvey, 2009). It is therefore possible that cleaved SNAP25 would be detected in the reticular formation in the brainstem, where this tract orginates. Tissue from the brainstem was not analysed on this occasion, however, this staining would be conducted if this experiment was to be repeated.

Although likely, it has not yet been confirmed that the cleaved SNAP25, detected in the thoracic spinal cord, is specifically contained within the lateral reticulospinal tract. The intermediolateral nucleus, which contains preganglionic sympathetic neurons, is located proximal to the lateral reticulospinal tract. It is thus possible that the SNAP25 cleavage visualised could instead be contained within the preganglionic sympathetic neurons of the intermediolateral nucleus, that innervate the abdominal viscera. This would thus suggest that 2xTetBot had somehow enterred the systemic circulation, from the peripheral injection site, to gain access to the abdomen.

It is important that this matter is resolved before further developing double tetanus binding domain as a delivery tool. One way to achieve this would be to retrogradely label the preganglionic neurons by injection of Fluorogold to the abdomen, and then investigate whether the cleaved SNAP25 staining colocalises with the tracer (Appel and Elde, 1988; Clemens et al., 2005). Alternatively, tyrosine hydroxylase could be used to label the sympathetic neurons, again looking for colocalisation with the cleaved SNAP25 marker. Notably, the cleaved SNAP25 staining demonstrated here does appear very similar to the tyrosine hydroxylase labelling of the IML, reported by Clemens et al. (2005), who described this labelling to be descending inhibitory dopaminergic axonal arborisations. Notably, the descending pathways regulating the activity of the sympathetic neurons project from the ventrolateral medulla (Zagon and Smith, 1993), again suggesting that it is possible that LcTd/A could reach the brainstem, after peripheral injection of 2xTetBot, albeit, via an alternative pathway to that previously considered.

5.3.3 Tetanus chimeras do not produce motor paralysis despite high levels of SNAP25 cleavage detected in the ventral horn

One of the most suprising findings, following intraplantar injection of 2xTetBot, was the absence of any signs of motor paralysis or motor impairment despite the large amount of SNAP25 cleavage detected in the ventral horn of the lumbar region. Laminae IX, located in the lateral ventral horn of the spinal cord, is responsible for the motor

innervation of the distal flexor muscles and appears to be the centre point of the SNAP25 cleavage in both the 2xTetBot- and TetBot- injected rats. Native tetanus toxin transcytoses from motor neurons into synapsing inhibitory interneurons where it cleaves the SNARE protein, synaptobrevin, thus blocking the release of inhibitory neurotransmitters, and consequently producing spastic paralysis (Surana et al., 2017). Accordingly, it would be expected that both TetBot and 2xTetBot would likewise produce spastic paralysis provided that the Tbd should target the chimera to the neurons natively targeted by tetanus, the inhibitory interneurons. This, however, remains to be confirmed by immunostaining.

In support of the observations made here, Ferrari et al. (2013) likewise did not observe any signs of motor paralysis in mice, even after intramuscular injection of 500 ng TetBot, equivalent to 100,000 times the lethal dose of native BoNT/A. It is, however, possible that while no obvious muscle paralysis was perceived, that the rats could have experienced compromised function of the hindpaw. In future, a grip test should be used to discriminate whether rats have any less obvious muscular paralysis.

5.3.4 Utilising tetanus chimeras to treat lysosomal disorders

The potential for motor paralysis associated with drug delivery to the interneurons and higher motor pathways by Tbd would not be a concern if the aim was to deliver a therapeutic protein, such as a neuroprotective factor, to neurons rather than a functional enzyme. It remains to be investigated whether Tetanus toxin can be used to deliver other proteins, rather than another clostridial subunit, as shown here. Tbd has previously been used to target the enzyme, beta-hexosaminidase, responsible for the degradation of the ganglioside GM2 in neurons, to the lysosomes of neurons to treat GM2 gangliosidosis, a neurodegenerative lysosomal storage disease (Dobrenis et al., 1992). A reduction in the accumulation of GM2 was noted after the incubation of neuronal cultures with the Tbd-beta-hexosaminidase construct. It was thus concluded that Tbd had successfully chaperoned the enzyme to the lysosome, to enable effective degradation of GM2. The stapling technology could therefore conceivably be applied to enhance drug delivery for the treatment of lysosomal disorders.

5.3.5 The cholera toxin-derived targeting domain is not suitable for delivery of therapeutics to the central nervous system

In contrast, potentially undetected motor effects remain an issue with regards to the other objective of this thesis, to design a neuronal blocker to be used as a novel analgesic, as

this would require the inclusion of the LcTd/A catalytic domain. Although a greater amount of fluorescence was visualised in the motor soma of the ventral horn following intraplantar injection of CTB-488, than single Tbd-Cy3, the cholera targeting subunit, AB5, was largley unsuccessful at chaperoning and delivering LcTd/A to the spinal cord. The lack of retrograde transport demonstrated could prove beneficial, however, when developing an analgesic for pain conditions where the pain is restricted to a peripheral site. If the catalytic activity of ChoBot is equally confined to the peripheral injection site then this would greatly reduce the risk of off-target, central effects.

It is worthwhile to note, however, that although more fluorescence was detected after intraplantar injection of CTB-488, compared to TetBot, a larger amount of CTB-488 than Tbd-Cy3 was injected, almost three times as much (20 µg CTB-488 opposed to 7.5 µg Tbd-Cy3), in line with recommendations gathered from previous studies (Conte et al., 2009; Mantilla et al., 2009). Accordingly, there was approximately a 3.5 fold increase in the amount of fluorescence detected, thus implying that, overall, cholera CTB subunit did not offer a huge advantage over single Tbd, with regards to the delivery of fluorescent dyes. Additionally, CTB was conjugated to AlexaFluor488, opposed to Cy3. The AlexaFluor dyes provide much greater photostability than the traditional fluorophores (ThermoFisher, n.d.; Mahmoudian et al., 2011) and are therefore more resistant to photobleaching. This could prove particularly advantageous when using confocal microscopy and thus might haved biased the perceived fluorescence.

It should also be acknowledged that CTB-488 was not constructed using the SNARE stapling technology used to produce Tbd-Cy3 and 2xTbd-Cy3. It was instead purchased as a recombinantly expressed protein, whereby the genes encoding CTB and AlexaFluor488 were fused, prior to expression (ThermoFisher, 2003). The ChoBot chimera used later in the experiment was, however, constructed using the stapling technology. It would therefore be of benefit to construct AB5-Cy3, using the SNARE-stapling approach, to determine whether fluorscence can still be detected in the spinal cord when using the same method of conjugation, and the same fluorophore.

Notably, in contrast to the CTB-488 conjugate, when constructing ChoBot, the LcTd/A was conjugated to the AB_5 domain, rather than directly to the B subunit. It has been reported that the B subunit dissociates from the pentameric structure at low pH, typically lower than pH 4.0 (De Wolf et al., 1987). BoNT/A must enter acidic vesicles, upon internalisation, to permit the unfolding of the translocation domain, in order for the enzymatic light chain to escape to the cytosol (Pirazzini et al., 2011). There are therefore two possible theories for the perceived lack of SNAP25 cleavage in the spinal cord. Firstly, ChoBot could have entered the acidic vesicles, consequently causing the targeting domain, CTB, to dissociate away from the chimera. This would have resulted

in LcTd/A being left at the peripheral terminal whilst CTB continued to be retrogradely transported to the central synapse, hence explaining the immunoreactivity for CTB detected in the motor soma post-intraplantar injection of ChoBot, and the absence of SNAP25 cleavage. Conversely, the AB_5 domain could have chaperoned LcTd/A into neutral vesicles, resulting in the catalytic light chain being unable to escape the vesicle, and therefore, the Lc would have been delivered to the central motor neuron soma but remained trapped inside the endosome, rendering LcTd/A inactive. This again provides valid explanation for the positive CTB staining, despite the lack of cleaved SNAP25.

5.3.6 Conclusion

In conclusion, it has been shown that tetanus toxin is an efficacious tool for drug delivery to the central nervous system. The in vivo data collected from TetBot and 2xTetBot injected-rats highlights that the pioneered stapling technique can be successfully used to enhance the efficacy of chimeras by attachment of a second targeting domain. 2xTetBot remains a proof of principle due to the associated immunogenicity of tetanus toxin in humans (Maple et al., 2000). The transferability of the technology to other chimeras still requires further investigation but appears promising. Moreover, the opportunity exists to attach another binding domain, or therapeutic protein, by splitting the SNARE complex into 4 individual peptides. Each of SNARE peptides could, in theory, be recombinantly expressed with an attached protein, creating a 4-domain SNARE-stapled chimera.

Separately, Cholera toxin was investigated as an alternative toxin for development as a drug delivery tool but failed to deliver large proteins to the central nervous system. The suspected limited penetration of the central nervous system by ChoBot could, however, prove beneficial in the development of analgesics. Although no motor paralysis following injection of either TetBot or 2xTetBot was observed, the long-term effects of SNAP25 cleavage within the motor area of the spinal cord are unknown and should thus be avoided when developing a future analgesic. Furthermore, if SNAP25 cleavage is only observed in the periphery following intraplantar injection of ChoBot, it could help to resolve the earlier questions of whether the therapeutic effect of BoNT/A is due to its peripheral or central catalytic activity. The use of ChoBot as a novel analgesic will consequently be explored in the next chapter.

Chapter 6. New bacterial chimera for the alleviation of post-operative pain and chemotherapy-induced peripheral neuropathy

6.1 Introduction

Two aforementioned novel clostridial chimeras, BiTox/A (Mangione et al., 2016) and TetBot (Ferrari et al., 2013), have been shown to be analgesic against mechanical hypersensitivity in separate pain conditions. Further investigation here has demonstrated that both chimeras produce large amounts of SNAP25 cleavage at the level of spinal cord, thus indicating that they must undergo retrograde transport from the periphery to the spinal cord. Consequently, although no signs of motor paralysis or compromised well-being were observed, there are concerns about any possible long-distance, off-target adverse effects, associated with the retrograde transport of these chimeras.

By comparison, ChoBot, containing the binding domain of Cholera Toxin (AB5) and the light chain translocation domain of Botulinum Neurotoxin A (LcTd/A), produced negligible amounts of cleaved SNAP25 in the spinal cord following intraplantar injection. This therefore implies that there is minimal retrograde transport of LcTd/A to the central spinal cord and that the catalytic activity of LcTd/A is instead restricted to the peripheral injection site. Not only is this beneficial to prevent off target effects but, if ChoBot was similarly shown to be analgesic, it would help to further elucidate whether the therapeutic benefit of SNAP25 cleavage by LcTd/A is due to a peripheral or central mechanism (Mangione et al., 2016).

Firstly, this chapter aims to confirm whether ChoBot does retain the catalytic activity of LcTd/A in vivo, and, if so, determine whether this catalytic activity is largely constrained to the injection site. If shown to be true, it will next be pursued whether ChoBot can similarly provide analgesia in pain models. Thus, either generating support for, or negating, the hypothesis that the analgesic effect of LcTd/A is peripherally mediated.

6.2 Results

6.2.1 ChoBot retains the enzymatic activity of Botulinum Neurotoxin A in vitro

As described in the previous chapter, the novel chimera, ChoBot, was constructed from a truncated version of the AB_5 cholera toxin, which was then stapled to the LcTd/A, by the addition of a SNARE peptide staple.

The native Cholera Toxin A subunit is expressed as a single polypeptide consisting of two domains, A1 and A2, which are joined by a disulphide bond. The A1 domain contains

the catalytic activity of cholera toxin (Beddoe et al., 2010). Consequently, the truncated A subunit used here to form the chimera contained only the rod-like, linker portion of the A subunit, the A2 domain, fused to the SNARE peptide, synaptobrevin. Specifically, the A2 domain is an α-helix which associates with the B subunit, via the central pore. There is a total of five B subunits which assemble into a pentameric arrangement, around the A2 domain, hence the name, AB_5. The removal of the A1 subunit eliminated the catalytic activity associated with Cholera toxin. Instead, here, the chimera's catalytic activity was inferred by the addition of the LcTd/A, which facilitates the cleavage of SNAP25. LcTd/A was fused to the SNARE- peptide, α-SNAP25, which, with the addition of the staple, syntaxin, enabled the formation of a SNARE complex between the two separate components of the chimera, the truncated AB5-synaptobrevin and LcTd/A-αSNAP25, to form an irreversibly conjugated chimera (Fig. 6.1A).

The stability of the chimera is highlighted during the running of a coomassie-stained SDS-PAGE gel. In the unboiled sample, the chimera is seen as a single band and does not dissociate back into the separate LcTd/A-αSNAP25 and A2-synaptobrevin domains, showing that the SNARE-complex is SDS-page resistant (Fig. 6.1A). The A2-synaptobrevin band represents excess material that was unable to conjugate to LcTd/A-αSNAP25 due to there being no more available to conjugate to, hence the absence of

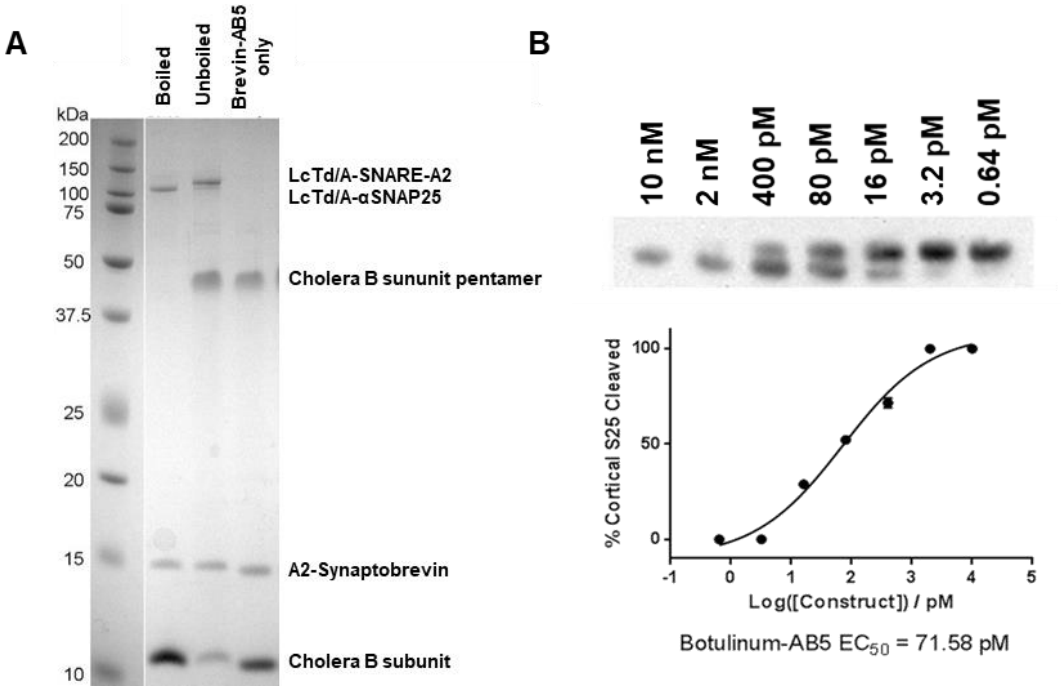

Figure 6.1 ChoBot successfully cleaves SNAP25 in rat cortical neuron cultures (A) *A coomassie-stained SDS-PAGE gel showing the assembly of the chimera, ChoBot.* ***(B)*** *Western blot showing cleavage of SNAP25 in rat cortical neuron cultures following 65 hour incubation with 0.64 pM- 10 nM ChoBot (N=2). Complete cleavage of SNAP25 is observed at concentrations of 2 nM and greater. Quantification of the western blot data displayed in the dose-response curve shows that the EC_{50} for SNAP25 cleavage was 71.58 pM. Data provided courtesy of Dr C. Leese.*

a LcTd/A-αSNAP25 band in the unboiled sample. Conversely, in the boiled sample, all components can be seen in their individual bands. It is noted on the gel, however, that the pentameric and singular B-subunits dissociate from the A subunit in all lanes, including in the unboiled sample. This is because the A2 subunit is non-covalently bound to the B-pentamer meaning that the two easily dissociate with the addition of SDS-page. Hence, also explaining the B-pentamer and singular B-subunit bands visible in each lane (Fig. 6.1A) (Beddoe et al., 2010).

After demonstrating the successful assembly of the chimera, the functionality of ChoBot was assessed in vitro to ensure that ChoBot remained capable of binding and internalising into neurons, as well as effectively retaining the catalytic activity of BoNT/A. ChoBot was added to dissociated cortical neuron cultures in varying concentrations. Complete cleavage of SNAP25 was shown in rat cortical neurons after 65 hour incubation with concentrations of 2 nM ChoBot and higher. Moreover, SNAP25 cleavage was produced by concentrations as low as 16 pM, thus demonstrating that ChoBot can effectively bind and internalise into neurons, and cleave SNAP25, in vitro (Fig. 6.1B).

6.2.2 ChoBot produces SNAP25 cleavage in myelinated sensory neurons in vitro

The ultimate intention is to design a chimera to be used as an analgesic. ChoBot's enzymatic activity was therefore further assessed in dorsal root ganglion cultures to determine whether ChoBot is able to preferentially bind to, and consequently cleave SNAP25 in, a subset of sensory neurons, specifically nociceptive neurons. For this purpose, we compared the binding profile of ChoBot to the two chimeras which have previously been demonstrated to produce analgesia in animal models, TetBot and BiTox/A (Ferrari et al., 2013; Mangione et al., 2016).

After 65 hour incubation with 10 nM ChoBot, cleaved SNAP25 was observed in a subset of sensory neurons with an average cell diameter of 21.0 ± 1.0 µm, again identified using the pan-neuronal marker, βTubulin III (Fig. 6.2A). According to the frequency distribution histogram, cleaved SNAP25 was most often visualised in neurons with a cell diameter between 18-20 µm. Another peak was noted at 28 µm cell diameter, (Fig. 6.2B), reminiscent of the frequency distribution histograms associated with incubation of cultures with BiTox/D (Fig. 4.4B).

Similarly, incubation with TetBot resulted in detectable SNAP25 cleavage in a subset of neurons with a mean cell diameter of 22.1 ± 1.1 µm (Fig. 6.2A). Again, two peaks were noted in the frequency distribution histogram, one peak at 16-20 µm cell diameter, and the other at 26 µm cell diameter (Fig. 6.2B). There was no significant difference between

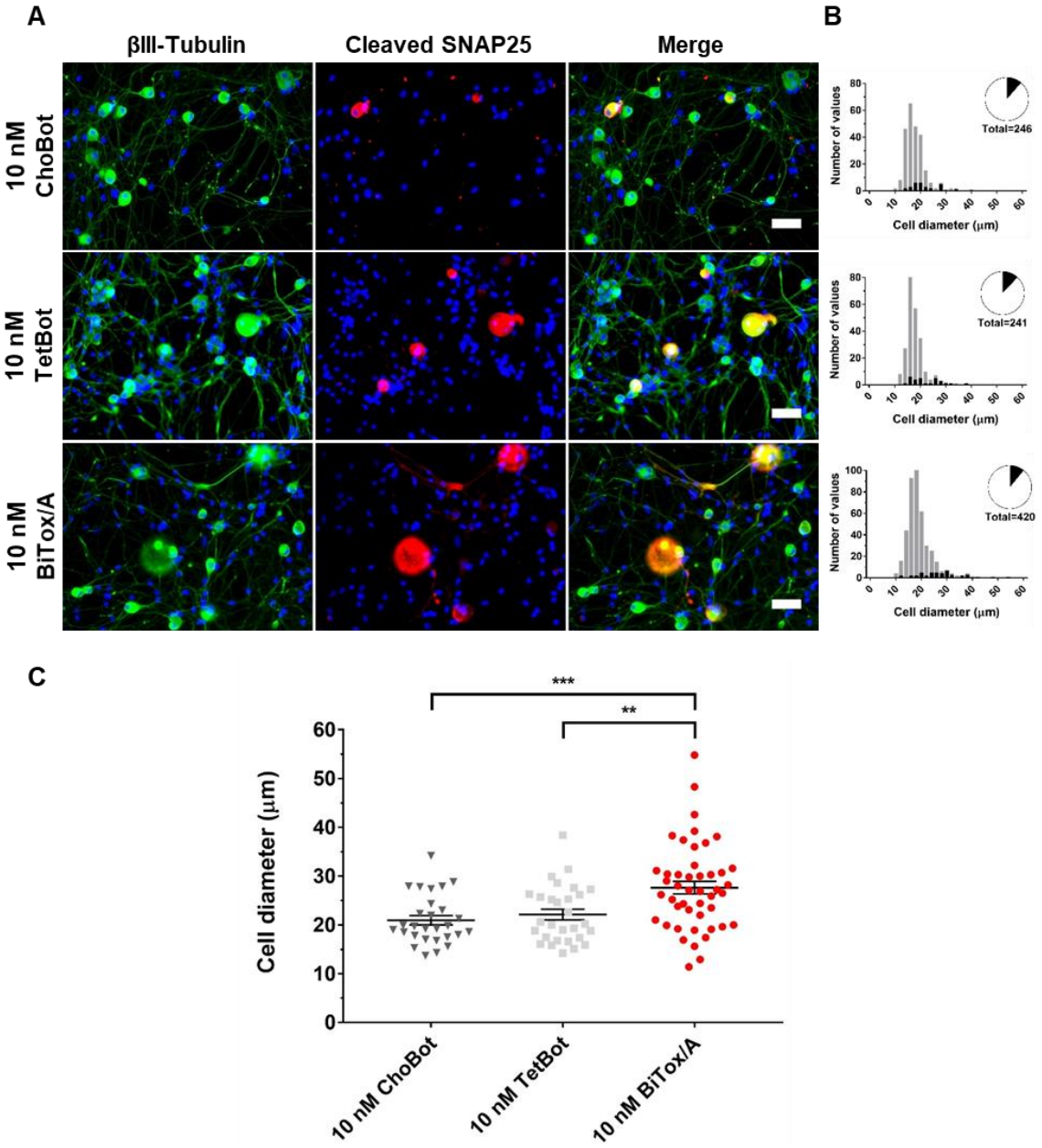

Figure 6.2 ChoBot cleaves SNAP25 in a subpopulation of cultured sensory neurons. (A) *Epifluorescent images of SNAP25 cleavage (red) in dissociated dorsal root ganglion neurons, identified using pan-neuronal marker, βTubulin III (BTIII) (green) after 65 hour incubation of cultures with 10 nM ChoBot (N=3, n=3), 10 nM TetBot (N=3, n=3) and 10 nM BiTox/A (N=5, n=3). The health of sensory neurons was confirmed by identification of an intact nucleus using DAPI (blue). Cleaved SNAP25 immunoreactivity was not detected in vehicle or untreated neuronal cultures (data not shown).* ***(B)*** *Images were quantified to produce frequency distribution histograms showing the number and diameter of neurons displaying both BTIII and cSNAP25 staining (black) compared to neurons displaying BTIII staining only (grey). Inserted pie charts (top right) show the percentage of the total neurons identified, that displayed SNAP25 cleavage (black). Scale bar = 50 μm.* ***(C)*** *The data points plotted represent the identified neurons positive for cleaved SNAP25 after incubation with each of the chimeras. Incubations with BiTox/A (27.6 ± 1.3 μm) resulted in cleaved SNAP25 being detected in neurons with a significantly higher mean cell diameter compared to ChoBot (21.0 ± 1.0 μm) and TetBot (22.1 ± 1.1 μm). All data is presented as mean ± S.E.M.** P=0.01, *** P=0.001.*

the average cell diameter of neurons displaying cleaved SNAP25 after incubation of ChoBot compared to TetBot (One-way ANOVA, $F_{(2,100)} = 9.355$, P=0.8158, Fig 6.2C).

In contrast, incubation with BiTox/A produced cleaved SNAP25 in a subpopulation of neurons with significantly larger mean cell diameter (27.6 ± 1.3 µm) than following incubation with ChoBot (One-way ANOVA, $F_{(2,100)} = 9.355$, P=0.0005) and TetBot (One-way ANOVA, $F_{(2,100)} = 9.355$, P=0.0045, Fig 6.2C). This is well exemplified by the frequency distribution histogram were the neurons displaying positive cleaved SNAP25 can be seen distributed across the upper values of the histogram. There was no significant difference in the percentage of neurons showing positive-cleaved SNAP25 staining between the three chimeras (One-way ANOVA, $F_{(2, 8)} = 0.34433$, P=0.7187, Fig. 6.2B).

The neuronal markers, Neurofilament 200 and peripherin, were subsequently used to distinguish whether this difference in binding between BiTox/A and the two other chimeras, ChoBot and TetBot, occurred within the population of larger, myelinated Aβ- and thinly myelinated Aδ- sensory neurons, or within the population of smaller unmyelinated neurons. Labelling the larger, myelinated neurons, using anti-NF200 antibody, likewise revealed that the neurons displaying positive cleaved SNAP25 staining after incubation with BiTox/A had a significantly larger mean cell diameter (28.2 ± 1.2 µm) in comparison to those showing cleaved SNAP25 after addition of ChoBot (20.9 ± 1.3 µm; One-way ANOVA, $F_{(2,90)} = 10.68$, P=0.0004) and TetBot (21.5 ± 1.3 µm; One-way ANOVA, $F_{(2,90)} = 10.68$, P=0.0015) (Fig. 6.3C). For both ChoBot and TetBot, the frequency distribution histogram indicated that the peak in the number of neurons displaying SNAP25 cleavage occurred below 20 µm (Fig. 6.3B). BiTox/A again produced a histogram were the neurons displaying cleaved SNAP25 spanned the upper values of the histogram, with a peak specifically observed at 30 µm cell diameter (Fig. 6.3B). There was, however, no perceived difference in the percentage of neurons displaying cleaved SNAP25, dependent on the treatment of cultures with the different chimeras (One-way ANOVA, $F_{(2,7)} = 0.1389$, P=0.8727, Fig 6.3B).

In contrast, identification of the unmyelinated, peripherin-positive neurons did not indicate any significant differences in either the mean cell diameter of the neurons co-labelled for cleaved SNAP25 (One-way ANOVA, $F_{(2,27)} = 0.3012$, P=0.7423; Fig. 6.4C), or in the percentage of peripherin-positive neurons displaying cleaved SNAP25 (One-way ANOVA, $F_{(2,6)} = 0.6665$, P=0.5478, Fig. 6.4B), following incubation with the different chimeras. All three chimeras produced cleaved SNAP25 in a subpopulation of unmyelinated neurons with a mean cell diameter below 20 µm (Fig. 6.4C).

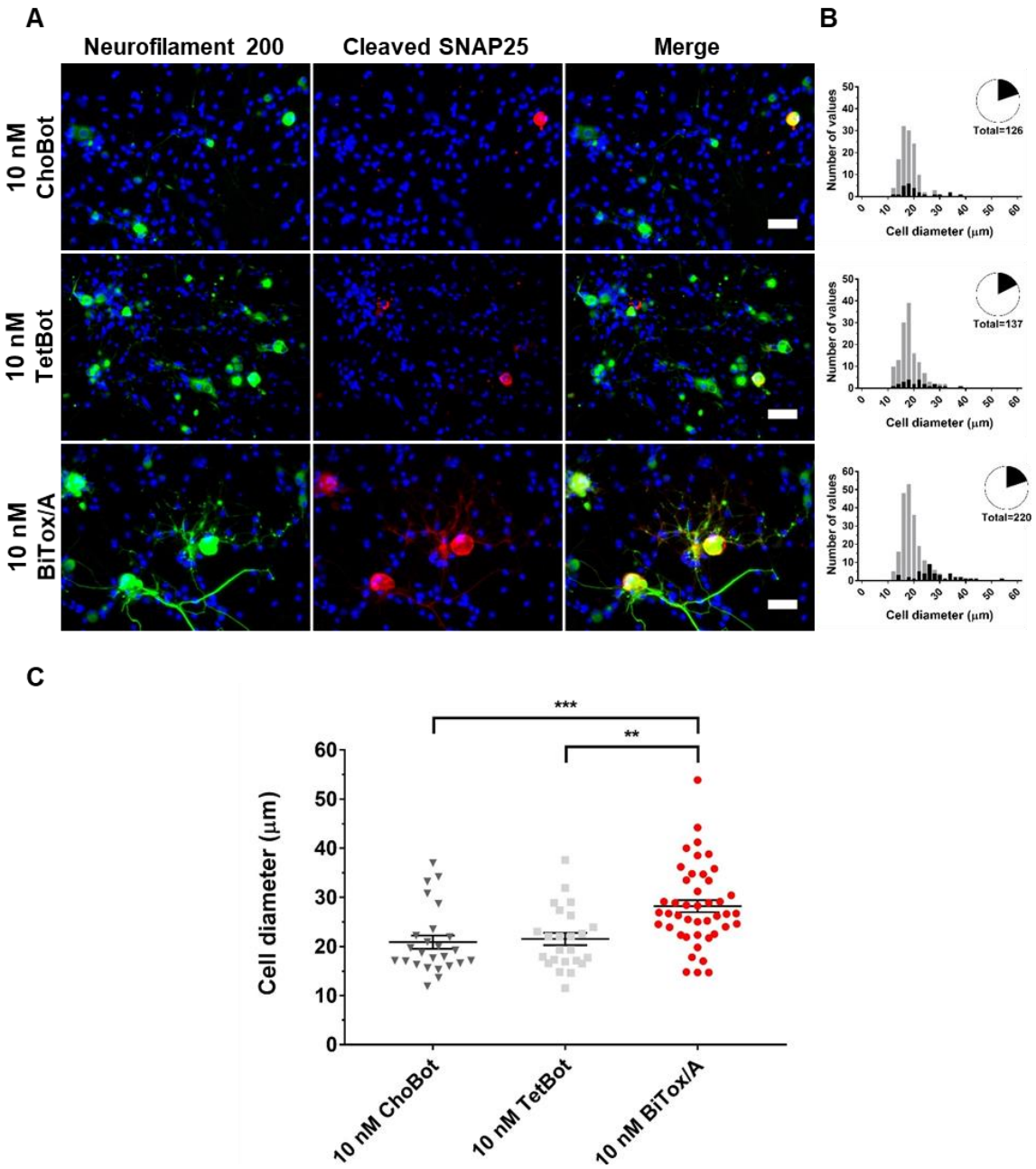

Figure 6.3 ChoBot cleaves SNAP25 in a subpopulation of myelinated sensory neurons. (A) *Representative images of cleaved SNAP25 (red) in myelinated sensory neurons, defined using anti-neurofilament 200 (NF200) antibody (green), following 65 hour incubation of dissociated dorsal root ganglion cultures with 10 nM ChoBot (N=3, n=3), TetBot (N=3, n=3) and BiTox/A (N=4, n=3). The nucleus is indicated by DAPI (blue). Scale bar= 50 µm.* ***(B)*** *Quantification of images was used to generate frequency distribution histograms which show the distribution of NF200-labelled neurons displaying cleaved SNAP25 (black), dependent on cell diameter, compared to NF200-positive neurons negative for cleaved SNAP25 (grey). Pie charts (top right) display the percentage of total NF200-positive neurons that were colabelled for cleaved SNAP25 (black).* ***(C)*** *Plotting the cell diameter of individual neurons colabelled for NF200 and cleaved SNAP25, after incubation with each of the chimeras, revealed that BiTox/A cleaves SNAP25 in myelinated sensory neurons with a larger mean cell diameter (28.2 ± 1.2 µm) than ChoBot (20.9 ± 1.3 µm) and TetBot (21.5 ± 1.3 µm). All data is presented as mean ± S.E.M.** P=0.01, *** P=0.001.*

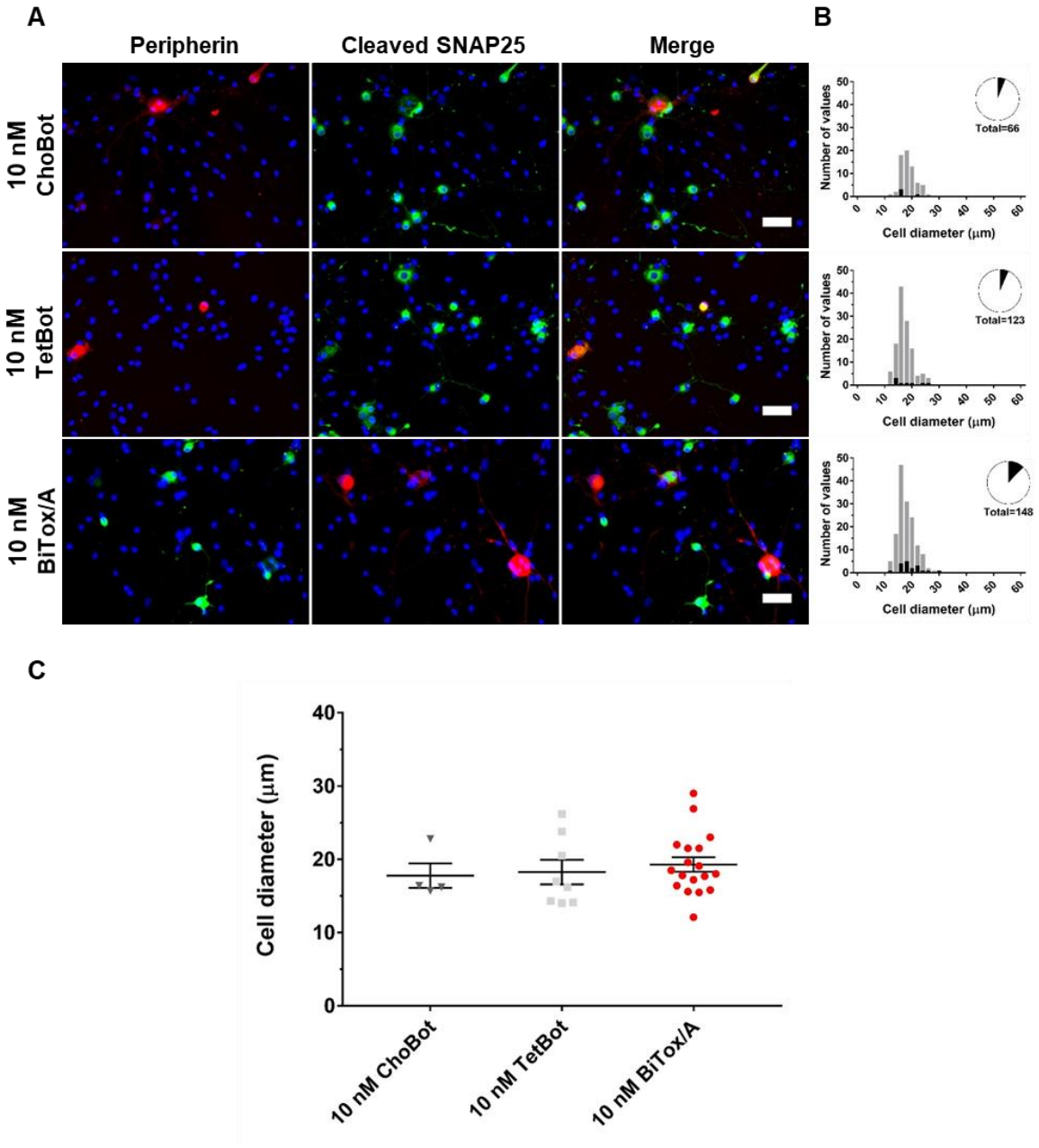

Figure 6.4 ChoBot cleaves SNAP25 in a small proportion of unmyelinated sensory neurons in vitro. (A) *Representative epifluorescent images of cleaved SNAP25 (red) in unmyelinated sensory neurons, marked using anti-peripherin antibody (green), taken after 65 hour incubation of 2 day old dissociated dorsal root ganglion cultures with 10 nM ChoBot (N=2, n=3), 10 nM TetBot (N=3, n=3) and 10 nM BiTox/A (N=4, n=3). DAPI (blue) marks the cell nuclei. Scale bar = 50 µm.* ***(B)*** *Frequency distribution histograms show the distribution of peripherin-positive neurons displaying cleaved SNAP25 (black), dependent on cell diameter, compared to peripherin marked neurons, negative for cleaved SNAP25 (grey). Pie charts (top right) illustrate the number of neurons colabelled for peripherin and cleaved SNAP25 (black) expressed as a percentage of the total number of peripherin-positive neurons.* ***(C)*** *The cell diameter of neurons colabelled for peripherin and cleaved SNAP25 was plotted to reveal no significant difference in the mean cell diameter of unmyelinated neurons displaying cleaved SNAP25 after incubation with each of the chimeras. All data is presented as mean ± S.E.M.*

6.2.3 Cleaved SNAP25 is detected in the peripheral sensory neurons of the glabrous skin following intraplantar injection of ChoBot

Subsequent in vivo investigations were used to evaluate whether the in vitro binding profile of ChoBot could be replicated in vivo. The pan-neuronal marker, βIII-Tubulin, was firstly used to label the neuronal fibres, innervating the glabrous skin. βIII-Tubulin recognises all nerve fibres and subsequently stains both motor and sensory neurons. The location of the nerve terminals was therefore used to distinguish the sensory nerve fibres from the motor nerve fibres. Sensory neurons terminate inside the dermis, proximal to the epidermis. Conversely, motor neurons project directly to the muscle fibres which are located much deeper in the dermis and are easily identified by their striated appearance.

Subsequent immunostaining using anti βIII-Tubulin antibody, revealed positive cleaved SNAP25 staining in the sensory neurons of the glabrous skin of the ipsilateral paw, following intraplantar injection of 200 ng ChoBot (Fig. 6.5A). SNAP25 cleavage was not detected in the sensory neurons of contralateral paw of ChoBot-injected animals (Fig. Fig. 6.5A). Likewise, cleaved SNAP25 was not observed in the ipsilateral paw of vehicle-injected or naïve rats.

Further staining was next conducted to elucidate which subtype of sensory neurons, specifically, contained cleaved SNAP25. Comparable to the in vitro labelling, cleaved SNAP25 was visualised in the larger, myelinated NF200 positive-neurons, however, it was not present in all NF200-stained neurons (Fig. 6.5B). SNAP25 cleavage was also seen in neurons expressing CGRP, described to be peptidergic neurons (Fig. 6.5B).

6.2.4 ChoBot significantly reduced KCl-evoked CGRP release in cultured sensory neurons

Consequent to the evidence that ChoBot can internalise into peptidergic neurons, it was investigated whether ChoBot could modulate neuropeptide release. Peptidergic neurons are heavily involved in neurogenic inflammation and are implicated in inflammatory pain conditions (Kilo et al., 1997; Benemei et al., 2009). In a CGRP release ELISA assay, conducted by Dr Marta L.A. Simoes, 65 hour incubation of dissociated mouse dorsal root ganglion cultures with 10 nM ChoBot significantly reduced KCl-evoked CGRP release (Fig. 6.5C). Incubation with ChoBot did not, however, significantly impact either basal or capsaicin-induced CGRP release, although there was a trend for both to be reduced. This therefore confirms that, in vitro, ChoBot has a functional effect on the sensory neurons implicated in pain and the development of pain conditions.

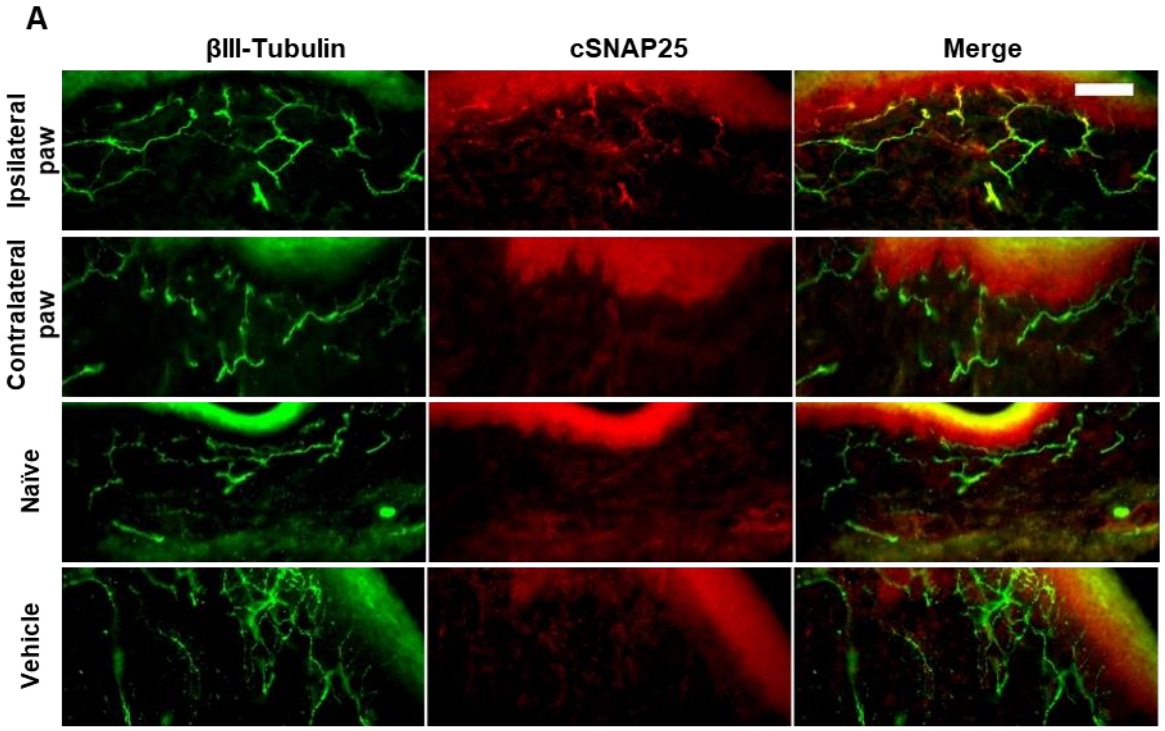
A
βIII-Tubulin
cSNAP25
Merge
Ipsilateral paw
Contralateral paw
Naïve
Vehicle

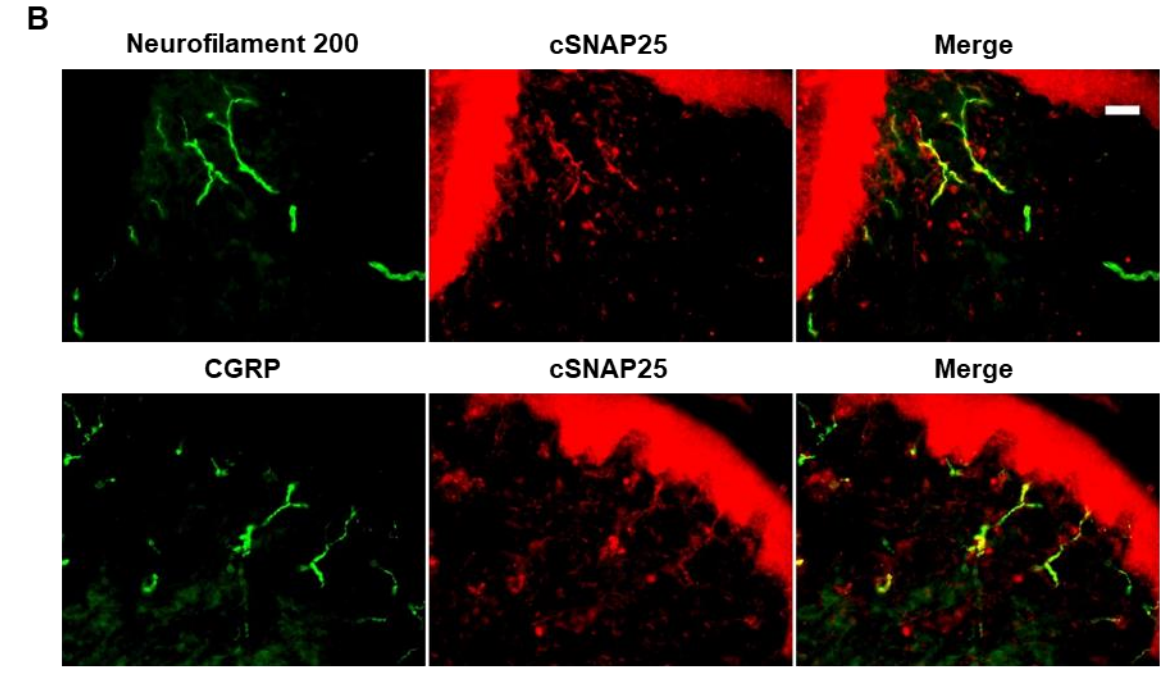
B
Neurofilament 200
cSNAP25
Merge
CGRP
cSNAP25
Merge

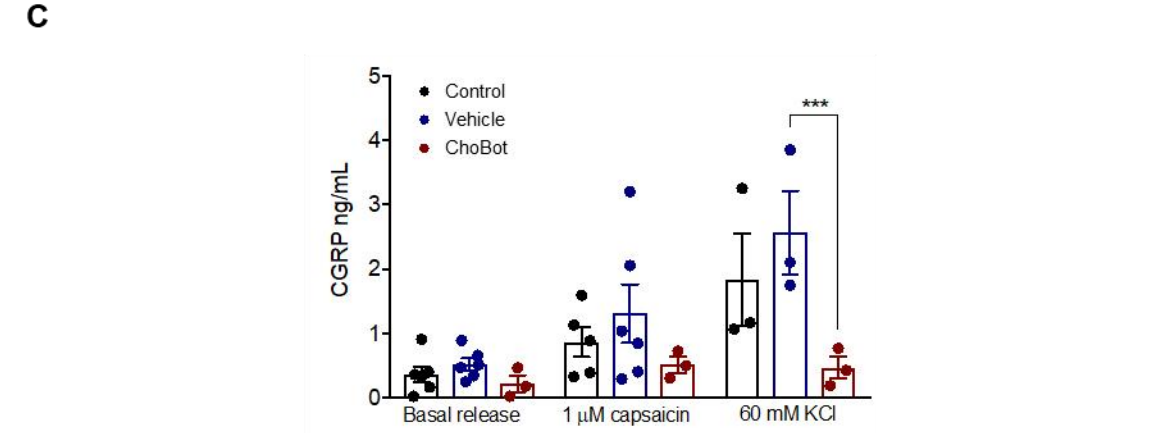
C
CGRP ng/mL
Control
Vehicle
ChoBot
***
Basal release
1 µM capsaicin
60 mM KCl

Figure 6.5 ChoBot cleaves SNAP25 in peripheral sensory neurons in vivo and prevents KCl-evoked CGRP release in vitro. *ChoBot-injected rats (200 ng/ 30 µl, N=2) and vehicle-injected rats (30 µl 0.4% OG in Buffer A, N=2) were perfused with 4% paraformaldehyde 7 days post-injection. Naïve rats were also perfused but received no prior treatment.* ***(A)*** *Epifluorescent images of 30 µm glabrous skin sections, isolated from the plantar surface of the hindpaw, reveal cleaved SNAP25 (red) in the sensory neurons, marked using βIII-Tubulin (green), within the dermis of the ChoBot-injected paw (ipsilateral paw, N=2). Cleaved SNAP25 was absent in the paw contralateral to the ChoBot-injected paw (N=2), in the ipsilateral hindpaw of vehicle-injected rats (N=2) and in naïve animals (N=2). Autofluorescence is generated by the dermal layer and is visible at the top of all of the images. It can thus be ignored. Scale bar = 100 µm* ***(B)*** *Cleaved SNAP25 colocalised with both CGRP-positive and NF200-positive neurons (N=2). Scale bar = 50 µm.* ***(C)*** *65 hour incubation with 10 nM ChoBot significantly attenuated KCl-evoked CGRP release from dissociated mouse dorsal root ganglion neuron cultures (N=3). Reduced capsaicin-evoked CGRP release was also noted but was not significant. All data presented as mean ± S.E.M, *** P<0.001. ELISA data provided courtesy of Dr. M.L.A. Simoes.*

6.2.5 Cleaved SNAP25 is detected at the neuromuscular junction in the glabrous skin of the hindpaw following intraplantar injection of ChoBot

It was also of importance to determine whether ChoBot would display any affinity for motor neurons, provided the paralytic nature of native BoNT/A. Visualisation of the neuromuscular junction, using α-Bungarotoxin-488, showed cleaved SNAP25 localised to the neuromuscular junction, as well as in some of the motor nerve fibres innervating the synapse (Fig. 6.6). Cleaved SNAP25 was absent at the neuromuscular junction in the contralateral paw. Expectedly, cleaved SNAP25 was not detected at the neuromuscular junction in vehicle-injected rats or in naïve animals (Fig. 6.6).

6.2.6 Pre-emptive intraplantar injection of ChoBot attenuates the development of mechanical hypersensitivity following surgery

The identification of SNAP25 cleavage in the peripheral sensory neurons combined with the overall absence of cleaved SNAP25 in the ventral lumbar spinal cord, or the contralateral paw, suggests that the catalytic activity of ChoBot is largely restricted to the peripheral injection site. The analgesic potential of ChoBot was consequently investigated as it would circumvent the concerns over the long-distance effects of BoNT chimeras, resulting from the retrograde transport, and possible transcytosis, routinely observed with these chimeras. ChoBot was primarily trialled in an incisional post-operative pain model. Briefly, 200 ng ChoBot was administered via intraplantar injection to the left hindpaw of rats, five days prior to the induction of the incisional post-operative pain model. Post-operative pain was induced by performing a longitudinal incision to the ipsilateral hindpaw (Brennan et al., 1996).

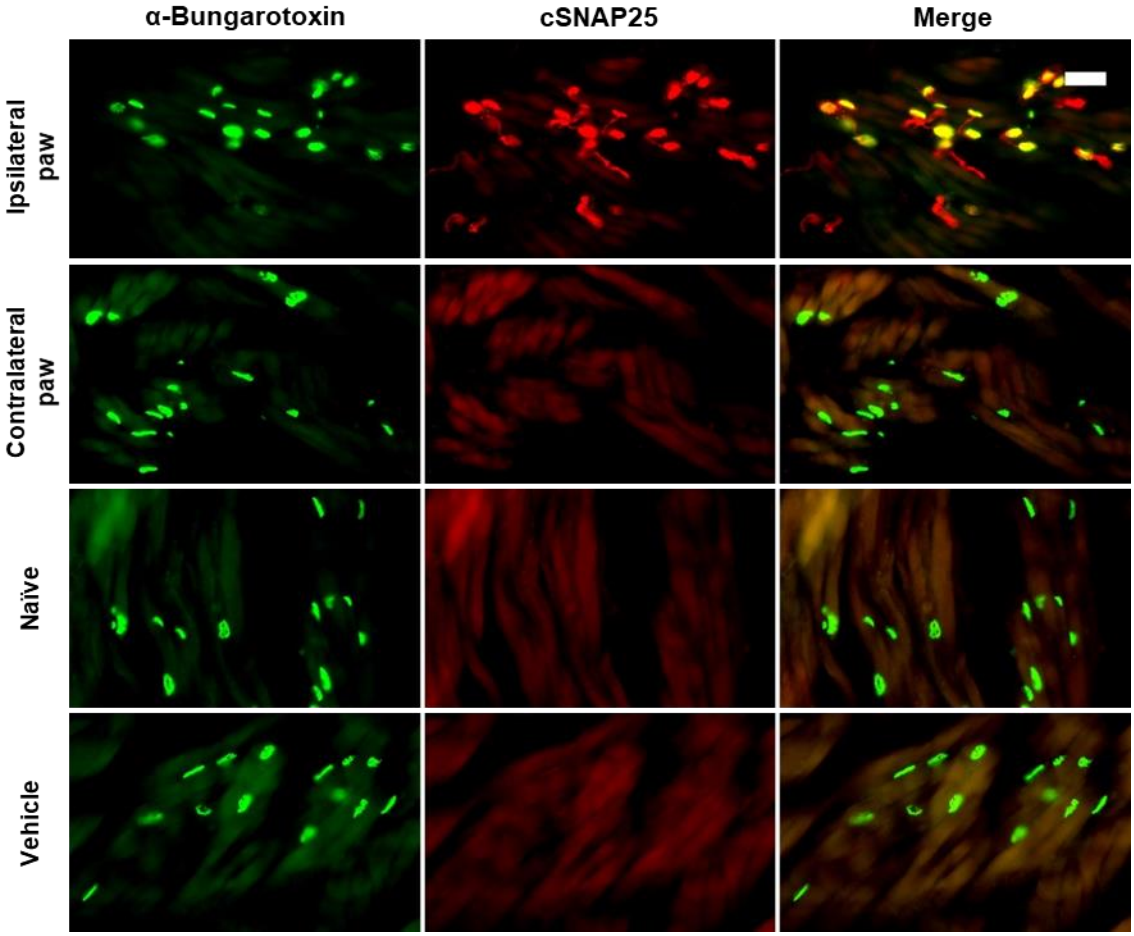

Figure 6.6 Cleaved SNAP25 is detected at the neuromuscular junction after intraplantar injection of ChoBot. *α-Bungarotoxin-488 was used to identify the neuromuscular junction (green) in glabrous skin sections, cryosectioned from the plantar surface of the hindpaw. Cleaved SNAP25 (red) was found colocalised to neuromuscular junction in the ipsilateral ChoBot-injected hindpaw, 7 days post intraplantar injection (N=2). Cleaved SNAP25 was not detected at the neuromuscular junction of contralateral hindpaw (N=2), in the ipsilateral paw of vehicle injected rats (N=2), or naïve rats (N=2).*

Injection of ChoBot did not influence either thermal (Two-way ANOVA, *Treatment: Baseline - Day -1: Ipsilateral paw*, $F_{(1, 8)}$ =0.4712, P= 0.5118, Fig. 6.7B; *Contralateral Paw*, $F_{(1, 8)}$ =0.0060, P= 0.9404, Fig. 6.7D) or mechanical basal thresholds (Two-way ANOVA, *Treatment: Baseline - Day -1: Ipsilateral paw*, $F_{(1, 8)}$ =1.275, P= 0.2915, Fig. 6.7A; *Contralateral Paw*, $F_{(1, 8)}$ = 0.0358, P= 0.8546, Fig. 6.7C). Pre-treatment with ChoBot did, however, significantly attenuate the development of mechanical hypersensitivity in the ipsilateral paw following incision, compared to rats that received vehicle injection (Two-way ANOVA, *Treatment: Day -1 – Day 7*, $F_{(1, 8)}$ = 23.6, P= 0.0013, Fig. 6.7A). ChoBot-injected rats maintained a significantly higher mechanical withdrawal threshold in the ipsilateral paw, than vehicle-injected rats, between days 1-3 post-incision (Sidak's multiple comparisons test, *Day 1*, P= 0.0065; *Day 2 and 3*, P= 0.0033). By day

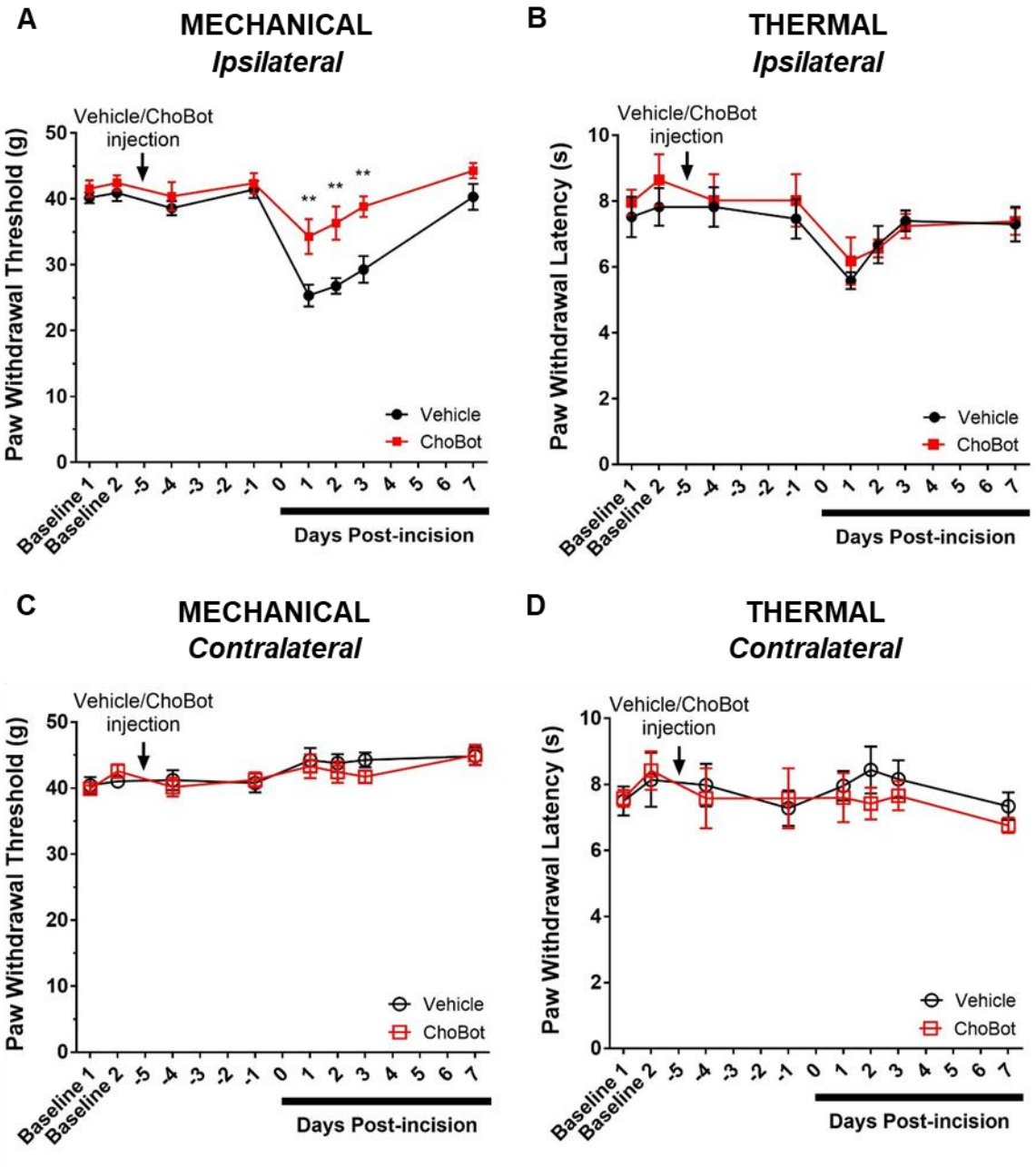

Figure 6.7 Pre-emptive intraplantar injection of ChoBot prevents the development of mechanical hypersensitivity following surgery. *5 week old male Sprague-Dawley rats received intraplantar injection of 200 ng/ 30 µl ChoBot (N=5) or vehicle (N=5) 5 days prior to the induction of the incisional post-operative pain model* ***(A)*** *Injection of ChoBot partially prevented the development of mechanical hypersensitivity in the ipsilateral paw, as shown by the increased mechanical withdrawal threshold, assessed using Electronic von Frey, between days 1 and 3 post-surgery compared to vehicle-injected rats.* ***(B)*** *The paw withdrawal latency, measured using Hargreaves Plantar test, revealed that ChoBot had no effect on thermal hyperalgesia produced in the ipsilateral paw following incision.* ***(C)*** *The mechanical threshold and* ***(D)*** *the thermal threshold of the contralateral hindpaw remained unaffected by either incision and intraplantar injection of ChoBot to the ipsilateral paw. All data presented as mean ± S.E.M, ** P<0.01.*

7 post-incision, the mechanical threshold had returned to basal levels for both ChoBot- and vehicle-injected rats and there was no longer a significant difference in mechanical threshold between the two groups (Sidak's multiple comparisons test, *Day 7*, P= 0.5056).

By comparison, ChoBot had no effect on the development of thermal hypersensitivity in the ipsilateral paw following incision (Two-way ANOVA, *Treatment: Day -1 – Day 7*, $F_{(1, 8)} = 0.1672$, P= 0.6933, Fig. 6.7B). Additionally, it was evident that the mechanical threshold (Two-way ANOVA, *Interaction*, $F_{(7, 56)} = 0.6173$, P= 0.7393, Fig. 6.7C) and thermal threshold (Two-way ANOVA, *Interaction*, $F_{(7, 56)} = 0.4969$, P= 0.8328, Fig. 6.7D) of the contralateral paw remained stable throughout the experiment and were unaffected by either injection of ChoBot or incision to the opposing hindpaw.

6.2.7. Post-operative intraplantar injection of ChoBot does not reverse mechanical hypersensitivity in a post-operative pain model

Encouraged by these results, it was next investigated whether ChoBot could be administered post-incision to reverse the mechanical hypersensitivity normally developed. In contrast, ChoBot injected intraplantar 1 day post-incision failed to significantly reduce the mechanical hypersensitivity developed in the ipsilateral paw (Two-way ANOVA, *Treatment: Day 1 – Day 4*, $F_{(1, 7)} = 1.339$, P= 0.2852, Fig. 6.8A) and remained ineffective against the thermal hypersensitivity component (Two-way ANOVA, *Treatment: Day 1 – Day 4*, $F_{(1, 7)} = 0.1988$, P= 0.6692, Fig. 6.8B). Again, the mechanical threshold (Two-way ANOVA, *Interaction*, $F_{(5, 35)}$ 0.7433, P= 0.5964, Fig. 6.8C) and thermal threshold (Two-way ANOVA, *Interaction*, $F_{(5, 35)} = 1.594$, P= 0.1876, Fig. 6.8D) of the contralateral paw remained unaffected throughout the experiment.

6.2.8 Pre-emptive intraplantar injection of ChoBot does not prevent the development of mechanical hypersensitivity in females following surgery

Over more recent years, there has been an increased emphasis placed on the need to include female subjects in pain studies (Mogil and Chanda, 2005). A large volume of evidence has shown that females not only experience more severe clinical pain, but also differ in their responsiveness to analgesic drugs (Greenspan et al., 2007; Fillingim et al., 2009; Hurley and Adams, 2009). With specific reference to post-operative pain, it has, however, been demonstrated that both male and female rodents develop mechanical hypersensitivity to an equal degree in the incisional post-operative pain model (Kroin et al., 2003; Banik et al., 2006). Consequently, the analgesic potential of ChoBot was studied in female Sprague-Dawley rats, undergoing the incisional post-operative pain

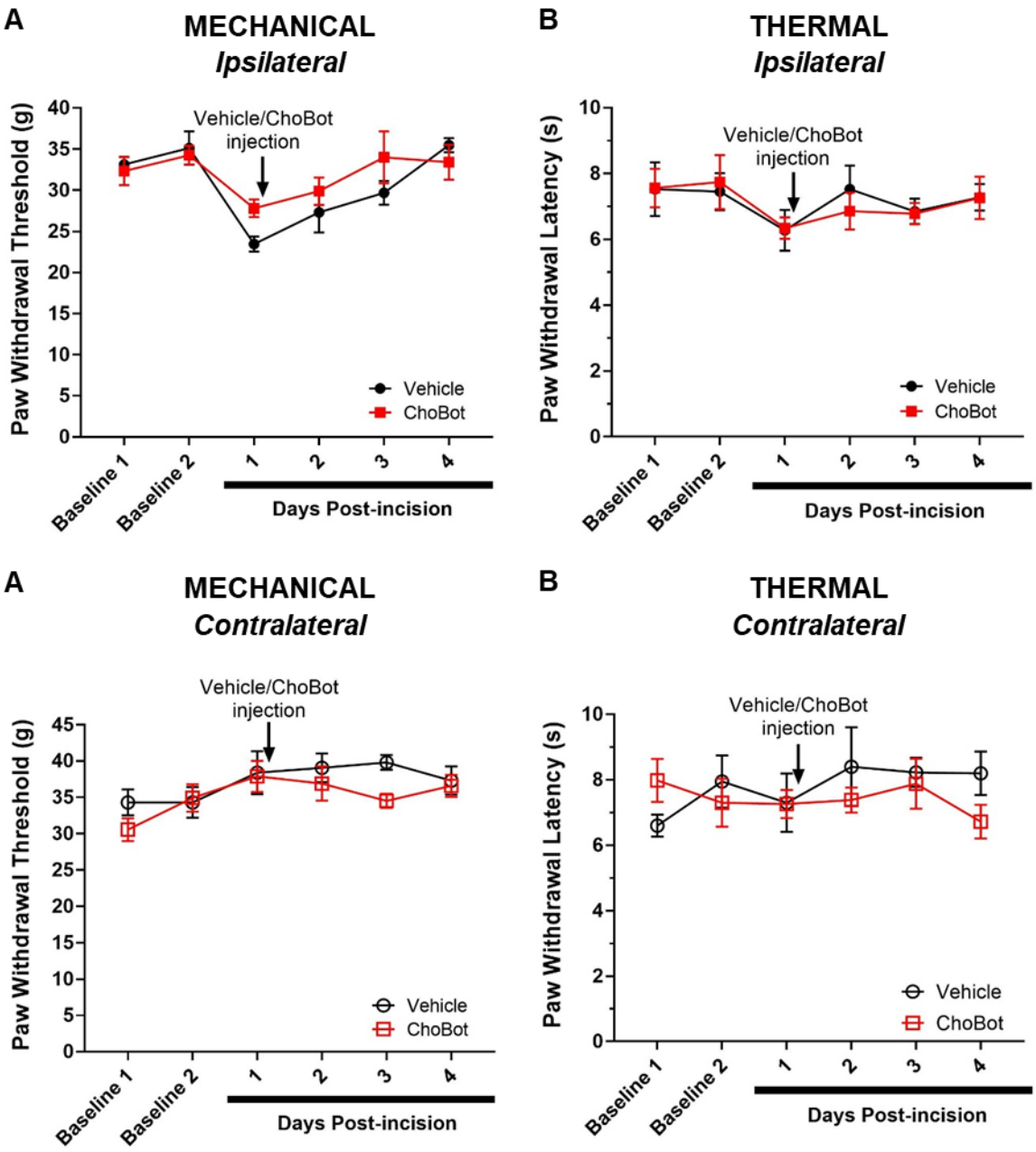

Figure 6.8 Post-operative intraplantar injection of ChoBot does not reverse mechanical hypersensitivity in an incisional pain model. *5 weeks old male Sprague-Dawley rats received intraplantar injection of either 30 µl vehicle (N=4) or 200 ng/ 30 µl ChoBot (N=5) one day post incision, after day 1 behavioural testing had been conducted. Injection of ChoBot post-incision did not significantly reverse the observed* ***(A)*** *mechanical hypersensitivity or* ***(B)*** *thermal hypersensitivity in the ipsilateral hindpaw.* ***(C)*** *The mechanical threshold and* ***(D)*** *the thermal threshold of the contralateral hindpaw remained stable and were unaffected by either incision or intraplantar injection to the ipsilateral paw. All data presented as mean ± S.E.M.*

model, to evaluate whether ChoBot was similarly as efficacious at attenuating the development of mechanical hypersensitivity in females, as was demonstrated in males.

There was no significant difference observed in either the mechanical (Two-way ANOVA, *Sex*, $F_{(1,16)} = 0.2569$, P= 0.6191) or thermal threshold (Two-way ANOVA, *Sex*, $F_{(1, 16)} = 3.034$, P= 0.1007) of the ipsilateral hindpaw between males and females, recorded at baseline. Again, intraplantar injection of ChoBot did not significantly affect either the basal mechanical threshold of the contralateral paw (Two-way ANOVA, *Treatment: Baseline 1 - Day -1*, $F_{(1, 6)} = 0.2291$, P= 0.6491, Fig. 6.9C) or the thermal threshold of the contralateral or ipsilateral paw in female rats (Two-way ANOVA, *Treatment: Baseline 1 - Day -1: Ipsilateral paw*, $F_{(1, 6)} = 0.8546$, P= 0.3909, Fig. 6.9B; *Contralateral Paw*, $F_{(1, 6)} = 3.316$, P= 0.1185, Fig. 6.9D). A significant effect on the mechanical threshold of the ipsilateral hindpaw was detected (Two-way ANOVA*: Baseline 1 - Day -1: Ipsilateral paw*, $F_{(1, 6)} = 6.12$, P=0.0482, Fig. 6.9A), however, this was due to differences observed in the initial baseline measurement of the ipsilateral paw between the two treatment groups, prior to injection of either vehicle or ChoBot. Once this data point was removed, injection of ChoBot was no longer shown to have a significant effect on the basal mechanical threshold of the ipsilateral hindpaw (Two-way ANOVA, *Treatment: Baseline 2 - Day -1: Ipsilateral paw*, $F_{(1, 6)} = 1.438$, P=0.2756, Fig. 6.9A).

In contrast to that observed in male rats, pre-emptive intraplantar injection of ChoBot in female rats did not hinder the development of mechanical hypersensitivity in the ipsilateral paw, following plantar incision (Two-way ANOVA, *Treatment*, $F_{(1, 6)} = 0.9955$, P= 0.3569, Fig. 6.9A). Again, ChoBot did not significantly alter the thermal hypersensitivity observed post-incision (Two-way ANOVA, *Treatment*, $F_{(1, 6)} = 3.744$, P= 0.1012), although a trend for a reduced thermal threshold was noted in the ipsilateral paw of ChoBot-injected females (Fig. 6.9B). There does, however, appear to be a much larger variation in the paw withdrawal latency in female rats, compared to male rats, which could explain the observed trend.

Once more, neither injection of ChoBot, nor the establishment of the post-operative pain model, had any significant effect on the mechanical threshold of the contralateral paw (Two-way ANOVA, *Interaction*, $F_{(8, 48)} = 1.051$, P= 0.4123, Fig. 6.9C) or the thermal threshold (Two-way ANOVA, *Interaction*, $F_{(8, 48)} = 0.8011$, P= 0.6046, Fig. 6.9D).

6.2.9. Intraplantar injection of ChoBot does not reverse the thermal or mechanical hypersensitivity observed in Complete Freund's Adjuvant inflammatory pain model

Post-operative pain encompasses clinical features from a range of different pain conditions including nociceptive pain, inflammatory pain and neuropathic pain (Kehlet et al., 2006; Pogatzki-zahn et al., 2017). The observation that ChoBot had no effect on

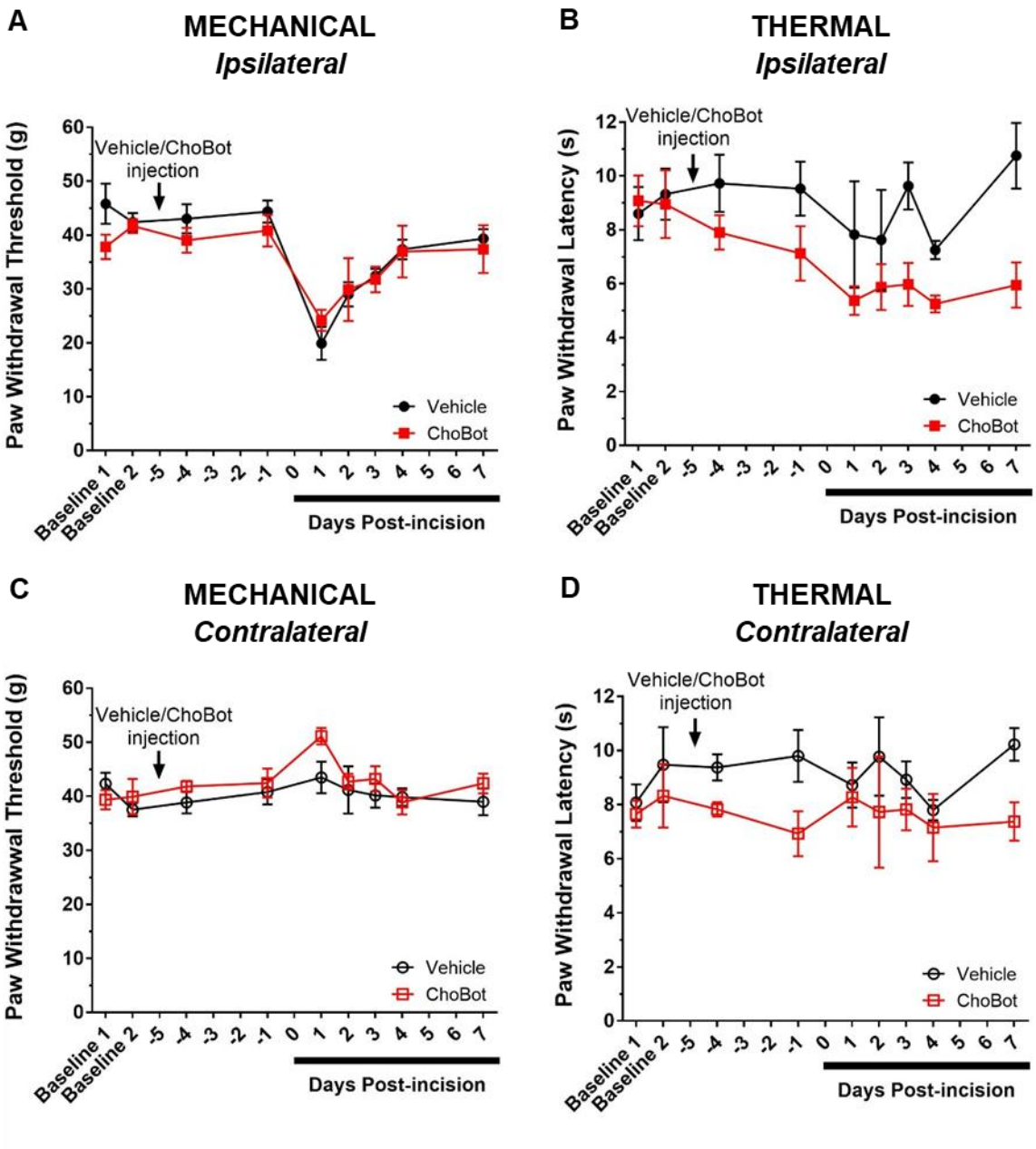

Figure 6.9 Pre-emptive intraplantar injection of ChoBot does not prevent incision-induced mechanical hypersensitivity in female rats. *Intraplantar injection of 30 µl vehicle (N=4) or 200 ng/ 30 µl ChoBot (N=4) was administered to the left hindpaw of 6 week old female Sprague-Dawley rats 5 days prior to plantar incision of the ipsilateral paw.* ***(A)*** *Pre-emptive injection of ChoBot did not attenuate the development of mechanical hypersensitivity in the ipsilateral hindpaw.* ***(B)*** *ChoBot was also ineffective against the development of thermal hyperalgesia in the ipsilateral paw. ChoBot- injected rats remained hyperalgesic to thermal stimuli 7 days post-incision whereas the thermal threshold of vehicle-injected recovered to approximately basal values.* ***(C)*** *The mechanical threshold and the* ***(D)*** *the thermal threshold of the contralateral paw were unaffected by injection of vehicle or ChoBot or incision to the ipsilateral paw. All data presented as mean ± S.E.M, * P<0.05.*

basal pain thresholds indicates that ChoBot is not affecting acute nociception and therefore implies that ChoBot must instead be combatting either the inflammatory or

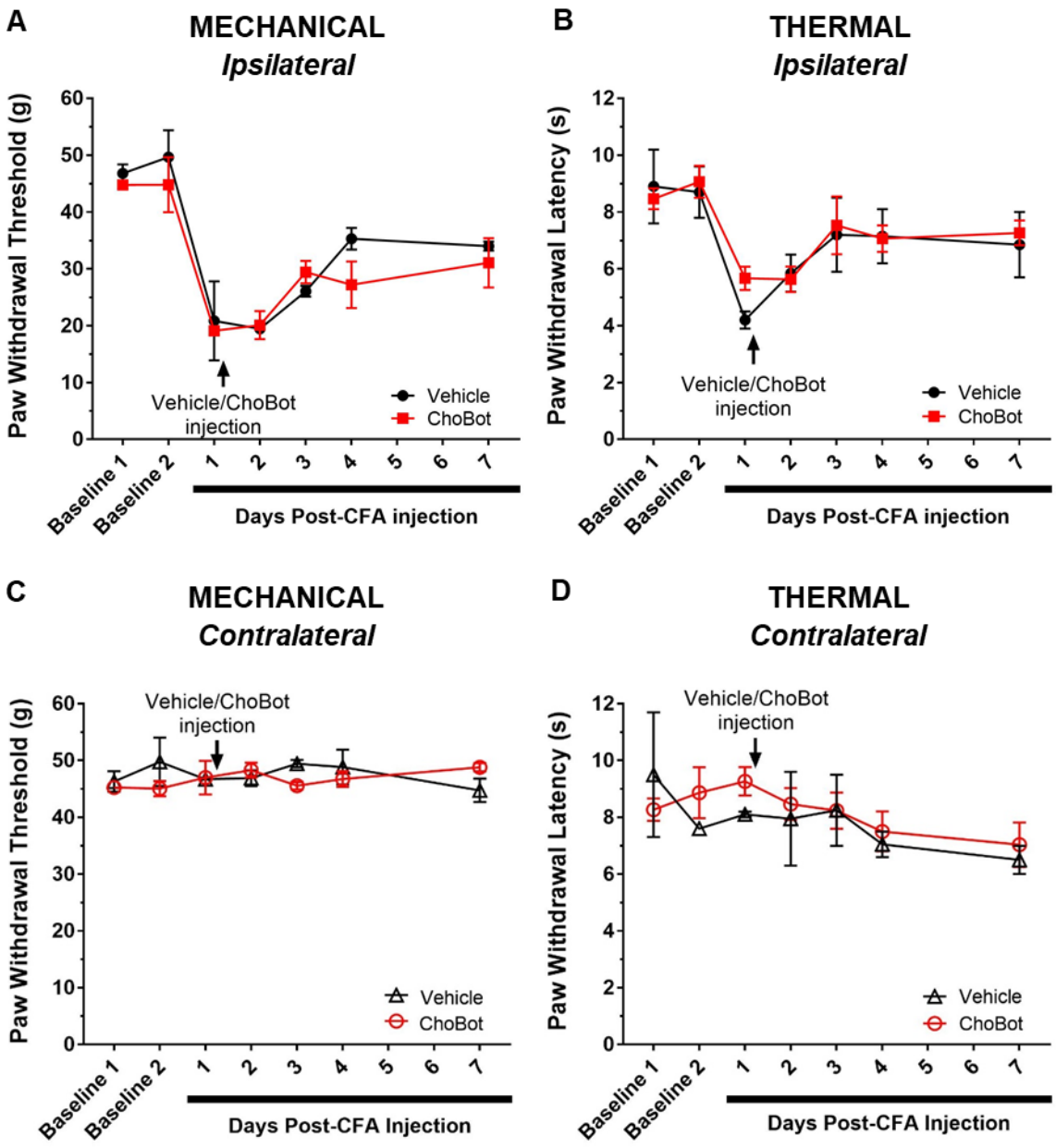

Figure 6.10 Intraplantar injection of ChoBot does not reverse thermal or mechanical hypersensitivity in Complete Freund's Adjuvant (CFA) inflammatory pain model. *Intraplantar injection of either 30 µl vehicle (N=2) or 200 ng/ 30 µl ChoBot (N=3) was delivered to the left hindpaw of 6 week old male Sprague-Dawley rats 24 hours after injection of 15 µl CFA to the ipsilateral hindpaw. Day 1 behavioural testing was conducted prior to injection of ChoBot and vehicle. Injection of ChoBot failed to reverse CFA-induced* ***(A)*** *mechanical hypersensitivity or* ***(B)*** *thermal hypersensitivity in the ipsilateral hindpaw.* ***(C)*** *The mechanical threshold and* ***(D)*** *the thermal threshold remained consistent in the contralateral hindpaw in both groups, regardless of treatment. All data presented as mean ± S.E.M.*

neuropathic component of postoperative pain. To elucidate whether the perceived analgesic effect of ChoBot was due to an effect on inflammation, ChoBot was injected intraplantar in the Complete Freund's Adjuvant inflammatory pain model to determine whether it would similarly reverse the pain phenotype.

ChoBot administered to the hindpaw 1 day after intraplantar injection of CFA did not influence the recovery of either the mechanical (Two-way ANOVA, *Treatment*, $F_{(1, 3)} = 0.9798$, P= 0.3952, Fig. 6.10A) or the thermal threshold (Two-way ANOVA, *Treatment*, $F_{(1, 3)} = 0.1846$, P= 0.6964, Fig. 6.10B) compared to rats which instead received vehicle. Mechanical (Two-way ANOVA, *Time*, $F_{(6, 18)} = 0.387$, P= 0.8777, Fig. 6.10C) and thermal thresholds (Two-way ANOVA, *Time*, $F_{(6, 18)} = 2.017$, P= 0.1163, Fig. 6.10D) measured in the contralateral paw remained consistent throughout the experiment and were therefore unaffected by either injection of CFA or ChoBot to the ipsilateral paw.

6.2.10 Intraplantar injection of ChoBot reduces mechanical hypersensitivity in paclitaxel-induced peripheral neuropathy

The lack of effect of ChoBot observed on both acute nociception and inflammatory pain suggests that ChoBot might instead be mediating its therapeutic effect against the possible neuropathic component of post-operative pain. Consequently, it was investigated whether ChoBot would produce analgesia in a neuropathic pain model.

Repeated intraperitoneal injection of Paclitaxel (2 mg/ml/kg), a chemotherapy drug, was successfully used to establish paclitaxel-induced peripheral neuropathy (PIPN), the chosen neuropathic pain model (Polomano et al., 2001). Rats who received repeated injection of paclitaxel displayed significant mechanical hypersensitivity in both paws compared to rats that received intraperitoneal injection of the vehicle control (Two-way ANOVA, *Treatment: Ipsilateral Hindpaw*, $F_{(1, 8)} = 38.02$, P= 0.0003; *Treatment: Contralateral Hindpaw*, $F_{(1, 8)} = 91.48$, P< 0.0001 Fig. 6.11A).

The perceived mechanical hypersensitivity in paclitaxel-treated rats was significantly reversed by intraplantar injection of ChoBot to left hindpaw, subsequently referred to as the ipsilateral paw (Two-way ANOVA, *Treatment: Day 14 - 28*, $F_{(1, 10)} = 13.47$, P= 0.0043, Fig. 6.12A). A significant overall reduction in mechanical hypersensitivity following injection of ChoBot was also observed in the contralateral paw (Two-way ANOVA, *Treatment: Day 14 - 28*, $F_{(1, 10)} = 9.227$, P= 0.0125, Fig. 6.12B). The mechanical threshold of ChoBot-injected PIPN animals was, however, only shown to be significantly higher than vehicle-injected PIPN animals at one time point (Sidak's multiple comparisons test, *Day 17*, P= 0.0296). The analgesic effect was apparent in both paws by day 17 and persisted until the experiment was terminated on day 28 (Fig. 6.12A and Fig. 6.12B).

Although thermal hyperalgesia has previously been described in the PIPN model, it was only observed in animals treated with lower doses of paclitaxel and was absent in animals receiving the higher dosage of 2 mg/ kg Paclitaxel (Polomano et al., 2001). Similarly, here, thermal hyperalgesia was not observed following repeated injection of 2

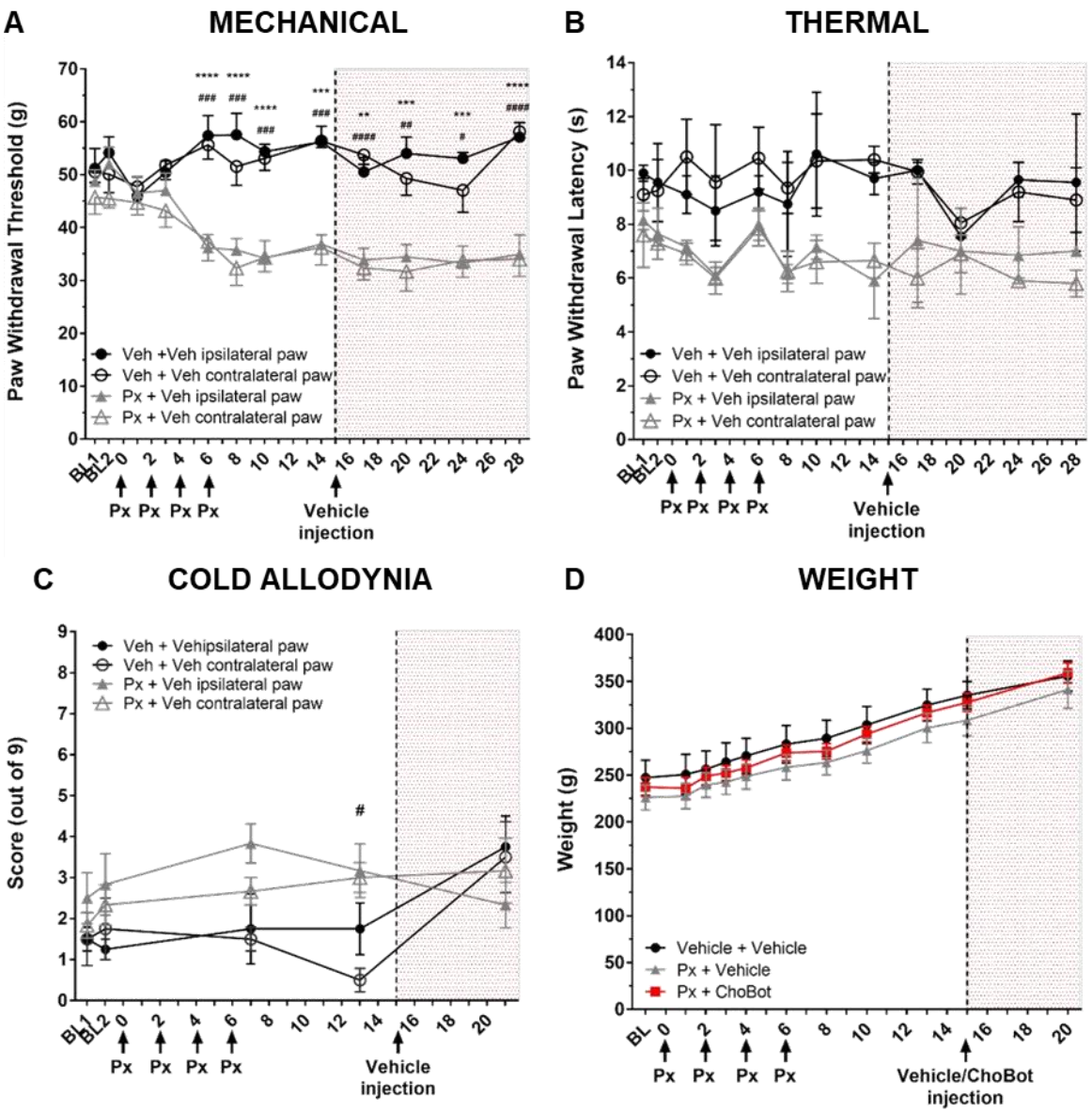

Figure 6.11 Repeated intraperitoneal injection of paclitaxel successfully produces paclitaxel-induced peripheral neuropathy (A) *6 week old male Sprague-Dawley rats received four intraperitoneal injections of either vehicle (1:1 ethanol:kolliphor) (N=4) or 2 mg/ml/kg Paclitaxel (N=6) on four alternate days (Day 0, 2, 4, 6). Repeated IP injection of paclitaxel (Px) successfully established paclitaxel-induced peripheral neuropathy (PIPN), as demonstrated by the development of mechanical hypersensitivity (decreased paw withdrawal threshold) in both the ipsilateral and contralateral paw of paclitaxel-injected rats, apparent by day 6. The mechanical threshold was not affected by intraplantar injection of vehicle (30 µl 0.4% OG in Buffer A) to the left hindpaw (ipsilateral paw) of both groups on day 15.* ***(B)*** *Plotting the mean weight per treatment group, including Px + ChoBot (N=6), revealed no significant difference in the average weight gain dependent on treatment group. Repeated injection of Px did not produce robust* ***(C)*** *thermal hypersensitivity or* ***(D)*** *cold allodynia, as assessed by acetone test. All data presented as mean ± S.E.M. Significance between groups for the ipsilateral paw: * P<0.05, ** P<0.01, *** P<0.001, **** P<0.0001; Significance between groups for the contralateral paw: # P<0.05, ## P<0.01, ### P<0.001, #### P<0.0001.*

mg/kg paclitaxel treatment (Two-way ANOVA, *Treatment: Ipsilateral Hindpaw*, $F_{(1, 2)}$ = 4.341, P= 0.1726; *Treatment: Contralateral Hindpaw*, $F_{(1, 2)}$ = 10.36, P= 0.0845, Fig. 6.11C). In contrast, cold allodynia has been reported by previous studies were rats received 2 mg/kg paclitaxel (Polomano et al., 2001; Flatters and Bennett, 2004). This pain phenotype was not, however, replicated in this current study (Fig. 6.11D). All data points were shown to be statistically insignificant, except for day 13 when paclitaxel-treated rats displayed a significantly higher score in the contralateral paw during the acetone test, compared to vehicle-treated rats, implying the development of cold allodynia (Mann–Whitney unpaired t-test, *Day 13*, P= 0.0095). Yet, this result was not reproduced at the succeeding time point, highlighting major inconsistency in the acetone test scores. The lack of overall significance could therefore be due to the high level of variation in the test scores as well as inadequate power due to limited N numbers. As a result, the acetone test was abandoned in subsequent experiments.

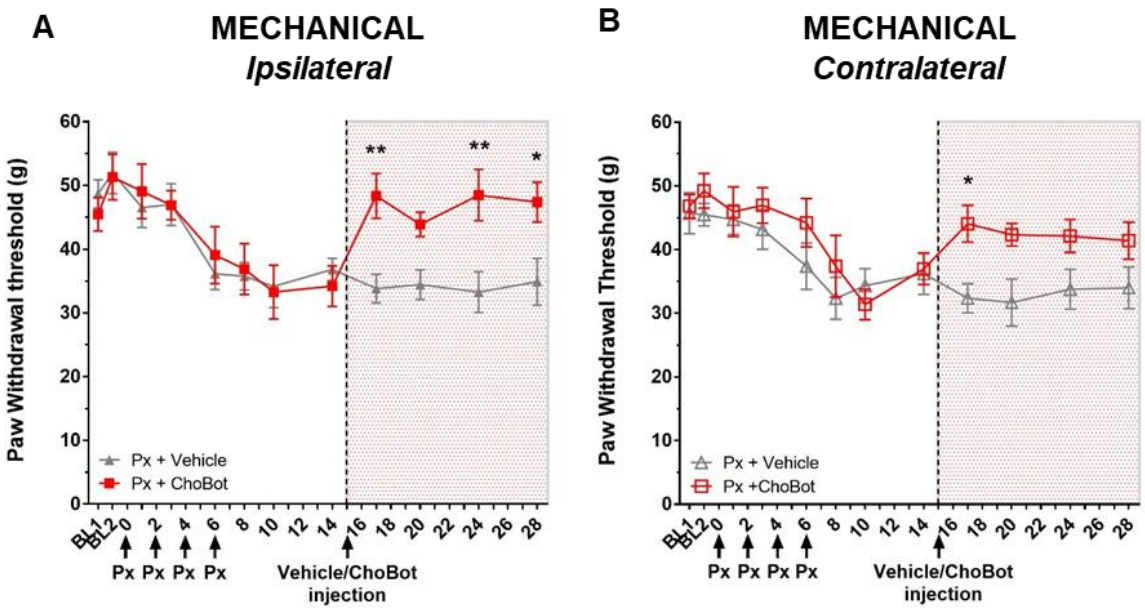

Figure 6.12 Intraplantar injection of ChoBot reduces mechanical hypersensitivity in paclitaxel-induced peripheral neuropathy (PIPN). *6 week old male Sprague-Dawley rats received four intraperitoneal injections of 2 mg/ml/kg Paclitaxel (N=6) on four alternate days (Day 0, 2, 4, 6). Maximal mechanical hypersensitivity was observed in the ipsilateral (left) hindpaw and contralateral (right) hindpaw by day 10. On day 15, rats received intraplantar injection of either 30 µl vehicle (N=6) or 200 ng/ 30 µl ChoBot (N=6) to the ipsilateral hindpaw.* ***(A)*** *Injection of ChoBot reversed the paclitaxel-induced mechanical hypersensitivity whereas vehicle-injected PIPN rats remained hypersensitive.* ***(B)*** *ChoBot also reversed mechanical hypersensitivity in the contralateral paw, compared to vehicle-injected PIPN rats, but with a less pronounced effect than that observed in the ipsilateral paw. All data presented as mean ± S.E.M, * P<0.05, ** P<0.01.*

Notably, the three groups of rats all continued to gain weight normally throughout the experiment, regardless of the induced-neuropathy or treatment condition (Two-way ANOVA, *Treatment*, $F_{(2, 13)}$ =0.7047, P= 0.5122, Fig. 6.11B). Neither group displayed any signs of ill-health, decreased well-being or motor impairment.

6.2.11 Female rats experiencing paclitaxel-induced peripheral neuropathy show a trend towards a reduction in mechanical hypersensitivity following intraplantar injection of ChoBot

After the earlier post-operative pain experiment revealed that ChoBot was efficacious at preventing the development of mechanical hyperalgesia following surgical incision in males, but not females, and furthermore, after confirming that ChoBot was again analgesic in a neuropathic pain model, it was deemed important that the current neuropathic pain model should be repeated in female rats, to determine whether the effects of ChoBot are indeed gender-specific.

It has previously been demonstrated that there are no sex-differences in the development of PIPN between male and female Sprague-Dawley rats (Hwang et al., 2012). Similarly, here, no significant difference in the paw withdrawal threshold between male and female rats who received vehicle treatment (Two-way ANOVA, *Sex*, $F_{(1, 5)}$ = 5.408, P= 0.0676) or paclitaxel treatment was detected (Two-way ANOVA, *Sex*, $F_{(1, 7)}$ =0.4492, P= 0.512, Fig. 6.13). Likewise to the male rats, the female rats which received repeated injection of paclitaxel showed a reduced mechanical withdrawal threshold compared to female rats that received repeated injection of vehicle. This trend, however, was not shown to be significant (Two-way ANOVA, *Treatment: Ipsilateral Hindpaw*, $F_{(1, 4)}$ = 2.183, P= 0.2136; *Treatment: Contralateral Hindpaw*, $F_{(1, 4)}$ = 6.605, P= 0.062, Fig. 6.14A). Furthermore, following injection of ChoBot on day 15 post-first paclitaxel injection, a recovery of the mechanical threshold was observed. Again, however, this was not shown to be significant (Two-way ANOVA, *Treatment Day 14 - 28*, $F_{(1, 4)}$ = 4.94, P= 0.0903, Fig. 6.14C). This lack of significance is most likely due to low n numbers rather than a lack of effect.

The analgesic effect observed in the contralateral hindpaw following injection of ChoBot to the ipsilateral paw was not as clear in female rats (Two-way ANOVA, *Treatment Day 14 - 28*, $F_{(1, 4)}$ = 0.3788 P= 0.5715, Fig. 6.14D). Only one timepoint indicated an increased mechanical threshold in the contralateral paw of ChoBot-injected rats compared to vehicle-injected rats. Conversely, in male rats, a higher mechanical withdrawal threshold was consistently measured in the contralateral paw at every time point, subsequent to ChoBot injection in comparison to vehicle-injected rats (Fig. 6.12B).

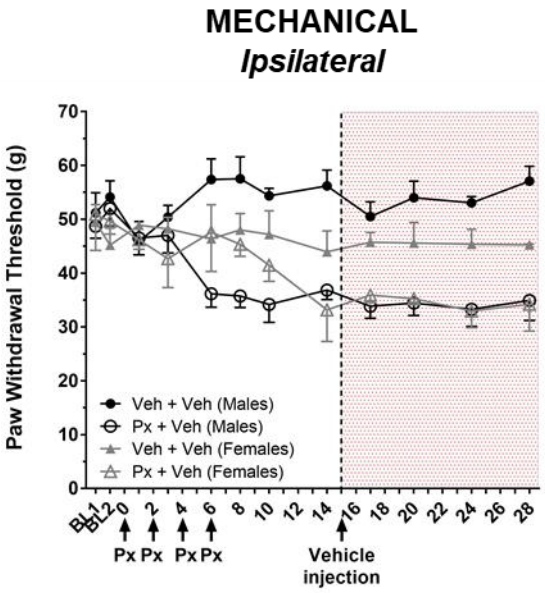

Figure 6.13 Male and female rats similarly develop mechanical hypersensitivity after repeated injection of Paclitaxel. *6 week old male and 7 week old female Sprague-Dawley rats received four intraperitoneal injections of either vehicle (1:1 ethanol:kolliphor) (Male, N=4; Female, N=3) or 2 mg/ml/kg Paclitaxel (Px) (Male, N=6; Female, N=3) on four alternate days (Day 0, 2, 4, 6). Reduced mechanical withdrawal threshold was observed in left hindpaw following repeated IP injection of Px in both male and female rats. No significant difference in the mechanical withdrawal threshold of the left hindpaw between male and female vehicle-injected rats, or between male and female Px-injected rats was detected. Intraplantar injection of vehicle (30 µl 0.4% OG in Buffer A) to the ipsilateral (left) paw of all groups on day 15 did not affect mechanical withdrawal threshold. All data presented as mean ± S.E.M.*

As previously demonstrated, all three groups of female rats continued to gain weight normally throughout the experiment (Two-way ANOVA, *Treatment*, $F_{(2, 22)} = 0.1609$, P= 0.8523, Fig. 6.14B). No signs of decreased well-being or motor impairment were detected in any of the animals.

6.2.12 The combined behavioural results of male and female PIPN rats highlights an analgesic effect of ChoBot against Paclitaxel-induced mechanical hypersensitivity

Subsequently, after confirming that the mechanical pain thresholds were not significantly different between male and female rats undergoing the PIPN pain model, and after observing similar trends in the pain thresholds of female rats to those observed in male rats, it was decided that the data collected from both male and female rats could be effectively combined to increase the number of subjects, and consequently increase the statistical power of the data analysis.

Combining the results from both the male and female rats once more highlighted a significant decrease in the mechanical withdrawal threshold of both the ipsilateral and the contralateral hindpaw in animals that received repeated injection of paclitaxel, opposed to vehicle control (Two-way ANOVA, Treatment: Ipsilateral Hindpaw, $F_{(1, 14)} = 22.8$, P= 0.0003; Treatment: Contralateral Hindpaw, $F_{(1, 14)} = 49.25$, P< 0.0001, Fig.

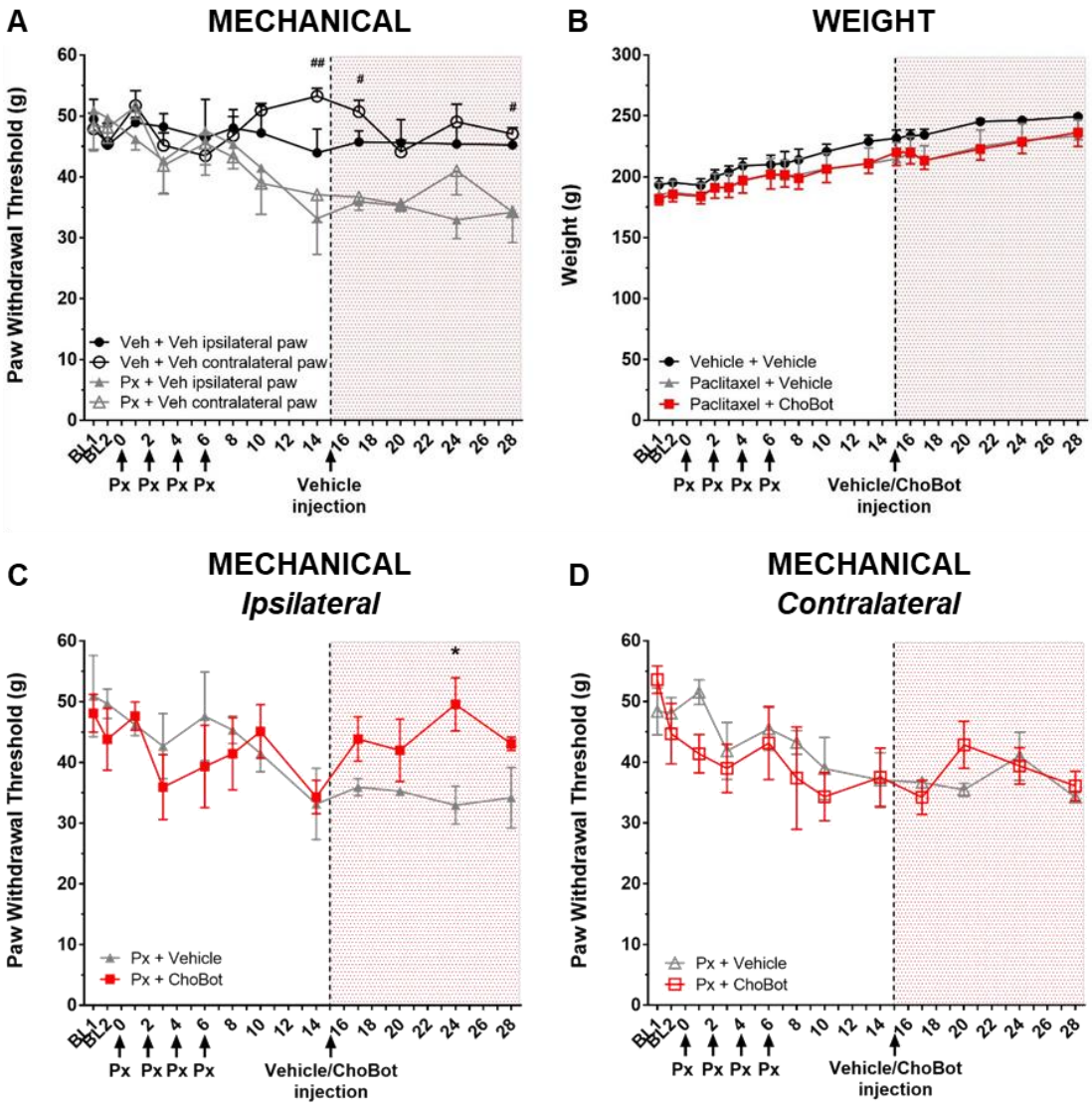

Figure 6.14 A trend towards reduced Paclitaxel-induced mechanical hypersensitivity is observed in female rats after intraplantar injection of ChoBot. *7 week old female Sprague-Dawley rats received four intraperitoneal injections of either vehicle (1:1 ethanol:kolliphor) (N=3) or 2 mg/ml/kg Paclitaxel (N=3) on four alternate days (Day 0, 2, 4, 6).* ***(A)*** *Repeated injection of (Px) resulted in a reduced mechanical threshold in the ipsilateral and contralateral paw of Px-injected rats which was maximal by day 14. This reduction was not shown to be significant when compared to vehicle-injected females. The mechanical threshold was not affected by intraplantar injection of vehicle (30 µl 0.4% OG in Buffer A) to the left (ipsilateral) hindpaw on day 15.* ***(B)*** *The mean weight of each treatment group, including Px + ChoBot (N=3), was plotted to reveal no significant difference in the average weight gain between treatment groups.* ***(C)*** *Injection of ChoBot appeared to reverse the paclitaxel-induced mechanical hypersensitivity. Treatment was not shown to have an overall significant effect on mechanical threshold (P= 0.09), however, the mechanical withdrawal threshold was consistently higher in ChoBot-injected females and significance was reported on day 24.* ***(D)*** *The mechanical withdrawal threshold was also measured in the contralateral hindpaw. A reduced mechanical threshold is visualised by day 10 but does not show a clear recovery after intraplantar injection of ChoBot to the ipsilateral hindpaw. All data presented as mean ± S.E.M, Significance between groups for the ipsilateral paw: * P<0.05; Significance between groups for the contralateral paw: # P<0.05, ## P<0.01.*

6.15A). Intraplantar injection of ChoBot, 15 days after the first paclitaxel injection, reversed the mechanical hypersensitivity associated with PIPN in the ipsilateral paw such that the mechanical threshold returned to basal values (Two-way ANOVA, *Treatment*, $F_{(1, 16)} = 20.4$, P= 0.0004, Fig. 6.15C). Intraplantar injection of ChoBot to the ipsilateral hindpaw was furthermore shown to significantly reduce mechanical hypersensitivity in the contralateral paw, compared to rats injected with vehicle (Two-way ANOVA, *Treatment*, $F_{(1, 16)} = 8.531$, P= 0.01, Fig. 6.15D). This was shown despite that the mechanical threshold of contralateral hindpaw was only significantly increased in the ChoBot-injected rats, compared to the vehicle-injected rats, at day 20 (Sidak's multiple comparisons test, *Day 20*, P= 0.015).

6.3 Discussion

Throughout this project, widespread SNAP25 cleavage has been visualised in the ventral horn of the lumbar spinal cord after peripheral injection of the clostridial chimeras so far tested, namely BiTox/A (Chapter 3), BiTox/D (Chapter 4) and TetBot (Chapter 5). In the absence of any perceived motor impairments, the SNAP25 cleavage in the ventral horn has raised concerns about the possible off-target effects of the clostridial chimeras and has further stimulated discussion about whether any associated analgesic effects are centrally or peripherally mediated. In contrast, data collected in the previous chapter suggested that the novel chimera, ChoBot, lacked catalytic activity at the central motor synapse, and from this, it was surmised that ChoBot might exclusively act at the peripheral terminal. Here, it was shown that ChoBot does successfully cleave SNAP25 in peripheral neurons, located at the intraplantar injection site. Consequent evaluation of the analgesic potential of ChoBot, across multiple pain models, revealed that, like BiTox/A, ChoBot produces analgesia specifically in pain conditions comprising a neuropathic component, and is ineffective against inflammatory pain conditions.

6.3.1 ChoBot cleaves SNAP25 at the peripheral injection site

The identification of cleaved SNAP25 in the sensory neurons of the hindpaw, following intraplantar injection, confirmed that ChoBot was able to internalise into sensory neurons in vivo and successfully cleave SNAP25. Immunolabelling in vivo largely agreed with the data gathered after in vitro incubation of dorsal root ganglion cultures with ChoBot. Cleaved SNAP25 was detected within a subset of NF200-positive, myelinated neurons, both in vivo and in vitro. In vitro data specified that ChoBot was enzymatically active in myelinated neurons of a significantly smaller average cell diameter than those neurons displaying cleaved SNAP25 after incubation with BiTox/A. This was repeatedly shown when labelling with both pan-neuronal marker, βIII-Tubulin, and with NF200.

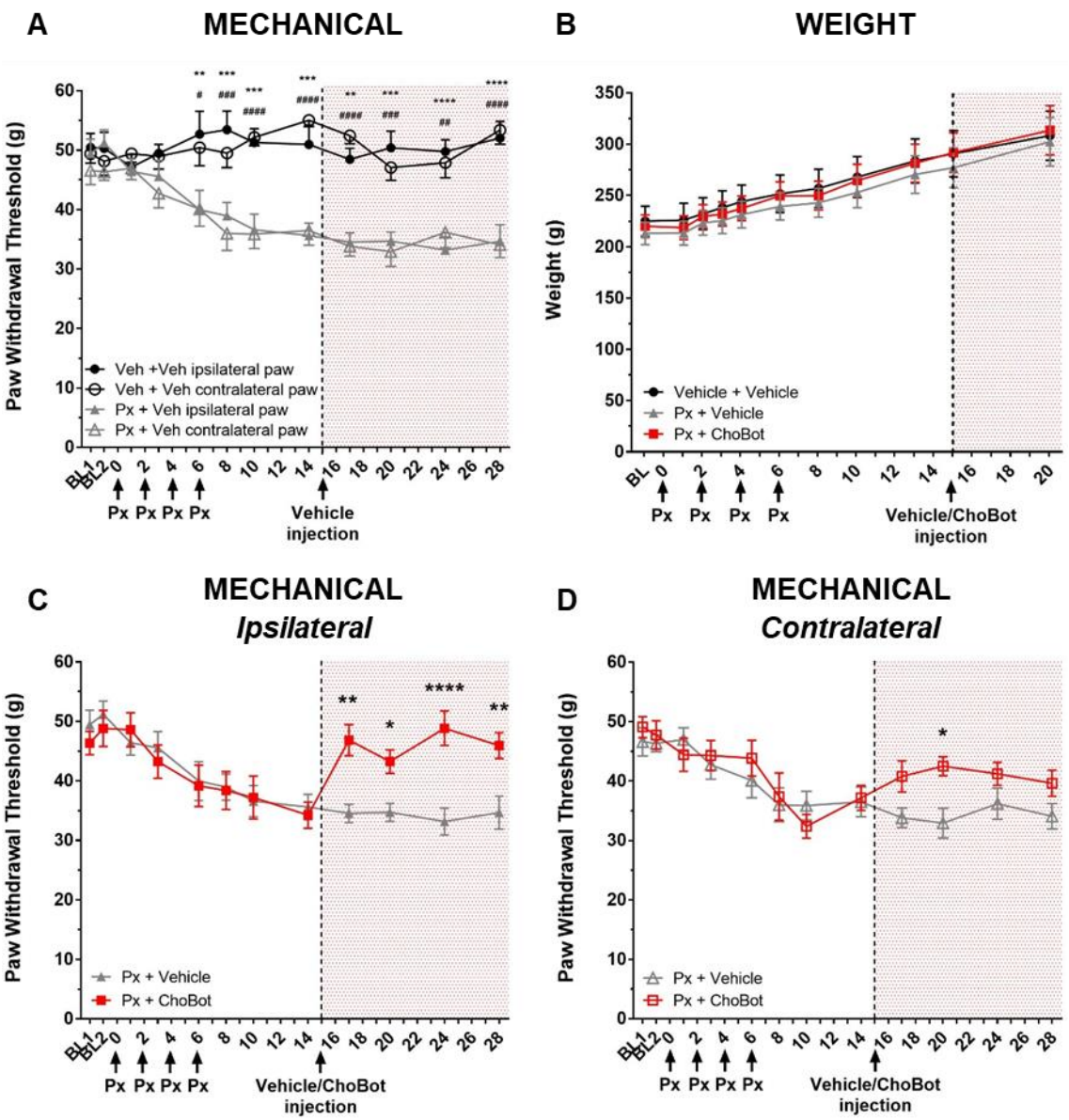

Figure 6.15 The combined behavioural results of male and female PIPN rats highlights an analgesic effect of ChoBot against Paclitaxel-induced mechanical hypersensitivity. (A) *Rats received four intraperitoneal injections of either vehicle (1:1 ethanol: kolliphor) (N=7, 4 male, 3 female) or 2 mg/ml/kg Paclitaxel(Px) (N=9, 6 male, 3 female) on four alternate days. Repeated Px injection produced mechanical hypersensitivity in both the ipsilateral and contralateral hindpaw. Intraplantar injection of vehicle (30 µl 0.4% OG in Buffer A) on day 15 had no effect on the observed mechanical hypersensitivity.* ***(B)*** *Weight gain was not affected by treatment group.* ***(C)*** *Intraplantar injection of 200 ng/ 30 µl ChoBot to the left (ipsilateral) hindpaw on day 15 (N=9, 6 male, 3 female), reversed the paclitaxel-induced mechanical hypersensitivity observed. Vehicle-injected PIPN rats maintained mechanical hypersensitivity until the experiment was terminated on day 28.* ***(D)*** *Injection of ChoBot to the ipsilateral paw also attenuated mechanical hypersensitivity displayed in the contralateral paw with ChoBot-injected animals demonstrating a significantly higher mechanical withdrawal threshold compared to vehicle-injected PIPN rats on day 20. All data presented as mean ± S.E.M. Significance between groups for the ipsilateral paw: * P<0.05, ** P<0.01, *** P<0.001, **** P<0.0001; Significance between groups for the contralateral paw: # P<0.05, ## P<0.01, ### P<0.001, #### P<0.0001.*

Notably, however, there were fewer larger diameter neurons present in the cultures that were incubated with ChoBot and TetBot, than those incubated with BiTox/A. This could potentially bias the mean cell diameter of neurons displaying cleaved SNAP25, after incubation with ChoBot and TetBot, to a smaller value. Importantly, however, there was a consistently large increase in the number of small diameter neurons in cultures incubated with BiTox/A, compared to ChoBot and TetBot, indicating that there was no overall difference in the distribution of the cell diameter of neurons between the cultures. This is clearly demonstrated by the consistency of the median cell diameter between the different culture conditions. For example, with regards to the βIII-Tubulin staining, all three median cell diameters were 17 µm -18.1 µm. Consequently, there would have been an equal opportunity for both BiTox/A, TetBot and ChoBot to enter neurons of varying cell diameters, thus implying that the mean cell diameter should not have been drastically influenced by the number of large diameter neurons present. This is well demonstrated in the frequency histogram for neurons, identified using βIII-Tubulin, where only one larger neuron with a cell diameter greater than 30 µm displayed cleaved SNAP25 after incubation with ChoBot. The other five large neurons available remained negative for cleaved SNAP25. The mean cell diameter therefore remains a true representation of the neurons in which the chimeras preferentially cleave SNAP25.

The presence of cleaved SNAP25 in myelinated neurons agrees with previous studies that demonstrated immunofluorescence in laminae III-V of the dorsal horn, where the myelinated Aβ fibres terminate, following intraneural injection of labelled-cholera subunit B (Woolf et al., 1992; Tong et al., 1999; Shehab et al., 2003). Minimal CTB labelling was detected in lamina I and II where the unmyelinated neurons terminate. Accordingly, here, cleaved SNAP25 is visualised in a much smaller percentage of peripherin-labelled unmyelinated neurons, than NF200- labelled myelinated neurons, following incubation with ChoBot, similarly demonstrating that ChoBot has a greater affinity for myelinated neurons.

In contrast here, however, ChoBot produced cleaved SNAP25 in a subset of smaller myelinated neurons, more suggestive of Aδ-nociceptors, rather than Aβ low-threshold mechanoreceptors. Nevertheless, following nerve transection, previous studies did characterise increased immunoreactivity in lamina I-II of the dorsal horn, where the C- and Aδ-neurons project, and reported increased CTB labelling in smaller neurons (Woolf et al., 1992; Tong et al., 1999; Shehab et al., 2003). This was suggested to be due to the increased uptake of CTB by undamaged unmyelinated and lightly myelinated neurons, post-nerve injury. This possibly results from the increased expression of the ganglioside to which CTB binds, GM1, which is associated with nerve repair and regeneration (Toffano et al., 1983; Leon et al., 1984). As described earlier, the protocol for producing

dissociated DRG cultures involves mutliple axotomies, required to excise DRGs. Again, this methodological process could perturb the expression levels of gangliosides and consequently impact the perceived in vitro binding profile of ChoBot.

The presence of cleaved SNAP25 in CGRP-positive neurons following intraplantar injection of ChoBot, however, negates that the in vitro binding profile is solely a product of the culturing process. Although CGRP can be expressed by all subpopulations of sensory neurons, its expression is most prevalent in the smaller neurons, the C- and Aδ nociceptors (Ferri et al., 1990; McCarthy and Lawson, 1990; Lawson et al., 2002; Bae et al., 2015). Cleaved SNAP25 was detected in both NF200- positive and CGRP-positive neurons in vivo, again suggesting that ChoBot could be catalytically active in Aδ nociceptors as this neuronal subtype would be most likely to produce immunoreactivity to both markers. Additional triple immunolabelling is, however, still required to confirm this.

6.3.2 ChoBot demonstrates potential as a future analgesic

Regardless, together, the verification of the catalytic activity of ChoBot in the peripheral sensory neurons, presumed to be Aδ-nociceptors, and the lack of activity noted at the central terminal, supported the decision to investigate ChoBot as a potential analgesic. ChoBot was shown to significantly attenuate the development of mechanical hypersensitivity following surgical incision to the hindpaw. Post-operative pain occurs in 10–50% of surgical cases, for example, following breast surgery, amputation, and major heart surgery (Kehlet et al., 2006). Effective management of post-operative pain is essential to increase early mobilisation, reduce hospital stay length and to lessen the associated medical costs (Gupta et al., 2010).

This analgesic effect was only observed when ChoBot was delivered pre-emptively, prior to surgery. Provided that cleaved SNAP25 was detected in the peripheral sensory neurons, this suggests that ChoBot could be preventing the initial sensitisation of peripheral afferents, which occurs around the incision site, and potentially the central sensitisation which occurs secondary to the increased nociceptive input from the peripheral afferents, by blocking neurotransmission (Pogatzki-zahn et al., 2017). The inefficacy of ChoBot post-incision suggests that once this hypersensitivity has been established, ChoBot is unable to reverse these changes.

Pre-emptive analgesia is highly desirable from a clinical perspective as it reduces the need for post-operative pain management, for example, with the use of opioids which are prone to abuse. It has also been suggested that pre-emptive treatments are more effective methods for treating postoperative pain (Møiniche et al., 2002). There is a huge

emphasis placed on the need for pre-emptive analgesia to be preventative, meaning that the treatment must stop peripheral and central sensitisation which leads to the chronification of post-operative pain, rather than simply blocking the initial perioperative nociceptive signalling.

Unfortunately, this analgesic effect was not reproduced in females. Clinical studies show that female patients experience more severe post-operative pain than males, according to reported visual analogue scale (VAS) pain scores, and require more frequent analgesics to manage their pain (Logan and Rose, 2004; Uchiyama et al., 2006; Pereira and Pogatzki-Zahn, 2015). These sex differences have so far not been replicated in rodents. Instead, there were no perceived differences in the development of either mechanical or thermal hypersensitivity between male and female rodents in the incisional post-operative pain model, and both sexes responded equally to analgesic interventions (Kroin et al., 2003; Banik et al., 2006). It is therefore unclear why male and female rats responded differently to incision following intraplantar injection of ChoBot

Notably, here, the stage of the menstrual cycle was not measured. Recently, in light of mixed reports on the significance of the estrous cycle on pain thresholds, it has been shown that the estrous cycle in females does not introduce any additional variability in pain measurements, compared to male rodents, thus negating the need to record the stage of the estrous cycle (Mogil and Chanda, 2005; Prendergast et al., 2014; Becker et al., 2016). Instead, both studies suggest that males display their own intrinsic variability resulting from fighting, aggressive behaviours and instinctive hierarchy, behaviours which are largely absent in females. Therefore, the frequency of these behaviours should be equally considered when making a case for measuring the hormone levels in females.

Although the menstrual cycle itself has been revealed to have little impact on pain thresholds, the mechanisms for the establishment of chronic pain have, however, been found to differ greatly between males and females (Mapplebeck et al., 2016). It has been shown that the development of mechanical allodynia in males relies upon the activation of microglia post-injury. This was demonstrated after the inhibition of, and the depletion of, microglia both significantly reversed mechanical allodynia in males separately subjected to the spared nerve injury model and the CFA model (Sorge et al., 2015). Conversely, although similar levels of microgliosis were observed in females, microglia were not implicated in the establishment of mechanical hypersensitivity in females as depletion and inhibition of microglia had no effect on mechanical pain thresholds. Consequently, this highlights that the difference in the efficacy of ChoBot, between the sexes, could potentially arise from a mechanism for the establishment of chronic pain which might only be active in males.

Despite the inflammatory component apparent in post-operative pain, ChoBot failed to induce analgesia in the Complete Freund's Adjuvant inflammatory pain model in male rats, thus demonstrating a lack of effectiveness of ChoBot in inflammatory pain conditions. It was hypothesised that ChoBot would have an analgesic effect in inflammatory conditions after in vitro incubation of DRG cultures with ChoBot caused a reduction in CGRP release, a process which occurs in neurogenic inflammation and contributes to both peripheral and central sensitisation (Benemei et al., 2009). It would thus be useful to repeat this assay, using rat DRG cultures, to ascertain whether the results are reproducible or are indeed species-dependent.

Conversely, when ChoBot was investigated in a neuropathic pain model, ChoBot had a profound analgesic effect. Interestingly, ChoBot was able to reverse the mechanical hypersensitivity observed in male and female PIPN rats. A full reversal of mechanical hypersensitivity was observed in the ipsilateral paw. Additionally, a partial, yet significant, recovery of the mechanical withdrawal threshold was demonstrated in the contralateral paw.

A bilateral analgesic effect has previously been shown following unilateral injection of BoNT/A, including after intraplantar injection specifically. This was reported in two separate neuropathic pain models, in the streptozotocin-induced model of diabetic peripheral neuropathy (Bach-Rojecky et al., 2010) and in the paclitaxel-induced peripheral neuropathy model, as used here (Favre-Guilmard et al., 2009). In a separate study, the bilateral analgesic effect, produced after intraplantar injection of BoNT/A in a saline-induced model of muscular hyperalgesia model, was abolished by intraneural injection of colchicine, a blocker of axonal transport, to the sciatic nerve (Bach-Rojecky and Lacković, 2009). Thus, highlighting that the observed analgesia was due to a central effect of BoNT/A, subsequent to retrograde transport. This was further accredited in a subsequent follow-on study whereby axonal transport within the sensory nerves specifically, was demonstrated (Matak et al., 2011).

In contrast, here, a negligible amount of cleaved SNAP25 was detected at the level of the spinal cord. This therefore opposes the theory for a central cause for the bilateral analgesia associated with peripherally-injected ChoBot. Due to the expansive cleavage of SNAP25 normally observed in the spinal cord after intraplantar injection of the other chimeras, it could be that investigation of the dorsal horn was neglected and that observations of cleaved SNAP25 were subsequently missed. This seems unlikely due to the thorough investigation of the tissue. Instead, the data suggests that ChoBot has a peripheral action, resulting in the blockade of neurotransmission in presumably the Aδ-nociceptors, although it is unclear how this would provide analgesia in the contralateral paw. To ascertain that there is no role for retrograde transport in the analgesic effect of

ChoBot, colchicine could be injected intraneurally at the same time, or prior to, injection of ChoBot. If analgesia was still produced in the contralateral hindpaw then this would prove that it was due to another mechanism, other than a centrally-mediated effect of ChoBot.

It is not yet clear why ChoBot produced an analgesic effect in both sexes experiencing PIPN but was only efficacious in males with regards to post-operative pain. Of note, however, the analgesic effect in the contralateral hindpaw was not as pronounced in female rats. There was only one data point that demonstrated a noticeably higher mechanical withdrawal threshold in the contralateral paw of ChoBot-injected PIPN females, compared to those receiving vehicle. It would be of interest to repeat this experiment, with a higher number of females, to allow a comprehensive comparison to made between the PIPN pain phenotype, and responsiveness to ChoBot, between males and females, to fully ascertain whether any subtler sex-differences do exist.

Given the therapeutic benefit of ChoBot administered pre-emptively in post-operative pain, it raises the additional question of whether ChoBot injected before repeated Paclitaxel exposure might similarly prevent the development of mechanical hyperalgesia. 64% of patients complain of chemotherapy-induced peripheral neuropathy whilst still receiving chemotherapy treatment. For 27% of these patients, this peripheral neuropathy develops into a long-lasting chronic neuropathic pain condition (Reyes-Gibby et al., 2009). From this perspective, an earlier interventive treatment could be beneficial to block the development of the neuropathy. Consequently, another promising future experiment to conduct would be to inject ChoBot in the days before paclitaxel injection, to determine whether ChoBot would similarly prevent the development of the neuropathic pain condition.

6.3.3 Justification of the behavioural assessment method utilised

All of the observations made above relied upon the use of an electronic von Frey aesthesiometer to assess the mechanical withdrawal threshold. Electronic von Frey has been highlighted as a sensitive test by which to assess mechanical hypersensitivity (Ängeby Möller et al., 1998; Vivancos et al., 2004). The major advantage associated with using electronic von Frey is the reduced experimental time. Each animal requires a maximum of 4 applications of the electronic von Frey aesthesiometer compared to the repeated applications of single filaments, during manual von Frey testing. This lead can to the sensitisation of the paw, as well as learnt behaviours to subsequent von Frey filament applications (Deuis et al., 2017).

The accuracy and suitability of electronic von Frey for the evaluation of mechanical threshold, compared to manual methods, specifically in neuropathic pain models has, however, been questioned. It was found that electronic von Frey was unable to produce reliable readings of the mechanical threshold in neuropathic pain models which feature severe deformity of the hindpaw, resulting from denervation. For example, in the chronic constriction injury model were all three branches of the sciatic nerve are damaged (Nirogi et al., 2012). In the partial sciatic nerve ligation model, however, were the hindpaw maintains postural control due to the partial innervation that remains, electronic von Frey provided consistent readings. From this perspective, electronic von Frey would be able to reliably assess the mechanical threshold in the PIPN model as this model does not produce a motor deficit and does not feature any degeneration of the motor fibres, meaning that the posture and form of the hindpaws are unaffected (Polomano et al., 2001). Furthermore, Electronic von Frey has already been successfully used to investigate mechanical threshold in both the incisional post-operative pain model (Whiteside et al., 2004) and the PIPN model (Rahn et al., 2008). Importantly, the values generated here, match those previously reported in the literature whilst using an electronic von Frey aesthesiometer, highlighting the high reproducibility between investigators (Moalem et al., 2004; Papers et al., 2004; Rahn et al., 2008). Furthermore, specifically, in this study, electronic von Frey has produced consistent results and its' use is therefore justified.

6.3.4 Considerations for the use of ChoBot as an analgesic

For a novel chimera to be used as an analgesic, it is important that it can be easily administrated, and that the method of delivery is minimally invasive. The previously designed chimera, TetBot, produced analgesia in an inflammatory pain model (Ferrari et al., 2013), however, this effect was only noted after intrathecal injection and could not be replicated following peripheral injection (data unpublished). In humans, intrathecal injection is a complicated procedure that requires administration by a trained anaesthetist and is associated with serious adverse complications such as persistent parathesias, arachnoiditis, and, more rarely, temporary respiratory depression (Goodman et al., 2008). The analgesic effects of ChoBot were reported after intraplantar injection. ChoBot could therefore be easily delivered by subcutaneous injection to a chosen peripheral site. Subcutaneous injection would not require highly specialist medical personnel, thus reducing any associated medical costs. Furthermore, whilst TetBot contains the receptor binding domain of Tetanus toxin, which the majority of humans are immunised against (Maple et al., 2000), most humans are not immunised against cholera toxin meaning that

it can be developed into a therapeutic intervention for humans. By contrast, TetBot is essentially redundant for human use.

Unfortunately, however, ChoBot was no more efficacious at producing analgesia in inflammatory pain conditions than BiTox/A. Thus far, TetBot is the only chimera which has been demonstrated to be analgesic in inflammatory pain conditions. Notably, the clostridial toxins bind to specific gangliosides expressed within the cell membrane. As described in Chapter 4, specific gangliosides, including GT1b, GD1a and GM1, associate with myelin-associated glycoprotein (MAG), which is essential for the stability of the myelin sheath of neurons (Yang et al., 1996; Schnaar, 2010). Expression of these gangliosides is hence, more associated with myelinated neurons. Therefore, in order to target the unmyelinated c-fibres which are more commonly implicated in chronic inflammatory pain conditions (Weng et al., 2012), it may be important to expand the search for a targeting domain, away from toxins, and perhaps towards neuropeptides. If this was successful, then LcTd/A could, in theory, be targeted to neurons which normally become sensitised following neuropeptide release from peptidergic neurons, for example, during neurogenic inflammation (Xanthos and Sandkühler, 2014).

Before further pursuing the use of ChoBot as an analgesic, it will be important to fully determine the stability of the chimera in vivo. During SDS-page, ChoBot can be seen to dissociate into LcTd/A-SNARE-A2 and the singular and pentameric B subunit. In contrast, the previous chimeras, BiTox/A (Ferrari et al., 2011) and TetBot (Ferrari et al., 2013) remained stable following SDS-page, demonstrating that an irreversible assembly of the individual components had occurred. Moreover, immunoreactivity for the CTB subunit was still detected in the ventral spinal cord in the absence of any SNAP25 cleavage. It is thus possible that the B subunit had dissociated away from the chimera, whilst in the periphery, before retrogradely transporting to the soma, leaving LcTd/A-SNARE-A2 in the peripheral terminals, hence explaining why cleaved SNAP25 was only detected in the peripheral neurons. From this perspective, it might be necessary to conjugate LcTd/A directly to the singular CTB subunit, to avoid any potential adverse effects associated with any dissociated CTB subunits.

Further to this, there were additional concerns about the significance of cleaved SNAP25 detected at the neuromuscular junction. Rats injected with ChoBot were observed for any signs of stress or compromised wellbeing. Specifically, they were observed for indications of dehydration, such as weight loss, symptomatic of cholera, and for flaccid muscle paralysis, indicative of botulism. The ChoBot-injected rats continued to gain weight after receiving the injection of ChoBot and did not exhibit any visible signs of muscular paralysis, such as lameness or inability to grasp during the inverted wire mesh test. Furthermore, it has repeatedly been demonstrated that the engineered clostridial

chimeras do not cause muscular paralysis. For example, in Chapter 3 it was shown that BiTox/A produces cleaved SNAP25 at both the NMJ, as well as in the ventral horn, but fails to elicit muscular paralysis (Ferrari et al., 2011, 2013; Mangione et al., 2016). This suggests that the lethality and toxic effects associated with the two native toxins were successfully eliminated from the chimera, despite the cleavage visualised at the neuromuscular junction.

6.3.5 Conclusion

In summary, it has been demonstrated that ChoBot can be effectively assembled using the established protein-stapling technology. The novel chimera, ChoBot, successfully retained the catalytic activity of LcTd/A, both in vitro and in vivo. Here, ChoBot is highlighted as a promising analgesic for pre-emptive use in post-operative pain and for the management of chemotherapy-induced neuropathies. It would be of great interest to investigate whether ChoBot can similarly reverse the mechanical hypersensitivity, characteristic of other neuropathic pain conditions. Importantly, considering that cleaved SNAP25 was largely absent at the level of the spinal cord, the analgesia associated with ChoBot provides evidence for a peripheral action, namely at the peripheral afferents, being at least partially accountable for the analgesia observed with BiTox/A.

Chapter 7. General Discussion

The primary objective of this project was to identify a novel analgesic to provide long-lasting pain relief in a variety of chronic pain conditions. Botulinum Neurotoxin A was chosen as the ideal biologic for development because of its well-known ability to silence neurons and effectively block neurotransmission. The multidomain structure of BoNT/A, combined with the expertise and knowledge of biochemistry and protein modification in the laboratory, made BoNT/A highly suitable for protein engineering. By exploiting protein modification techniques, it was hypothesised that BoNT/A would be safely retargeted to the sensory neurons, selectively involved in pain signalling pathways, whilst simultaneously excluding its entry to the neuromuscular junction to remove the flaccid motor paralysis, normally associated with botulism.

Previous efforts to reengineer BoNT/A have resulted in the chimera, BiTox/A. For the chimera, BiTox/A, the LcTd/A, responsible for the enzymatic activity of BoNT/A, was reassembled to the receptor binding domain of BoNT/A, using the pioneered stapling technology, to produce an elongated version of native BoNT/A (Ferrari et al., 2011). Subsequent behavioural investigations had demonstrated that BiTox/A is analgesic in certain pain conditions, and is especially effective at reducing the mechanical hypersensitivity developed in neuropathic pain (Mangione et al., 2016). A significant portion of this project focused on the investigation of the in vivo behaviour of the published chimera, BiTox/A, to elucidate the mechanisms by which it might mediate its analgesic effect, subsequent to peripheral delivery (Mangione et al., 2016).

7.1 The in vivo activity of clostridial chimeras

Despite that, previously, Mangione et al. (2016) had failed to detect SNAP25 cleavage at either the peripheral injection site or in the lumbar dorsal horn after intraplantar injection of BiTox/A using western blot, here, immunohistochemical staining successfully revealed cleaved SNAP25 at both locations. This consequently provides the first evidence for both a peripherally- and centrally- mediated mechanism for the analgesia produced by BiTox/A.

7.1.1 Cleaved SNAP25 is consistently detected in the peripheral sensory afferent terminals following intraplantar injection of clostridial chimeras

Specifically, cleaved SNAP25 staining was visualised in the peripheral sensory afferents following intraplantar injection of BiTox/A and colocalised with Neurofilament 200, the marker of myelinated neurons, and IB_4, indicative of non-peptidergic neurons. This binding profile, established in vivo, was subsequently replicated in vitro, following immunolabelling of dissociated DRG cultures. In vitro, BiTox/A produced cleavage in the larger, myelinated neurons, suggestive of Aβ sensory neurons. Interestingly, in vivo, cleaved SNAP25 also partially colocalised with CGRP, a neuropeptide released by sensory afferents which contributes to pain signalling and neurogenic inflammation (Benemei et al., 2009). This was reminiscent of the peripherin-positive subpopulation of sensory neurons that were identified to contain cleaved SNAP25 in BiTox/A-incubated cultures, given that CGRP is primarily expressed by the unmyelinated C-fibre nociceptors (McCarthy and Lawson, 1990; Lawson et al., 2002).

Likewise, ChoBot, investigated in chapter 6, was shown to produce SNAP25 cleavage in the peripheral sensory afferents, specifically within a subset of NF200 and CGRP-positive afferents. This thus suggests that this peripheral action at the sensory afferents is conserved across the clostridial chimeras.

7.1.2 Clostridial chimeras do not produce muscular paralysis despite cleaving SNAP25 at the neuromuscular junction

Despite successfully demonstrating the enzymatic activity of BoNT/A in the peripheral sensory afferents, the issue with all the chimeras so far tested, including ChoBot, is the unexpected presence of cleaved SNAP25, repeatedly detected at the neuromuscular junction of the glabrous skin. It has, however, been consistently reported that animals injected with clostridial chimeras, do not display any visible signs of motor paralysis or impaired motor function of the hindlimb. More thorough assessments are, however, required to effectively disprove this concern before developing the chimeras for use in humans. As explained earlier, CatWalk gait analysis could elucidate any more subtle change in gait as a result of less obvious motor paralysis (Kappos et al., 2017). Electromyography recordings would also be recommended to ensure that there is no change in the electrical activity of the skeletal muscle, as this would likely be the most convincing argument to confirm that there is no motor effect.

It is, however, possible that the function of the hindpaw muscles could be preserved, despite the cleavage of SNAP25 at the neuromuscular junction, if a suboptimal amount of SNAP25 has been cleaved. Keller and Neale (2001) depicted a model which predicted that for each percentage of SNAP25 cleaved, there is a two times equivalent reduction in the percentage of neurotransmitter released. The model illustrates that cleaved

SNAP25 is a competitive antagonist of full length SNAP25. In accordance with this, it has previously been described that half of the SNAP25 present is required to be cleaved to effectively block glutamate release from synaptosomes (Otto et al., 1995). Consequently, this shows that the negative effect of cleaved SNAP25 can be overcome if there is enough full length cleaved SNAP25 available to out-compete the cleaved, non-functional SNAP25. These observations are therefore consistent with the proposed hypothesis that BiTox/A displays reduced penetration of the neuromuscular junction (Darios et al., 2010; Ferrari et al., 2011). If a lower level of SNAP25 is cleaved by BiTox/A, due to the reduced penetration and internalisation rate compared with native BoNT/A, then the limited amount of cleaved SNAP25 present could be successfully out-competed, and thus compensated for, by the full-length SNAP25. This could thereby justify the lack of motor impairment observed, despite the SNAP25 cleavage which occurs.

7.1.3 The relevance of sensorimotor connectivity for the SNAP25 cleavage observed within the lumbar spinal cord following peripheral injection

Further to the SNAP25 cleavage detected at the neuromuscular junction, the significance of the large area of SNAP25 cleavage reported in the ventral spinal cord, surrounding the motor neurons, following peripheral injection of not only BiTox/A, but also BiTox/D, TetBot and 2xTetBot, remains to be elucidated. As suggested previously, this could represent SNAP25 cleavage in the sensorimotor pathways within the spinal cord, which modulate motor output and are important for proprioception (Cai et al., 2017). For example, there are sensory neurons, namely the Ia sensory afferents, which respond to muscle stretch and project from the dorsal horn to then form synapses directly with the proximal dendrites and soma of the motor neurons in laminae IX (Snider et al., 1992). These afferents could thus provide direct access for BiTox/A, to the dorsal horn, via retrograde axonal transport, and could potentially represent the single fibres of SNAP25 cleavage in the dorsal horn. Furthermore, there are also GABAergic interneurons, present in the spinal cord, which modulate the sensory input to motor neurons, both by presynaptic inhibition of sensory neurotransmitter release to motor neurons, as well as inhibition of the motor neurons post-synaptically to reduce excitability (Betley et al., 2009). Again, this emphasises the interconnectivity which exists between the dorsal and ventral horn, even beyond direct contacts.

Additionally, there is also the corticospinal tract which projects from the somatosensory and motor cortices to both the dorsal and ventral horn of the spinal cord. It is important for the execution of voluntary motor movements and sensory feedback (Scheibel and Scheibel, 1966; Moreno-López et al., 2016). The corticospinal tract thus represents yet

another interface between the sensory and motor systems, and collectively illustrates how well interconnected these two systems are. This hence demonstrates that even if the BiTox/A protease is solely transported by the motor neurons to reach the central spinal cord, considering that cleaved SNAP25 cannot be detected in the DRG, the protease could still gain indirect access to the neurons which constitute the sensory system, in order to impact sensory processing.

In view of this, future experiments will be required to identify the neuronal subtypes which contain cleaved SNAP25, indicating the presence of active BiTox/A protease in the spinal cord to effectively delineate the neuronal networks by which BiTox/A might mediate its possible central effect. Two methods by which to achieve this would firstly be the use of neuronal tracers, such as DiI and DiA, that can be injected using a microelectrode to either the DRG or the dorsal root to label the sensory neurons, or to the ventral root to separately label the motor neurons (Snider et al., 1992). Alternatively, neuronal subtypes can be identified by immunolabelling, using specific markers. For example, vGlut1 can be used to selectively label the sensory terminals in the spinal cord, whilst parvalbumin can be used to label the motor neurons (Betley et al., 2009). Furthermore, vGlut2 and GAD65 can be used to identify the excitatory and inhibitory interneurons, respectively (Betley et al., 2009). Both techniques should label the entirety of the neuron, including the axonal and dendritic projections, rather than being confined to the neuronal nucleus and cytoplasm as is seen with the NeuN marker, used here. This will help to conclude whether the cleaved SNAP25 detected in the dorsal and ventral horn, is present within the dendritic arborisations of the motor neurons or within the spinal interneurons.

Interestingly, the synaptic bouton labelling of sensory terminals, produced by vGlut1 (Betley et al., 2009), resembles the cleaved SNAP25 staining observed immediately adjacent to the motor neurons, following intraplantar injection of BiTox/A, which was hypothesised to represent synaptic end-feet. This theory contrasts Cai et al. (2017) who claimed that the cleaved SNAP25 stain, resultant from peripheral injection of BoNT/A, remained contained within motor neurons. The two techniques detailed could be used to effectively disprove this theory if cleaved SNAP25 staining was found colocalised with either a tracer, or a respective neuronal marker, used to label the sensory afferents. If shown to be true, this experiment would further determine whether BiTox/A might enter the sensory afferents directly, or whether it instead enters connective interneurons.

It will also be important to conduct an experiment whereby colchicine, a blocker of axonal transport, is injected intraneurally prior to intraplantar injection of BiTox/A (Bach-Rojecky and Lacković, 2009; Matak et al., 2012). This will delineate whether it is necessary for BiTox/A to reach the central spinal cord, regardless of which neuronal subtype it is active in, in order to elicit its analgesic effect. It will also verify that the SNAP25 cleavage

detected distal from the injection site, for example at the spinal cord and in the contralateral paw, results from axonal transport of the BiTox/A protease and not from systemic diffusion.

Nevertheless, the lack of penetration of the spinal cord by ChoBot does, however, make it an attractive candidate for future development as an analgesic. Restricting the enzymatic activity of BoNT/A protease to the periphery greatly reduces the likelihood of any adverse off-target effects and improves the chimera's safety profile, accordingly.

7.2 The development and behavioural assessment of novel chimeras

In addition to attempting to elucidate the in vivo activity of clostridial chimeras, an effort was made to produce a chimera efficacious against thermal hyperalgesia. Consequently, it was investigated whether chimeras produced by combining LcTd/A with the binding domains of other botulinum serotypes, namely Rbd/C, -/D and -/E, would show specificity for other sensory neuron subpopulations. If shown to be correct, this method would enable the targeting of separate sensory neuron subpopulations, whilst maintaining the long-duration blockade, characteristic of BoNT/A (Eleopra et al., 1998). It was hypothesised that the novel chimeras would then preferentially silence other distinct subpopulations of sensory neurons, and thus, be more efficacious against other pain conditions, such as inflammatory pain.

Two of the novel chimeras, BiTox/D and -/E, did actively target LcTd/A to a different subpopulation of sensory neurons, however, when further pursued in a behavioural model of inflammatory pain, BiTox/D was unfortunately suspected to be pro-hyperalgesic. Specifically, the behavioural assessment of BiTox/D in CFA-injected rats suggested that it might instead prolong the period of thermal hyperalgesia. This is not, however, to say that this stapling technology, or this approach, is therefore redundant. Recent research in collaboration with the Hunt lab at the University College London, investigated the conjugation of LcTd/A to neuropeptides, implicated in pain signalling, such as substance P, again using the stapling technique described (Maiarù et al., 2016). Given intrathecally, LcTd/A conjugated to Substance P successfully reduced mechanical hypersensitivity in both a chronic inflammatory pain model, induced by CFA injection, and in the spared nerve injury model of neuropathic pain.

7.2.1 Methodological considerations for the perceived lack of analgesic effect of chimeras in inflammatory pain models

Here, in this project, the stapling technology was used to construct the chimera, ChoBot. Again, ChoBot consisted of the LcTd/A which was then attached to the AB_5 cholera toxin binding domain. ChoBot was similarly shown to be analgesic. However, like with BiTox/A, this therapeutic effect was specifically observed against the mechanical component of pain conditions. Specifically, ChoBot was effective at attenuating the mechanical hypersensitivity experienced in the incisional pain model for post-operative pain and in the PIPN model of neuropathic pain. ChoBot was not, however, shown to relieve thermal hyperalgesia or to produce analgesia in purely inflammatory conditions, i.e. the CFA-induced inflammatory pain model. This finding was demonstrated despite that, in vitro, ChoBot produced SNAP25 cleavage in a subpopulation of neurons which, based on their size distribution and myelination, were significantly distinct from the subpopulation in which BiTox/A cleaves SNAP25. Instead, the subpopulation of sensory neurons appeared very similar to that which TetBot is catalytically active in. Notably, TetBot was previously shown to reduce mechanical hypersensitivity in CFA-induced inflammatory pain (Ferrari et al., 2013). It is thus surprising that ChoBot did not also display an anti-nociceptive effect in an inflammatory pain model. This could, nevertheless, result from the method of administration.

The analgesic effect of TetBot was observed after intrathecal injection whereas, for this project, ChoBot was injected intraplantar. Similarly, the aforementioned BoNT/A-Substance P construct, which reduced mechanical hypersensitivity in the CFA inflammatory pain model, was delivered via intrathecal injection (Maiarù et al., 2016). The method of administration could thus be essential for the observed therapeutic effect of clostridial chimeras in inflammatory pain conditions as, noticeably, all of BiTox/A behavioural experiments likewise utilised intraplantar injection (Mangione et al., 2016). Besides which, interestingly, immunolabelling of spinal cord sections, isolated from ChoBot-injected rats, showed minimal immunoreactivity for cleaved SNAP25 in the spinal cord, thereby suggesting that there had been insufficient transport of the BoNT/A protease to the spinal cord. Together, this suggests that clostridial chimeras might require direct access to the central terminal in order to elicit an analgesic effect in inflammatory pain conditions. Given the consistency of the results, dependent on the method of delivery, this might occur regardless of the targeting domain utilised.

An alternative explanation regards the timing of the delivery of the chimeras. Both of the peripherally-injected chimeras, BiTox/A and ChoBot, were administered to the hindpaw one day after CFA injection. At this time point, one day post-CFA injection, significant oedema is already observed in the CFA-injected hindpaw, indicative of an inflammatory response (Iadarola et al., 1988; Stein et al., 1988). Accordingly, in both behavioural experiments, pain behaviour was maximal after 24 hours, consistent with previous

reports (Fehrenbacher et al., 2012; Mangione et al., 2016). The heightened immune response in the hindpaw at this time, and the infiltration of immune cells could result in the quick removal of the injected chimera before it is able to internalise into the sensory neurons that innervate the site of inflammation, thus leading to a diminished analgesic effect.

Interestingly, BiTox/A administered to the hindpaw one day post-CFA injection elicited a very transient relief of mechanical hypersensitivity in the CFA-inflammatory pain model between days 2-3 post CFA-injection. Although the difference was shown to be significant, the improvement in the mechanical threshold was minimal. By comparison, when CFA was instead injected into the ankle joint, intraplantar injection of BiTox/A, 3 days after CFA induction, resulted in a more significant, sustained reversal of the mechanical hypersensitivity, observed in the hindpaw. In this instance, BiTox/A was injected distal to the site of inflammation and would thus be less vulnerable to immune cells clearance which, consequently, could explain the improved analgesic effect observed.

7.3 Additional methodological considerations

7.3.1 The use of the in-house anti-cleaved SNAP25 antibody

One of the major limitations of this project is the reliance of the conclusions made on the validity of the in-house anti-cleaved SNAP25 antibody. Rhéaume et al. (2015) previously questioned the specificity of some of the commercially available anti-cleaved SNAP25 antibodies. Consequently, they tested the validity of these antibodies alongside their own in-house anti-cleaved SNAP25 antibodies. It was found that the validity of the commercial antibodies depended on the assay in which they were used, whether that be western blot or immunohistochemistry, and moreover, with specific reference to immunohistochemistry, the type of tissue used. The presence of immunoreactivity in vehicle-treated samples was regarded as evidence that the antibody lacked specificity and was instead binding both cleaved and full length SNAP25. The in-house anti-cleaved SNAP25 used here did not produce an immunofluorescent signal in tissue taken from either vehicle-injected or naïve animals or in vehicle or untreated DRG cultures, thus validating the antibody used here. It can thus be confirmed that the conclusions made are valid and based upon reliable evidence. It would, however, be recommended to ensure that these findings can replicated using an alternative anti-cleaved SNAP25 antibody to negate any reservations and create more support for the hypothesis.

7.3.2 The inclusion of the SNAP25 linker when generating clostridial chimeras

With regards to the cleaved SNAP25 immunoreactivity, it has repeatedly been questioned whether the chimeras themselves would contribute to the positive cleaved SNAP25 signal. The chimeras have all been constructed using the SNARE stapling approach which involves the assembly of a SNARE complex at the centre of the conjugated subunits (Darios et al., 2010; Ferrari et al., 2011, 2013; Mangione et al., 2016; Mavlyutov et al., 2016). Consequently, all the chimeras contain the SNAP25 peptide, the cleavage target of BoNT/A protease. The presence of the BoNT/A protease within the chimera can thus result in self-cleavage. As detailed by Rhéaume et al. (2015), the amount of BoNT/A injected to elicit therapeutic effects is fairly negligible and therefore it would be extremely difficult to detect BoNT/A directly. This is why the proteolytic product is instead labelled as this provides signal amplification and acts as a reporter for the location of the BoNT/A protease. Similarly, the positive cleaved SNAP25 staining, generated directly by the cleaved SNAP25 linker-peptide contained within the chimeras, should be insignificant, perhaps even undetectable, compared to the signal produced by the cleavage of cellular SNAP25, the intended proteolytic product of the chimeras, due to the nanogram amounts injected.

The other concern generally expressed regards the ability of the chimera to form in addition to its subsequent stability, following self-cleavage. Interestingly, SNAP25 which has been cleaved by BoNT/A, fully retains the ability to assemble into the SNARE-complex (Hayashi et al., 1994; Otto et al., 1995). Once BoNT/A-cleaved SNAP25 enters the SNARE-complex, however, the complex is rendered non-functional and is consequently unable to fuse the vesicular and the plasma membrane, hence explaining why cleaved SNAP25 acts as a competitive antagonist to full length SNAP25 (Keller and Neale, 2001). Likewise, in the context of the SNARE-stapling technique, self-cleavage of the SNAP25 linker does not interfere with the assembly of the SNARE complex, and thus, does not impact chimera formation (Darios et al., 2010). Additionally, BoNT/A is unable to access and cleave SNAP25 once it is already engaged in a SNARE complex (Hayashi et al., 1994). Therefore, if the chimera assembles before self-cleavage occurs then the chimera will comprise full-length SNAP25 thus making the above justification inconsequential.

7.4 Versatility in the SNARE-stapling technology

Apart from demonstrating novel chimeras as potential future analgesics, this project also illustrated how advancements can be made to the stapling technology to successfully increase the efficacy of chimeric proteins. At this time, the project moved away from the

original aim of developing a novel pain therapeutic and instead concentrated on spinal cord delivery. It was shown that instead of using syntaxin solely as a staple, syntaxin could equally be utilised to attach an additional domain to the chimeric protein, via recombinant expression, comparable to that demonstrated with the other SNARE components. The additional subunit, here, an extra binding domain, did not interfere with the normal activity of the chimera but, instead, augmented it. One of the other linker peptides, α-SNAP25 is in fact composed of two individual helixes and could thus be split to enable the attachment of another additional domain. In theory, the potential exists to join a total of 8 individual subunits, if both ends of each of the four helices of the tetrahelical SNARE complex were utilised (Darios et al., 2010).

7.5 Conclusions

In conclusion, this project has demonstrated the ability of the SNARE-stapling technology to produce safer, novel analgesics for use in a range of chronic pain conditions. During this project, ChoBot, specifically, has been highlighted as a promising analgesic for pre-emptive use in post-surgical pain and for the management of neuropathic pain conditions. Meanwhile, the potential mechanisms by which BiTox/A might mediates its analgesic effect have been elucidated. All chimeras were administered without producing motor paralysis or compromising the wellbeing of animals.

This project has also emphasised the versatility of the stapling technology. In chapter 4, it was shown how the stapling technology allows for the combinatorial engineering of proteins. This enabled the efficient substitution of receptor binding domain of the BiTox chimera and consequently, allowed for the exploration of the differential binding profiles resulting from the alternative targeting of the BoNT/A protease. Furthermore, it has been demonstrated that the stapling technology is not restricted to use with clostridial neurotoxin subunits, exclusively. ChoBot utilised the binding domain of an alternative bacterial toxin, cholera toxin. Additionally, the stapling technology has also been used to conjugate BoNT/A protease to neuropeptides implicated in pain signalling (Maiarù et al., 2016), as well as to surrogate targeting domains intended to target the protease to neuroblastoma cell lines, for the treatment of cancer (Rust, 2016; Hart, 2017).This further demonstrates the multiple disease applications for the stapling technology.

In this project, the use of chimeras for spinal cord delivery was investigated. With further development, chimeras could provide a therapeutic delivery tool for use in central nervous system conditions, including amyotrophic lateral sclerosis (ALS) and spinal muscular atrophy (SMA), which, with the aid of advancements to the stapling technology such as the attachment of additional targeting domains, could lead to an augmented

therapeutic effect. The most promising application does, however, remain the use of clostridial chimeras in chronic pain.

Multiple chimeras have now been tested across multiple pain models to successfully produce analgesia (Ferrari et al., 2013; Maiarù et al., 2016; Mangione et al., 2016). These chimeras have the capability to selectively target and provide long-term silencing of pain signalling pathways. With the aid of future experiments to further validate the safety profile of clostridial chimeras, they offer a potential solution to the inadequacy of current pharmacological intervention for chronic pain and could provide the first therapeutic designed specifically for use in chronic pain conditions.

References

Abraira, V. E. and Ginty, D. D. (2013) ‘The sensory neurons of touch.’ *Neuron*, 79(4) pp. 618–39.

Al-Khater, K. M. and Todd, A. J. (2009) ‘Collateral projections of neurons in laminae I, III, and IV of rat spinal cord to thalamus, periaqueductal gray matter, and lateral parabrachial area.’ *The Journal of comparative neurology*, 515(6) pp. 629–46.

Almeida, T. F., Roizenblatt, S. and Tufik, S. (2004) ‘Afferent pain pathways: A neuroanatomical review.’ *Brain Research*, 1000(1–2) pp. 40–56.

Amaya, F., Izumi, Y., Matsuda, M. and Sasaki, M. (2013) ‘Tissue injury and related mediators of pain exacerbation.’ *Current neuropharmacology*, 11(6) pp. 592–7.

Andersen, K. G. and Kehlet, H. (2011) ‘Persistent Pain After Breast Cancer Treatment: A Critical Review of Risk Factors and Strategies for Prevention.’ *The Journal of Pain*, 12(7) pp. 725–746.

Ängeby Möller, K., Johansson, B. and Berge, O.-G. (1998) ‘Assessing mechanical allodynia in the rat paw with a new electronic algometer.’ *Journal of Neuroscience Methods*, 84(1–2) pp. 41–47.

Angelucci, A., Clascá, F. and Sur, M. (1996) ‘Anterograde axonal tracing with the subunit B of cholera toxin: a highly sensitive immunohistochemical protocol for revealing fine axonal morphology in adult and neonatal brains.’ *Journal of Neuroscience Methods*, 65(1) pp. 101–112.

Antonucci, F., Rossi, C., Gianfranceschi, L., Rossetto, O. and Caleo, M. (2008) ‘Long-Distance Retrograde Effects of Botulinum Neurotoxin A.’ *The Journal of Neuroscience*, 28(14) pp. 3689–3696.

Aoki, K. R. (2005) ‘Review of a proposed mechanism for the antinociceptive action of botulinum toxin type A.’ *NeuroToxicology*, 26(5) pp. 785–793.

Aoki, K. R. and Guyer, B. (2001) ‘Botulinum toxin type A and other botulinum toxin serotypes: a comparative review of biochemical and pharmacological actions.’ *European Journal of Neurology*, 8 pp. 21–29.

Appel, N. M. and Elde, R. P. (1988) ‘The intermediolateral cell column of the thoracic spinal cord is comprised of target-specific subnuclei: evidence from retrograde transport studies and immunohistochemistry.’ *The Journal of neuroscience : the official journal of the Society for Neuroscience*, 8(5) pp. 1767–1775.

Arsenault, J., Ferrari, E., Niranjan, D., Cuijpers, S. A. G., Gu, C., Vallis, Y., O'Brien, J. and Davletov, B. (2013) 'Stapling of the botulinum type A protease to growth factors and neuropeptides allows selective targeting of neuroendocrine cells.' *Journal of Neurochemistry*, 126(2) pp. 223–233.

Ashton, F. A., Levison, S. W. and Mccarthy, K. D. (1990) 'Anti-ganglioside antibodies reveal subsets of cultured rat dorsal root ganglion neurons.' *Brain Research*, 529 pp. 349–353.

Attal, N., de Andrade, D. C., Adam, F., Ranoux, D., Teixeira, M. J., Galhardoni, R., Raicher, I., Üçeyler, N., Sommer, C. and Bouhassira, D. (2016) 'Safety and efficacy of repeated injections of botulinum toxin A in peripheral neuropathic pain (BOTNEP): A randomised, double-blind, placebo-controlled trial.' *The Lancet Neurology*, 15(6) pp. 555–565.

Averbeck, B., Izydorczyk, I. and Kress, M. (2000) 'Inflammatory mediators release calcitonin gene-related peptide from dorsal root ganglion neurons of the rat.' *Neuroscience*, 98(1) pp. 135–40.

Azurin, J. C. and Alvero, M. (1974) 'Field evaluation of environmental sanitation measures against cholera.' *Bulletin of the World Health Organization*, 51(1) pp. 19–26.

Baba, H., Doubell, T. P. and Woolf, C. J. (1999) 'Peripheral inflammation facilitates Abeta fiber-mediated synaptic input to the substantia gelatinosa of the adult rat spinal cord.' *The Journal of neuroscience : the official journal of the Society for Neuroscience*, 19(2) pp. 859–67.

Baba, H., Ji, R.-R., Kohno, T., Moore, K. A., Ataka, T., Wakai, A., Okamoto, M. and Woolf, C. J. (2003) 'Removal of GABAergic inhibition facilitates polysynaptic A fiber-mediated excitatory transmission to the superficial spinal dorsal horn.' *Molecular and Cellular Neuroscience*, 24(3) pp. 818–830.

Bach-Rojecky, L. and Lacković, Z. (2005) 'Antinociceptive effect of botulinum toxin type a in rat model of carrageenan and capsaicin induced pain.' *Croatian medical journal*, 46 pp. 201–208.

Bach-Rojecky, L. and Lacković, Z. (2009) 'Central origin of the antinociceptive action of botulinum toxin type A.' *Pharmacology Biochemistry and Behavior*, 94(2) pp. 234–238.

Bach-Rojecky, L., Šalković-Petrišić, M. and Lacković, Z. (2010) 'Botulinum toxin type A reduces pain supersensitivity in experimental diabetic neuropathy: Bilateral effect after unilateral injection.' *European Journal of Pharmacology*, 633 pp. 10–14.

Backonja, M.-M. (2003) 'Defining Neuropathic Pain.' *Anesthesia & Analgesia* pp. 785–

790.

Bae, J. Y., Kim, J. H., Cho, Y. S., Mah, W. and Bae, Y. C. (2015) 'Quantitative analysis of afferents expressing substance P, calcitonin gene-related peptide, isolectin B4, neurofilament 200, and Peripherin in the sensory root of the rat trigeminal ganglion.' *Journal of Comparative Neurology*, 523(1) pp. 126–138.

Bajjalieh, S. M., Frantz, G. D., Weimann, J. M., McConnell, S. K. and Scheller, R. H. (1994) 'Differential expression of synaptic vesicle protein 2 (SV2) isoforms.' *The Journal of neuroscience : the official journal of the Society for Neuroscience*, 14(9) pp. 5223–35.

Baker, M. D. and Bostock, H. (1997) 'Low-threshold, persistent sodium current in rat large dorsal root ganglion neurons in culture.' *Journal of neurophysiology*, 77(3) pp. 1503–13.

Banik, R. K., Woo, Y. C., Park, S. S. and Brennan, T. J. (2006) 'Strain and sex influence on pain sensitivity after plantar incision in the mouse.' *Anesthesiology*, 105(6) pp. 1246–1253.

Basbaum, A. I., Bautista, D. M., Scherrer, G. and Julius, D. (2009) 'Cellular and Molecular Mechanisms of Pain.' *Cell*, 139(2) pp. 267–284.

Becker, J. B., Prendergast, B. J. and Liang, J. W. (2016) 'Female rats are not more variable than male rats: A meta-analysis of neuroscience studies.' *Biology of Sex Differences*, 7(1) pp. 1–7.

Beddoe, T., Paton, A. W., Nours, J. Le, Rossjohn, J. and James, C. (2010) 'Structure, biological functions and applications of the AB5 toxins,' 35(7) pp. 411–418.

Benemei, S., Nicoletti, P., Capone, J. G. and Geppetti, P. (2009) 'CGRP receptors in the control of pain and inflammation.' *Current Opinion in Pharmacology*, 9(1) pp. 9–14.

Betley, J. N., Wright, C. V. E., Kawaguchi, Y., Erdélyi, F., Szabó, G., Jessell, T. M. and Kaltschmidt, J. A. (2009) 'Stringent Specificity in the Construction of a GABAergic Presynaptic Inhibitory Circuit.' *Cell*, 139(1) pp. 161–174.

Bhave, G. and Gereau IV, R. W. (2004) 'Posttranslational mechanisms of peripheral sensitization.' *Journal of Neurobiology*, 61(1) pp. 88–106.

Blyth, F. M., March, L. M., Brnabic, A. J., Jorm, L. R., Williamson, M. and Cousins, M. J. (2001) 'Chronic pain in Australia: a prevalence study.' *Pain*, 89(2–3) pp. 127–34.

Boehm, J., Kang, M.-G., Johnson, R. C., Esteban, J., Huganir, R. L. and Malinow, R. (2006) 'Synaptic Incorporation of AMPA Receptors during LTP Is Controlled by a PKC Phosphorylation Site on GluR1.' *Neuron*, 51(2) pp. 213–225.

Breivik, H., Collett, B., Ventafridda, V., Cohen, R. and Gallacher, D. (2006) ‘Survey of chronic pain in Europe: Prevalence, impact on daily life, and treatmentBreivik, H., Collett, B., Ventafridda, V., Cohen, R. and Gallacher, D. (2006) “Survey of chronic pain in Europe: Prevalence, impact on daily life, and treatment.” European Jo.’ *European Journal of Pain*, 10(4) pp. 287–333.

Brennan, T. J., Vandermeulen, E. P. and Gebhart, G. F. (1996) ‘Characterization of a rat model of incisional pain.’ *Pain*, 64(3) pp. 493–501.

Brin, M. F., Fahn, S., Moskowitz, C., Friedman, A., Shale, H. M., Greene, P. E., Blitzer, A., List, T., Lange, D., Lovelace, R. E. and McMahon, D. (1987) ‘Localized injections of botulinum toxin for the treatment of focal dystonia and hemifacial spasm.’ *Movement Disorders*, 2(4) pp. 237–254.

Broide, R. S., Rubino, J., Nicholson, G. S., Ardila, M. C., Brown, M. S., Aoki, K. R. and Francis, J. (2013) ‘The rat Digit Abduction Score (DAS) assay: A physiological model for assessing botulinum neurotoxin-induced skeletal muscle paralysis.’ *Toxicon*, 71 pp. 18–24.

Brower, M., Grace, M., Kotz, C. M. and Koya, V. (2015) ‘Comparative analysis of growth characteristics of Sprague Dawley rats obtained from different sources.’ *Laboratory animal research*, 31(4) pp. 166–73.

Cai, B. B., Francis, J., Brin, M. F. and Broide, R. S. (2017) ‘Botulinum neurotoxin type A-cleaved SNAP25 is confined to primary motor neurons and localized on the plasma membrane following intramuscular toxin injection.’ *Neuroscience*. Pergamon, 352, June, pp. 155–169.

Caleo, M. and Schiavo, G. (2009) ‘Central effects of tetanus and botulinum neurotoxins.’ *Toxicon*, 54(5) pp. 593–599.

Caterina, M. J. and Julius, D. (1999) ‘Sense and specificity: a molecular identity for nociceptors.’ *Current Opinion in Neurobiology*, 9(5) pp. 525–530.

Cazalets, J.-R., Borde, M. and Claraci, F. (1995) ‘Localization and Organization of the Central Pattern Generator for Hindlimb Locomotion in Newborn Rat.’ *The Journal of Neuroscience*, 75(7) pp. 4943–4951.

Cervero, F., Laird, J. M. A. and García-Nicas, E. (2003) ‘Secondary hyperalgesia and presynaptic inhibition: An update.’ *European Journal of Pain*, 7(4) pp. 345–351.

Cheung, N. K., Lazarus, H., Miraldi, F. D., Abramowsky, C. R., Kallick, S., Saarinen, U. M., Spitzer, T., Strandjord, S. E., Coccia, P. F. and Berger, N. A. (1987) ‘Ganglioside GD2 specific monoclonal antibody 3F8: a phase I study in patients with neuroblastoma

and malignant melanoma.' *Journal of Clinical Oncology*, 5(9) pp. 1430–1440.

Chian, R.-J., Li, J., Ay, I., Celia, S. A., Kashi, B. B., Tamrazian, E., Matthews, J. C., Bronson, R. T., Rossomando, A., Pepinsky, R. B., Fishman, P. S., Brown, R. H. and Francis, J. W. (2009) 'IGF-1:Tetanus toxin fragment C fusion protein improves delivery of IGF-1 to spinal cord but fails to prolong survival of ALS mice.' *Brain Research*, 1287 pp. 1–19.

Choi, E., Cho, C. W., Kim, H. Y., Lee, P. B. and Nahm, F. S. (2015) 'Lumbar sympathetic block with botulinum toxin type b for complex regional pain syndrome: A case study.' *Pain Physician*, 18(5) pp. E911–E916.

Christie, R. J., Fleming, R., Bezabeh, B., Woods, R., Mao, S., Harper, J., Joseph, A., Wang, Q., Xu, Z.-Q., Wu, H., Gao, C. and Dimasi, N. (2015) 'Stabilization of cysteine-linked antibody drug conjugates with N-aryl maleimides.' *Journal of Controlled Release*, 220 pp. 660–670.

Chuang, Y. C., Yoshimura, N., Huang, C. C., Chiang, P. H. and Chancellor, M. B. (2004) 'Intravesical botulinum toxin a administration produces analgesia against acetic acid induced bladder pain responses in rats.' *Journal of Urology*, 172(4 I) pp. 1529–1532.

Ciaramitaro, P., Mondelli, M., Logullo, F., Grimaldi, S., Battiston, B., Sard, A., Scarinzi, C., Migliaretti, G., Faccani, G. and Cocito, D. (2010) 'Traumatic peripheral nerve injuries: epidemiological findings, neuropathic pain and quality of life in 158 patients.' *Journal of the Peripheral Nervous System*, 15(2) pp. 120–127.

Ciriza, J., Moreno-Igoa, M., Calvo, A. C., Yague, G., Palacio, J., Miana-Mena, F. J., Muñoz, M. J., Zaragoza, P., Brûlet, P. and Osta, R. (2008) 'A genetic fusion GDNF-C fragment of tetanus toxin prolongs survival in a symptomatic mouse ALS model.' *Restorative neurology and neuroscience*, 26(6) pp. 459–65.

Clemens, S., Sawchuk, M. A. and Hochman, S. (2005) 'Reversal of the circadian expression of tyrosine-hydroxylase but not nitric oxide synthase levels in the spinal cord of dopamine D3 receptor knockout mice.' *Neuroscience*, 133(2) pp. 353–357.

Conte, W. L., Kamishina, H. and Reep, R. L. (2009) 'Multiple neuroanatomical tract-tracing using fluorescent Alexa Fluor conjugates of cholera toxin subunit B in rats.' *Nature Protocols*, 4(8) pp. 1157–1166.

Cook, B. Y. A. J. and Woolf, C. J. (1985) 'Cutaneous receptive field and morphological properties of hamstring flexor alpha-motoneurones in the rat.' *Journal of Physiology*, 364 pp. 249–263.

Cook, S. P. and McCleskey, E. W. (2002) 'Cell damage excites nociceptors through

release of cytosolic ATP.' *Pain*, 95(1–2) pp. 41–7.

Corzo, J. (2006) 'Time, the forgotten dimension of ligand binding teaching.' *Biochemistry and Molecular Biology Education*, 34(6) pp. 413–416.

Cui, M., Khanijou, S., Rubino, J. and Aoki, K. R. (2004) 'Subcutaneous administration of botulinum toxin a reduces formalin-induced pain.' *Pain*, 107(1–2) pp. 125–133.

Darios, F., Niranjan, D., Ferrari, E., Zhang, F., Soloviev, M., Rummel, A., Bigalke, H., Suckling, J., Ushkaryov, Y., Naumenko, N., Shakirzyanova, A., Giniatullin, R., Maywood, E., Hastings, M., Binz, T. and Davletov, B. (2010) 'SNARE tagging allows stepwise assembly of a multimodular medicinal toxin.' *Proceedings of the National Academy of Sciences of the United States of America*, 107(42) pp. 18197–18201.

Davies, M., Brophy, S., Williams, R. and Taylor, A. (2006) 'The prevalence, severity, and impact of painful diabetic peripheral neuropathy in type 2 diabetes.' *Diabetes Care*, 29(7) pp. 1518–1522.

Davis, K. D., Meyer, R. A. and Campbell, J. N. (1993) 'Chemosensitivity and sensitization of nociceptive afferents that innervate the hairy skin of monkey.' *Journal of neurophysiology*, 69(4) pp. 1071–81.

Davletov, B., Bajohrs, M. and Binz, T. (2005) 'Beyond BOTOX: advantages and limitations of individual botulinum neurotoxins.' *Trends in Neurosciences*, 28(8) pp. 446–452.

Derkach, V., Barria, A. and Soderling, T. R. (1999) 'Ca2+/calmodulin-kinase II enhances channel conductance of alpha-amino-3-hydroxy-5-methyl-4-isoxazolepropionate type glutamate receptors.' *Proceedings of the National Academy of Sciences of the United States of America*, 96(6) pp. 3269–74.

Deuis, J. R., Dvorakova, L. S. and Vetter, I. (2017) 'Methods Used to Evaluate Pain Behaviors in Rodents.' *Frontiers in Molecular Neuroscience*, 10(September) pp. 1–17.

Dickenson, A. H. (1995) 'Spinal cord pharmacology of pain.' *British Journal of Anaesthesia*, 75(2) pp. 193–200.

Dobrenis, K., Joseph, A. and Rattazzi, M. C. (1992) 'Neuronal lysosomal enzyme replacement using fragment C of tetanus toxin.' *Proc Natl Acad Sci U S A*, 89(6) pp. 2297–2301.

Dodick, D. W., Turkel, C. C., Degryse, R. E., Aurora, S. K., Silberstein, S. D., Lipton, R. B., Diener, H., Silberstein, S. D. and Einstein, A. (2010) 'OnabotulinumtoxinA for Treatment of Chronic Migraine : Pooled Results From the Double-Blind , Randomized , Placebo-Controlled Phases of the PREEMPT Clinical Program.'

Dolly, J. O. and O'Connell, M. A. (2012) 'Neurotherapeutics to inhibit exocytosis from sensory neurons for the control of chronic pain.' *Current Opinion in Pharmacology*, 12(1) pp. 100–108.

Dong, M., Liu, H., Tepp, W. H., Johnson, E. A., Janz, R. and Chapman, E. R. (2008) 'Glycosylated SV2A and SV2B mediate the entry of botulinum neurotoxin E into neurons.' *Molecular biology of the cell*, 19(12) pp. 5226–37.

Dong, M., Yeh, F., Tepp, W. H., Dean, C., Johnson, E. A., Janz, R. and Chapman, E. R. (2006) 'SV2 Is the Protein Receptor for Botulinum Neurotoxin A.' *Science*, 312(5773) pp. 592–596.

Dressler, D., Mander, G. and Fink, K. (2012) 'Measuring the potency labelling of onabotulinumtoxinA (Botox®) and incobotulinumtoxinA (Xeomin®) in an LD50 assay.' *Journal of Neural Transmission*, 119(1) pp. 13–15.

Drew, G. M., Siddall, P. J. and Duggan, A. W. (2004) 'Mechanical allodynia following contusion injury of the rat spinal cord is associated with loss of GABAergic inhibition in the dorsal horn.' *Pain*, 109(3) pp. 379–388.

Drinovac, V., Bach-Rojecky, L. and Lacković, Z. (2014) 'Association of antinociceptive action of botulinum toxin type A with GABA-A receptor.' *Journal of Neural Transmission*, 121(6) pp. 665–669.

Drinovac, V., Bach-Rojecky, L. and Lacković, Z. (2016) 'Antinociceptive action of botulinum toxin type A in carrageenan-induced mirror pain.' *Journal of Neural Transmission*, 123(12) pp. 1403–1413.

Drinovac, V., Bach-Rojecky, L., Matak, I. and Lacković, Z. (2013) 'Involvement of μ-opioid receptors in antinociceptive action of botulinum toxin type A.' *Neuropharmacology*, 70 pp. 331–337.

Dubin, A. E. and Patapoutian, A. (2010) 'Nociceptors: the sensors of the pain pathway.' *The Journal of clinical investigation*, 120(11) pp. 3760–72.

Duggan, M. J., Quinn, C. P., Chaddock, J. A., Purkiss, J. R., Alexander, F. C. G., Doward, S., Fooks, S. J., Friis, L. M., Hall, Y. H. J., Kirby, E. R., Leeds, N., Moulsdale, H. J., Dickenson, A., Mark Green, G., Rahman, W., Suzuki, R., Shone, C. C. and Foster, K. A. (2002) 'Inhibition of release of neurotransmitters from rat dorsal root ganglia by a novel conjugate of a Clostridium botulinum toxin A endopeptidase fragment and Erythrina cristagalli lectin.' *Journal of Biological Chemistry*, 277(38) pp. 34846–34852.

Durham, P. L., Cady, R., Cady, R. and Blumenfeld, A. J. (2004) 'Regulation of Calcitonin Gene-Related Peptide Secretion from Trigeminal Nerve Cells by Botulinum Toxin Type

A: Implications for Migraine Therapy.' *Headache*, 44(1) pp. 35–43.

Dworkin, R. H., O'Connor, A. B., Backonja, M., Farrar, J. T., Finnerup, N. B., Jensen, T. S., Kalso, E. A., Loeser, J. D., Miaskowski, C., Nurmikko, T. J., Portenoy, R. K., Rice, A. S. C., Stacey, B. R., Treede, R.-D., Turk, D. C. and Wallace, M. S. (2007) 'Pharmacologic management of neuropathic pain: Evidence-based recommendations.' *Pain*, 132(3) pp. 237–251.

Eleopra, R., Tugnoli, V., Rossetto, O., De Grandis, D. and Montecucco, C. (1998) 'Different time courses of recovery after poisoning with botulinum neurotoxin serotypes A and E in humans.' *Neuroscience letters*, 256(3) pp. 135–8.

England, S., Bevan, S. and Docherty, R. J. (1996) 'PGE2 modulates the tetrodotoxin-resistant sodium current in neonatal rat dorsal root ganglion neurones via the cyclic AMP-protein kinase A cascade.' *The Journal of physiology*, 495(2) pp. 429–440.

Fallon, M. T. (2013) 'Neuropathic pain in cancer.' *British Journal of Anaesthesia*, 111(1) pp. 105–111.

Favre-Guilmard, C., Auguet, M. and Chabrier, P. E. (2009) 'Different antinociceptive effects of botulinum toxin type A in inflammatory and peripheral polyneuropathic rat models.' *European Journal of Pharmacology*, 617(1–3) pp. 48–53.

Fehrenbacher, J. C., Vasko, M. R. and Duarte, D. B. (2012) 'Models of inflammation: Carrageenan- or complete Freund's Adjuvant (CFA)-induced edema and hypersensitivity in the rat.' *Current protocols in pharmacology*, Chapter 5 p. Unit5.4.

De Felice, M., Sanoja, R., Wang, R., Vera-Portocarrero, L., Oyarzo, J., King, T., Ossipov, M. H., Vanderah, T. W., Lai, J., Dussor, G. O., Fields, H. L., Price, T. J. and Porreca, F. (2011) 'Engagement of descending inhibition from the rostral ventromedial medulla protects against chronic neuropathic pain.' *Pain*, 152(12) pp. 2701–9.

Ferrari, E., Gu, C., Niranjan, D., Restani, L., Rasetti-Escargueil, C., Obara, I., Geranton, S. M., Arsenault, J., Goetze, T. A., Harper, C. B., Nguyen, T. H., Maywood, E., O'Brien, J., Schiavo, G., Wheeler, D. W., Meunier, F. A., Hastings, M., Edwardson, J. M., Sesardic, D., Caleo, M., Hunt, S. P. and Davletov, B. (2013) 'Synthetic self-assembling clostridial chimera for modulation of sensory functions.' *Bioconjugate Chemistry*, 24(10) pp. 1750–1759.

Ferrari, E., Maywood, E. S., Restani, L., Caleo, M., Pirazzini, M., Rossetto, O., Hastings, M. H., Niranjan, D., Schiavo, G. and Davletov, B. (2011) 'Re-assembled botulinum neurotoxin inhibits CNS functions without systemic toxicity.' *Toxins*, 3(4) pp. 345–355.

Ferrari, E., Soloviev, M., Niranjan, D., Arsenault, J., Gu, C., Vallis, Y., O'Brien, J. and

Davletov, B. (2012) ‘Assembly of protein building blocks using a short synthetic peptide.’ *Bioconjugate Chemistry*, 23(3) pp. 479–484.

Ferri, G.-L., Sabani, A., Abelli, L., Polak, J. M., Dahl, D. and Portier, M.-M. (1990) ‘Neuronal intermediate filaments in rat dorsal root ganglia: differential distribution of peripherin and neurofilament protein immunoreactivity and effect of capsaicin.’ *Brain Research*, 515(1–2) pp. 331–335.

Figueiredo, D. M., Hallewell, R. A., Chen, L. L., Fairweather, N. F., Dougan, G., Savitt, J. M., Parks, D. A. and Fishman, P. S. (1997) ‘Delivery of Recombinant Tetanus–Superoxide Dismutase Proteins to Central Nervous System Neurons by Retrograde Axonal Transport.’ *Experimental Neurology*, 145(2) pp. 546–554.

Filipović, B., Matak, I., Bach-Rojecky, L. and Lackovi, Z. (2012) ‘Central Action of Peripherally Applied Botulinum Toxin Type A on Pain and Dural Protein Extravasation in Rat Model of Trigeminal Neuropathy.’ *PLoS ONE*, 7(1) p. e29803.

Fillingim, R. B., King, C. D., Ribeiro-Dasilva, M. C., Rahim-Williams, B. and Riley, J. L. (2009) ‘Sex, Gender, and Pain: A Review of Recent Clinical and Experimental Findings.’ *Journal of Pain*, 10(5) pp. 447–485.

Finnerup, N. B., Attal, N., Haroutounian, S., McNicol, E., Baron, R., Dworkin, R. H., Gilron, I., Haanpää, M., Hansson, P., Jensen, T. S., Kamerman, P. R., Lund, K., Moore, A., Raja, S. N., Rice, A. S. C., Rowbotham, M., Sena, E., Siddall, P., Smith, B. H. and Wallace, M. (2015) ‘Pharmacotherapy for neuropathic pain in adults: A systematic review and meta-analysis.’ *The Lancet Neurology*, 14(2) pp. 162–173.

Fischer, A. and Montal, M. (2007) ‘Crucial Role of the Disulfide Bridge between Botulinum Neurotoxin Light and Heavy Chains in Protease Translocation across Membranes *.’ *The Journal of biological chemistry*, 282(40) pp. 29604–29611.

Fischer, A., Mushrush, D. J., Lacy, D. B. and Montal, M. (2008) ‘Botulinum neurotoxin devoid of receptor binding domain translocates active protease.’ *PLoS Pathogens*, 4(12).

Flatters, S. J. L. and Bennett, G. J. (2004) ‘Ethosuximide reverses paclitaxel- and vincristine-induced painful peripheral neuropathy.’ *Pain*, 109(1–2) pp. 150–161.

Fontaine, S. D., Reid, R., Robinson, L., Ashley, G. W. and Santi, D. V. (2015) ‘Long-term stabilization of maleimide-thiol conjugates.’ *Bioconjugate Chemistry*, 26(1) pp. 145–152.

Foran, P. G., Mohammed, N., Lisk, G. O., Nagwaney, S., Lawrence, G. W., Johnson, E., Smith, L., Aoki, K. R. and Dolly, J. O. (2003) ‘Evaluation of the Therapeutic Usefulness of Botulinum Neurotoxin B, C1, E, and F Compared with the Long Lasting Type A.’ *Journal of Biological Chemistry*, 278(2) pp. 1363–1371.

Fornaro, M., Lee, J. M., Raimondo, S., Nicolino, S., Geuna, S. and Giacobini-Robecchi, M. (2008) 'Neuronal intermediate filament expression in rat dorsal root ganglia sensory neurons: An in vivo and in vitro study.' *Neuroscience*, 153(4) pp. 1153–1163.

Francis, J. W., Figueiredo, D., VanderSpek, J. C., Ayala, L. M., Kim, Y. S., Remington, M. P., Young, P. J., Lorson, C. L., Ikebe, S., Fishman, P. S. and Brown, R. H. (2004) 'A survival motor neuron:tetanus toxin fragment C fusion protein for the targeted delivery of SMN protein to neurons.' *Brain Research*, 995(1) pp. 84–96.

Freund, B. and Schwartz, M. (2003) 'Temporal relationship of muscle weakness and pain reduction in subjects treated with botulinum toxin A.' *The Journal of Pain*, 4(3) pp. 159–165.

Frevert, J. (2010) 'Content of botulinum neurotoxin in Botox®/Vistabel®, Dysport®/Azzalure®, and Xeomin®/Bocouture®.' *Drugs in R&D*, 10(2) pp. 67–73.

Friebel, U., Eickhoff, S. B. and Lotze, M. (2011) 'Coordinate-based meta-analysis of experimentally induced and chronic persistent neuropathic pain.' *NeuroImage*, 58(4) pp. 1070–1080.

Gold, M. S. and Gebhart, G. F. (2010) 'Nociceptor sensitization in pain pathogenesis.' *Nature medicine*, 16(11) pp. 1248–57.

Gold, M. S., Levine, J. D. and Correa, A. M. (1998) 'Modulation of TTX-R INa by PKC and PKA and their role in PGE2-induced sensitization of rat sensory neurons in vitro.' *The Journal of neuroscience : the official journal of the Society for Neuroscience*, 18(24) pp. 10345–55.

Goldstein, M. E., House, S. B. and Gainer, H. (1991) 'NF-L and peripherin immunoreactivities define distinct classes of rat sensory ganglion cells.' *Journal of Neuroscience Research*, 30(1) pp. 92–104.

Goodman, B. S., Posecion, L. W. F., Mallempati, S. and Bayazitoglu, M. (2008) 'Complications and pitfalls of lumbar interlaminar and transforaminal epidural injections.' *Ethics in Science and Environmental Politics* pp. 1–11.

Gottrup, H., Andersen, J., Arendt-Nielsen, L. and Jensen, T. S. (2000) 'Psychophysical examination in patients with post-mastectomy pain.' *Pain* pp. 275–284.

Greenspan, J. D., Craft, R. M., LeResche, L., Arendt-Nielsen, L., Berkley, K. J., Fillingim, R. B., Gold, M. S., Holdcroft, A., Lautenbacher, S., Mayer, E. A., Mogil, J. S., Murphy, A. Z. and Traub, R. J. (2007) 'Studying sex and gender differences in pain and analgesia: A consensus report.' *Pain*, 132(SUPPL. 1) pp. 26–45.

Gupta, A., Kaur, K., Sharma, S., Goyal, S., Arora, S. and Murthy, R. S. R. (2010) 'Clinical

aspects of acute post-operative pain management & its assessment.' *Journal of advanced pharmaceutical technology & research*, 1(2) pp. 97–108.

Hall, D. H. and Treinin, M. (2011) 'How does morphology relate to function in sensory arbors?' *Trends in neurosciences*, 34(9) pp. 443–51.

Handgretinger, R., Anderson, K., Lang, P., Dopfer, R., Klingebiel, T., Schrappe, M., Reuland, P., Gillies, S. D., Reisfeld, R. A. and Niethammer, D. (1995) 'A phase I study of human/mouse chimeric antiganglioside GD2 antibody ch14.18 in patients with neuroblastoma.' *European Journal of Cancer*, 31(2) pp. 261–267.

Handgretinger, R., Baader, P., Dopfer, R., Klingebiel, T., Reuland, P., Treuner, J., Reisfeld, R. A. and Niethammer, D. (1992) 'A phase I study of neuroblastoma with the anti-ganglioside GD2 antibody 14.G2a.' *Cancer Immunology Immunotherapy*, 35(3) pp. 199–204.

Hargreaves, K., Hargreaves, K., Dubner, R., Dubner, R., Brown, F., Brown, F., Flores, C., Flores, C., Joris, J. and Joris, J. (1988) 'A new and sensitive method for measuring thermal nociception in cutaneous hyperalgesia.' *Pain*, 32(1) p. 11.

Harper, B. Y. A. A. and Lawson, S. N. (1985) 'Electrical properties of rat dorsal root ganglion neurones with different peripheral nerve conduction velocities.' *Journal of Physiology*, 359 pp. 47–63.

Hart, R. (2017) *Developing protein conjugation techniques to enhance cell delivery of therapeutic enzymes*. University of Sheffield.

Harvey, R. J., Depner, U. B., Wässle, H., Ahmadi, S., Heindl, C., Reinold, H., Smart, T. G., Harvey, K., Schütz, B., Abo-Salem, O. M., Zimmer, A., Poisbeau, P., Welzl, H., Wolfer, D. P., Betz, H., Zeilhofer, H. U. and Müller, U. (2004) 'GlyR alpha3: an essential target for spinal PGE2-mediated inflammatory pain sensitization.' *Science*, 304(5672) pp. 884–7.

Hatai, S. (1902) 'Number and size of the spinal ganglion cells and dorsal root fibers in the white rat at different ages.' *Journal of Comparative Neurology*, 12(2) pp. 107–124.

Hayashi, T., McMahon, H., Yamasaki, S., Binz, T., Hata, Y., Südhof, T. C. and Niemann, H. (1994) 'Synaptic vesicle membrane fusion complex: action of clostridial neurotoxins on assembly.' *The EMBO journal*, 13(21) pp. 5051–61.

van Hecke, O., Austin, S. K., Khan, R. A., Smith, B. H. and Torrance, N. (2014) 'Neuropathic pain in the general population: A systematic review of epidemiological studies.' *Pain*, 155(4) pp. 654–662.

Heckmann, M., Ceballos-Baumann, A. O., Plewig, G. and Hyperhidrosis Study Group

(2001) ‘Botulinum Toxin A for Axillary Hyperhidrosis (Excessive Sweating).’ *New England Journal of Medicine*, 344(7) pp. 488–493.

von Hehn, C. A., Baron, R. and Woolf, C. J. (2012) ‘Deconstructing the neuropathic pain phenotype to reveal neural mechanisms.’ *Neuron*, 73(4) pp. 638–52.

Helgason, S., Petursson, G., Gudmundsson, S. and Sigurdsson, J. A. (2000) ‘Prevalence of postherpetic neuralgia after a single episode of herpes zoster: prospective study with long term follow up.’ *BMJ*, 321 pp. 1–4.

Hepp, R., Perraut, M., Chasserot-Golaz, S., Galli, T., Aunis, D., Langley, K. and Grant, N. J. (1999) ‘Cultured glial cells express the SNAP-25 analogue SNAP-23.’ *Glia*, 27(2) pp. 181–7.

Hirayama, A., Saitoh, Y., Kishima, H., Shimokawa, T., Oshino, S., Hirata, M., Kato, A. and Yoshimine, T. (2006) ‘Reduction of intractable deafferentation pain by navigation-guided repetitive transcranial magnetic stimulation of the primary motor cortex.’ *Pain*, 122(1) pp. 22–27.

Hoot, M. R., Sim-Selley, L. J., Selley, D. E., Scoggins, K. L. and Dewey, W. L. (2011) ‘Chronic neuropathic pain in mice reduces μ-opioid receptor-mediated G-protein activity in the thalamus.’ *Brain research*, 1406 pp. 1–7.

Hösl, K., Reinold, H., Harvey, R. J., Müller, U., Narumiya, S. and Zeilhofer, H. U. (2006) ‘Spinal prostaglandin E receptors of the EP2 subtype and the glycine receptor α3 subunit, which mediate central inflammatory hyperalgesia, do not contribute to pain after peripheral nerve injury or formalin injection.’ *Pain*, 126(1–3) pp. 46–53.

Huang, J., Zhang, X. and McNaughton, P. A. (2006) ‘Modulation of temperature-sensitive TRP channels.’ *Seminars in Cell & Developmental Biology*, 17(6) pp. 638–645.

Hurley, R. W. and Adams, M. C. B. (2009) ‘Sex, Gender, and Pain: An Overview of a Comple.’ *Anesthesia & Analgesia*, 107(1) pp. 309–317.

Hwang, B. Y., Kim, E. S., Kim, C. H., Kwon, J. Y. and Kim, H. K. (2012) ‘Gender differences in paclitaxel-induced neuropathic pain behavior and analgesic response in rats.’ *Korean Journal of Anesthesiology*, 62(1) pp. 66–72.

Iadarola, M. J., Brady, L. S., Draisci, G. and Dubner, R. (1988) ‘Enhancement of dynorphin gene expression in spinal cord following experimental inflammation: stimulus specificity, behavioral parameters and opioid receptor binding.’ *Pain*, 35(3) pp. 313–326.

Ikeda, H., Stark, J., Fischer, H., Wagner, M., Drdla, R., Jäger, T. and Sandkühler, J. (2006) ‘Synaptic Amplifier of Inflammatory Pain in the Spinal Dorsal Horn.’ *Science*, 312(5780) pp. 1659–1662.

Jacoby, S., Sims, R. E. and Hartell, N. A. (2001) ‘Nitric oxide is required for the induction and heterosynaptic spread of long-term potentiation in rat cerebellar slices.’ *The Journal of Physiology*, 535(3) pp. 825–839.

Jaffe, J., Natanson-Yaron, S., Caparon, M. G. and Hanski, E. (1996) ‘Protein F2, a novel fibronectin-binding protein from Streptococcus pyogenes, possesses two binding domains.’ *Molecular microbiology*, 21(2) pp. 373–384.

Jankovic, J., Schwartz, K. and Donovan, D. T. (1990) ‘Botulinum toxin treatment of cranial-cervical dystonia, spasmodic dysphonia, other focal dystonias and hemifacial spasm.’ *Journal of Neurology, Neurosurgery, and Psychiatry*, 53 pp. 633–639.

Jensen, T. S., Baron, R., Haanpää, M., Kalso, E., Loeser, J. D., Rice, A. S. C. and Treede, R.-D. (2011) ‘A new definition of neuropathic pain.’ *Pain*, 152(10) pp. 2204–2205.

Ji, R.-R., Samad, T. A., Jin, S.-X., Schmoll, R. and Woolf, C. J. (2002) ‘p38 MAPK Activation by NGF in Primary Sensory Neurons after Inflammation Increases TRPV1 Levels and Maintains Heat Hyperalgesia.’ *Neuron*, 36 pp. 57–68.

Julius, D. and Basbaum, A. I. (2001) ‘Molecular mechanisms of nociception.’ *Nature*, 413 pp. 203–210.

Kappos, E. A., Sieber, P. K., Engels, P. E., Mariolo, A. V., D’Arpa, S., Schaefer, D. J. and Kalbermatten, D. F. (2017) ‘Validity and reliability of the CatWalk system as a static and dynamic gait analysis tool for the assessment of functional nerve recovery in small animal models.’ *Brain and Behavior*, 7(7) pp. 1–12.

Karl, A., Birbaumer, N., Lutzenberger, W., Cohen, L. G. and Flor, H. (2001) ‘Reorganization of motor and somatosensory cortex in upper extremity amputees with phantom limb pain.’ *The Journal of neuroscience : the official journal of the Society for Neuroscience*, 21(10) pp. 3609–18.

Kaye, A. D., Baluch, A. and Scott, J. T. (2010) ‘Pain Management in the Elderly Population: A Review.’ *The Oschner Journal*, 10(3) pp. 179–187.

Kehlet, H., Jensen, T. S. and Woolf, C. J. (2006) ‘Persistent postsurgical pain: risk factors and prevention.’ *The Lancet*, 367(9522) pp. 1618–1625.

Keller, J. E. and Neale, E. A. (2001) ‘The Role of the Synaptic Protein SNAP-25 in the Potency of Botulinum Neurotoxin Type A.’ *Journal of Biological Chemistry*, 276(16) pp. 13476–13482.

Kilo, S., Harding-Rose, C., Hargreaves, K. M. and Flores, C. M. (1997) ‘Peripheral CGRP release as a marker for neurogenic inflammation: A model system for the study of

neuropeptide secretion in rat paw skin.' *Pain*, 73(2) pp. 201–207.

Kogelman, L. J. A., Christensen, R. E., Pedersen, S. H., Bertalan, M., Hansen, T. F., Jansen-Olesen, I. and Olesen, J. (2017) 'Whole transcriptome expression of trigeminal ganglia compared to dorsal root ganglia in Rattus Norvegicus.' *Neuroscience*, 350 pp. 169–179.

Koriazova, L. K. and Montal, M. (2003) 'Translocation of botulinum neurotoxin light chain protease through the heavy chain channel.' *Nature Structural Biology*, 10(1) pp. 13–18.

Kress, M., Koltzenburg, M., Reeh, P. W. and Handwerker, H. O. (1992) 'Responsiveness and functional attributes of electrically localized terminals of cutaneous C-fibers in vivo and in vitro.' *Journal of Neurophysiology*, 68(2) pp. 581–595.

Kroin, J. S., Buvanendran, A., Nagalla, S. K. S. and Tuman, K. J. (2003) 'Postoperative pain and analgesic responses are similar in male and female Sprague-Dawley rats.' *Canadian Journal of Anesthesia*, 50(9) pp. 904–908.

Kroken, A. R., Karalewitz, A. P.-A. A., Fu, Z., Kim, J.-J. J. P. and Barbieri, J. T. (2011) 'Novel ganglioside-mediated entry of botulinum neurotoxin serotype D into neurons.' *The Journal of biological chemistry*, 286(30) pp. 26828–37.

Kumar, V., Krone, K. and Mathieu, A. (2004) 'Neuraxial and sympathetic blocks in herpes zoster and postherpetic neuralgia: An appraisal of current evidence.' *Regional Anesthesia and Pain Medicine*, 29(5) pp. 454–461.

van Laar, M., Pergolizzi, J. V, Mellinghoff, H.-U., Merchante, I. M., Nalamachu, S., O'Brien, J., Perrot, S., Raffa, R. B. and Raffa, R. B. (2012) 'Pain treatment in arthritis-related pain: beyond NSAIDs.' *The open rheumatology journal*. Bentham Science Publishers, 6 pp. 320–30.

Lacy, D. B. and Stevens, R. C. (1999) 'Sequence homology and structural analysis of the clostridial neurotoxins.' *Journal of Molecular Biology*, 291(5) pp. 1091–1104.

LaMotte, R. H., Shain, C. N., Simone, D. a and Tsai, E. F. (1991) 'Neurogenic hyperalgesia: psychophysical studies of underlying mechanisms.' *Journal of neurophysiology*, 66(1) pp. 190–211.

Lan, J., Skeberdis, V. A., Jover, T., Grooms, S. Y., Lin, Y., Araneda, R. C., Zheng, X., Bennett, M. V. L. and Zukin, R. S. (2001) 'Protein kinase C modulates NMDA receptor trafficking and gating.' *Nature Neuroscience*, 4(4) pp. 382–390.

Larivière, R. C., Nguyen, M. D., Ribeiro-Da-Silva, A. and Julien, J. P. (2002) 'Reduced number of unmyelinated sensory axons in peripherin null mice.' *Journal of Neurochemistry*, 81(3) pp. 525–532.

Latremoliere, A. and Woolf, C. J. (2009) ‘Central Sensitization: A Generator of Pain Hypersensitivity by Central Neural Plasticity.’ *Journal of Pain*, 10(9) pp. 895–926.

Lawrence, G. W., Ovsepian, S. V, Wang, J., Aoki, K. R. and Dolly, J. O. (2012) ‘Extravesicular intraneuronal migration of internalized botulinum neurotoxins without detectable inhibition of distal neurotransmission.’ *Biochem. J*, 441 pp. 443–452.

Lawson, S. N., Crepps, B. and Perl, E. R. (2002) ‘Calcitonin gene-related peptide immunoreactivity and afferent receptive properties of dorsal root ganglion neurones in guinea-pigs.’ *The Journal of physiology*, 540(3) pp. 989–1002.

Lawson, S. N., Harper, A. A., Harper, E. I., Garson, J. A. and Anderton, B. H. (1984) ‘A monoclonal antibody against neurofilament protein specifically labels a subpopulation of rat sensory neurones.’ *The Journal of Comparative Neurology*. Alan R. Liss, Inc., 228(2) pp. 263–272.

Lawson, S. N. and Waddell, P. J. (1991) ‘Soma neurofilament immunoreactivity is related to cell size and fibre conduction velocity in rat primary sensory neurons.’ *The Journal of Physiology*, 435(1) pp. 41–63.

Lefaucheur, J.-P., André-Obadia, N., Antal, A., Ayache, S. S., Baeken, C., Benninger, D. H., Cantello, R. M., Cincotta, M., De Carvalho, M., De Ridder, D., Devanne, H., Di Lazzaro, V., Filipovi, S. R., Hummel, F. C., Jääskeläinen, S. K., Kimiskidis, V. K., Koch, G., Langguth, B., Nyffeler, T., Oliviero, A., Padberg, F., Poulet, E., Rossi, S., Rossini, P. M., Rothwell, J. C., Schönfeldt-Lecuona, C., Siebner, H. R., Slotema, C. W., Stagg, C. J., Valls-Sole, J., Ziemann, U., Paulus, W. and Garcia-Larrea, L. (2014) ‘Evidence-based guidelines on the therapeutic use of repetitive transcranial magnetic stimulation (rTMS).’ *Clinical Neurophysiology*, 125 pp. 2150–2206.

Lefaucheur, J.-P., Drouot, X., Ménard-Lefaucheur, I. and Nguyen, J. . (2004) ‘Neuropathic pain controlled for more than a year by monthly sessions of repetitive transcranial magnetic stimulation of the motor cortex.’ *Neurophysiologie Clinique/Clinical Neurophysiology*, 34(2) pp. 91–95.

Lefaucheur, J.-P., Ménard-Lefaucheur, I., Goujon, C., Keravel, Y. and Nguyen, J.-P. (2011) ‘Predictive value of rTMS in the identification of responders to epidural motor cortex stimulation therapy for pain.’ *The journal of pain : official journal of the American Pain Society*, 12(10) pp. 1102–11.

Lefaucheur, J. P., Drouot, X., Menard-Lefaucheur, I., Keravel, Y. and Nguyen, J. P. (2006) ‘Motor cortex rTMS restores defective intracortical inhibition in chronic neuropathic pain.’ *Neurology*, 67(9) pp. 1568–1574.

Legrain, V., Iannetti, G. D., Plaghki, L. and Mouraux, A. (2011) 'The pain matrix reloaded: A salience detection system for the body.' *Progress in Neurobiology*, 93(1) pp. 111–124.

Leon, A., Benvegnù, D., Toso, R. D., Presti, D., Facci, L., Giorgi, O. and Toffano, G. (1984) 'Dorsal root ganglia and nerve growth factor: A model for understanding the mechanism of GM 1 effects on neuronal repair.' *Journal of Neuroscience Research*, 12(2–3) pp. 277–287.

Lima, M. C. and Fregni, F. (2008) 'Motor cortex stimulation for chronic pain: systematic review and meta-analysis of the literature.' *Neurology*, 70(24) pp. 2329–37.

Lisman, J. E., Raghavachari, S. and Tsien, R. W. (2007) 'The sequence of events that underlie quantal transmission at central glutamatergic synapses.' *Nature Reviews Neuroscience*, 8(8) pp. 597–609.

Logan, D. E. and Rose, J. B. (2004) 'Gender differences in post-operative pain and patient controlled analgesia use among adolescent surgical patients.' *Pain*, 109(3) pp. 481–487.

Love, S. and Coakham, H. B. (2001) 'Trigeminal neuralgia: Pathology and pathogenesis.' *Brain*, 124(12) pp. 2347–2360.

Lu, W.-Y., Man, H.-Y., Ju, W., Trimble, W. S., MacDonald, J. F. and Wang, Y. T. (2001) 'Activation of Synaptic NMDA Receptors Induces Membrane Insertion of New AMPA Receptors and LTP in Cultured Hippocampal Neurons.' *Neuron*, 29(1) pp. 243–254.

Lundy, C. T., Doherty, G. M. and Fairhurst, C. B. (2009) 'Botulinum toxin type A injections can be an effective treatment for pain in children with hip spasms and cerebral palsy.' *Developmental Medicine & Child Neurology*, 51(9) pp. 705–710.

Ma, H., Meng, J., Wang, J., Hearty, S., Dolly, J. O. and O'Kennedy, R. (2014) 'Targeted delivery of a SNARE protease to sensory neurons using a single chain antibody (scFv) against the extracellular domain of P2X 3 inhibits the release of a pain mediator.' *Biochemical Journal*, 462(2) pp. 247–256.

Macrae, W. A. (2008) 'Chronic post-surgical pain: 10 Years on.' *British Journal of Anaesthesia*, 101(1) pp. 77–86.

Magerl, W., Fuchs, P. N., Meyer, R. A. and Treede, R.-D. (2001) 'Roles of capsaicin-insensitive nociceptors in cutaneous pain and secondary hyperalgesia.' *Brain*, 124(9) pp. 1754–1764.

Mahmoudian, J., Hadavi, R., Jeddi-Tehrani, M., Mahmoudi, A. R., Bayat, A. A., Shaban, E., Vafakhah, M., Darzi, M., Tarahomi, M. and Ghods, R. (2011) 'Comparison of the Photobleaching and Photostability Traits of Alexa Fluor 568- and Fluorescein

Isothiocyanate- conjugated Antibody.' *Cell journal*. Royan Institute, 13(3) pp. 169–72.

Maiarù, M., Certo, M., Echeverria Altuna, I., M Geranton, S., S Mangione, A., Tassorelli, C., Ferrari, E., Leese, C., Davletov, B. and Hunt, S. (2016) 'New botulinum conjugates targeting NK1 and opiate receptor expressing neurons for the control of chronic pain.' *In Society for Neuroscience's 46th Annual Meeting*. San Diego.

Malan, T. P., Mata, H. P. and Porreca, F. (2002) 'Spinal GABA(A) and GABA(B) receptor pharmacology in a rat model of neuropathic pain.' *Anesthesiology*, 96(5) pp. 1161–7.

Manfridi, A. and Forloni, G. L. (1992) 'CULTURE OF DORSAL AGED RATS : EFFECTS GANGLION NEURONS FROM OF ACETYL-L-CARNITINE AND NGF,' 10(4) pp. 321–329.

Mangione, A. S., Obara, I., Maiarú, M., Geranton, S. M., Tassorelli, C., Ferrari, E., Leese, C., Davletov, B. and Hunt, S. P. (2016) 'Nonparalytic botulinum molecules for the control of pain.' *Pain*, 157(5) pp. 1045–55.

Mantilla, C. B., Zhan, W.-Z. and Sieck, G. C. (2009) 'Retrograde labeling of phrenic motoneurons by intrapleural injection.' *Journal of neuroscience methods*, 182(2) pp. 244–9.

Maple, P. A. C., Jones, C. S., Wall, E. C., Vyse, A., Edmunds, W. J., Andrews, N. J. and Miller, E. (2000) 'Immunity to diphtheria and tetanus in England and Wales.' *Vaccine*, 19(2–3) pp. 167–173.

Mapplebeck, J. C. S., Beggs, S. and Salter, M. W. (2016) 'Sex differences in pain.' *PAIN*, 157 pp. S2–S6.

Marinelli, S., Vacca, V., Ricordy, R., Uggenti, C., Tata, A. M., Luvisetto, S. and Pavone, F. (2012) 'The Analgesic Effect on Neuropathic Pain of Retrogradely Transported botulinum Neurotoxin A Involves Schwann Cells and Astrocytes.' *PLoS ONE*, 7(10) p. e47977.

Marino, M. J., Terashima, T., Steinauer, J. J., Eddinger, K. A., Yaksh, T. L. and Xu, Q. (2014) 'Botulinum toxin B in the sensory afferent: Transmitter release, spinal activation, and pain behavior.' *Pain*, 155(4) pp. 674–684.

Martyn, C. N. and Hughes, R. A. C. (1997) 'Epidemiology of peripheral neuropathy.' *Neurosurgery, and Psychiatry*, 62 pp. 310–318.

Matak, I., Bach-Rojecky, L., Filipović, B. and Lacković, Z. (2011) 'Behavioral and immunohistochemical evidence for central antinociceptive activity of botulinum toxin A.' *Neuroscience*, 186 pp. 201–207.

Matak, I. and Lacković, Z. (2014) ‘Botulinum toxin A, brain and pain.’ *Progress in Neurobiology*, 119–120 pp. 39–59.

Matak, I., Riederer, P. and Lacković, Z. (2012) ‘Botulinum toxin’s axonal transport from periphery to the spinal cord.’ *Neurochemistry International*, 61(2) pp. 236–239.

Matak, I., Tékus, V., Bölcskei, K., Lacković, Z. and Helyes, Z. (2017) ‘Involvement of substance P in the antinociceptive effect of botulinum toxin type A: Evidence from knockout mice.’ *Neuroscience*, 358 pp. 137–145.

Mavlyutov, T. A., Duellman, T., Kim, H. T., Epstein, M. L., Leese, C., Davletov, B. A. and Yang, J. (2016) ‘Sigma-1 receptor expression in the dorsal root ganglion: Reexamination using a highly specific antibody.’ *Neuroscience*, 331 pp. 148–157.

May, A. (2008) ‘Chronic pain may change the structure of the brain.’ *PAIN*®, 137(1) pp. 7–15.

McCarthy, P. W. and Lawson, S. N. (1990) ‘Cell type and conduction velocity of rat primary sensory neurons with calcitonin gene-related peptide-like immunoreactivity.’ *Neuroscience*, 34(3) pp. 623–632.

McCorry, L. K. (2007) ‘Teachers’ topics: Physiology of the Autonomic Nervous System.’ *American Journal of Pharmaceutical Education*, 71(4)(78) pp. 1–11.

McCutcheon, J. E. and Marinelli, M. (2009) ‘Age matters.’ *The European journal of neuroscience*, 29(5) pp. 997–1014.

Melin, C., Jacquot, F., Vitello, N., Dallel, R. and Artola, A. (2017) ‘Different processing of meningeal and cutaneous pain information in the spinal trigeminal nucleus caudalis.’ *Cephalalgia*, 37(12) pp. 1189–1201.

Melli, G. and Höke, A. (2009) ‘Dorsal Root Ganglia Sensory Neuronal Cultures: a tool for drug discovery for peripheral neuropathies.’ *Expert opinion on drug discovery*, 4(10) pp. 1035–1045.

Mense, S. (2004) ‘Neurobiological basis for the use of botulinum toxin in pain therapy.’ *J Neurol*, 251(Suppl 1) pp. 1–7.

Merskey, H. and Bogduk, N. (2012) *Classification of Chronic Pain*. 2nd ed., Seattle: IASP Press.

Midha, R. (1997) ‘Epidemiology of Brachial Plexus Injuries.’ *Neurosurgery*, 40(6) pp. 1182–1189.

Mirkovic, S., Rystedt, A., Balling, M. and Swartling, C. (2018) ‘Hyperhidrosis Substantially Reduces Quality of Life in Children: A Retrospective Study Describing

Symptoms, Consequences and Treatment with Botulinum Toxin.' *Acta Dermato Venereologica*, 98(1) pp. 103–107.

Moalem, G., Xu, K. and Yu, L. (2004) 'T LYMPHOCYTES PLAY A ROLE IN NEUROPATHIC PAIN FOLLOWING PERIPHERAL NERVE INJURY IN RATS,' 129 pp. 767–777.

Mogil, J. S. and Chanda, M. L. (2005) 'The case for the inclusion of female subjects in basic science studies of pain.' *Pain*, 117(1–2) pp. 1–5.

Møiniche, S., Kehlet, H. and Dahl, J. B. (2002) 'A Qualitative and Quantitative Systematic Review of Preemptive Analgesia for Postoperative Pain Relief.' *Anesthesiology*, 96(3) pp. 725–741.

Montal, M. (2010) 'Botulinum neurotoxin: a marvel of protein design.' *Annual review of biochemistry*, 79 pp. 591–617.

Montecucco, C. (1994) 'Molecular mechanism of action of tetanus toxin and botulinum neurotoxins.' *Molecular Microbiology*, 13(1) pp. 1–8.

Montecucco, C., Schiavo, G. and Pantano, S. (2005) 'SNARE complexes and neuroexocytosis: how many, how close?' *Trends in Biochemical Sciences*, 30(7) pp. 367–372.

Moore, K. A., Kohno, T., Karchewski, L. A., Scholz, J., Baba, H. and Woolf, C. J. (2002) 'Partial peripheral nerve injury promotes a selective loss of GABAergic inhibition in the superficial dorsal horn of the spinal cord.' *The Journal of neuroscience : the official journal of the Society for Neuroscience*, 22(15) pp. 6724–31.

Morenilla-Palao, C., Planells-Cases, R., García-Sanz, N. and Ferrer-Montiel, A. (2004) 'Regulated exocytosis contributes to protein kinase C potentiation of vanilloid receptor activity.' *The Journal of biological chemistry*, 279(24) pp. 25665–72.

Moreno-López, Y., Olivares-Moreno, R., Cordero-Erausquin, M. and Rojas-Piloni, G. (2016) 'Sensorimotor Integration by Corticospinal System.' *Frontiers in neuroanatomy*, 10(March) p. 24.

Moxon, K. A., Oliviero, A., Aguilar, J. and Foffani, G. (2014) 'Cortical reorganization after spinal cord injury: always for good?' *Neuroscience*, 283, December, pp. 78–94.

Mujumdar, R. B., Ernst, L. A., Mujumdar, S. R., Lewis, C. J. and Waggoner, A. S. (1993) 'Cyanine dye labeling reagents: sulfoindocyanine succinimidyl esters.' *Bioconjugate chemistry*, 4(2) pp. 105–11.

Mustafa, G., Anderson, E. M., Bokrand-Donatelli, Y., Neubert, J. K. and Caudle, R. M.

(2013) ‘Anti-nociceptive effect of a conjugate of substance P and light chain of botulinum neurotoxin type A.’ *Pain*, 154(11) pp. 2547–2553.

Nickel, F. T., Seifert, F., Lanz, S. and Maihöfner, C. (2012) ‘Mechanisms of neuropathic pain.’ *European Neuropsychopharmacology*. British Journal of Anaesthesia, 22(2) pp. 81–91.

Nirogi, R., Goura, V., Shanmuganathan, D., Jayarajan, P. and Abraham, R. (2012) ‘Comparison of manual and automated filaments for evaluation of neuropathic pain behavior in rats.’ *Journal of Pharmacological and Toxicological Methods*, 66(1) pp. 8–13.

Nurmikko, T., MacIver, K., Bresnahan, R., Hird, E., Nelson, A. and Sacco, P. (2016) ‘Motor Cortex Reorganization and Repetitive Transcranial Magnetic Stimulation for Pain—A Methodological Study.’ *Neuromodulation*, 19(7).

O’Connell, N. E., Wand, B. M., Gibson, W., Carr, D. B., Birklein, F. and Stanton, T. R. (2016) ‘Local anaesthetic sympathetic blockade for complex regional pain syndrome.’ *Cochrane Database of Systematic Reviews*, 7, July, p. CD004598.

Ogawa-Goto, K., Funamoto, N., Ohta, Y., Abe, T. and Nagashima, K. (1992) ‘Myelin gangliosides of human peripheral nervous system: an enrichment of GM1 in the motor nerve myelin isolated from cauda equina.’ *Journal of neurochemistry*, 59(5) pp. 1844–9.

Okuse, K. (2007) ‘Pain signalling pathways: From cytokines to ion channels.’ *International Journal of Biochemistry and Cell Biology*, 39(3) pp. 490–496.

Olbrich, K., Costard, L., Moser, C. V., Syhr, K. M. J., King-Himmelreich, T. S., Wolters, M. C., Schmidtko, A., Geisslinger, G. and Niederberger, E. (2017) ‘Cleavage of SNAP-25 ameliorates cancer pain in a mouse model of melanoma.’ *European Journal of Pain*, 21(1) pp. 101–111.

Otto, H., Hanson, P. I., Chapman, E. R., Blasi, J. and Jahn, R. (1995) ‘Poisoning by Botulinum Neurotoxin A Does Not Inhibit Formation or Disassembly of the Synaptosomal Fusion Complex.’ *Biochemical and Biophysical Research Communications*, 212(3) pp. 945–952.

Oyler, G. A., Higgins, G. A., Hart, R. A., Battenberg, E., Billingsley, M., Bloom, F. E. and Wilson, M. C. (1989) ‘The identification of a novel synaptosomal-associated protein, SNAP-25, differentially expressed by neuronal subpopulations.’ *The Journal of cell biology*. Rockefeller University Press, 109(6 Pt 1) pp. 3039–52.

Papers, J. B. C., Doi, M., Hong, S., Morrow, T. J., Paulson, P. E., Isom, L. L. and Wiley, J. W. (2004) ‘Early Painful Diabetic Neuropathy Is Associated with Differential Changes

in Tetrodotoxin-sensitive and -resistant Sodium Channels in Dorsal Root Ganglion Neurons in the Rat *,' 279(28) pp. 29341–29350.

Park, C., Kim, J.-H., Yoon, B.-E., Choi, E.-J., Lee, C. J. and Shin, H.-S. (2010) 'T-type channels control the opioidergic descending analgesia at the low threshold-spiking GABAergic neurons in the periaqueductal gray.' *Proceedings of the National Academy of Sciences of the United States of America*, 107(33) pp. 14857–62.

Parysek, L. M. and Goldman, R. D. (1988) 'Distribution of a novel 57 kDa intermediate filament (IF) protein in the nervous system.' *The Journal of neuroscience : the official journal of the Society for Neuroscience*, 8(2) pp. 555–63.

Passmore, G. M. (2005) 'Dorsal root ganglion neurones in culture: A model system for identifying novel analgesic targets?' *Journal of Pharmacological and Toxicological Methods*, 51(3 SPEC. ISS.) pp. 201–208.

Pereira, M. P. and Pogatzki-Zahn, E. (2015) 'Gender aspects in postoperative pain.' *Current Opinion in Anaesthesiology*, 28(5) pp. 546–558.

Peuker, S., Cukkemane, A., Held, M., Noé, F., Kaupp, U. B. and Seifert, R. (2013) 'Kinetics of ligand-receptor interaction reveals an induced-fit mode of binding in a cyclic nucleotide-activated protein.' *Biophysical journal*, 104(1) pp. 63–74.

Phillips, C. J. (2009) 'The Cost and Burden of Chronic Pain.' *Reviews in pain*, 3(1) pp. 2–5.

Pickett, A. (2010) 'Re-engineering clostridial neurotoxins for the treatment of chronic pain: Current status and future prospects.' *BioDrugs*, 24(3) pp. 173–182.

Pirazzini, M., Rossetto, O., Bolognese, P., Shone, C. C. and Montecucco, C. (2011) 'Double anchorage to the membrane and intact inter-chain disulfide bond are required for the low pH induced entry of tetanus and botulinum neurotoxins into neurons.' *Cellular Microbiology*, 13(11) pp. 1731–1743.

Pirazzini, M., Tehran, D. A., Zanetti, G., Megighian, A., Scorzeto, M., Fillo, S., Shone, C. C., Binz, T., Rossetto, O., Lista, F. and Montecucco, C. (2014) 'Thioredoxin and Its Reductase Are Present on Synaptic Vesicles, and Their Inhibition Prevents the Paralysis Induced by Botulinum Neurotoxins.' *Cell Reports*, 8 pp. 1870–1878.

Pocock, G., Richards, C. D. and Richards, D. A. (Biochemist) (2018) '13. The Somatosensory System.' *In Human Physiology*. 5th ed., Oxford: Oxford University Press, p. 203.

Pogatzki-zahn, E. M., Segelcke, D. and Schug, S. A. (2017) 'Postoperative pain — from mechanisms to treatment.' *PAIN Reports*, 2(2) p. e588.

Polgár, E., Gray, S., Riddell, J. S. and Todd, A. J. (2004) 'Lack of evidence for significant neuronal loss in laminae I-III of the spinal dorsal horn of the rat in the chronic constriction injury model.' *Pain*, 111(1–2) pp. 144–150.

Polomano, R. C., Mannes, A. J., Clark, U. S. and Bennett, G. J. (2001) 'A painful peripheral neuropathy in the rat produced by the chemotherapeutic drug, paclitaxel.' *Pain*, 94(3) pp. 293–304.

Porreca, F., Lai, J., Bian, D., Wegert, S., Ossipov, M. H., Eglen, R. M., Kassotakis, L., Novakovic, S., Rabert, D. K., Sangameswaran, L. and Hunter, J. C. (1999) 'A comparison of the potential role of the tetrodotoxin-insensitive sodium channels, PN3/SNS and NaN/SNS2, in rat models of chronic pain.' *Proceedings of the National Academy of Sciences of the United States of America*, 96(14) pp. 7640–4.

Porreca, F., Ossipov, M. H. and Gebhart, G. F. (2002) 'Chronic pain and medullary descending facilitation.' *Trends in Neurosciences*, 25(6) pp. 319–325.

Portier, M.-M., de Néchaud, B. and Gros, F. (1983) 'Peripherin, a New Member of the Intermediate Filament Protein Family.' *Developmental Neuroscience*, 6(6) pp. 335–344.

Posse de Chaves, E. and Sipione, S. (2010) 'Sphingolipids and gangliosides of the nervous system in membrane function and dysfunction.' *FEBS Letters*, 584(9) pp. 1748–1759.

Premkumar, L. S. and Ahern, G. P. (2000) 'Induction of vanilloid receptor channel activity by protein kinase C.' *Nature*, 408(6815) pp. 985–990.

Prendergast, B. J., Onishi, K. G. and Zucker, I. (2014) 'Female mice liberated for inclusion in neuroscience and biomedical research.' *Neuroscience and Biobehavioral Reviews*, 40 pp. 1–5.

Purkiss, J., Welch, M., Doward, S. and Foster, K. (2000) 'Capsaicin-stimulated release of substance P from cultured dorsal root ganglion neurons: Involvement of two distinct mechanisms.' *Biochemical Pharmacology*, 59(11) pp. 1403–1406.

Rahn, E. J., Zvonok, A. M., Thakur, G. a, Khanolkar, A. D., Makriyannis, A. and Hohmann, A. G. (2008) 'Selective activation of cannabinoid CB2 receptors suppresses neuropathic nociception induced by treatment with the chemotherapeutic agent paclitaxel in rats.' *The Journal of pharmacology and experimental therapeutics*, 327(2) pp. 584–591.

Reddi, D. and Curran, N. (2014) 'Chronic pain after surgery: Pathophysiology, risk factors and prevention.' *Postgraduate Medical Journal*, 90(1062) pp. 222–227.

Reinold, H., Ahmadi, S., Depner, U. B., Layh, B., Heindl, C., Hamza, M., Pahl, A., Brune,

K., Narumiya, S., Müller, U. and Zeilhofer, H. U. (2005) ‘Spinal inflammatory hyperalgesia is mediated by prostaglandin E receptors of the EP2 subtype.’ *The Journal of clinical investigation*, 115(3) pp. 673–9.

Relja, M. and Klepac, N. (2002) ‘Different doses of botulinum toxin A and pain responsiveness in cervical dystonia.’ *Neurology*, 58(7) p. 474.

Restani, L., Antonucci, F., Gianfranceschi, L., Rossi, C., Rossetto, O. and Caleo, M. (2011) ‘Evidence for Anterograde Transport and Transcytosis of Botulinum Neurotoxin A (BoNT/A).’ *Journal of Neuroscience*, 31(44) pp. 15650–15659.

Reyes-Gibby, C. C., Morrow, P. K., Buzdar, A. and Shete, S. (2009) ‘Chemotherapy-induced peripheral neuropathy as a predictor of neuropathic pain in breast cancer patients previously treated with paclitaxel.’ *The journal of pain : official journal of the American Pain Society*, 10(11) pp. 1146–50.

Rhéaume, C., Cai, B. B., Wang, J., Fernández-Salas, E., Roger Aoki, K., Francis, J. and Broide, R. S. (2015) ‘A highly specific monoclonal antibody for botulinum neurotoxin type A-cleaved SNAP25.’ *Toxins*, 7(7) pp. 2354–2370.

Rosano, G. L. and Ceccarelli, E. A. (2014) ‘Recombinant protein expression in Escherichia coli: advances and challenges.’ *Frontiers in microbiology*, 5 pp. 1–17.

Rossetto, O. (2017) ‘The binding of botulinum neurotoxins to different peripheral neurons.’ *Toxicon* pp. 1–5.

Rowbotham, M., Harden, N., Stacey, B., Bernstein, P. and Magnus-Miller, L. (1998) ‘Gabapentin for the treatment of postherpetic neuralgia: A randomized controlled trial.’ *Journal of the American Medical Association*, 280(21) pp. 1837–1842.

Rummel, A. (2012) ‘Double Receptor Anchorage of Botulinum Neurotoxins Accounts for their Exquisite Neurospecificity.’ *In* Rummel, A. and Binz, T. (eds) *Botulinum Neurotoxins*. 1st ed., Berlin: Springer-Verlag Berlin Heidelberg, pp. 61–90.

Rummel, A., Häfner, K., Mahrhold, S., Darashchonak, N., Holt, M., Jahn, R., Beermann, S., Karnath, T., Bigalke, H. and Binz, T. (2009) ‘Botulinum neurotoxins C, e and F bind gangliosides via a conserved binding site prior to stimulation-dependent uptake with botulinum neurotoxin F utilising the three isoforms of SV2 as second receptor.’ *Journal of Neurochemistry*, 110(6) pp. 1942–1954.

Rummel, A., Mahrhold, S., Bigalke, H. and Binz, T. (2004) ‘The HCC-domain of botulinum neurotoxins A and B exhibits a singular ganglioside binding site displaying serotype specific carbohydrate interaction.’ *Molecular microbiology*, 51(3) pp. 631–43.

Rust, A. (2016) *Novel payloads for immunotoxin-based treatment of neuroblastoma*.

University of Sheffield.

Said, G., Slama, G. and Selva, J. (1983) ‘PROGRESSIVE CENTRIPETAL DEGENERATION OF AXONS IN SMALL FIBRE DIABETIC POLYNEUROPATHY: A CLINICAL AND PATHOLOGICAL STUDY.’ *Brain*, 106 pp. 791–807.

Schaible, H. G., Ebersberger, A. and Natura, G. (2011) ‘Update on peripheral mechanisms of pain: Beyond prostaglandins and cytokines.’ *Arthritis Research and Therapy*, 13(2) p. 210.

Scheibel, M. E. and Scheibel, A. B. (1966) ‘Terminal axonal patterns in cat spinal cord I. The lateral corticospinal tract.’ *Brain Research*, 2(4) pp. 333–350.

Schiavo, G., Matteoli, M. and Montecucco, C. (2000) ‘Neurotoxins affecting neuroexocytosis.’ *Physiological reviews*, 80(2) pp. 717–766.

Schmader, K. E. (2002) ‘Epidemiology and impact on quality of life of postherpetic neuralgia and painful diabetic neuropathy.’ *The Clinical journal of pain*, 18(6) pp. 350–4.

Schmidt, R., Schmelz, M., Forster, C., Ringkamp, M., Torebjiirk, E. and Handwerker, H. (1995) ‘Novel Classes of Responsive and Unresponsive C Nociceptors in Human Skin.’ *The Journal of Neuroscience*, 15(l) pp. 333–341.

Schnaar, R. L. (2010) ‘Brain gangliosides in axon-myelin stability and axon regeneration.’ *FEBS letters*, 584(9) pp. 1741–7.

Scholz, J., Broom, D. C., Youn, D.-H., Mills, C. D., Kohno, T., Suter, M. R., Moore, K. A., Decosterd, I., Coggeshall, R. E. and Woolf, C. J. (2005) ‘Blocking Caspase Activity Prevents Transsynaptic Neuronal Apoptosis and the Loss of Inhibition in Lamina II of the Dorsal Horn after Peripheral Nerve Injury.’ *The Journal of Neuroscience*, 25(32) pp. 7317–7323.

Shehab, S. A. S., Spike, R. C. and Todd, A. J. (2003) ‘Evidence against cholera toxin B subunit as a reliable tracer for sprouting of primary afferents following peripheral nerve injury.’ *Brain Research*, 964(2) pp. 218–227.

Shimizu, T., Shibata, M., Toriumi, H., Iwashita, T., Funakubo, M., Sato, H., Kuroi, T., Ebine, T., Koizumi, K. and Suzuki, N. (2012) ‘Reduction of TRPV1 expression in the trigeminal system by botulinum neurotoxin type-A.’ *Neurobiology of Disease*, 48(3) pp. 367–378.

Sikandar, S., Gustavsson, Y., Marino, M. J., Dickenson, A. H., Yaksh, T. L., Sorkin, L. S. and Ramachandran, R. (2016) ‘Effects of intraplantar botulinum toxin-B on carrageenan-induced changes in nociception and spinal phosphorylation of GluA1 and Akt.’ *European Journal of Neuroscience*, 44(1) pp. 1714–1722.

Simpson, L. L. (1981) ‘The origin, structure, and pharmacological activity of botulinum toxin.’ *Pharmacological Reviews*, 33(3) pp. 155–188.

Sivilotti, L. and Woolf, C. J. (1994) ‘The contribution of GABAA and glycine receptors to central sensitization: disinhibition and touch-evoked allodynia in the spinal cord.’ *Journal of Neurophysiology*, 72(1) pp. 169–179.

Sleed, M., Eccleston, C., Beecham, J., Knapp, M. and Jordan, A. (2005) ‘The economic impact of chronic pain in adolescence: Methodological considerations and a preliminary costs-of-illness study.’ *Pain*, 119(1–3) pp. 183–190.

Snider, W. D., Zhang, L., Yusoof, S., Gorukanti, N. and Tsering, C. (1992) ‘Interactions between dorsal root axons and their target motor neurons in developing mammalian spinal cord.’ *The Journal of neuroscience : the official journal of the Society for Neuroscience*, 12(9) pp. 3494–3508.

Söllner, T., Bennett, M. K., Whiteheart, S. W., Scheller, R. H. and Rothman, J. E. (1993) ‘A protein assembly-disassembly pathway in vitro that may correspond to sequential steps of synaptic vesicle docking, activation, and fusion.’ *Cell*, 75(3) pp. 409–418.

Sorge, R. E., Mapplebeck, J. C. S., Rosen, S., Beggs, S., Taves, S., Alexander, J. K., Martin, L. J., Austin, J.-S., Sotocinal, S. G., Chen, D., Yang, M., Shi, X. Q., Huang, H., Pillon, N. J., Bilan, P. J., Tu, Y., Klip, A., Ji, R.-R., Zhang, J., Salter, M. W. and Mogil, J. S. (2015) ‘Different immune cells mediate mechanical pain hypersensitivity in male and female mice.’ *Nature Neuroscience*, 18(8) pp. 1081–1083.

Sorkin, L. S., Otto, M., Baldwin, W. M., Vail, E., Gillies, S. D., Handgretinger, R., Barfield, R. C., Ming Yu, H. and Yu, A. L. (2010) ‘Anti-GD2 with an FC point mutation reduces complement fixation and decreases antibody-induced allodynia.’ *PAIN*®, 149(1) pp. 135–142.

Sorkin, L. S., Yu, A. L., Junger, H. and Doom, C. M. (2002) ‘Antibody directed against GD2 produces mechanical allodynia, but not thermal hyperalgesia when administered systemically or intrathecally despite its dependence on capsaicin sensitive afferents.’ *Brain Research*, 930(1–2) pp. 67–74.

Southwick, P. L., Ernst, L. A., Tauriello, E. W., Parker, S. R., Mujumdar, R. B., Mujumdar, S. R., Clever, H. A. and Waggoner, A. S. (1990) ‘Cyanine Dye Labeling Reagents - Carboxymethylindocyanine Succinimidyl Esters.’ *Cytometry*, 11 pp. 418–430.

Starobova, H. and Vetter, I. (2017) ‘Pathophysiology of Chemotherapy-Induced Peripheral Neuropathy.’ *Frontiers in molecular neuroscience*, 10 p. 174.

Steeds, C. E. (2016) ‘The anatomy and physiology of pain.’ *Surgery (Oxford)*, 34(2) pp.

55–59.

Stein, C., Millan, M. J. and Herz, A. (1988) ‘Unilateral inflammation of the hindpaw in rats as a model of prolonged noxious stimulation: Alterations in behavior and nociceptive thresholds.’ *Pharmacology, Biochemistry and Behavior*, 31(2) pp. 445–451.

Stoeckel, K., Schwab, M. and Thoenen, H. (1977) ‘Role of gangliosides in the uptake and retrograde axonal transport of cholera and tetanus toxin as compared to nerve growth factor and wheat germ agglutinin.’ *Brain Research*, 132(2) pp. 273–285.

Straube, S., Derry, S., Moore, R. A. and Cole, P. (2013) ‘Cervico-thoracic or lumbar sympathectomy for neuropathic pain and complex regional pain syndrome.’ *Cochrane Database of Systematic Reviews*, (9) September, p. CD002918.

Strotmeier, J., Lee, K., Völker, A. K., Mahrhold, S., Zong, Y., Zeiser, J., Zhou, J., Pich, A., Bigalke, H., Binz, T., Rummel, A. and Jin, R. (2010) ‘Botulinum neurotoxin serotype D attacks neurons via two carbohydrate-binding sites in a ganglioside-dependent manner.’ *Biochemical Journal*, 431(2) pp. 207–216.

Surana, S., Tosolini, A. P., Meyer, I. F. G., Fellows, A. D., Novoselov, S. S. and Schiavo, G. (2017) ‘The travel diaries of tetanus and botulinum neurotoxins.’ *Toxicon*.

Tao-Cheng, J. H., Du, J. and McBain, C. J. (2000) ‘SNAP-25 is polarized to axons and abundant along the axolemma: An immunogold study of intact neurons.’ *Journal of Neurocytology*, 29(1) pp. 67–77.

ThermoFisher (2003) *Cholera Toxin Subunit B (CT-B) Conjugates*.

ThermoFisher (n.d.) *Alexa Fluor Dyes—Excellent Photostability*.

Thompson, D. E., Brehm, J. K., Oultram, J. D., Swinfield, T. J., Shone, C. C., Atkinson, T., Melling, J. and Minton, N. P. (1990) ‘The complete amino acid sequence of the Clostridium botulinum type A neurotoxin, deduced by nucleotide sequence analysis of the encoding gene.’ *European journal of Biochemistry*, 189(1) pp. 73–81.

Thompson, S. W., Woolf, C. J. and Sivilotti, L. G. (1993) ‘Small-caliber afferent inputs produce a heterosynaptic facilitation of the synaptic responses evoked by primary afferent A-fibers in the neonatal rat spinal cord in vitro.’ *Journal of Neurophysiology*, 69(6) pp. 2116–2128.

Todd, A. J. (2010) ‘Neuronal circuitry for pain processing in the dorsal horn.’ *Nature Reviews Neuroscience*, 11(12) pp. 823–836.

Todd, A. J. (2017) ‘Identifying functional populations among the interneurons in laminae I-III of the spinal dorsal horn.’ *Molecular pain*, 13 p. 1744806917693003.

Toffano, G., Savoini, G., Moroni, F., Lombardi, G., Calza, L. and Agnati, L. F. (1983) 'GM1 ganglioside stimulates the regeneration of dopaminergic neurons in the central nervous system.' *Brain Research*, 261(1) pp. 163–166.

Toivonen, J. M., Oliván, S. and Osta, R. (2010) 'Tetanus toxin c-fragment: The courier and the cure?' *Toxins*, 2(11) pp. 2622–2644.

De Toledo, I. P., Conti Réus, J., Fernandes, M., Porporatti, A. L., Peres, M. A., Takaschima, A., Linhares, M. N., Guerra, E. and De Luca Canto, G. (2016) 'Prevalence of trigeminal neuralgia: A systematic review.' *The Journal of the American Dental Association*. Elsevier, 147(7) p. 570–576.e2.

Tong, Y. G., Wang, H. F., Ju, G., Grant, G., Hökfelt, T. and Zhang, X. (1999) 'Increased uptake and transport of cholera toxin B-subunit in dorsal root ganglion neurons after peripheral axotomy: Possible implications for sensory sprouting.' *Journal of Comparative Neurology*, 404(2) pp. 143–158.

Tracey, I. and Mantyh, P. W. (2007) 'The Cerebral Signature for Pain Perception and Its Modulation.' *Neuron*, 55(3) pp. 377–391.

Treede, R.-D., Rief, W., Barke, A., Aziz, Q., Bennett, M. I., Benoliel, R., Cohen, M., Evers, S., Finnerup, N. B., First, M. B., Giamberardino, M. A., Kaasa, S., Kosek, E., Lavand'homme, P., Nicholas, M., Perrot, S., Scholz, J., Schug, S., Smith, B. H., Svensson, P., Vlaeyen, J. W. S. and Wang, S.-J. (2015) 'A classification of chronic pain for ICD-11.' *Pain*, 156(6) pp. 1003–7.

Treede, R. D., Meyer, R. A., Raja, S. N. and Campbell, J. N. (1992) 'Peripheral and central mechanisms of cutaneous hyperalgesia.' *Progress in Neurobiology*, 38(4) pp. 397–421.

Tsukamoto, K., Kohda, T., Mukamoto, M., Takeuchi, K., Ihara, H., Saito, M. and Kozaki, S. (2005) 'Binding of Clostridium botulinum type C and D neurotoxins to ganglioside and phospholipid: Novel insights into the receptor for clostridial neurotoxins.' *Journal of Biological Chemistry*, 280(42) pp. 35164–35171.

Turton, K., Chaddock, J. A. and Acharya, K. R. (2002) 'Botulinum and tetanus neurotoxins: structure, function and therapeutic utility.' *Trends in Biochemical Sciences*, 27(11) pp. 552–558.

Uchiyama, K., Kawai, M., Tani, M., Ueno, M., Hama, T. and Yamaue, H. (2006) 'Gender differences in postoperative pain after laparoscopic cholecystectomy.' *Surgical Endoscopy*, 20(3) pp. 448–451.

UgoBasile (2013) *Instruction Manual: Plantar Test (Hargreaves Apparatus)*. Varese: Ugo

Basile.

Usoskin, D., Zilberter, M., Linnarsson, S., Hjerling-Leffler, J., Uhlén, P., Harkany, T. and Ernfors, P. (2010) 'En masse in vitro functional profiling of the axonal mechanosensitivity of sensory neurons.' *Proceedings of the National Academy of Sciences of the United States of America*, 107(37) pp. 16336–41.

Vacca, V., Marinelli, S., Eleuteri, C., Luvisetto, S. and Pavone, F. (2012) 'Botulinum neurotoxin A enhances the analgesic effects on inflammatory pain and antagonizes tolerance induced by morphine in mice.' *Brain, Behavior, and Immunity*, 26(3) pp. 489–499.

Vanegas, H. and Schaible, H.-G. (2004) 'Descending control of persistent pain: inhibitory or facilitatory?' *Brain Research Reviews*, 46(3) pp. 295–309.

Vinson, M., Strijbos, P. J., Rowles, A., Facci, L., Moore, S. E., Simmons, D. L. and Walsh, F. S. (2001) 'Myelin-associated glycoprotein interacts with ganglioside GT1b. A mechanism for neurite outgrowth inhibition.' *The Journal of biological chemistry*, 276(23) pp. 20280–5.

Vivancos, G. G., Verri, W. A., Cunha, T. M., Schivo, I. R. S., Parada, C. A., Cunha, F. Q. and Ferreira, S. H. (2004) 'An electronic pressure-meter nociception paw test for rats.' *Brazilian Journal of Medical and Biological Research*, 37(3) pp. 391–399.

Vyas, A. A., Patel, H. V, Fromholt, S. E., Heffer-Lauc, M., Vyas, K. A., Dang, J., Schachner, M. and Schnaar, R. L. (2002) 'Gangliosides are functional nerve cell ligands for myelin-associated glycoprotein (MAG), an inhibitor of nerve regeneration.' *Proceedings of the National Academy of Sciences of the United States of America*, 99(12) pp. 8412–7.

Watson, C. and Harvey, A. R. (2009) 'Projections from the Brain to the Spinal Cord.' *In The Spinal Cord*. Elsevier, pp. 168–179.

Welch, M. J., Purkiss, J. R. and Foster, K. A. (2000) 'Sensitivity of embryonic rat dorsal root ganglia neurons to Clostridium botulinum neurotoxins.' *Toxicon*, 38(2) pp. 245–258.

Wen, J., Sun, D., Tan, J. and Young, W. (2015) 'A Consistent, Quantifiable, and Graded Rat Lumbosacral Spinal Cord Injury Model.' *Journal of neurotrauma*, 892 pp. 875–892.

Weng, X., Smith, T., Sathish, J. and Djouhri, L. (2012) 'Chronic inflammatory pain is associated with increased excitability and hyperpolarization-activated current (Ih) in C- but not Aδ-nociceptors.' *Pain*, 153(4) pp. 900–914.

Werner, M. U. and Kongsgaard, U. E. (2014) 'Defining persistent post-surgical pain: Is an update required?' *British Journal of Anaesthesia*, 113(1) pp. 1–4.

Whiteside, G. T., Harrison, J., Boulet, J., Mark, L., Pearson, M. and Walker, K. (2004) 'Pharmacological characterisation of a rat model of incisional pain' pp. 85–91.

Wilhelm, B. G., Mandad, S., Truckenbrodt, S., Kröhnert, K., Schäfer, C., Rammner, B., Koo, S. J., Claßen, G. A., Krauss, M., Haucke, V., Urlaub, H. and Rizzoli, S. O. (2014) 'Composition of isolated synaptic boutons reveals the amounts of vesicle trafficking proteins.' *Science*, 344(6187) pp. 1023–1028.

De Wolf, M. J. S., Lagrou, A. R., Hilderson, H. J. J., Van Dessel, G. A. F. and Dierick, W. S. H. (1987) 'pH-Induced Transitions in Cholera Toxin Conformation: A Fluorescence Study.' *Biochemistry*, 26(13) pp. 3799–3806.

Woolf, C. J. (1983) 'Evidence for a central component of post-injury pain hypersensitivity.' *Nature*, 306(5944) pp. 686–688.

Woolf, C. J. (2011) 'Central sensitization: Implications for the diagnosis and treatment of pain.' *Pain*, 152(S.3) pp. S2–S15.

Woolf, C. J. and King, A. E. (1990) 'Dynamic alterations in the cutaneous mechanoreceptive fields of dorsal horn neurons in the rat spinal cord.' *The Journal of neuroscience : the official journal of the Society for Neuroscience*, 10(8) pp. 2717–26.

Woolf, C. J., Shortland, P. and Coggeshall, R. E. (1992) 'Peripheral nerve injury triggers central sprouting of myelinated afferents.' *Nature*, 355(6355) pp. 75–78.

Wu, C., Xie, N., Lian, Y., Xu, H., Chen, C., Zheng, Y., Chen, Y. and Zhang, H. (2016) 'Central antinociceptive activity of peripherally applied botulinum toxin type A in lab rat model of trigeminal neuralgia.' *SpringerPlus*, 5 p. 431.

Xanthos, D. N. and Sandkühler, J. (2014) 'Neurogenic neuroinflammation: inflammatory CNS reactions in response to neuronal activity.' *Nature Reviews Neuroscience*, 15(1) pp. 43–53.

Xiao, L., Cheng, J., Zhuang, Y., Qu, W., Muir, J., Liang, H. and Zhang, D. (2013) 'Botulinum Toxin Type A Reduces Hyperalgesia and TRPV1 Expression in Rats with Neuropathic Pain...Transient Receptor Potential Vanilloid Type 1.' *Pain Medicine*, 14(2) pp. 276–286.

Xiao, W., Yu, A. L. and Sorkin, L. S. (1997) 'Electrophysiological characteristics of primary afferent fibers after systemic administration of anti-GD2 ganglioside antibody.' *Pain*, 69(1–2) pp. 145–151.

Xie, W., Chen, S., Strong, J. A., Li, A.-L., Lewkowich, I. P. and Zhang, J.-M. (2016) 'Localized Sympathectomy Reduces Mechanical Hypersensitivity by Restoring Normal Immune Homeostasis in Rat Models of Inflammatory Pain.' *The Journal of Neuroscience*,

36(33) pp. 8712–8725.

Xu, Q. and Yaksh, T. L. (2011) ‘A brief comparison of the pathophysiology of inflammatory versus neuropathic pain.’ *Current opinion in anaesthesiology*, 24(4) pp. 400–7.

Yang, L. J., Zeller, C. B., Shaper, N. L., Kiso, M., Hasegawa, A., Shapiro, R. E. and Schnaar, R. L. (1996) ‘Gangliosides are neuronal ligands for myelin-associated glycoprotein.’ *Proceedings of the National Academy of Sciences of the United States of America*, 93(2) pp. 814–8.

Young, M. J., Boulton, A. J., MacLeod, A. F., Williams, D. R. and Sonksen, P. H. (1993) ‘A multicentre study of the prevalence of diabetic peripheral neuropathy in the United Kingdom hospital clinic population.’ *Diabetologia*, 36(2) pp. 150–4.

Zagon, A. and Smith, A. D. (1993) ‘Monosynaptic projections from the rostral ventrolateral medulla oblongata to identified sympathetic preganglionic neurons.’ *Neuroscience*, 54(3) pp. 729–743.

Ziegler, E. A., Magerl, W., Meyer, R. A. and Treede, R. D. (1999) ‘Secondary hyperalgesia to punctate mechanical stimuli. Central sensitization to A-fibre nociceptor input.’ *Brain*, 122(12) pp. 2245–2257.

Zychowska, M., Rojewska, E., Makuch, W., Luvisetto, S., Pavone, F., Marinelli, S., Przewlocka, B. and Mika, J. (2016) ‘Participation of pro- and anti-nociceptive interleukins in botulinum toxin A-induced analgesia in a rat model of neuropathic pain.’ *European Journal of Pharmacology*, 791 pp. 377–388.